

R AND O ADIOLOGY ONCOLOGY

vol.45 no.4

december 2011



AROMASIN[®]

eksemestan



ENDOKRINO ZDRAVLJENJE BOLNIC Z RAKOM DOJK PO MENOPAVZI



BISTVENE INFORMACIJE IZ POVZETKA GLAVNIH ZNAČILNOSTI ZDRAVILA

AROMASIN 25 mg obložene tablete

Sestava in oblika zdravila: obložena tableta vsebuje 25 mg eksemestana. **Indikacije:** Adjuvantno zdravljenje žensk po menopavzi, ki imajo invazivnega zgodnjega raka dojke s pozitivnimi estrogenskimi receptorji in so se uvodoma vsaj 2 do 3 leta zdravile s tamoksifenom. Zdravljenje napredovelega raka dojke pri ženskah z naravno ali umetno povzročeno menopavzo, pri katerih je bolezen napredovala po antiestrogenskem zdravljenju. Učinkovitost še ni bila dokazana pri bolnicah, pri katerih tumorske celice nimajo estrogenskih receptorjev. **Odmerjanje in način uporabe:** 25 mg enkrat na dan, najbolje po jedi. Pri bolnicah z zgodnjim rakom dojke je treba zdravljenje nadaljevati do dopolnjenega petega leta adjuvantnega hormonskega zdravljenja oz. do recidiva tumorja. Pri bolnicah z napredovalim rakom dojke je treba zdravljenje nadaljevati, dokler ni razvidno napredovanje tumorja. **Kontraindikacije:** znana preobčutljivost na učinkovino zdravila ali na katero od pomožnih snovi, ženske pred menopavzo, nosečnice in doječe matere. **Posebna opozorila in previdnostni ukrepi:** predmenopavzni endokrini status, jetrna ali ledvična okvara, bolniki z redko dedno intoleranco za fruktozo, malabsorpcijo glukoze/galaktoze ali pomanjkanjem sahara-izomaltaze. Lahko povzroči alergijske reakcije ali zmanjšanje mineralne gostote kosti ter večjo pogostost zlomov. Ženskam z osteoporozo ali tveganjem zanjo je treba na začetku zdravljenja izmeriti mineralno kostno gostoto s kostno denzitometrijo. Čeprav še ni dovolj podatkov, kako učinkujejo zdravila za zdravljenje zmanjšane mineralne kostne gostote, ki jo povzroča Aromasin, je treba pri bolnicah s tveganjem uvesti zdravljenje ali profilakso osteoporozе ter bolnice natančno spremljati. **Medsebojno delovanje z drugimi zdravili:** Sočasna uporaba zdravil – npr. rifampicina, antiepileptikov (npr. fenitoina ali karbamazepina) ali zdravil rastlinskega izvora s šentjaževko – ki inducirajo CYP 3A4, lahko zmanjša učinkovitost Aromasina. Uporabljati ga je treba previdno z zdravili, ki se presnavljajo s pomočjo CYP 3A4 in ki imajo ozek terapevtski interval. Kliničnih izkušenj s sočasno uporabo zdravila Aromasin in drugih zdravil proti raku ni. Ne sme se jemati sočasno z zdravili, ki vsebujejo estrogen, saj bi ta izničila njegovo farmakološko delovanje. **Vpliv na sposobnost vožnje in upravljanja s stroji:** Po uporabi zdravila je lahko psihofizična sposobnost za upravljanje s stroji ali vožnjo avtomobila zmanjšana. **Neželeni učinki:** neželeni učinki so bili v študijah, v katerih so uporabljali standardni odmerek 25 mg, ponavadi blagi do zmerni. Zelo pogosti (> 10 %): vročinski oblivi, bolečine v sklepih, mišicah in kosteh, utrujenost, navzea, nespečnost, glavobol, močnejše znojenje, ginekološke motnje. **Način in režim izdajanja:** zdravilo se izdaja le na recept, uporablja pa se po navodilu in pod posebnim nadzorom zdravnika specialista ali od njega pooblaščenega zdravnika. **Imetnik dovoljenja za promet:** Pfizer Luxembourg SARL, 51, Avenue J. F. Kennedy, L-1855, Luksemburg. **Datum zadnje revizije besedila:** 11.12.2009

Pred predpisovanjem se seznanite s celotnim povzetkom glavnih značilnosti zdravila.

“SAMO ZA STROKOVNO JAVNOST”



Pfizer Luxembourg SARL, Grand Duchy of Luxembourg, 51, Avenue J.F. Kennedy, L-1855,
PFIZER, Podružnica za svetovanje s področja farmacevtske dejavnosti, Ljubljana, Letališka 3c, 1000 Ljubljana, SLOVENIJA

ARO-01-11



Publisher

Association of Radiology and Oncology

Affiliated with

Slovenian Medical Association – Slovenian Association of Radiology, Nuclear Medicine Society,
Slovenian Society for Radiotherapy and Oncology, and Slovenian Cancer Society
Croatian Medical Association – Croatian Society of Radiology
Societas Radiologorum Hungarorum
Friuli-Venezia Giulia regional groups of S.I.R.M.
Italian Society of Medical Radiology

Aims and scope

Radiology and Oncology is a journal devoted to publication of original contributions in diagnostic and interventional radiology, computerized tomography, ultrasound, magnetic resonance, nuclear medicine, radiotherapy, clinical and experimental oncology, radiobiology, radiophysics and radiation protection.

Editor-in-Chief

Gregor Serša Ljubljana, Slovenia

Executive Editor

Viljem Kovač Ljubljana, Slovenia

Deputy Editors

Andrej Čör Izola, Slovenia

Igor Kocijančič Ljubljana, Slovenia

Editorial Board

Karl H. Bohuslavizki Hamburg, Germany
Maja Čemažar Ljubljana, Slovenia
Christian Dittrich Vienna, Austria
Metka Filipič Ljubljana, Slovenia
Tullio Giraldi Trieste, Italy
Maria Gódey Budapest, Hungary
Vassil Hadjidekov Sofia, Bulgaria
Marko Hočevar Ljubljana, Slovenia
Maksimilijan Kadivec Ljubljana, Slovenia
Miklós Kásler Budapest, Hungary
Michael Kirschfink Heidelberg, Germany
Janko Kos Ljubljana, Slovenia
Tamara Lah Turnšek Ljubljana, Slovenia
Damijan Miklavčič Ljubljana, Slovenia
Luka Milas Houston, USA

Damir Miletić Rijeka, Croatia
Maja Osmak Zagreb, Croatia
Branko Palčič Vancouver, Canada
Dušan Pavčnik Portland, USA
Geoffrey J. Pilkington Portsmouth, UK
Ervin B. Podgoršak Montreal, Canada
Uroš Smrdel Ljubljana, Slovenia
Primož Strojčan Ljubljana, Slovenia
Borut Štabuc Ljubljana, Slovenia
Ranka Štern-Padovan Zagreb, Croatia
Justin Teissié Toulouse, France
Sándor Tóth Orosháza, Hungary
Gillian M. Tozer Sheffield, UK
Andrea Veronesi Aviano, Italy
Branko Zakotnik Ljubljana, Slovenia

Advisory Committee

Marija Auersperg Ljubljana, Slovenia
Tomaž Benulič Ljubljana, Slovenia
Jure Fettich Ljubljana, Slovenia
Valentin Fidler Ljubljana, Slovenia
Berta Jereb Ljubljana, Slovenia
Vladimir Jevtič Ljubljana, Slovenia
Stojan Plesničar Ljubljana, Slovenia
Mirjana Rajer Ljubljana, Slovenia
Živa Zupančič Ljubljana, Slovenia

Editorial office

Radiology and Oncology

Zaloška cesta 2

P. O. Box 2217

SI-1000 Ljubljana

Slovenia

Phone: +386 1 5879 369

Phone/Fax: +386 1 5879 434

E-mail: gsersa@onko-i.si

Copyright © Radiology and Oncology. All rights reserved.

Reader for English

Vida Kološa

Secretary

Mira Klemenčič

Zvezdana Vukmirović

Design

Monika Fink-Serša, Samo Rován, Ivana Ljubanović

Layout

Matjaž Lužar

Printed by

Tiskarna Ozimek, Slovenia

Published quarterly in 600 copies

Beneficiary name: DRUŠTVO RADIOLOGIJE IN ONKOLOGIJE

Zaloška cesta 2

1000 Ljubljana

Slovenia

Beneficiary bank account number: SI56 02010-0090006751

IBAN: SI56 0201 0009 0006 751

Our bank name: Nova Ljubljanska banka, d.d.,

Ljubljana, Trg republike 2,

1520 Ljubljana; Slovenia

SWIFT: LJBAS12X

Subscription fee for institutions EUR 100, individuals EUR 50

The publication of this journal is subsidized by the Slovenian Book Agency.

Indexed and abstracted by:

Science Citation Index Expanded (SciSearch®)

Journal Citation Reports/Science Edition

Scopus

EMBASE/Excerpta Medica

DOAJ

Open J-gate

Chemical Abstracts

Biomedicina Slovenica

This journal is printed on acid-free paper

On the web: ISSN 1581-3207

<http://versitaopen.com/ro>

<http://versita.com/science/medicine/ro/>

<http://www.onko-i.si/radioloncol/>

contents

review

- 227 **Titanium dioxide in our everyday life; is it safe?**
Matej Skocaj, Metka Filipic, Jana Petkovic, Sasa Novak

radiology

- 248 **Assessing renal function in children with hydronephrosis - additional feature of MR urography**
George Hadjidekov, Savina Hadjidekova, Zahari Tonchev, Rumiana Bakalova, Ichio Aoki

experimental oncology

- 259 **Cathepsin H indirectly regulates morphogenetic protein-4 (BMP-4) in various human cell lines**
Matija Rojnik, Zala Jevnikar, Bojana Mirkovic, Damjan Janes, Nace Zidar, Danijel Kikelj, Janko Kos

clinical oncology

- 267 **Sinonasal inverted papilloma associated with squamous cell carcinoma**
Jasna But-Hadzic, Klemen Jenko, Mario Poljak, Bostjan J Kocjan, Nina Gale, Primoz Strojan
- 273 **Comparison of survival of patients receiving laparoscopic and open radical resection for stage II colon cancer**
Cui-Zhen Fan, Yu-Ping Chu, Ping Wei, Hong Dai, Wenming Chen
- 279 **Expression of NF- κ B p65 phosphorylated at serine-536 in rectal cancer with or without preoperative radiotherapy**
Andreas Lewander, Jinfang Gao, Gunnar Adell, Hong Zhang, Xiao-Feng Sun

contents

- 285 **Efficacy of first-line systemic treatment in correlation with BRAF V600E and different KRAS mutations in metastatic colorectal cancer - a single institution retrospective analysis**
Martina Rebersek, Marko Boc, Petra Cerkovnik, Jernej Benedik, Zvezdana Hlebanja, Neva Volk, Srdjan Novakovic, Janja Ocvirk
- 292 **Hepatocellular carcinoma with subcutaneous metastasis of the scalp**
Yilmaz Tezcan and Mehmet Koc
- 296 **Genotyping of *BRCA1*, *BRCA2*, *p53*, *CDKN2A*, *MLH1* and *MSH2* genes in a male patient with secondary breast cancer**
Ana Lina Vodusek, Srdjan Novakovic, Vida Stegel, Berta Jereb
- 300 **Periampullary localized pancreatic intraepithelial neoplasia-3 (PanIN-3): evaluation with contrast-enhanced MR cholangiography (MRCP)**
Oktay Algin, Evrim Ozmen, Pamir Eren Ersoy, Mustafa Karaoglanoglu
- 304 **Brain meningioma invading and destructing the skull bone: replacement of the missing bone *in vivo***
Tomaz Velnar, Rado Pregelj, Clara Limbaeck-Stokin

radiophysics

- 310 **Dosimetric verification of compensated beams using radiographic film**
Slaven Jurkovic, Gordana Zauhar, Dario Faj, Deni Smilovic Radojcic, Manda Svabic, Mladen Kasabasic, Ana Diklic

I *slovenian abstracts*

VIII *authors Index 2011*

X *subject Index 2011*

RADIOLOGY AND ONCOLOGY is covered in Science Citation Index Expanded (SciSearch®), Journal Citation Reports/Science Edition, Scopus,

DOAJ, EMBASE/Excerpta Medica, Open J-gate, Chemical Abstracts, Biomedicina Slovenica

Titanium dioxide in our everyday life; is it safe?

Matej Skocaj¹, Metka Filipic², Jana Petkovic², Sasa Novak¹

¹ Jožef Stefan Institute, Department for Nanostructured Materials, Ljubljana, Slovenia

² National Institute of Biology, Department for Genetic Toxicology and Cancer Biology, Ljubljana, Slovenia

Received 7 October 2011

Accepted 27 October 2011

Correspondence to: Saša Novak, Jožef Stefan Institute, Department for Nanostructured Materials, Jamova 39, SI-1000 Ljubljana, Slovenia. Phone: +386 1 4773 271; Fax: +386 1 4773 221; E-mail: sasa.novak@ijs.si

Disclosure: No potential conflicts were disclosed.

Background. Titanium dioxide (TiO₂) is considered as an inert and safe material and has been used in many applications for decades. However, with the development of nanotechnologies TiO₂ nanoparticles, with numerous novel and useful properties, are increasingly manufactured and used. Therefore increased human and environmental exposure can be expected, which has put TiO₂ nanoparticles under toxicological scrutiny. Mechanistic toxicological studies show that TiO₂ nanoparticles predominantly cause adverse effects via induction of oxidative stress resulting in cell damage, genotoxicity, inflammation, immune response etc. The extent and type of damage strongly depends on physical and chemical characteristics of TiO₂ nanoparticles, which govern their bioavailability and reactivity. Based on the experimental evidence from animal inhalation studies TiO₂ nanoparticles are classified as "possible carcinogenic to humans" by the International Agency for Research on Cancer and as occupational carcinogen by the National Institute for Occupational Safety and Health. The studies on dermal exposure to TiO₂ nanoparticles, which is in humans substantial through the use of sunscreens, generally indicate negligible transdermal penetration; however data are needed on long-term exposure and potential adverse effects of photo-oxidation products. Although TiO₂ is permitted as an additive (E171) in food and pharmaceutical products we do not have reliable data on its absorption, distribution, excretion and toxicity on oral exposure. TiO₂ may also enter environment, and while it exerts low acute toxicity to aquatic organisms, upon long-term exposure it induces a range of sub-lethal effects.

Conclusions. Until relevant toxicological and human exposure data that would enable reliable risk assessment are obtained, TiO₂ nanoparticles should be used with great care.

Key words: titanium dioxide; nanoparticles; toxicity; applications; safety

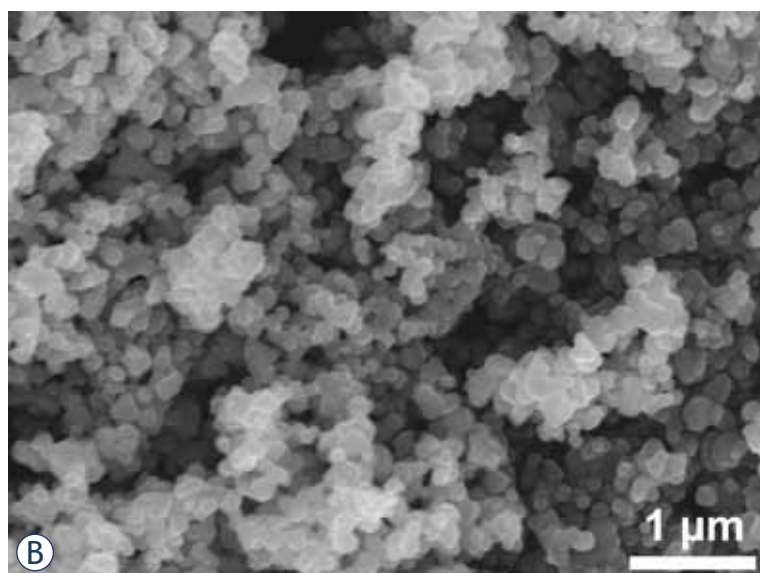
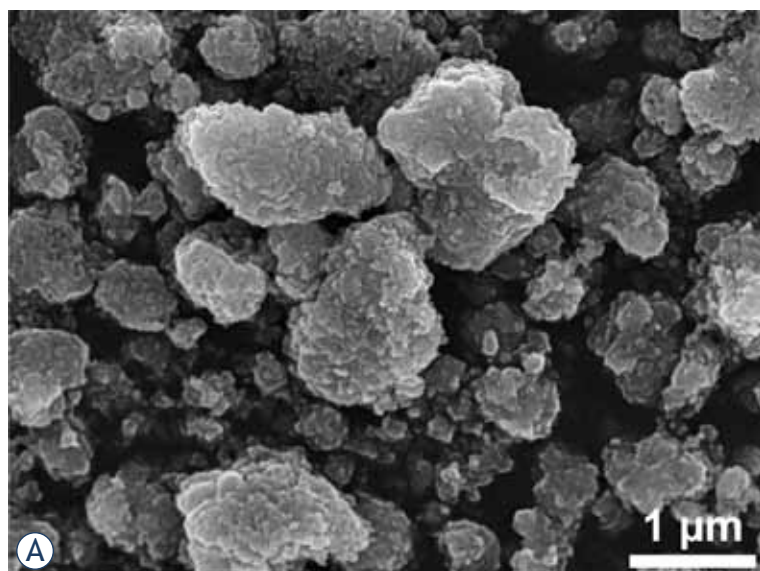
Introduction

Titanium dioxide (titania, TiO₂) is chemically inert, semiconducting material that also exhibits photocatalytic activity in the presence of light with an energy equal to or higher than its band-gap energy. These characteristics offer a wide range of applications. For these reasons, and because of the relatively low price of the raw material and its processing, titania has gained widespread attention over recent decades.

TiO₂ has been classified in humans and animals as biologically inert^{1,2}, and is widely considered to be a "natural" material, which at least partially contributes to its relatively positive acceptance by the public. In fact, most TiO₂ has been synthesized from the mineral ilmenite, FeTiO₃, using the "sulphate" or "chloride" process for nearly 100 years.

The annual worldwide production of titania powder in 2005 has been estimated to be around 5 million tons³, provoking the question as to its abundance in the environment. The proportion of nano-sized titania is estimated to have been approximately 2.5 % in 2009, increasing to 10 % by 2015⁴, with an exponential increase over the past decade.

During recent decades, TiO₂ powders have begun to appear in many applications, mainly due to their ability to confer whiteness and opacity on various products, such as paints, papers and cosmetics. Its high technological attractiveness originates from its light-scattering properties and very high refractive index, which mean that relatively low levels of the pigment are required to achieve a white, opaque coating. The range of light that is scattered depends on the particle size. Numerous technological improvements, based on nano-sized



TiO₂ have been introduced that enable its use for antifogging and self-cleaning coatings on glass, for building facades, in confectionary, in the plastics industry, and so on. Furthermore, TiO₂ is accepted as a food and pharmaceutical additive.⁵ In the United States it is included in the Food and Drug Administration (FDA) Inactive Ingredients Guide for dental paste, oral capsules, suspensions, tablets, dermal preparations and in non-parenteral medicines.

The increasing production of nano-sized TiO₂ powder has led to growing concerns about the consequences of exposure of humans and the environ-

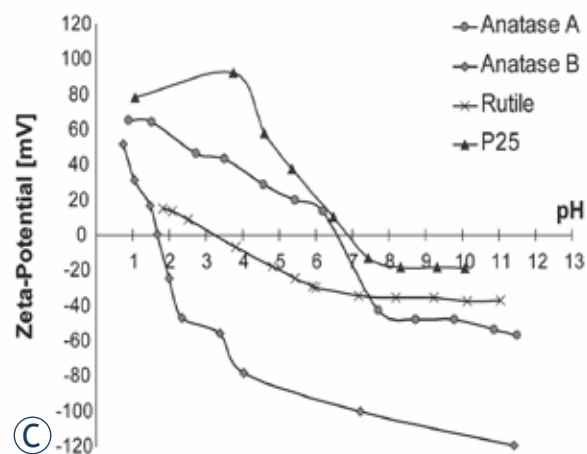


FIGURE 1. Field emission electron micrographs of different TiO₂ powders: A) Anatase A (Sigma 637254), B) Anatase B (Sigma T8141); C) Zeta-potential of these two powders, Rutile (Sigma 637262) and P25 (Degussa).

ment.⁶ In the present paper we review and discuss the latest findings on potential hazard of exposure to nano-sized TiO₂ for humans and environment, in regard to the particle size and the crystal structure of TiO₂, the route of exposure as well as the effect of ultraviolet (UV) irradiation-induced photocatalysis.

Chemical and physical properties of TiO₂ nanoparticles

Nanoparticles (NPs) are generally defined as particles having at least one dimension smaller than 100 nm. Accordingly, particles with different morphologies, from equi-axial shapes, whiskers, and nanotubes to nanorods, need to be considered. Although micron-sized and nano-sized TiO₂ powders are, in general, chemically identical, due to their significantly higher specific surface area, nano-powders may exhibit physical and chemical properties that differ from those of the coarser grades, and so should not be treated in the same way. In a recent paper⁷ the size-dependent properties of a variety of inorganic NPs were reviewed and it was suggested that they are likely to be of concern due to the appearance of unique properties when they have diameters of ≤ 30 nm. In this size range, many particles undergo dramatic changes in behaviour that enhance their interfacial reactivity. While less than 20 % of the constituent atoms are at the surface of 30 nm NPs, approximately 35-40 % of the atoms are localized at the surface of a 10 nm particle.

In practice, it is difficult to draw a clear borderline between nano- and submicron-sized particles. Submicron-sized powders always contain a certain proportion of nano-sized particles and, conversely, NPs tend to associate to form relatively strongly bonded aggregates (Figure 1A) or soft agglomerates (Figure 1B). The latter can usually be disintegrated easily in a liquid; however, their dispersion depends strongly on the zeta-potential. As illustrated in Figure 1C, the zeta-potential of TiO₂ powders may differ significantly over a wide range of pH values. The reported isoelectric points for TiO₂ powders range from pH 3.5 to 8⁸ which may greatly affect the bioavailability in the region of physiological pH values. The effective size of particles and their zeta-potential have been neglected almost completely in most of the studies of the interaction of TiO₂ NPs with biological systems.

Crystalline TiO₂ occurs naturally in three polymorphs – anatase, rutile and brookite – among which rutile is the most stable. A powder with an average particle size of 230 nm scatters visible light, while its counterpart, with an average size of 60 nm, scatters UV light and reflects visible light. Under UV, TiO₂ exhibits photocatalytic activity, which is a consequence of the electronic structure of the titania, and is, to a large extent, more characteristic of anatase than of rutile and brookite. In the presence of light with energy equal to or higher than the TiO₂ band-gap energy, an electron is promoted from the valence band to the conduction band, leaving behind a positive hole. The extrapolated optical absorption gaps of anatase and rutile are 3.2 and 3.0 eV at room temperature, which correspond to wavelengths of around 413 nm and 387 nm. Consequently, the photo-activation of nano-TiO₂ can be achieved by irradiation with UV-A, B and C, visible, fluorescent light, and X-ray radiation. The photocatalytic activity results in formation of highly reactive radicals, that are capable of reacting with most of the surrounding organic substances.⁹⁻¹²

Mechanisms of TiO₂ NPs toxicity

As already discussed, the physicochemical properties of particles depend on their size, so that, at the nanometre level, the material is chemically more reactive. This can be exploited as a desirable property, *e.g.*, as a catalyst. However, at the same time, the material may possess biological activities that can be either desirable (*e.g.*, carrier capacity

for therapeutics, penetration of cellular barriers for drug delivery) or undesirable (*e.g.*, toxicity, induction of oxidative stress or cellular dysfunction), or a mix of the two.

Cellular uptake of TiO₂ NPs

From a toxicological point of view the important characteristics of NPs are their size, surface area, surface chemistry and charge, crystallinity, shape, solubility and agglomeration/aggregation state. Surface groups may render NPs hydrophilic or hydrophobic, lipophilic or lipophobic, catalytically active or passive. Cellular uptake, subcellular localization, and ability to cause toxic effects depend on these properties of NPs.¹³ The two main pathways of NP uptake in the cell are active uptake by endocytosis, and passive uptake by free diffusion. Phagocytosis is an actin-dependent, endocytic mechanism, typical of “professional” phagocytes like macrophages. Geiser *et al.*¹⁴ reported that, in rats exposed to TiO₂ powders by inhalation, alveolar macrophages effectively cleared micron-sized (3–6 μm) but not nano-sized (20 nm) TiO₂ particles. This is important, since phagocytes generally remove particulate matter >500 nm¹⁵ and, as they are unable to phagocytose smaller particles, the latter are retained in the tissue, leading to a sustained burden on other tissues and cells. It was demonstrated that the uptake of 50 nm nano-TiO₂, by endocytosis with alveolar A549 epithelial cells, was limited to aggregated particles.¹⁶ After inhalation exposure of rats to TiO₂ NPs, free particles were found within the cytoplasm of epithelial and endothelial cells and fibroblasts.¹⁷ Rothen-Rutishauser *et al.*¹⁸, used an *in vitro* airway wall model, and found membrane-bound aggregates (>200 nm) of TiO₂ as well as smaller unbound aggregates within the cell cytoplasm. In an *in vitro* study Kocbek *et al.*¹⁹ demonstrated the endocytotic uptake of 25 nm-sized anatase TiO₂ by human keratinocytes. They observed highly aggregated NPs within early and late endosomes and in amphisomes, confirming endocytotic uptake. Experiments with red blood cells, which lack phagocytic receptors¹⁸, revealed that TiO₂ NP aggregates smaller than 200 nm are able to enter red blood cells, while larger particles were only found attached to the cell's surface. Xia *et al.*²⁰ showed that fluorescence-labelled TiO₂ NPs (11 nm) were taken up and localized in late endosomal and caveolar compartments in phagocytic RAW 246.7 and lung endothelial BEAS-2B cells.

Oxidative stress induced by TiO₂ NPs

Oxidative stress is thought to be a key mechanism responsible for adverse biological effects exerted by NPs.^{21,22} The role of oxidative stress in TiO₂-induced adverse effects has been confirmed by evidence that it induces an increase in reactive oxygen species (ROS) production and oxidative products (*i.e.*, lipid peroxidation), as well as the depletion of cellular antioxidants.²³⁻²⁹

TiO₂ mediates oxidative stress under UV irradiation as well as without it. Uchino *et al.*³⁰ showed that, under UV irradiation, the TiO₂ NPs of different crystalline structures and sizes produces different amounts of hydroxyl radicals, and that cytotoxicity against Chinese hamster ovary cells correlates with the production of radicals. Dodd and Jha³¹ confirmed that hydroxyl radicals are the primary damaging species produced by UV irradiated nano-sized TiO₂, and react to give carboxyl radicals. A number of studies have shown photo-activated anatase TiO₂ to induce higher cytotoxicity and genotoxicity than similarly activated rutile TiO₂. These differences could arise from the fact that anatase particles possess a wider absorption gap and a smaller electron effective mass, resulting in the higher mobility of the charge carriers and the greater generation of ROS. On the other hand, there is evidence that TiO₂ also induces ROS formation and the associated adverse effects in the absence of photo-activation. For instance, Gurr *et al.*²⁴ found that anatase TiO₂ NPs and mixtures of anatase and rutile TiO₂ NPs induced oxidative damage in human bronchial epithelial (BEAS-2B) cells, and Petković *et al.*³² reported that in human hepatoma cells (HepG2), non-irradiated anatase nano-TiO₂ induced significantly higher levels of intracellular ROS than the corresponding rutile-TiO₂, and only anatase nano-TiO₂ caused oxidative DNA damage. Recently, Petković *et al.*³³ compared cytotoxicity and genotoxicity of non-irradiated and UV pre-irradiated anatase TiO₂ of two sizes (<25 nm and >100 nm). They showed that non-irradiated TiO₂ particles did not affect survival of the cells; they caused slight increase in number of DNA strand breaks, while only TiO₂ NPs caused increase in oxidative DNA damage. After pre-irradiation with UV both sizes of anatase TiO₂ particles reduced cell viability, induced DNA strand breaks and oxidative DNA damage. This is an important finding that, for the first time, showed that photo-activated TiO₂ particles retained higher cytotoxic and genotoxic potential also when UV irradiation was discontinued and that it was not particle size dependent.

ROS are also important signalling modulators, therefore exposure of cells to NPs may, via elevated ROS formation, affect cellular signalling cascades that control processes such as cell proliferation, inflammation and cell death.³⁴ The role of oxidative stress in TiO₂-induced inflammation has recently been confirmed by Kang *et al.*³⁵ In the mouse peritoneal macrophage cell line RAW 246.7 exposed to nano-TiO₂, ROS production was associated with the activation of pro-inflammatory cascade, as indicated by extracellular signal-regulated kinases ERK1/2 phosphorylation, tumour necrosis factor TNF α production and macrophage inflammatory protein MIP-2 secretion.

Taken together, these studies indicate that the high level of oxidative stress that is related to an exposure to a high concentration of TiO₂ NPs leads to cell damage-associated responses, whereas at moderate levels of oxidative stress, inflammatory responses may be stimulated by the activation of ROS-sensitive signalling pathways.

Genotoxicity of TiO₂ NPs

Several studies show that nano-TiO₂ induces genotoxic effects, including DNA damage, and micronuclei formation that is indicative of chromosomal aberrations in different cell lines.^{32, 35-38} The studies also showed that genotoxic effects elicited by TiO₂ NPs strongly depended upon their size and form. For instance, Gurr *et al.*²⁴ showed that anatase TiO₂ NPs up to 20 nm in size induced an increase in micronuclei formation, while 200 nm anatase or 200 nm rutile TiO₂ did not. Zhu *et al.*³⁹ demonstrated clear differences in the cytotoxicity and the extent of DNA strand scission, together with the formation of 8-hydroxy-2-deoxyguanosine (8-OHdG) adducts in isolated DNA, after a treatment with different types of TiO₂ NPs in the order 10-20 nm anatase > 50-60 nm anatase > 50-60 nm rutile. At the molecular level it has been shown that the exposure of peripheral human lymphocytes to TiO₂ NPs caused the activation of DNA damage check points and the accumulation of tumour suppressor protein p53, the main regulator of the cellular response to DNA damage.⁴⁰ Exposure of human hepatoma HepG2 cells under similar conditions led to the elevated expression of tumor suppressor p53 mRNA and its downstream regulated DNA damage response genes (cyclin-dependent kinase inhibitor p21, growth arrest and DNA damage-inducible gene *GADD45a* and the E3 ubiquitin ligase *MDM2*).³²

On the other hand, TiO₂ NPs were devoid of mutagenic activity in microbial mutation assays (with *Salmonella typhimurium*) and in chromosomal aberration in Chinese hamster ovary cells.⁴¹ Similarly, Theogaraj *et al.*⁴² reported that nano-sized TiO₂ (eight different anatase and rutile forms) at concentrations up to 5 mg/ml did not induce any increase in the chromosomal aberration frequency in Chinese hamster ovary cells, in either the absence or the presence of UV light. However, in this study only a short-term, 3-hour, and no continuous (*i.e.*, 20 hours) exposure, was performed.

In an early study Driscoll *et al.*⁴³ reported that in rats intratracheal instillation of TiO₂ NPs (100 mg/kg BW) induced increased HPRT mutation frequency in alveolar cells. They also showed that mutagenicity in alveolar cells was associated with inflammation. Trouiller *et al.*⁴⁴ recently reported that oral exposure of mice to TiO₂ NPs through drinking water (50-500 mg/kg BW/day for 5 days) induced oxidative DNA damage, micronuclei formation and γ -H2AX foci, the indicators of DNA double strand breaks. Since also high-level gene expression of pro-inflammatory cytokines was also observed, the authors suggested the inflammatory effects were responsible for the induction of genotoxic effects.

The *in vitro* and *in vivo* genotoxicity studies using different experimental models indicate that nano-TiO₂ may cause genotoxic effects via secondary mechanisms that include oxidative stress and inflammation.^{32,38,40,43,44} However, there is some evidence that nano-sized TiO₂ can locate in nuclei¹⁷, and recently Li *et al.*⁴⁵ reported the presence of anatase nano-sized TiO₂ in DNA extracted from the liver of mice exposed intraperitoneally to these NPs (5-150 mg/kg BW/day for 14 days). The authors showed that Ti inserted between DNA base pairs or bound to DNA nucleotides, in such a way that it altered the conformation of the DNA and, at higher doses, caused DNA cleavage. These findings indicate that TiO₂ may also induce genetic damage by a direct interaction with the DNA.

Immunotoxic effects of TiO₂ NPs

Depending on physicochemical properties of NPs, they are recognized and taken up by immune cells, such as macrophages, monocytes, platelets, leukocytes and dendritic cells, and can trigger an inflammatory response. In a human monoblastoid cell line (U937) exposure to TiO₂ NPs induced apoptosis and necrosis in concentrations corresponding to those found in blood, plasma, or in tissues sur-

rounding Ti implants⁴⁶. Palomäki *et al.*⁴⁷ reported that rutile TiO₂ NPs and silica-coated rutile TiO₂ NPs induced the enhanced expression of a variety of proinflammatory cytokines in murine dendritic cells (bm-DC) and in murine macrophages (RAW 246.7). The particles were for dendritic cells more toxic than for macrophages. In dendritic cells nano-sized TiO₂ led to an upregulation of maturation markers and activated the NLRP3 inflammasome, a multiprotein complex within the cytoplasm of antigen-presenting cells, leading to significant IL 1 β -secretion. It was demonstrated for neutrophils that the short-term exposure of neutrophils to nano-anatase TiO₂ induces changes in their morphology, indicating its potential to activate these cells, while longer exposure resulted in the inhibition of apoptosis and cytokine production, confirming that *in vitro* TiO₂ exerts neutrophil agonist properties.

Immunomodulating effects after exposure to TiO₂ NPs have been observed also in *in vivo* studies. Larsen *et al.*⁴⁸ showed that in ovalbumin immunized mice intraperitoneal exposure to TiO₂ NPs promoted a T-helper type 2 cells mediated dominant immune response with high levels of ovalbumin-specific immunoglobulins IgE and IgG1 in serum and influx of eosinophils, neutrophils and lymphocytes in bronchoalveolar lavage fluid. Airway inflammation and immune adjuvant activity in ovalbumin immunized mice was observed also after intranasal exposure to TiO₂ NPs^{48,49} indicating that airborne exposure to TiO₂ NPs may induce respiratory allergy, where the possible mechanism could be an adjuvant-like activity of NPs on allergic sensitization. Associated with the impairment of the immune response, recently Moon *et al.*⁵⁰ showed that the intraperitoneal exposure of mice to TiO₂ NPs enhanced the growth of subcutaneously implanted B16F10 melanoma through the immunomodulation of B- and T-lymphocytes, macrophages, and natural killer cells.

Neurotoxic effects of TiO₂ NPs

It has been reported that inhaled NPs can translocate to the central nervous system through the olfactory pathway²² and by crossing the blood-brain barrier.^{51,52} *In vitro* studies of non-irradiated TiO₂ NPs (Degussa P25) showed that they cause oxidative stress in the brain microglia BV2 cell line⁵³ that was associated with the up-regulation of genes involved in the inflammation, apoptosis, and the cell cycle, and down-regulation of genes involved in energy metabolism.²⁵ While Degussa

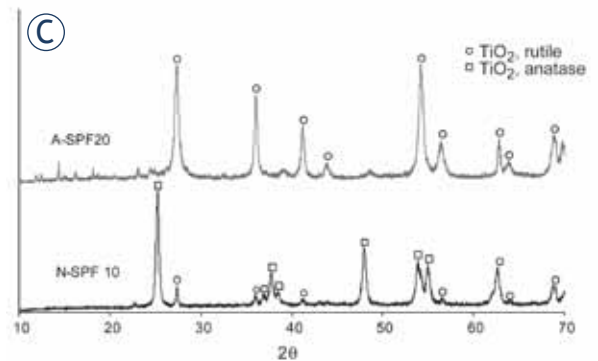
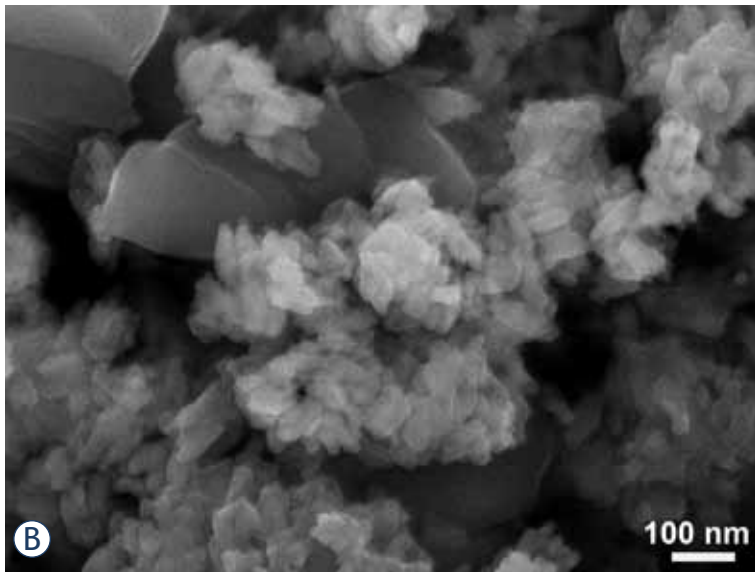
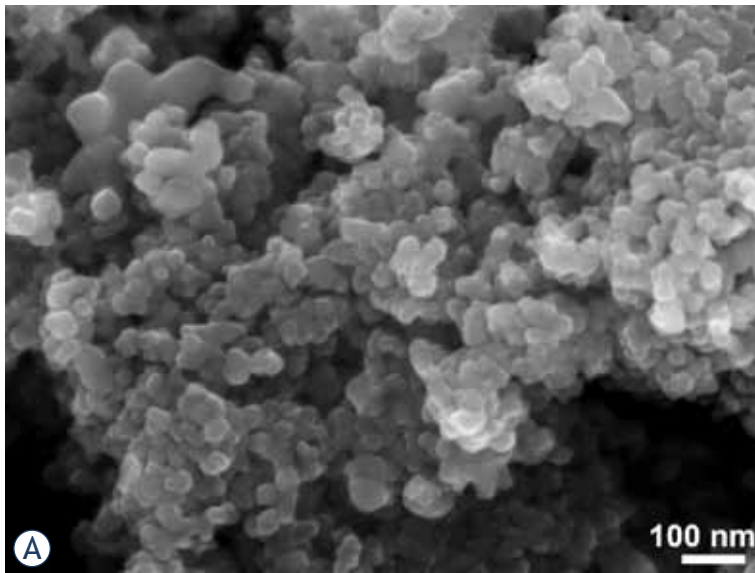


FIGURE 2. Field emission electron micrographs of the powders from two commercial sunscreens: A-SPF 20 (A) and N-SPF 10 (B), and their XRD diffraction (C).

stem cells towards neurons. These results indicate that the responses may be cell-type dependent and oxidative stress-mediated.

Recently Scuri *et al.*⁵⁶ reported that inhalation exposure of newborn (2-day-old) and weanling (2-week-old), but not adult, rats to TiO₂ NPs (12 mg/m³; 5.6 h/day for 3 days) up-regulates the expression of lung neurotrophins, key regulatory elements of neuronal development and responsiveness that play a critical role in the pathophysiology of childhood asthma. The effect was associated with the development of airway hyperreactivity (AHR) and mild airway inflammation. These results suggest the presence of a critical window of vulnerability in the earlier stages of lung development, which may lead to a higher risk of developing asthma.

TiO₂ NPs in everyday life

Nano-sized TiO₂ in various forms is used widely in everyday life in a variety of products, such as anti-fouling paints, household products, plastic goods, medications, cosmetics, sunscreens, pharmaceutical additives and food colorants, and many new applications are under development or already in pilot production. In the following sections we consider the main entry ports of nano-sized TiO₂ into the human body and potential adverse effects.

Dermal exposure to TiO₂ NPs

TiO₂ NPs as a component of the sunscreen-technology revolution

During recent decades, skin cancer has become the most frequent neoplastic disease among the Caucasian population in Europe, North America

P25 NPs stimulated ROS formation in BV2 microglia, they were nontoxic to isolated N27 neurons. However, in complex brain cultures the Degussa P25 particles rapidly damaged neurons, plausibly through microglial generated ROS. In contrast, Liu *et al.*⁵⁴ reported that, in the neuronal cell line PC12, exposure to nano-TiO₂ induced dose-dependent oxidative stress and apoptosis that was partly prevented by pre-treatment with a ROS scavenger. Surprisingly, it was shown recently⁵⁵ that TiO₂ NPs (rutile TiO₂ coated with SiO₂; 80-100 nm) might be an inducer of the differentiation of (mouse) neural

and Australia, and its incidence has reached epidemic proportions.⁵⁷ As a consequence, the trend in sun protection in daily cosmetics is towards increased use of organic and inorganic UV filters. It is estimated that worldwide use of nano-sized TiO₂ in sunscreens is around 1000 tons per year.⁵¹

TiO₂ has been used in sunscreens since 1952, however the Food and Drug Administration (FDA) approved the use of TiO₂ in sunscreens in 1999.^{58,59} Currently it is not required to label sunscreens as containing nano-TiO₂.⁶⁰ The situation could change if the European Union (EU) commission adopts a proposed new regulation within EU Cosmetic Directive, under which all cosmetics that contain more than 1 % w/w of NPs will have to declare it on the packaging. Since TiO₂ is considered as low-irritating, it is the only inorganic UV filter allowed by European legislation in concentrations as high as 25 %.^{61,62} There is also some confusion regarding the classification of sunscreens. In the EU they are classified as cosmetics, while in the USA, they are classified as over the counter (OTC) drugs.⁶³

The average size of the TiO₂ particles in sunscreens ranges between 10 and 100 nm, while some products contain particles down to 5 nm or up to 500 nm.⁶⁴ TiO₂ particles in the size range between 200 and 500 nm are opaque and act as a true sunblock when applied to the skin.^{61,65,66} However, this opacity is lost when much finer particles are used. Such sunscreens are more transparent, less viscous, and blend into the skin more easily. Therefore, the optimum size of TiO₂ particles was suggested to be around 50 nm, which provides good protection against UV light, while the dispersion of visible light is such that sunscreens do not appear white on the skin.⁶⁷

Sunscreens typically, but not exclusively, contain rutile TiO₂ powder, which is less photo-active than the anatase TiO₂. Micrographs of the powders extracted from two commercial sunscreens from different producers are shown in Figures 2A and B. From the X-ray diffractograms (Figure 2C) it is evident that the TiO₂ powder in the sunscreen "N-SPF10" is predominantly in the anatase form, with an estimated particle size of around 50 nm (Figure 2A, C), while the powder in the sunscreen "A-SPF20" contained rutile TiO₂ with two size populations (Figure 2B, C). (The original commercial names of the products were adapted for this study.)

To minimize the harmful effects of photo-active nano-TiO₂, various coatings such as magnesia, silica, alumina or zirconia⁶⁸⁻⁷¹ were introduced. However, certain coating materials may have side effects, such as aluminium-based ones (Figure 3),

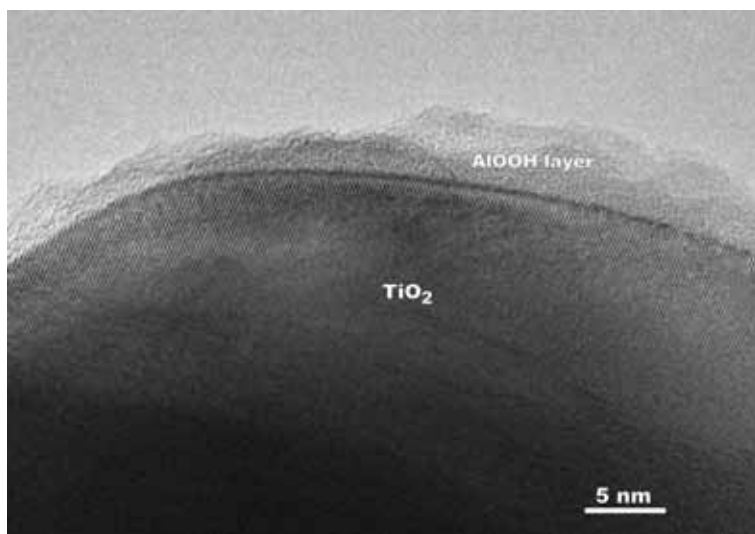


FIGURE 3. Transmission electron micrograph of an AlOOH-coated TiO₂ NP (Courtesy of dr. G. Dražić).

and it is also not clear how stable the coatings are and what is the lifetime of the "inert" particle released from sunscreens.

Cytotoxic and genotoxic effects of TiO₂ NPs in dermal cells and skin models

Different dermal cell types have been reported to differ in their sensitivity to nano-sized TiO₂. Kiss *et al.*⁷² exposed human keratinocytes (HaCaT), human dermal fibroblast cells, sebaceous gland cells (SZ95) and primary human melanocytes to 9 nm-sized TiO₂ particles at concentrations from 0.15 to 15 µg/cm² for up to 4 days. The particles were detected in the cytoplasm and perinuclear region in fibroblasts and melanocytes, but not in keratinocytes or sebaceous cells. The uptake was associated with an increase in the intracellular Ca²⁺ concentration. A dose- and time-dependent decrease in cell proliferation was evident in all cell types, whereas in fibroblasts an increase in cell death via apoptosis has also been observed. Anatase TiO₂ in 20–100 nm-sized form has been shown to be cytotoxic in mouse L929 fibroblasts.⁷³ The decrease in cell viability was associated with an increase in the production of ROS and the depletion of glutathione. The particles were internalized and detected within lysosomes. In human keratinocytes exposed for 24 h to non-illuminated, 7 nm-sized anatase TiO₂, a cluster analysis of the gene expression revealed that genes involved in the "inflammatory response" and "cell adhesion", but not those involved in "oxidative stress" and "apoptosis", were up-regulated.⁷³ The results suggest that non-illu-

minated TiO₂ particles have no significant impact on ROS-associated oxidative damage, but affect the cell-matrix adhesion in keratinocytes in extracellular matrix remodelling. In human keratinocytes, Kocbek *et al.*¹⁹ investigated the adverse effects of 25 nm-sized anatase TiO₂ (5 and 10 µg/ml) after 3 months of exposure and found no changes in the cell growth and morphology, mitochondrial function and cell cycle distribution. The only change was a larger number of nanotubular intracellular connections in TiO₂-exposed cells compared to non-exposed cells. Although the authors proposed that this change may indicate a cellular transformation, the significance of this finding is not clear. On the other hand, Dunford *et al.*²³ studied the genotoxicity of UV-irradiated TiO₂ extracted from sunscreen lotions, and reported severe damage to plasmid and nuclear DNA in human fibroblasts. Manitol (antioxidant) prevented DNA damage, implying that the genotoxicity was mediated by ROS.

Recently, Yanagisawa *et al.*⁷⁴ reported that the transdermal exposure (mimicking skin-barrier dysfunction or defect) of NC/Nga mice to TiO₂ NPs (15, 50, or 100 nm), in combination with allergen, aggravated atopic dermatitis-like lesions through a T-helper type 2 (Th2) dominant immune response. The study also indicated that TiO₂ NPs can play a role in the initiation and/or progression of skin diseases, since histamine was released, even in the absence of allergen.

Skin-penetration studies

The skin of an adult person is, in most places, covered with a relatively thick (~10 µm) barrier of keratinised dead cells. One of the main questions is still whether TiO₂ NPs are able to penetrate into the deeper layers of the skin.⁷⁵ The majority of studies suggest that TiO₂ NPs, neither uncoated nor coated (SiO₂, Al₂O₃ and SiO₂/Al₂O₃) of different crystalline structures, penetrate normal animal or human skin.^{76,77-82} However, in most of these studies the exposures were short term (up to 48 h); only few long-term or repeated exposure studies have been published. Wu *et al.*⁸³ have shown that dermal application of nano-TiO₂ of different crystal structures and sizes (4-90 nm) to pig ears for 30 days did not result in penetration of NPs beyond deep epidermis. On the other hand, in the same study the authors reported dermal penetration of TiO₂ NPs with subsequent appearance of lesions in multiple organs in hairless mice, that were dermal exposed to nano-TiO₂ for 60 days. However,

the relevance of this study for human exposure is not conclusive because hairless mice skin has abnormal hair follicles, and mice stratum corneum has higher lipid content than human stratum corneum, which may contribute to different penetration. Recently Sadrieh *et al.*⁸⁴ performed a 4 week dermal exposure to three different TiO₂ particles (uncoated submicron-sized, uncoated nano-sized and coated nano-sized) in 5 % sunscreen formulation with minipigs. They found elevated titanium levels in epidermis, dermis and in inguinal lymph nodes, but not in precapsular and submandibular lymph nodes and in liver. With the energy dispersive X-ray spectrometry and transmission electron microscopy (TEM) analysis the authors confirmed presence of few TiO₂ particles in dermis and calculated that uncoated nano-sized TiO₂ particles observed in dermis represented only 0.00008 % of the total applied amount of TiO₂ particles. Based on the same assumptions used by the authors in their calculations it can be calculated that the total number of particles applied was 1.8×10^{13} /cm² and of these 1.4×10^7 /cm² penetrated. The surface area of skin in humans is around 1.8 m²⁸⁵ and for sun protection the cream is applied over whole body, which would mean that 4 week usage of such cream with 5 % TiO₂ would result in penetration of totally 2.6×10^{10} particles. Although Sadrieh *et al.*⁸⁴ concluded that there was no significant penetration of TiO₂ NPs through intact normal epidermis, the results are not completely confirmative.

TiO₂ NPs intake by food

TiO₂ has been well accepted in the food industry and can be found as the E171 additive in various food products, mainly for whitening and texture. It is present in some cottage and Mozzarella cheeses, horseradish cream and sauces, lemon curd, and in low-fat products such as skimmed milk and ice-cream. Even if the product is labelled as containing E171, no information is usually given about the quantity, particle size and particle structure. FDA claims that TiO₂ may be safely used as a colour additive for colouring foods in quantities up to 1 % by weight of the food.⁸⁶ Interestingly, TiO₂ is frequently declared as a "natural colouring agent" and is therefore well accepted by consumers.

TiO₂ is also used in oral pharmaceutical formulations⁵, and the Pharmaceutical Excipients handbook considers nano-sized TiO₂ a non-irritant and non-toxic excipient. Despite the fact that TiO₂ submicron- and nano-sized particles are widely used as food and pharmaceutical additives, information

on their toxicity and distribution upon oral exposure is very limited.

Potential hazards of oral exposure to TiO₂ NPs

The gastrointestinal tract is a complex barrier/exchange system, and is the most important route by which macromolecules can enter the body. The main absorption takes place through villi and microvilli of the epithelium of the small and large intestines, which have an overall surface of about 200 m². Already in 1922, it was recognized by Kumagai⁸⁷, that particles can translocate from the lumen of the intestinal tract via aggregation of intestinal lymphatic tissue (Peyer's patch, containing M-cells (phagocytic enterocytes)). Uptake can also occur via the normal intestinal enterocytes. Solid particles, once in the sub-mucosal tissue, are able to enter both the lymphatic and blood circulation.

In an early study Jani *et al.*⁸⁸ administered rutile TiO₂ (500 nm) as a 0.1 ml of 2.5 % w/v suspension (12.5 mg/kg BW) to female Sprague Dawley rats, by oral gavage daily for 10 days and detected presence of particles in all the major gut associated lymphoid tissue as well as in distant organs such as the liver, spleen, lung and peritoneal tissue, but not in heart and kidney. The distribution and toxicity of nano- (25 nm, 80 nm) and submicron-sized (155 nm) TiO₂ particles were evaluated in mice administered a large, single, oral dosing (5 g/kg BW) by gavage.⁸⁹ In the animals that were sacrificed two weeks later, ICP-MS analysis showed that the particles were retained mainly in liver, spleen, kidney, and lung tissues, indicating that they can be transported to other tissues and organs after uptake by the gastrointestinal tract. Interestingly, although an extremely high dose was administered, no acute toxicity was observed. In groups exposed to 80 nm and 155 nm particles, histopathological changes were observed in the liver, kidney and in the brain. The biochemical serum parameters also indicated liver, kidney and cardiovascular damage and were higher in mice treated with nano-sized (25 or 80 nm) TiO₂ compared to submicron-sized (155 nm) TiO₂. However, the main weaknesses of this study are the use of extremely high single dose and insufficient characterisation of the particles.

Duan *et al.*⁹⁰ administered 125 mg/kg BW or 250 mg/kg BW of anatase TiO₂ (5 nm) intragastrically to mice continuously for 30 days. The exposed mice lost body weight, whereas the relative liver, kidney, spleen and thymus weights increased. Particles seriously affected the haemostasis of the blood and the immune system. The decrease in the immune response could be the result of damage to

the spleen, which is the largest immune organ in animals and plays an important role in the immune response. Powel *et al.*⁹¹ demonstrated that TiO₂ NPs may trigger immune reactions of the intestine after oral intake. They showed that TiO₂ NPs conjugated with bacterial lipopolysaccharide, but not TiO₂ NPs or lipopolysaccharide alone, trigger the immune response in human peripheral blood mononuclear cells and in isolated intestinal tissue. This indicates that TiO₂ NPs may be important mediators in overcoming normal gut-cell hyporesponsiveness to endogenous luminal molecules, which may be particularly relevant to patients with inflammatory bowel disease, which is characterized by an abnormal intestinal permeability.

The National Cancer Institute tested TiO₂ for possible carcinogenicity by the oral route of exposure by feeding rats and mice with TiO₂ (size not specified) at doses 25,000 or 50,000 ppm TiO₂ for 103 weeks. They concluded that TiO₂ was not carcinogenic.⁹² Also, the study with rats fed diets containing up to 5 % TiO₂ coated mica for 130 weeks showed no treatment-related carcinogenicity.⁹³ Since the size and other TiO₂ properties were not specified or determined, we cannot generalize this conclusion and we have to take into account other possible outcomes of this scenario in different exposure conditions (other size/crystalline structure of TiO₂ etc.).

It should also be considered that due to the low pH in the stomach, the increased dissolution of the TiO₂ particles may increase its bioavailability and may facilitate the entry of titanium ions into the blood circulation.⁹⁴ Despite the relatively large consumption of TiO₂ as a food additive, no studies on the effect of pH on its absorption and bioavailability have been found in the literature. This can be attributed to a general belief that TiO₂ is completely insoluble. However, this is not completely true, as TiO₂ particles show a certain degree of solubility.³³

Exposure to TiO₂ NPs by inhalation

Inhalation exposure to TiO₂ particles occurs predominantly in occupational settings during production of TiO₂ powders and manufacturing the products containing TiO₂.⁹⁵ The highest levels of exposure occur during packing, milling and site cleaning however, the empirical data regarding airborne TiO₂ particle concentrations in occupational settings is very limited. Fryzek *et al.*⁹⁶ reported that packers, micronizers and addbacks had the highest TiO₂ exposure levels measuring 6.2±9.4 mg/m³, whereas ore handlers had lower TiO₂ exposure lev-

el of 1.1 ± 1.1 mg/m³. Boffetta *et al.*⁹⁷ reported that the yearly averaged estimated exposure to TiO₂ dust in EU factories varied from 0.1 to 1.0 mg/m³, and the average levels ranged up to 5 mg/m³ for individual job categories. However, in these studies the particle size distribution has not been determined. Nevertheless, the data indicate that in certain jobs categories the exposure exceed the values of time-weighted average (10 h TWA) concentrations of 2.4 mg/m³ for submicron-sized TiO₂ and 0.3 mg/m³ for nano-sized TiO₂, which are recommended as exposure limits by National Institute for Occupational Safety and Health (NIOSH).⁹⁸

Potential hazards of inhalation exposure to TiO₂ NPs

The lung consists of about 2300 km of airways and 300 million alveoli. The epithelium of airways is protected by a viscous layer of mucus, and is a relatively robust barrier. In alveoli, the barrier between the alveolar wall and the capillaries is very thin, about 0.5 μm. Thus, the large surface area of the alveoli and the intense air-blood contact in this region makes the alveoli less protected against environmental damage than other parts of the respiratory system.⁷⁵ The clearance of particles from the upper airways is achieved through the mucociliary escalator, while clearance from the deep lung is supposed to be achieved predominantly by macrophage phagocytosis. Deposited particles can lead to the activation of cytokine production and inflammation by macrophages and epithelial cells. It has been reported that besides the pulmonary and systemic inflammation, inhaled insoluble NPs can also accelerate atherosclerosis and alter the cardiac autonomic function.⁹⁹⁻¹⁰²

Following administration of nano-sized TiO₂ to rats by inhalation the particles were detected in the cytoplasm of all lung-cell types in a non-membrane bound manner.¹⁷ Ferin *et al.*¹⁰³ reported that 20 nm-sized TiO₂ particles penetrate more easily into the pulmonary interstitial space of rats than 250 nm-sized TiO₂ particles. Three-month inhalation exposure in rats demonstrated that the clearance of 20 nm TiO₂ particles was significantly slower than that of 200 nm TiO₂ particles, and more particles translocated to interstitial sites and regional lymph nodes.¹⁰⁴ Geiser *et al.*¹⁴ confirmed that alveolar macrophages were not primarily responsible for the uptake and clearance of TiO₂ NPs. These findings are in agreement with the known size limitations of uptake processes such as phagocytosis, which is thought to be restricted to particles that are 1 to

5 μm in size, while NPs might escape macrophage phagocytosis.^{101,105}

Inhaled TiO₂ NPs can enter the alveoli of the lung and consequently the blood circulation^{106,107} and can then translocate to other organs.^{102,108,109} In addition to several reports on the absence of toxicity following the inhalation of TiO₂ NPs in rodents, the majority of lung-inhalation and instillation studies have pointed out obvious toxic effects, like inflammation and damage to pulmonary epithelium.¹¹⁰ The studies also showed that TiO₂ NPs induced greater pulmonary inflammation and tissue damage than an equal dose of submicron-sized TiO₂ particles. The greater toxicity of TiO₂ NPs has been explained as being related to their larger surface area and their increased internalization.¹¹¹ Multiple studies showed the reversibility of the inflammatory response after cessation of the exposure to TiO₂ particles. After a single instillation exposure to different types of submicron- and nano-sized TiO₂, acute inflammatory response returned to control levels within one week¹¹² or 90 days¹¹³ after the instillation. In mice that were exposed to TiO₂ NPs (2-5 nm) by whole body inhalation (0.77 or 7.22 mg/m³ 4 h/day 10 days) the recovery was observed during the third week after exposure.¹¹⁴

Pulmonary toxicity studies suggest that, besides the particle size and surface area, crystal structure and surface treatment are also important parameters. Warheit *et al.*¹¹⁵ demonstrated higher pulmonary toxicity of anatase than rutile TiO₂ NPs. These observations were confirmed in a recent study by Roursgaard *et al.*¹¹⁶ who showed that the intratracheal instillation of submicron- and nano-sized rutile, nano-sized anatase, or amorphous TiO₂ to mice induced a dose-dependent acute inflammation, while subchronic inflammation was apparent only in mice exposed to nano-sized rutile and amorphous TiO₂.

Recently, toxicogenomic studies were published that may contribute to a better understanding of the mechanisms of TiO₂-mediated pulmonary toxicity. In mice exposed to a single intratracheal dose (0.1 or 0.5 mg/kg BW) of TiO₂ with an average particle size of 20 nm Chen *et al.*¹¹⁷ showed that changes in the morphology and histology of the lungs were associated with the differential expression of hundreds of genes, including those involved in cell cycle regulation, apoptosis, chemokines, and complement cascades. In particular, TiO₂ NPs upregulated the expression of the placenta growth factor and other chemokines that are associated with pulmonary emphysema and alveolar epithelial cell apoptosis. Park *et al.*¹¹⁸ showed that exposure of mice

to nano-sized TiO₂ (5-50 mg /kg BW) by a single intratracheal instillation can, in addition to chronic inflammation, also trigger an autoimmune response. They found that many classes of genes related to antigen presentation and the induction of chemotaxis of immune cells were over-expressed.

The studies have shown that submicron-sized TiO₂¹¹⁹ and nano-sized TiO₂^{120,121} induce lung tumors in chronically exposed rats. TiO₂ NPs induced a significantly increased number of lung tumors during inhalation exposure to 10 mg/m³ (18 h/day, 2 years), while submicron-sized TiO₂ increased the number of lung tumors at exposure to 250 mg/m³ (6 h/day 2 years). In contrast, no tumours were observed in similarly exposed mice and hamsters.^{121,122} These apparent species differences suggest that the experimentally induced lung tumours may be a rat-specific, threshold phenomenon, depending on lung overloading accompanied by chronic inflammation to exert the observed tumorigenic response. Comparative toxicological studies of the development and possible progression of the lung response in rats, mice and hamsters exposed to a range of concentrations of submicron- or nano-sized TiO₂ over a period of 90 days showed distinct species differences in the lung responses. Rats and mice had similar lung burdens and clearance rates, while hamsters showed higher clearance rates. At high lung-particle burdens, rats showed a marked progression of the histopathological lesions during the post-exposure period, while mice and hamsters showed minimal initial lesions with apparent recovery during the post-exposure period.^{123,124} It has been thus argued that the dose response data from inhalation studies in rats should not be used when extrapolating the cancer risk to humans.⁹⁵ However, clearance of insoluble particles is in humans slower than in rats.¹²⁵ In addition, it has been shown that the lung-tumour response to exposure to non-soluble particles can be predicted by the particle surface area dose without the need to account for overloading.⁹⁸ Therefore, for workers with a high dust exposure the doses that cause overloading in rats may be relevant for estimating the health risk for humans.

Animal studies showed also other adverse effects after inhalation exposure to TiO₂ particles. Nurkiewicz *et al.*¹⁰⁹ showed that exposure to TiO₂ particles may cause cardiovascular effects at concentrations below those causing adverse pulmonary effects. In rats exposed to submicron-sized TiO₂ (<1 µm) or nano-sized TiO₂ (21 nm) at airborne exposures aimed at achieving similar particle mass deposition in the lungs (nano-sized: 1.5–12 mg/m³,

240–720 min; submicron-sized: 3–15 mg/m³, 240–480 min) they observed systemic microvessel dysfunction in the absence of pulmonary inflammation or lung damage. The effect was related to the adherence of polymorphonuclear leukocytes to the microvessel walls and the production of ROS in the microvessels. As already described previously, inhalation exposure to TiO₂ NPs may cause immune responses and neurotoxic effects that may lead to respiratory allergy and higher risk of developing asthma, respectively.

It has been reported that TiO₂ NPs can translocate to the central nervous system following nasal instillation, potentially via the olfactory bulb, and accumulate mainly within the cerebral cortex, thalamus and hippocampus.^{22,29,126} The absorption appears to occur via neuronal transport, bypassing the blood-brain barrier.^{29,126} The main target is the hippocampus, where TiO₂ NPs caused morphological alteration and the loss of neurones. In addition, TiO₂ induced oxidative stress and an inflammatory response within the whole brain, with anatase nano-TiO₂ inducing a stronger inflammatory response than rutile. However, from these studies it is not clear to what extent large local doses during nasal instillation reflect inhalation exposure.

Human epidemiological studies

Several case reports described adverse health effects in workers with potential TiO₂ exposure that later lead to epidemiological studies of a relationship between occupational exposure and observed cases.⁹⁸ The lung particle analyses indicated that workers exposed to respirable TiO₂ had particle retention in their lungs that included TiO₂, silica, and other minerals, sometimes years after cessation of exposure. In most cases of tissue-deposited TiO₂ was associated with a local macrophage response and fibrosis that was generally mild. In one case papillary adenocarcinoma and TiO₂ associated pneumoconiosis was reported in the lung of a 53-year-old male who had been engaged in packing TiO₂ for about 13 years and had 40-year smoking history.¹²⁷ The cohort epidemiological studies undertaken in the USA^{96,128} did not report excess risks of lung cancer; nor did a Canadian population-based case-control study.¹²⁹ The retrospective cohort lung cancer mortality study¹³⁰, which included workers in the TiO₂ production industry in six European countries, showed a small but significant elevation in lung cancer mortality among male TiO₂ workers when compared to the general

population. However, the data did not suggest an exposure-response relation.

TiO₂ has been classified by the International Agency for Research on Cancer (IARC) as an IARC Group 2B carcinogen, "possibly carcinogenic to humans" by inhalation.¹³¹ Although the IARC working group concluded that the epidemiological studies on TiO₂ provide inadequate evidence of carcinogenicity, they considered that the results from animal studies of inhalation and intratracheal instillation provide sufficient evidence to classify TiO₂ in Group 2B.¹³² Also NIOSH⁹⁸ has recently classified TiO₂ NPs as a potential occupational carcinogen but considered that there is insufficient evidence at this time to classify also submicron-sized TiO₂ as a potential occupational carcinogen. NIOSH also recommended new exposure limits at 2.4 mg/m³ for submicron-sized TiO₂ and 0.3 mg/m³ for nano-sized TiO₂, as time-weighted average concentrations for up to 10 hours per day during a 40-hour work week.

Exposure to TiO₂ NPs through body implants

A few-nanometres-thick layer of amorphous TiO₂ is commonly formed on the surface of orthopaedic and dental implants made of titanium metal or its alloys. In non-moving implants (hip stems, plates, screws, etc.) this does not appear to represent the same kind of risk for the body as free TiO₂ NPs discussed in previous sections. However, this is not the case for wear-exposed implants, such as hip and knee joints. There are many reports proving that under mechanical stress or altered physiological conditions, Ti-based implants can release biologically relevant amounts of debris, in both the micrometre and nanometre ranges, that can migrate to the surrounding tissues. During the wear process, a thin amorphous oxide layer is continuously being created and removed, resulting in large numbers of titanium particles. It is increasingly being suggested that they are associated with major inflammation and systemic diseases.¹³³ Furthermore, increasing numbers of reports indicate that the delayed hypersensitivity to titanium and its oxides may constitute a health risk for individuals with higher susceptibility.¹³⁴⁻¹³⁶

The effects of the TiO₂ particles released from implants were investigated by Wang *et al.*¹³⁷ in rats by intra-articular injection of 0.2 to 20 mg of anatase nano-TiO₂ per kg BW. Their results demonstrate that particles can potentially affect major organs like the heart, lung and liver.

Generally, the maximum diameter of particles that move across the synovial capillary wall was suggested to be 50 nm. The released TiO₂ NPs resulted in synovial hypotrophy, lymphocyte and plasma infiltration, and fibroblast proliferation in the knee joint. Oxidative stress and lipid peroxidation was detected in exposed synovial fluid. Seven days after the initial exposure a brown particulate deposit was observed in vascular endothelial cells and in alveolar macrophages. Similar results have been reported by Urban *et al.*¹³⁸, who found TiO₂ particles in the liver and in the spleen of the patients with implants. TiO₂ NPs were observed in joint simulators and in joint periprosthetic tissues. Margevicius *et al.*¹³⁹ characterized the debris around the total hip joint prosthesis and found up to 140.10⁹ particles/g dry weight, in diameters ranging from 0.58 to 100 µm. Agins *et al.*¹⁴⁰ found concentration of wear particles in the tissue adjacent to a prosthesis in the range between 56 µg/g and 3.7 mg/g dry weight. Thus, due to the natural tendency of titanium to oxidise, Ti-based implants should not be neglected as a possible source of TiO₂ exposure.

On the other hand, the man-made (crystalline) TiO₂ coatings on the surfaces of pure Ti or Ti alloys are reported to be able to modulate protein absorption, cell adhesion, osseointegration and bone mineralization at the bone-biomaterial interface, both *in vivo* and *in vitro*.^{141,142} For this reason, the development of a more stable crystalline titania coating on Ti-based implants is in progress.¹⁴³

Environmental pollution by TiO₂ NPs

Toxic effects of TiO₂ NPs on aquatic organisms

The trend in the production of NPs is likely to lead to increasing amounts of nano-powders in the air, water and soil, which will consequently affect living organisms. Labielle *et al.*⁶⁸ demonstrated that 25 % of Al(OH)₃-coated TiO₂ particles from sunscreens are dispersed as a stable colloid and become available to microorganisms and filter-feeders, while the remaining 75 % are probably incorporated into geogenic sediments, where they could become available to benthic fauna. Solar UV irradiation may penetrate as far as 20 m in the water column¹⁴⁴ and therefore photo-activate the dispersed particles, which may have an adverse effect on various aquatic organisms.

Freshwater algae show low-to-moderate susceptibility to TiO₂ exposure, with more pronounced

toxic effects in the presence of UV irradiation. It has also been shown that nano-sized TiO₂ is significantly more toxic to algae *Pseudokirchneriella subcapitata* than submicron-sized TiO₂.¹⁴⁵ Hund-Rinke and Simon¹⁴⁶ reported that UV irradiated 25 nm TiO₂ NPs are more toxic to green freshwater algae *Desmodesmus subspicatus* than UV irradiated 50 nm particles, which is in agreement with Hartmann et al.¹⁴⁷ UV irradiated TiO₂ NPs also inactivated other algae species such as *Anabaena*, *Microcystis*, *Melsoira*¹⁴⁸ and *Chroococcus*.¹⁴⁹ It was demonstrated that smaller particles have a greater potential to penetrate the cell interior than submicron-sized particles and larger aggregates. Studies have shown that the amount of TiO₂ adsorbed on algal cells can be up to 2.3 times their own weight.¹⁴²

Nano-sized TiO₂ generally shows low or no acute toxicity in both invertebrates¹⁴⁶ and vertebrates.¹⁵⁰ However, exposure of *Daphnia magna* to 20 ppm TiO₂ for 8 consecutive days was found to cause 40 % mortality.¹⁵¹ Zhu et al.¹⁵² showed minimal toxicity to *D. magna* after 48 h exposure, while upon chronic exposure for 21 days, *D. magna* suffered severe growth retardation and mortality. A significant amount of nano-sized TiO₂ was found also accumulated in the body of the animals. Similar findings with coated nano-sized TiO₂ (T-Lite™ SF, T-Lite™ SF-S and T-Lite™ MAX; BASF SE) were reported by Wiench et al.¹⁵³ Biochemical measurements showed that exposure to TiO₂ NPs induces significant concentration-dependent antioxidant enzyme activities in *D. magna*.¹⁵⁴ Lee et al.¹⁵⁵ showed that 7 and 20 nm-sized TiO₂ induced no genotoxic effect in *D. magna* and in the larva of the aquatic midge *Chironomus riparius*.

No acute effects of nano-sized TiO₂ were observed in *Danio rerio* (zebrafish) embryos.¹⁵⁶ Exposure of rainbow trout to TiO₂ NPs triggered lipid peroxidation, influence on the respiratory tract, disturbance in the metabolism of Cu and Zn, induction of intestinal erosion¹⁵⁷ and accumulation in kidney tissue.¹⁵⁸ Linhua et al.¹⁵⁹ exposed juvenile carp to 100 and 200 mg/ml of TiO₂ particles and observed no mortality. However, the fish suffered from oxidative stress and pathological changes in gill and liver. In the infaunal species *Arenicola marina*, exposure to TiO₂ NPs in sediment caused sub-lethal effects including decrease in casting rate and increase in cellular and DNA damage.¹⁶⁰ Aggregated particles were visible in the lumen of the gut, but no uptake through the gut or the skin was observed.

Zhu et al.¹⁶¹ were the first to provide evidence that TiO₂ NPs (21 nm) can transfer from daphnia to

zebrafish by dietary exposure. Hence, dietary intake could be a major route of exposure to NPs for high trophic level aquatic organisms. Ecological research should therefore focus, not only on the concentration of NPs in the environment, but also on its bioconcentration, bioaccumulation and biomagnification. In addition it has been shown that TiO₂ NPs can increase accumulation of other environmental toxicants: enhanced accumulation of cadmium (Cd) and arsenic (As) was found in carp in the presence of TiO₂ NPs.^{162,163} The strong adsorption capacity for Cd and As was explained by the large specific surface area and strong electrostatic attraction of TiO₂ NPs that contribute to facilitated transport into different organs.

In vitro, in the hemocytes of the marine mussel *Mytilus hemocytes*, suspension of TiO₂ NPs (Degussa P25, 10 µg/ml) stimulated immune and inflammatory responses, such as lysozyme release, oxidative burst and nitric oxide production.¹⁶⁴ Vevers and Jha¹⁶⁵ demonstrated the intrinsic genotoxic and cytotoxic potential of TiO₂ NPs on a fish-cell line derived from rainbow-trout gonadal tissue (RTG-2 cells) after 24 h of exposure to 50 µg/ml. Reeves et al.¹⁶⁶ demonstrated a significant increase in the level of oxidative DNA damage in goldfish cells, and suggested that damage could not be repaired by DNA repair mechanisms. Another suggestion from the mentioned study was that hydroxyl radicals are generated also in the absence of UV light. It has been shown that fish cells are generally more susceptible to toxic/oxidative injury than mammalian cells.

Toxic effects of TiO₂ NPs on soil organisms

Drobne et al.¹⁶⁷ used the terrestrial arthropod *Porcellio scaber* as a test organism for determining the cytotoxic effect of TiO₂ NPs (anatase). The animals were exposed to TiO₂ NPs of two different sizes (25 nm and 75 nm) in the concentration range 10-1000 µg TiO₂/g dry food for 3 to 14 days. No adverse effects, such as mortality, body weight changes or reduced feeding, were observed. In fact, quite the opposite, an enhanced feeding rate, food absorption efficiency and increase in catalase activity were observed. The intensity of these responses appeared to be time- but not dose-dependent. It should also be noted that the concentrations tested in this study were much higher than the predicted concentration (4.8 µg/g soil) at high emission scenario of nano-sized TiO₂.¹⁶⁸ Using the same test organism another group¹⁶⁹ showed that exposure to

TiO₂ NPs induced destabilization of cell membrane in the epithelium of digestive glands isolated from exposed animals. They also showed that this effect can be observed after just 30 minutes of exposure.

TiO₂ NPs appeared to be more toxic to nematode *Caenorhabditis elegans* than submicron-sized TiO₂.¹⁷⁰ At a concentration of 1 mg/l, 7 nm particles affected its fertility and survival rate and were more toxic than 20 nm anatase particles.¹⁷¹ Similarly, Hu *et al.*¹⁷² showed that rutile particles (10-20 nm), at concentrations above 1 g/kg soil, can be bio-accumulated in earthworms, where they induce oxidative stress, inhibit the activity of cellulase and induce DNA and mitochondrial damage.

The effects of TiO₂ NPs in plants

In addition to the toxic effects of TiO₂ NPs, discussed in previous chapters, these NPs have been also shown to promote photosynthesis and nitrogen metabolism, resulting in the enhanced growth of spinach.¹⁷³⁻¹⁷⁵ It increases the absorption of light and accelerates the transfer and transformation of the light energy.¹⁷⁶ It was also found that treatment with nano-sized TiO₂ significantly increased the level of antioxidant enzymes, and decreased the ROS accumulation and malonyldialdehyde content in spinach chloroplasts under visible and UV irradiation.¹⁷⁷ TiO₂ NPs also increased the superoxide dismutase activity of germinating soybean, enhanced its antioxidant ability, and promoted seed germination and seedling growth.¹⁷⁸

Potential desirable effects of TiO₂ NPs

The same properties of nano-sized TiO₂ that are associated with undesirable, harmful effects can be exploited for certain useful applications. The antimicrobial effect of photo-activated TiO₂ NPs has been known since 1985¹⁷⁹ and since then numerous reports have described its potential antimicrobial activity against numerous microorganisms.¹⁸⁰ As expected, the antimicrobial effect increases with smaller particle sizes¹⁸¹; however, powder agglomeration may obscure this effect.¹⁵¹ When submitted to UV-C irradiation, TiO₂ depresses the photo-activation and dark repair of DNA in bacteria, which increases the bactericidal efficiency of UV-C irradiation.¹⁸²

TiO₂ NPs have potential application in removing or minimizing the effect of the red tides¹⁸³ that are associated with the harmful algae *K.brevis* that

produces neurotoxic brevetoxin (PbTx). Further, it can be used for disinfecting water, air and surfaces, with possible applications of TiO₂ in form of solid films or free particles. Given its use for eradicating toxins, pollutants and spores from water and air, it can be classified as a broad-spectrum oxidizing/cleaning substance. However, an informed balance between the benefits of such a cleaning system and its potential adverse effects needs to be maintained.

NPs are offering new possibilities for in medicine either for diagnostic or therapeutic purposes. For instance recent studies indicate that magnetic NPs may be used in cancer treatment for targeted drug delivery.¹⁸⁴ Several recent studies indicated that also cultured cancer cells are more sensitive to TiO₂ NPs than normal cells. Photo-activated TiO₂ exhibited selective cytotoxicity against highly malignant breast-cancer cells MDA-MB-468, in comparison with non-malignant MCF-7 cells.¹⁸⁵ Similarly, UV-irradiated Degussa P25 TiO₂ NPs reduced viability of sarcoma cells but were not toxic to cultured fibroblasts MCR-5.¹⁸⁶ In addition, UV-C photo-activated TiO₂ particles inhibited aggregation of sarcoma cells with human platelets, thus preventing the formation of metastases. Cai *et al.*¹⁸⁷ found that photo-activated (50 µg/ml), but not non-irradiated nano-sized TiO₂, was lethal for HeLa cells *in vitro* and suppressed the growth of HeLa tumours in nude mice. Photo-activated TiO₂ also showed antitumour activity *in vivo* against murine skin tumours.¹⁸⁸ The potential usefulness of nano-sized TiO₂ in cancer cell therapy has also been reported by other research groups.¹⁸⁹⁻¹⁹² Cytotoxicity against different cancer cell lines appears to depend on the cell type, the particle concentration and the surface chemistry.

The appearance of multidrug-resistant tumour cells is a major obstacle to the success of chemotherapy. Song *et al.*¹⁹³ reported an enhanced effect of nano-sized TiO₂ on drug uptake by drug-resistant leukaemia cells under UV irradiation. Very promising is also the finding that cancer cells can be effectively destroyed by the use of X-ray irradiated nano-sized TiO₂.¹⁹⁴ A combination of monoclonal antibody conjugated nano-sized TiO₂ with photoinduction¹⁹⁵ and electroporation¹⁹⁶ have also been proposed for selective cancer treatment. The monoclonal antibodies would enable selective targeting of cancer cells, photoinduction would trigger local generation of radicals and electroporation would accelerate the delivery of nano-sized TiO₂ into the cancer cells. A novel possibility of cancer treatment was recently suggested¹⁹⁷, in which TiO₂

NPs and folic acid were coupled and shown to be internalized by HeLa cells via the folate receptor.

Where we are and where to go

The mechanistic toxicological studies showed that TiO₂ NPs induced adverse effects are predominantly mediated by oxidative stress, which may lead to cell damage, genotoxic effects, inflammatory responses and changes in cell signalling. The studies also showed that these effects strongly depend on numerous chemical and physical characteristics of the TiO₂ particles: size, crystal structure, specific surface area, particle shape, purity, surface charge, solubility, agglomeration rate, photo-activation, etc. TiO₂ particles are without doubt associated with the hazardous properties, and the risk for human health and environment depends on the route and extent of exposure.

Based on the widespread use of creams with SPF based on nano-sized TiO₂, human exposure to TiO₂ NPs by dermal applications is apparently enormous. *In vitro* studies with skin models showed that TiO₂ NPs are taken up by keratinocytes, fibroblasts, and melanocytes, in which they cause toxic effects that are not different from the effects observed in other cell types. Current experimental evidence indicates that TiO₂ NPs do not penetrate through healthy skin and thus do not reach viable skin cells and distribute to other organs and tissues. However, the data on TiO₂ NPs skin penetration during long-term or repeated exposure and in the presence of UV, which is actually characteristic for real life exposure, are insufficient. Therefore, there is no simple answer to the question regarding safety of the use of TiO₂ NPs in sunscreens. The safety of the use of TiO₂ in cosmetics is often argued by the claim, that it has been used for decades without observing any adverse effects on human health. This, however, is not completely true, as no monitoring and post market health surveillance has been conducted, neither for submicron-sized nor for nano-sized TiO₂ in sunscreens. Such surveillance is currently impossible, since current legislation does not require labelling whether the products contain nano-sized TiO₂, which is also incorrect to customers who have no possibility to make a choice whether to use or not the sunscreen containing nano-sized TiO₂. In our opinion dermal applications of TiO₂ NPs as sunscreen should be limited until appropriate long-term experimental studies confirm their harmlessness. It is undeniable that long-term sun exposure can induce skin

cancer. It is questionable, however, whether people are, by using sunscreens, actually encouraged to expose themselves to the sun instead of avoiding it, and if the benefit provided by TiO₂ as a protection from UV compensates for the potential harm.

The available data on absorption, distribution, elimination or any consequent adverse effects after oral exposure to specific TiO₂ NPs are extremely limited. TiO₂ NPs have been shown to be absorbed from gastrointestinal tract and distributed to other organs, however this was observed at extremely high, for human exposure, irrelevant doses. On the other hand, it has been shown that at lower concentrations TiO₂ may induce different adverse effects. TiO₂ is an approved food additive with the limit set at 1 % by weight of the food; however, neither the size nor the structure is defined. It has been estimated that the average daily exposure to TiO₂ from food, medicines and toothpaste is around 5 mg/individual (*i.e.*, about 0.07 mg/kg BW)¹⁹⁸, which is a much lower dose than those that showed adverse effects in experimental animals. Currently there is no data if, and what proportion of TiO₂ NPs is absorbed at doses relevant for human exposure, and how different food matrices affect behaviour and absorption of TiO₂ NPs. However, even if very small portion of consumed nano-sized TiO₂ is absorbed from gastrointestinal tract and distributed to distant organs, this brings into question accumulation of TiO₂ NPs that may, through a constant lifetime oral exposure, reach concentrations that would trigger adverse effects. Another important question, which should not be neglected is, whether low exposure may trigger symptoms in subjects with an underlying susceptibility. Before *in vivo* toxicokinetic data for nano-sized TiO₂ are available, no conclusion about the risk of nano-sized TiO₂ by oral exposure is possible. Therefore, it should be seriously reconsidered if the use of TiO₂ NPs in nutrition and pharmacy just to shade or stabilise the products is justified at all.

Inhalation seems to be the most vulnerable entrance point of the TiO₂ NPs and the toxic effects of inhalation exposure are therefore by far the most studied. Animal studies showed that on inhalation exposure the particles deposit in the lung, where they may cause chronic inflammation and lung-tissue damage, which can lead to lung-tumour development. The important finding is that inhalation exposure to nano-sized TiO₂ represents a higher health risk than exposure to submicron-sized TiO₂ particles. Experimental data indicate that on inhalation exposure nano-sized TiO₂ may translocate to distant organs and tissues, which may be associ-

ated with systemic effects, such as allergy, asthma and cardiovascular effects, however further studies are needed to confirm these observations and to clarify if they are associated with increased risk for humans. In the scientific community there is still a debate whether the data from *in vivo* rodent toxicity studies are reliable enough to predict the effects in humans in particular regarding mode of exposure (instillation vs. inhalation exposure) and the differences in susceptibility between different experimental species. Nevertheless, the experimental evidence, although not clearly supported by human epidemiological data, was considered to be sufficient to classify TiO₂ (unrespectable to particle size and form) as “possible human carcinogen” upon inhalation exposure by IARC. Recently also NIOSH classified nano-sized, but not submicron-sized TiO₂ as occupational carcinogen, and accordingly established different limit values for occupational inhalation exposure for nano-sized (0.3 mg/m³) and submicron-sized (2.4 mg/m³) TiO₂. At present, through environmental air pollution general population is probably not at risk. However, occupational exposure should be controlled and protective measures applied, not only in TiO₂ production industries, but also in certain areas of TiO₂ applications; for instance when removing paints or destroying TiO₂ containing materials the workers may be exposed to high concentrations of TiO₂. Thus, accurate, portable, and cost effective measurement techniques should be developed and applied for effective exposure control and protection.

TiO₂ can also be released within the human body as a result of the wear of Ti-based implants. The released particles cause local inflammation, but even more importantly they distribute over the body and can potentially cause systemic effects. Generally the benefit provided by the implant compensates for the potential harm, in particular in the cases where there is no better alternative to the Ti-based implants available. However, although there is no direct experimental evidence that released TiO₂ can be deposited in the body or can cause systemic effects, it can be postulated from other exposure studies and mechanistic data that at least for individuals with hypersensitivity to titanium such exposure may represent a permanent health threat. Thus, it should be obligatory to test the patients for titanium hypersensitivity prior to implantation of titanium based implants.

Due to the widespread use TiO₂ can enter aquatic and terrestrial environment and potentially affect the indigenous organisms. Although data from

acute ecotoxicity tests in crustaceans, fish and algae indicate a low toxic potential of TiO₂ NPs for aquatic species, when chronic exposure was applied TiO₂ NPs induced a range of sub-lethal adverse effects. In addition it has been shown that nano-sized TiO₂ can enter the freshwater food chain, which means that it can be transferred from lower to higher trophic organisms, including humans.

Taken together, the overall exposure of an average individual TiO₂ NPs is not known; there are still opened questions regarding toxicokinetics and specific organ toxicity of TiO₂ NPs, in particular at oral and dermal exposure, and thus it is impossible to make a reliable quantitative risk assessment. One of the main observations of this review is that, due to the versatility of the TiO₂ NPs in terms of particle size, shape, crystal structure, dispersion in biological surroundings (bioavailability) and UV-induced photocatalytic activity, no single conclusion can be drawn, since different forms of TiO₂ may act very differently. Until we know more, in our opinion TiO₂ NPs should be used with great care, in particular in food and cosmetics. The least that should be done for the consumer is that a declaration of nano-sized TiO₂ in these products is obligatory, so that we will have the choice whether to use it or not.

Acknowledgement

The study was supported financially by the Slovenian Research Agency within the research programmes “Nanostructured Materials” (P2-0084) and “Ecotoxicology, Toxicological Genomics and Carcinogenesis (P1-0245). We thank Prof. Roger Pain and Assist. Prof. Paul McGuinness for critical reading of the manuscript. Authors would also like to thank Dr. Zoran Samardžija for field-emission-gun scanning electron microscopy observations of the TiO₂ powders.

References

1. Ophus EM, Rode L, Gylseth B, Nicholson DG, Saeed K. Analysis of titanium pigments in human lung tissue. *Scand J Work Environ Health* 1979; **53**: 290-6.
2. Lindenschmidt RC, Driscoll KE, Perkins MA, Higgins JM, Maurer JK, Belfiore KA. The comparison of a fibrogenic and two nonfibrogenic dusts by bronchoalveolar lavage. *Toxicol Appl Pharmacol* 1990; **102**: 268-81.
3. Backus R. Lighting up time for TiO₂. *Industrial Minerals* 2007; **473**: 28-39.
4. Robichaud CO, Uyar AE, Darby MR, Zucker LG, Wiesner MR. Estimates of upper bounds and trends in nano-TiO₂ production as a basis for exposure assessment. *Environ Sci Technol* 2009; **43**: 4227-33.

5. Rowe RC, Sheskey PJ, Weller PJ. Handbook of pharmaceutical excipients. Fourth ed. London: Pharmaceutical Press, London, United Kingdom, and the American Pharmaceutical Association; 2003.
6. Klaine SJ, Alvarez PJ, Batley GE, Fernandes TF, Handy RD, Lyon DY, et al. Nanomaterials in the environment: behaviour, fate, bioavailability, and effects. *Environ Toxicol Chem* 2008; **27**: 1825-51.
7. Auffan M, Rose J, Bottero JY, Lowry GV, Jolivet JP, Wiesner MR. Towards a definition of inorganic nanoparticles from an environmental, health and safety perspective. *Nat Nanotechnol* 2009; **4**: 634-41.
8. Kosmulski M. The pH-dependent surface charging and points of zero charge V. Update. *J Colloid Interface Sci* 2011; **353**: 1-15.
9. Tang H, Prasad K, Sanjinbs R, Schmid P E, Levy F. Electrical and optical properties of TiO₂ anatase thin films. *J Appl Phys* 2004; **75**: 2042-7.
10. Augustynski J. The role of the surface intermediates in the photoelectrochemical behaviour of anatase and rutile TiO₂. *Electrochimica Acta* 1993; **38**: 43-6.
11. Hewitt JP. Titanium dioxide: a different kind of sunshield. *Drug Cosmet Ind* 1992; **151**: 26-32.
12. Fujishima A, Zhang X, Tryk DA. TiO₂ photocatalysis and related surface phenomena. *Surf Sci Rep* 2008; **63**: 515-82.
13. Xia T, Kovochich M, Brant J, Hotze M, Sempf J, Oberley T, et al. Comparison of the abilities of ambient and manufactured nanoparticles to induce cellular toxicity according to an oxidative stress paradigm. *Nano Lett* 2006; **68**: 1794-807.
14. Geiser M, Casaulta M, Kupferschmid B, Schulz H, Semmler-Behnke M, Kreyling W. The role of macrophages in the clearance of inhaled ultrafine titanium dioxide particles. *Am J Respir Cell Mol Biol* 2008; **38**: 371-6.
15. Aderem A, Underhill DM. Mechanisms of phagocytosis in macrophages. *Annu Rev Immunol* 1999; **17**: 593-623.
16. Stearns RC, Paulauskis JD, Godleski JJ. Endocytosis of ultrafine particles by A549 cells. *Am J Respir Cell Mol Biol* 2001; **24**: 108-15.
17. Geiser M, Rothen-Rutishauser B, Kapp N, Schurch S, Kreyling W, Schulz H, et al. Ultrafine particles cross cellular membranes by nonphagocytic mechanisms in lungs and in cultured cells. *Environ Health Perspect* 2005; **113**: 1555-60.
18. Rothen-Rutishauser BM, Schurch S, Haenni B, Kapp N, Gehr P. Interaction of fine particles and nanoparticles with red blood cells visualized with advanced microscopic techniques. *Environ Sci Technol* 2006; **40**: 4353-9.
19. Kocbek P, Teskac K, Kreft ME, Kristl J. Toxicological aspects of long-term treatment of keratinocytes with ZnO and TiO₂ nanoparticles. *Small* 2010; **6**: 1908-17.
20. Xia T, Kovochich M, Liong M, Madler L, Gilbert B, Shi HB, et al. Comparison of the mechanism of toxicity of zinc oxide and cerium oxide nanoparticles based on dissolution and oxidative stress properties. *ACS Nano* 2008; **2**: 2121-34.
21. Donaldson K, Stone V, Clouter A, Renwick L, MacNee W. Ultrafine particles. *Occup Environ Med* 2001; **58**: 211-6.
22. Nel A, Xia T, Madler L, Li N. Toxic potential of materials at the nanolevel. *Science* 2006; **311**: 622-7.
23. Dunford R, Salinaro A, Cai LZ, Serpone N, Horikoshi S, Hidaka H, et al. Chemical oxidation and DNA damage catalysed by inorganic sunscreen ingredients. *Febs Lett* 1997; **418**: 87-90.
24. Gurr JR, Wang ASS, Chen CH, Jan KY. Ultrafine titanium dioxide particles in the absence of photoactivation can induce oxidative damage to human bronchial epithelial cells. *Toxicology* 2005; **213**: 66-73.
25. Long TC, Tajuba J, Sama P, Saleh N, Swartz C, Parker J, et al. Nanosize titanium dioxide stimulates reactive oxygen species in brain microglia and damages neurons in vitro. *Environ Health Persp* 2007; **115**: 1631-7.
26. Lu N, Zhu Z, Zhao X, Tao R, Yang X, Gao Z. Nano titanium dioxide photocatalytic protein tyrosine nitration: a potential hazard of TiO₂ on skin. *Biochem Biophys Res Commun* 2008; **370**: 675-80.
27. Park EJ, Yi J, Chung YH, Ryu DY, Choi J, Park K. Oxidative stress and apoptosis induced by titanium dioxide nanoparticles in cultured BEAS-2B cells. *Toxicol Lett* 2008; **180**: 222-9.
28. Sayes CM, Wahi R, Kurian PA, Liu Y, West JL, Ausman KD, et al. Correlating nanoscale titania structure with toxicity: a cytotoxicity and inflammatory response study with human dermal fibroblasts and human lung epithelial cells. *Toxicol Sci* 2006; **92**: 174-85.
29. Wang JX, Chen CY, Liu Y, Jiao F, Li W, Lao F, et al. Potential neurological lesion after nasal instillation of TiO₂ nanoparticles in the anatase and rutile crystal phases. *Toxicol Lett* 2008; **183**: 72-80.
30. Uchino T, Tokunaga H, Ando M, Utsumi H. Quantitative determination of OH radical generation and its cytotoxicity induced by TiO₂-UVA treatment. *Toxicol in Vitro* 2002; **16**: 629-35.
31. Dodd NJ, Jha AN. Titanium dioxide induced cell damage: a proposed role of the carboxyl radical. *Mutat Res* 2009; **660**: 79-82.
32. Petković J, Žegura B, Stevanović M, Drnovšek N, Uskoković D, Novak S et al. DNA damage and alterations in expression of DNA damage responsive genes induced by TiO₂ nanoparticles in human hepatoma HepG2 cells. *Nanotoxicology* 2011; **5**: 341-53.
33. Petković J, Kuzma T, Rade K, Novak S, Filipič M. Pre-irradiation of anatase TiO₂ particles with UV enhances their cytotoxic and genotoxic potential in human hepatoma HepG2 cells. *J Hazard Mater* 2011; doi: 10.1016/j.jhazmat.2011.09.004.
34. Barthel A, Klotz LO. Phosphoinositide 3-kinase signaling in the cellular response to oxidative stress. *Biol Chem* 2005; **386**: 207-16.
35. Kang JL, Moon C, Lee HS, Lee HW, Park EM, Kim HS, et al. Comparison of the biological activity between ultrafine and fine titanium dioxide particles in RAW 264.7 cells associated with oxidative stress. *J Toxicol Environ Health, Part A* 2008; **71**: 478-85.
36. Rahman Q, Lohani M, Dopp E, Pemsel H, Jonas L, Weiss DG, et al. Evidence that ultrafine titanium dioxide induces micronuclei and apoptosis in Syrian hamster embryo fibroblasts. *Environ Health Persp* 2002; **110**: 797-800.
37. Wang JJ, Sanderson BJS, Wang H. Cyto- and genotoxicity of ultrafine TiO₂ particles in cultured human lymphoblastoid cells. *Mutat Res-Gen Tox En* 2007; **628**: 99-106.
38. Xu A, Chai YF, Nohmi T, Hei TK. Genotoxic responses to titanium dioxide nanoparticles and fullerene in gpt delta transgenic MEF cells. *Part Fibre Toxicol* 2009; **6**: 3.
39. Zhu RR, Wang SL, Chao J, Shi DL, Zhang R, Sun XY, et al. Bio-effects of Nano-TiO₂ on DNA and cellular ultrastructure with different polymorph and size. *Mat Sci Eng C-Bio S* 2009; **29**: 691-6.
40. Kang SJ, Kim BM, Lee YJ, Chung HW. Titanium dioxide nanoparticles trigger p53-mediated damage response in peripheral blood lymphocytes. *Environ Mol Mutagen* 2008; **49**: 399-405.
41. Warheit DB, Hoke RA, Finlay C, Donner EM, Reed KL, Sayes CM. Development of a base set of toxicity tests using ultrafine TiO₂ particles as a component of nanoparticle risk management. *Toxicol Lett* 2007; **171**: 99-110.
42. Theogaraj E, Riley S, Hughes L, Maier M, Kirkland D. An investigation of the photo-clastogenic potential of ultrafine titanium dioxide particles. *Mutat Res-Gen Tox En* 2007; **634**: 205-19.
43. Driscoll KE, Deyo LC, Carter JM, Howard BW, Hassenbein DG, Bertram TA. Effects of particle exposure and particle-elicited inflammatory cells on mutation in rat alveolar epithelial cells. *Carcinogenesis* 1997; **18**: 423-30.
44. Trouiller B, Reliene R, Westbrook A, Solaimani P, Schiestl RH. Titanium dioxide nanoparticles induce DNA damage and genetic instability in vivo in mice. *Cancer Res* 2009; **69**: 8784-9.
45. Li N, Ma LL, Wang J, Zheng L, Liu J, Duan YM, et al. Interaction between nano-anatase TiO₂ and liver DNA from mice in vivo. *Nanoscale Res Lett* 2010; **51**: 108-15.
46. Vamanu CI, Cimpan MR, Hol PJ, Sornes S, Lie SA, Gjerdet NR. Induction of cell death by TiO₂ nanoparticles: Studies on a human monoblastoid cell line. *Toxicol in Vitro* 2008; **22**: 1689-96.
47. Palomaki J, Karisola P, Pylkkanen L, Savolainen K, Alenius H. Engineered nanomaterials cause cytotoxicity and activation on mouse antigen presenting cells. *Toxicology* 2010; **267**: 125-31.
48. Larsen ST, Roursgaard M, Jensen KA, Nielsen GD. Nano titanium dioxide particles promote allergic sensitization and lung inflammation in mice. *Basic Clin Pharmacol Toxicol* 2010; **106**: 114-7.

49. de Haar C, Hassing I, Bol M, Bleumink R, Pieters R. Ultrafine but not fine particulate matter causes airway inflammation and allergic airway sensitization to co-administered antigen in mice. *Clin Exp Allergy* 2006; **36**: 1469-79.
50. Moon EY, Yi GH, Kang JS, Lim JS, Kim HM, Pyo S. An increase in mouse tumor growth by an in vivo immunomodulating effect of titanium dioxide nanoparticles. *J Immunotoxicol* 2011; **81**: 56-67.
51. Borm PJ, Robbins D, Haubold S, Kuhlbusch T, Fissan H, Donaldson K, et al. The potential risks of nanomaterials: a review carried out for ECETOC. *Part Fibre Toxicol* 2006; **3**: 11.
52. Peters A, Veronesi B, Calderon-Garciduenas L, Gehr P, Chen LC, Geiser M, et al. Translocation and potential neurological effects of fine and ultrafine particles a critical update. *Part Fibre Toxicol* 2006; **3**: 13.
53. Long TC, Saleh N, Tilton RD, Lowry GV, Veronesi B. Titanium dioxide (P25) produces reactive oxygen species in immortalized brain microglia (BV2): Implications for nanoparticle neurotoxicity. *Environ Sci Technol* 2006; **40**: 4346-52.
54. Liu SC, Xu LJ, Zhang T, Ren GG, Yang Z. Oxidative stress and apoptosis induced by nanosized titanium dioxide in PC12 cells. *Toxicology* 2010; **267**: 172-7.
55. Liu XY, Ren XF, Deng XY, Huo YA, Xie J, Huang H, et al. A protein interaction network for the analysis of the neuronal differentiation of neural stem cells in response to titanium dioxide nanoparticles. *Biomaterials* 2010; **31**: 3063-70.
56. Scuri M, Chen BT, Castranova V, Reynolds JS, Johnson VJ, Samsell L, et al. Effects of titanium dioxide nanoparticle exposure on neuroimmune responses in rat airways. *J Toxicol Environ Health, Part A* 2010; **73**: 1353-69.
57. Nohynek GJ, Schaefer H. Benefit and risk of organic ultraviolet filters. *Regul Toxicol Pharmacol* 2001; **333**: 285-99.
58. FDA. Sunscreen drug products for over-the-counter human use, Final Monograph, Federal Register 64 27666, US Rockville, MD; 2000.
59. Newman MD, Stotland M, Ellis JI. The safety of nanosized particles in titanium dioxide- and zinc oxide-based sunscreens. *J Am Acad Dermatol* 2009; **61**: 685-92.
60. Breggin L, Falkner R, Jaspers N, Pendergrass J, Porter R. Securing the promise of nanotechnologies towards transatlantic regulatory cooperation. London: Affairs RIol; 2009.
61. Serpone N, Dondi D, Albini A. Inorganic and organic UV filters: Their role and efficacy in sunscreens and sun care products. *Inorg Chim Acta* 2007; **360**: 794-802.
62. Salvador A, Chisvert A. Sunscreen analysis - A critical survey on UV filters determination. *Anal Chim Acta* 2005; **537**: 1-14.
63. Nohynek GJ, Antignac E, Re T, Toutain H. Safety assessment of personal care products/cosmetics and their ingredients. *Toxicol Appl Pharmacol* 2010; **243**: 239-59.
64. Nohynek GJ, Lademann J, Ribaud C, Roberts MS. Grey goo on the skin? Nanotechnology, cosmetic and sunscreen safety. *Crit Rev Toxicol* 2007; **373**: 251-77.
65. Salinaro A, Emeline AV, Zhao J, Hidaka H., Ryabchuk V, Serpone KN. Terminology, relative photonic efficiencies and quantum yields in heterogeneous photocatalysis. Part II: Experimental determination of quantum yields (Technical Report). *Pure Appl Chem* 1999; **71**: 321-6.
66. Serpone N, Salinaro A, Hidaka H, Horikoshi S, Knowland J, Dunford R. Solar engineering. In: Morehouse JM, Hogan RE (eds). New York: ASME; 1998.
67. Jaroenworarluck A, Sunsaneeyametha W, Kosachan N, Stevens R. Characteristics of silica-coated TiO₂ and its UV absorption for sunscreen cosmetic applications. *Surf Interface Anal* 2006; **38**: 473-7.
68. Labiele J, Feng J, Botta C, Borschneck D, Sammut M, Cabie M, et al. Agging of TiO₂ nanocomposites used in sunscreens. Dispersion and fate of the degradation products in aqueous environment. *Environ Pollut* 2010; **158**: 1-8.
69. Mills A, Le Hunte S. An overview of semiconductor photocatalysis. *J Photochem Photobiol A* 1997; **108**: 1-35.
70. Wakefield G, Lipscomb S, Holland E, Knowland J. The effects of manganese doping on UVA absorption and free radical generation of micronised titanium dioxide and its consequences for the photostability of UVA absorbing organic sunscreen components. *Photochem Photobiol Sci* 2004; **37**: 648-52.
71. Pan Z, Lee W, Slutsky L, Clark RA, Pernodet N, Rafailovich MH. Adverse effects of titanium dioxide nanoparticles on human dermal fibroblasts and how to protect cells. *Small* 2009; **54**: 511-20.
72. Kiss B, Biro T, Czifra G, Toth BI, Kertesz Z, Szikszai Z, et al. Investigation of micronized titanium dioxide penetration in human skin xenografts and its effect on cellular functions of human skin-derived cells. *Exp Dermatol* 2008; **17**: 659-67.
73. Jin CY, Zhu BS, Wang XF, Lu QH. Cytotoxicity of titanium dioxide nanoparticles in mouse fibroblast cells. *Chem Res Toxicol* 2008; **219**: 1871-7.
74. Yanagisawa R, Takano H, Inoue K, Koike E, Kamachi T, Sadakane K, et al. Titanium Dioxide Nanoparticles Aggravate Atopic Dermatitis-Like Skin Lesions in NC/Nga Mice. *Exp Biol Med* 2009; **234**: 314-22.
75. Hoet PH, Bruske-Hohlfeld I, Salata OV. Nanoparticles - known and unknown health risks. *J Nanobiotechnology* 2004; **21**: 12.
76. Tyner KM, Wokovich AM, Godar DE, Doub WH, Sadrieh N. The state of nano-sized titanium dioxide (TiO₂) may affect sunscreen performance. *Int J Cosmetic Sci* 2010; **33**: 234-44.
77. Lademann J, Weigmann H, Rickmeyer C, Barthelmes H, Schaefer H, Mueller G, et al. Penetration of titanium dioxide microparticles in a sunscreen formulation into the horny layer and the follicular orifice. *Skin Pharmacol Appl Skin Physiol* 1999; **12**: 247-56.
78. Pflucker F, Wendel V, Hohenberg H, Gartner E, Will T, Pfeiffer S, et al. The human stratum corneum layer: an effective barrier against dermal uptake of different forms of topically applied micronised titanium dioxide. *Skin Pharmacol Appl Skin Physiol* 2001; **14**: 92-7.
79. Schulz J, Hohenberg H, Pflucker F, Gartner E, Will T, Pfeiffer S, et al. Distribution of sunscreens on skin. *Adv Drug Deliv Rev* 2002; **54**: S157-63.
80. Schilling K, Bradford B, Castelli D, Dufour E, Nash JF, Pape W, et al. Human safety review of "nano" titanium dioxide and zinc oxide. *Photochem Photobiol Sci* 2010; **9**: 495-509.
81. Senzui M, Tamura T, Miura K, Ikarashi Y, Watanabe Y, Fujii M. Study on penetration of titanium dioxide (TiO₂) nanoparticles into intact and damaged skin in vitro. *J Toxicol Sci* 2010; **35**: 107-13.
82. Tan MH, Commens CA, Burnett L, Snitch PJ. A pilot study on the percutaneous absorption of microfine titanium dioxide from sunscreens. *Australas J Dermatol* 1996; **37**: 185-7.
83. Wu J, Liu W, Xue C, Zhou S, Lan F, Bi L, et al. Toxicity and penetration of TiO₂ nanoparticles in hairless mice and porcine skin after subchronic dermal exposure. *Toxicol Letters* 2009; **191**: 1-8.
84. Sadrieh N, Wokovich AM, Gopee NV, Zheng JW, Haines D, Parmiter D, et al. Lack of Significant Dermal Penetration of Titanium Dioxide from Sunscreen Formulations Containing Nano- and Submicron-Size TiO₂(2) Particles. *Toxicol Sci* 2010; **115**: 156-66.
85. Mosteller RD. Simplified calculation of body-surface area. *N Engl J Med* 1987; **317**: 1098.
86. FDA [Internet]. Food and drugs chapter I, Listing of color additives exempt from certification. Federal Register 21CFR73, US Rockville, MD; 2010; [cited 2011 October 14]. Available from: <http://www.accessdata.fda.gov/scripts/cdrh/cfdocs/cfcr/CFRSearch.cfm?CFRPart=73&showFR=1>.
87. Kumagai K. Uber den Resorptionvergang der corpuscularen Bestandteile im Darm. **192**: 429-31.
88. Jani PU, McCarthy DE, Florence AT. Titanium dioxide (rutile) particle uptake from the rat GI tract and translocation to systemic organs after oral administration. *Int J Pharm* 1994; **105**: 157-68.
89. Wang JX, Zhou GQ, Chen CY, Yu HW, Wang TC, Ma YM, et al. Acute toxicity and biodistribution of different sized titanium dioxide particles in mice after oral administration. *Toxicol Lett* 2007; **168**: 176-85.
90. Duan Y, Liu J, Ma L, Li N, Liu H, Wang J, et al. Toxicological characteristics of nanoparticulate anatase titanium dioxide in mice. *Biomaterials* 2010; **31**: 894-9.

91. Powell JJ, Harvey RSJ, Ashwood P, Wolstencroft R, Gershwin ME, Thompson RPH. Immune potentiation of ultrafine dietary particles in normal subjects and patients with inflammatory bowel disease. *J Autoimmun* 2000; **14**: 99-105.
92. National Cancer Institute. Bioassay of titanium dioxide for possible carcinogenicity. Washington, DC: U.S. Department of Health, Education, and Welfare, Public Health Service, National Institutes of Health; 1979.
93. Bernard BK, Osheroff MR, Hofmann A, Mennear JH. Toxicology and carcinogenesis studies of dietary titanium dioxide-coated mica in male and female Fischer 344 rats. *J Toxicol Env Health* 1990; **29**: 417-29.
94. Okazaki Y, Gotoh E. Comparison of metal release from various metallic biomaterials in vitro. *Biomaterials* 2005; **26**: 11-21.
95. Hext PM, Tomenson JA, Thompson P. Titanium dioxide: inhalation toxicology and epidemiology. *Ann Occup Hyg* 2005; **49**: 461-72.
96. Fryzek JP, Chadda B, Marano D, White K, Schweitzer S, McLaughlin JK, et al. A cohort mortality study among titanium dioxide manufacturing workers in the United States. *J Occup Environ Med* 2003; **45**: 400-9.
97. Boffetta P, Soutar A, Cherrie JW, Granath F, Andersen A, Anttila A, et al. Mortality among workers employed in the titanium dioxide production industry in Europe. *Cancer Causes Control* 2004; **15**: 697-706.
98. NIOSH. Occupational Exposure to Titanium Dioxide. Department Of Health And Human Services, Centers for Disease Control and Prevention, National Institute for Occupational Safety and Health 2011.
99. Peters A, Dockery DW, Muller JE, Mittleman MA. Increased particulate air pollution and the triggering of myocardial infarction. *Circulation* 2001; **103**: 2810-5.
100. Peters A, Doring A, Wichmann HE, Koenig W. Increased plasma viscosity during an air pollution episode: a link to mortality? *Lancet* 1997; **349**: 1582-7.
101. McGuinness C, Duffin R, Brown S, Mills NL, Megson IL, MacNee W, et al. Surface derivatization state of polystyrene latex nanoparticles determines both their potency and their mechanism of causing human platelet aggregation in vitro. *Toxicol Sci* 2011; **119**: 359-68.
102. Donaldson K, Stone V, Seaton A, MacNee W. Ambient particle inhalation and the cardiovascular system: Potential mechanisms. *Environ Health Perspect* 2001; **109**: 523-27.
103. Ferin J, Oberdorster G, Penney DP. Pulmonary retention of ultrafine and fine particles in rats. *Am J Respir Cell Mol Biol* 1992; **65**: 535-42.
104. Oberdorster G, Ferin J, Lehnert BE. Correlation between particle-size, in vivo particle persistence, and lung injury. *Environ Health Perspect* 1994 **102**: 173-9.
105. Renwick LC, Donaldson K, Clouter A. Impairment of alveolar macrophage phagocytosis by ultrafine particles. *Toxicol Appl Pharmacol* 2001; **172**: 119-27.
106. van Ravenzwaay B, Landsiedel R, Fabian E, Burkhardt S, Strauss V, Ma-Hock L. Comparing fate and effects of three particles of different surface properties: nano-TiO₂, pigmentary TiO₂ and quartz. *Toxicol Lett* 2009; **186**: 152-9.
107. Kapp N, Studer D, Gehr P, Geiser M. Electron energy-loss spectroscopy as a tool for elemental analysis in biological specimens. *Methods Mol Biol* 2007; **369**: 431-47.
108. Nemmar A, Vanbilloen H, Hoylaerts MF, Hoet PH, Verbruggen A, Nemery B. Passage of intratracheally instilled ultrafine particles from the lung into the systemic circulation in hamster. *Am J Respir Crit Care Med* 2001; **164**: 1665-8.
109. Nurkiewicz TR, Porter DW, Hubbs AF, Cumpston JL, Chen BT, Frazer DG, et al. Nanoparticle inhalation augments particle-dependent systemic microvascular dysfunction. *Part Fibre Toxicol* 2008; **5**: 1.
110. Kim HW, Ahn EK, Jee BK, Yoon HK, Lee KH, Lim Y. Nanoparticle-induced toxicity and related mechanism in vitro and in vivo. *J Nanopart Res* 2009; **11**: 55-65.
111. Oberdorster G. Pulmonary effects of inhaled ultrafine particles. *Int Arch Occup Environ Health* 2001; **74**: 1-8.
112. Warheit DB, Webb TR, Sayes CM, Colvin VL, Reed KL. Pulmonary instillation studies with nanoscale TiO₂ rods and dots in rats: Toxicity is not dependent upon particle size and surface area. *Toxicol Sci* 2006; **91**: 227-36.
113. Rehn B, Seiler F, Rehn S, Bruch J, Maier M. Investigations on the inflammatory and genotoxic lung effects of two types of titanium dioxide: untreated and surface treated. *Toxicol Appl Pharmacol* 2003; **189**: 84-95.
114. Grassian VH, O'Shaughnessy PT, Adamcakova-Dodd A, Pettibone JM, Thorne PS. Inhalation exposure study of titanium dioxide nanoparticles with a primary particle size of 2 to 5 nm. *Environ Health Perspect* 2007; **115**: 397-402.
115. Warheit DB, Webb TR, Reed KL, Frerichs S, Sayes CM. Pulmonary toxicity study in rats with three forms of ultrafine-TiO₂ particles: Differential responses related to surface properties. *Toxicology* 2007; **230**: 90-104.
116. Roursgaard M, Jensen KA, Poulsen SS, Jensen NEV, Poulsen LK, Hammer M, et al. Acute and subchronic airway inflammation after intratracheal instillation of quartz and titanium dioxide agglomerates in mice. *Scientific World Journal* 2011; **11**: 801-25.
117. Chen HW, Su SF, Chien CT, Lin WH, Yu SL, Chou CC, et al. Titanium dioxide nanoparticles induce emphysema-like lung injury in mice. *FASEB J* 2006; **20**: 2393-5.
118. Park EJ, Yoon J, Choi K, Yi J, Park K. Induction of chronic inflammation in mice treated with titanium dioxide nanoparticles by intratracheal instillation. *Toxicology* 2009; **260**: 37-46.
119. Lee KP, Trochimowicz HJ, Reinhardt CF. Pulmonary Response of Rats Exposed to Titanium-Dioxide (TiO₂) by Inhalation for 2 Years. *Toxicol Appl Pharmacol* 1985; **79**: 179-92.
120. Borm PJA, Hohl D, Steinfartz Y, Zeittreger I, Albrecht C. Chronic inflammation and tumor formation in rats after intratracheal instillation of high doses of coal dusts, titanium dioxides, and quartz. *Inhal Toxicol* 2000; **12**: 225-31.
121. Heinrich U, Fuhst R, Rittinghausen S, Creutzenberg O, Bellmann B, Koch W, et al. Chronic inhalation exposure of Wistar rats and 2 different strains of mice to diesel-engine exhaust, carbon-black, and titanium-dioxide. *Inhal Toxicol* 1995; **74**: 533-56.
122. Muhle H, Bellmann B, Creutzenberg O, Koch W, Dasenbrock C, Ernst H, et al. Pulmonary response to toner, TiO₂ and crystalline silica upon chronic inhalation exposure in Syrian golden hamsters. *Inhal Toxicol* 1998; **10**: 699-729.
123. Bermudez E, Mangum JB, Asgharian B, Wong BA, Reverdy EE, Janszen DB, et al. Long-term pulmonary responses of three laboratory rodent species to subchronic inhalation of pigmentary titanium dioxide particles. *Toxicol Sci* 2002; **70**: 86-97.
124. Bermudez E, Mangum JB, Wong BA, Asgharian B, Hext PM, Warheit DB, et al. Pulmonary responses of mice, rats, and hamsters to subchronic inhalation of ultrafine titanium dioxide particles. *Toxicol Sci* 2004; **77**: 347-57.
125. Hsieh TH, Yu CP. Two-phase pulmonary clearance of insoluble particles in mammalian species. *Inhal Toxicol* 1998; **10**: 121-30.
126. Wang JX, Liu Y, Jiao F, Lao F, Li W, Gu YQ, et al. Time-dependent translocation and potential impairment on central nervous system by intranasally instilled TiO₂ nanoparticles. *Toxicology* 2008; **254**: 82-90.
127. Yamadori I, Ohsumi S, Taguchi K. Titanium dioxide deposition and adenocarcinoma of the lung. *Acta Pathol Jpn* 1986; **36**: 783-90.
128. Chen JL, Fayerweather WE. Epidemiologic-study of workers exposed to titanium-dioxide. *J Occup Environ Med* 1988; **30**: 937-42.
129. Ramanakumar AV, Parent ME, Latreille B, Siemiatycki J. Risk of lung cancer following exposure to carbon black, titanium dioxide and talc: results from two case-control studies in Montreal. *Int J Cancer* 2008; **122**: 183-9.
130. Boffetta P, Soutar A, Cherrie JW, Granath F, Andersen A, Anttila A, et al. Mortality among workers employed in the titanium dioxide production industry in Europe. *Cancer Causes Control* 2004; **15**: 697-706.
131. IARC. Carbon black, titanium dioxide, and talc. IARC monographs on the evaluation of carcinogenic risks to humans, vol. 93. International Agency for Research on Cancer: Lyon, France, 2006.
132. Baan R, Straif K, Grosse Y, Secretan B, El Ghissassi F, Coglianò V. Carcinogenicity of carbon black, titanium dioxide, and talc. *Lancet Oncol* 2006; **74**: 295-6.
133. Cadosch D, Chan E, Gautschi OP, Filgueira L. Metal is not inert: Role of metal ions released by biocorrosion in aseptic loosening-Current concepts. *J Biomed Mater Res A* 2009; **91**: 1252-62.

134. Sargeant A, Goswami T. Hip implants - Paper VI - Ion concentrations. *Mater Design* 2007; **28**: 155-71.
135. Valentine-Thon E, Schiwaro HW. Validity of MELISA (R) for metal sensitivity testing. *Neuroendocrinol Lett* 2003; **241**: 57-64.
136. Hallab N, Merritt K, Jacobs JJ. Metal sensitivity in patients with orthopaedic implants. *J Bone Joint Surg Am* 2001; **83**: 428-36.
137. Wang JX, Fan YB, Gao Y, Hu QH, Wang TC. TiO₂ nanoparticles translocation and potential toxicological effect in rats after intraarticular injection. *Biomaterials* 2009; **30**: 4590-600.
138. Urban RM, Jacobs JJ, Tomlinson MJ, Gavrilovic J, Black J, Peoc'h M. Dissemination of wear particles to the liver, spleen, and abdominal lymph nodes of patients with hip or knee replacement. *J Bone Joint Surg Am* 2000; **82**: 457-76.
139. Margevicius KJ, Bauer TW, McMahon JT, Brown SA, Merritt K. Isolation and characterization of debris in membranes around total joint prostheses. *J Bone Joint Surg Am* 1994; **76**: 1664-75.
140. Agins HJ, Alcock NW, Bansal M, Salvati EA, Wilson PD, Pellicci PM, et al. Metallic wear in failed titanium-alloy total hip replacements. A histological and quantitative analysis. *J Bone Joint Surg Am* 1988; **70**: 347-56.
141. Giavaresi G, Ambrosio L, Battiston GA, Casellato U, Gerbasi R, Finia M, et al. Histomorphometric, ultrastructural and microhardness evaluation of the osseointegration of a nanostructured titanium oxide coating by metal-organic chemical vapour deposition: an in vivo study. *Biomaterials* 2004; **25**: 5583-91.
142. Cui C, Liu H, Li Y, Sun J, Wang R, Liu S, et al. Fabrication and biocompatibility of nano-TiO₂/titanium alloys biomaterials. *Mater Lett* 2005; **59**: 3144-48.
143. Drnovsek N, Daneu N, Recnik A, Mazaj M, Kovac J, Novak S. Hydrothermal synthesis of a nanocrystalline anatase layer on Ti6Al4V implants. *Surf Coat Tech* 2009; **203**: 1462-68.
144. Tedetti M, Sempere R. Penetration of ultraviolet radiation in the marine environment. A review. *Photochem Photobiol* 2006; **82**: 389-97.
145. Aruoja V, Doubouguier H-C, Kasemets K, Kahru A. Toxicity of nanoparticles of CuO, ZnO and TiO₂ to microalgae *Pseudokirchneriella subcapitata*. *Sci Total Environ* 2009; **407**: 1461-68.
146. Hund-Rinke K, Simon M. Ecotoxic effect of photocatalytic active nanoparticles (TiO₂) on algae and daphnids. *Environ Sci Pollut Res Int* 2006; **134**: 225-32.
147. Hartmann NB, Von der Kammer F, Hofmann T, Baalousha M, Ottofuelling S, Baun A. Algal testing of titanium dioxide nanoparticles--Testing considerations, inhibitory effects and modification of cadmium bioavailability. *Toxicology* 2010; **269**: 190-7.
148. Kim S-C, Lee D-K. Preparation of TiO₂-coated hollow glass beads and their application to the control of algal growth in eutrophic water. *Microchem J* 2005; **80**: 227-32.
149. Hong J, Ma H, Otaki M. Controlling algal growth in photo-dependent decolorant sludge by photocatalysis. *J Biosci Bioeng* 2005; **99**: 592-7.
150. Velzeboer I, Hendriks AJ, Ragas AMJ, Van de Meent D. Aquatic ecotoxicity tests of some nanomaterials. *Environ Toxicol Chem* 2008; **27**: 1942-47.
151. Adams LK, Lyon DY, Alvarez PJ. Comparative eco-toxicity of nanoscale TiO₂, SiO₂, and ZnO water suspensions. *Water Res* 2006; **40**: 3527-32.
152. Zhu X, Chang Y, Chen Y. Toxicity and bioaccumulation of TiO₂ nanoparticle aggregates in *Daphnia magna*. *Chemosphere* 2010; **78**: 209-15.
153. Wiench K, Wohlleben W, Hisgen V, Radke K, Salinas E, Zok S, et al. Acute and chronic effects of nano- and non-nano-scale TiO₂ and ZnO particles on mobility and reproduction of the freshwater invertebrate *Daphnia magna*. *Chemosphere* 2009; **76**: 1356-65.
154. Kim KT, Klaine SJ, Cho J, Kim SH, Kim SD. Oxidative stress responses of *Daphnia magna* exposed to TiO₂ nanoparticles according to size fraction. *Sci Total Environ*; **408**: 2268-72.
155. Lee S-W, Kim S-M, Choi J. Genotoxicity and ecotoxicity assays using the freshwater crustacean *Daphnia magna* and the larva of the aquatic midge *Chironomus riparius* to screen the ecological risks of nanoparticle exposure. *Environ Toxicol Phar* 2009; **281**: 86-91.
156. Zhu X, Zhu L, Duan Z, Qi R, Li Y, Lang Y. Comparative toxicity of several metal oxide nanoparticle aqueous suspensions to Zebrafish (*Danio rerio*) early developmental stage. *J Environ Sci Health A Tox Hazard Subst Environ Eng* 2008; **433**: 278-84.
157. Federici G, Shaw BJ, Handy RD. Toxicity of titanium dioxide nanoparticles to rainbow trout (*Oncorhynchus mykiss*): Gill injury, oxidative stress, and other physiological effects. *Aquat Toxicol* 2007; **844**: 415-30.
158. Scown TM, van Aerle R, Johnston BD, Cumberland S, Lead JR, Owen R, et al. High Doses of Intravenously Administered Titanium Dioxide Nanoparticles Accumulate in the Kidneys of Rainbow Trout but with no Observable Impairment of Renal Function. *Toxicol Sci* 2009; **109**: 372-80.
159. Linhua H, Zhenyu W, Baoshan X. Effect of sub-acute exposure to TiO₂ nanoparticles on oxidative stress and histopathological changes in Juvenile Carp (*Cyprinus carpio*). *J Environ Sci* 2009; **21**: 1459-66.
160. Galloway T, Lewis C, Dolciotti I, Johnston BD, Moger J, Regoli F. Sublethal toxicity of nano-titanium dioxide and carbon nanotubes in a sediment dwelling marine polychaete. *Environ Pollut* 2010; **158**: 1748-55.
161. Zhu X, Wang J, Zhang X, Chang Y, Chen Y. Trophic transfer of TiO₂ nanoparticles from *Daphnia* to zebrafish in a simplified freshwater food chain. *Chemosphere* 2010; **79**: 928-33.
162. Zhang XZ, Sun HW, Zhang ZY, Niu Q, Chen YS, Crittenden JC. Enhanced bioaccumulation of cadmium in carp in the presence of titanium dioxide nanoparticles. *Chemosphere* 2007; **67**: 160-66.
163. Sun HW, Zhang XZ, Niu Q, Chen YS, Crittenden JC. Enhanced accumulation of arsenate in carp in the presence of titanium dioxide nanoparticles. *Water Air Soil Pollut* 2007; **178**: 245-54.
164. Canesi L, Ciacci C, Vallotto D, Gallo G, Marcomini A, Pojana G. In vitro effects of suspensions of selected nanoparticles (C60 fullerene, TiO₂, SiO₂) on *Mytilus hemocytes*. *Aquat Toxicol* 2010; **96**: 151-8.
165. Vevers WF, Jha AN. Genotoxic and cytotoxic potential of titanium dioxide (TiO₂) nanoparticles on fish cells in vitro. *Ecotoxicology* 2008; **175**: 410-20.
166. Reeves JF, Davies SJ, Dodd NJF, Jha AN. Hydroxyl radicals (OH) are associated with titanium dioxide (TiO₂) nanoparticle-induced cytotoxicity and oxidative DNA damage in fish cells. *Mutat Res-Fund Mol M* 2008; **640**: 113-22.
167. Drobne D, Jemec A, Pipan Tkalec Z. In vivo screening to determine hazards of nanoparticles: nanosized TiO₂. *Environ Pollut* 2009; **157**: 1157-64.
168. Mueller NC, Nowack B. Exposure modeling of engineered nanoparticles in the environment. *Environ Sci Technol* 2008; **421**: 4447-53.
169. Valant J, Drobne D, Sepcic K, Jemec A, Kogej K, Kostanjsek R. Hazardous potential of manufactured nanoparticles identified by in vivo assay. *J Hazard Mater* 2009; **171**: 160-5.
170. Wang H, Wick RL, Xing B. Toxicity of nanoparticulate and bulk ZnO, Al₂O₃ and TiO₂ to the nematode *Caenorhabditis elegans*. *Environ Pollut* 2009; **157**: 1171-7.
171. Roh J-Y, Park Y-K, Park K, Choi J. Ecotoxicological investigation of CeO₂ and TiO₂ nanoparticles on the soil nematode *Caenorhabditis elegans* using gene expression, growth, fertility, and survival as endpoints. *Environ Toxicol Phar* 2010; **29**: 167-72.
172. Hu CW, Li M, Cui YB, Li DS, Chen J, Yang LY. Toxicological effects of TiO₂ and ZnO nanoparticles in soil on earthworm *Eisenia fetida*. *Soil Biol Biochem* 2010; **42**: 586-91.
173. Yang F, Hong F, You W, Liu C, Gao F, Wu C, et al. Influence of nano-anatase TiO₂ on the nitrogen metabolism of growing spinach. *Biol Trace Elem Res* 2006; **110**: 179-90.
174. Gao F, Hong F, Liu C, Zheng L, Su M, Wu X, et al. Mechanism of nano-anatase TiO₂ on promoting photosynthetic carbon reaction of spinach. *Biol Trace Elem Res* 2006; **111**: 239-53.
175. Gao F, Liu C, Qu C, Zheng L, Yang F, Su M, et al. Was improvement of spinach growth by nano-TiO₂ treatment related to the changes of Rubisco activase? *BioMetals* 2008; **212**: 211-17.
176. Su MY, Liu C, Qu CX, Zheng L, Chen L, Huang H, et al. Nano-anatase relieves the inhibition of electron transport caused by linolenic acid in chloroplasts of spinach. *Biol Trace Elem Res* 2008; **122**: 73-81.
177. Lei Z, Mingyu S, Xiao W, Chao L, Chunxiang Q, Liang C, et al. Antioxidant Stress is Promoted by Nano-anatase in Spinach Chloroplasts Under UV-B Radiation. *Biol Trace Elem Res* 2008; **121**: 69-79.

178. Lu CM, Zhang CY, Wen JQ, Wu GR. (in Chinese). *Soybean Sci* 2002; **21**: 168-71.
179. Matsunaga T, Tomoda R, Nakajima T, Wake H. Photoelectrochemical sterilization of microbial cells by semiconductor powders. *FEMS Microbiol Lett* 1985; **29**: 211-4.
180. Ibáñez JA, Litter MI, Pizarro RA. Photocatalytic bactericidal effect of TiO₂ on *Enterobacter cloacae*: Comparative study with other Gram (-) bacteria. *J Photochem Photobiol, A* 2003; **157**: 81-5.
181. Jang HD, Kim S-K, Kim S-J. Effect of particle size and phase composition of titanium dioxide nanoparticles on the photocatalytic properties. *J Nanopart Res* 2001; **3**: 141-7.
182. Shang C, Cheung LM, Ho C-M, Zeng M. Repression of photoreactivation and dark repair of coliform bacteria by TiO₂-modified UV-C disinfection. *App Catal B* 2009; **89**: 536-42.
183. Khan U, Benabderrazik N, Bourdelais AJ, Baden DG, Rein K, Gardinali PR, et al. UV and solar TiO₂ photocatalysis of brevetoxins (PbTx_s). *Toxicol* 2010; **55**: 1008-16.
184. Prijic S, Sersa G. Magnetic nanoparticles as targeted delivery systems in oncology. *Radiol Oncol* 2011; **45**: 1-16.
185. Lagopati N, Kitsiou PV, Kontos AI, Venieratos P, Kotsopoulou E, Kontos AG, et al. Photo-induced treatment of breast epithelial cancer cells using nanostructured titanium dioxide solution. *J Photochem Photobiol, A* 2010; **214**: 215-23.
186. Stefanou E, Eyangelou A, Falaras P. Effects of UV-irradiated titania nanoparticles on cell proliferation, cancer metastasis and promotion. *Catal Today* 2010; **151**: 58-63.
187. Cai R, Kubota Y, Shuin T, Sakai H, Hashimoto K, Fujishima A. Induction of cytotoxicity by photoexcited TiO₂ particles. *Cancer Res* 1992; **52**: 2346-8.
188. Fujishima A, Hashimoto K, Watanabe T. *TiO₂ Photocatalysis: Fundamentals and Applications*. Tokyo: BKC, Inc; 1999.
189. Fujishima A, Call RX, Otsuki J, Hashimoto K, Iron K, Yamashita T, et al. Biochemical application of photoelectrochemistry: photokilling of malignant cells with TiO₂ powder. *Electrochim Acta* 1993; **38**: 153-7.
190. Kalbacova M, Macak MJ, Schmidt-Stein F, Mierke CT, Schmuki P. *Phys. Status Solidi (RRL)*. 2008; **2**: 194-8.
191. Kubota Y, Shuin T, Kawasaki C, Hosaka M, Kitamura H, Cai R et al. Photokilling of T-24 Human Bladder-Cancer Cells with Titanium-Dioxide. *Br J Cancer* 1994; **70**: 1107-11.
192. Thevenot P, Cho J, Wavhal D, Timmons RB, Tang L. Surface chemistry influences cancer killing effect of TiO₂ nanoparticles. *Nanomedicine* 2008; **43**: 226-36.
193. Song M, Zhang RY, Dai YY, Gao F, Chi HM, Lv G, et al. The in vitro inhibition of multidrug resistance by combined nanoparticulate titanium dioxide and UV irradiation. *Biomaterials* 2006; **27**: 4230-38.
194. Schmidt-Stein F, Hahn R, Gnichwitz JF, Song YY, Shrestha NK, Hirsch A, et al. X-ray induced photocatalysis on TiO₂ and TiO₂ nanotubes: Degradation of organics and drug release. *Electrochem Commun* 2009; **1111**: 2077-80.
195. Matsui K, Segawa M, Tanaka T, Kondo A, Ogino C. Antibody-immobilized TiO₂ nanoparticles for cancer therapy. *J Biosci Bioeng* 2009; **108**: S36-S37.
196. Xu J, Sun Y, Huang JJ, Chen CM, Liu GY, Jiang Y et al. Photokilling cancer cells using highly cell-specific antibody-TiO₂ bioconjugates and electroporation. *Bioelectrochem* 2007; **712**: 217-22.
197. Lai T-Y, Lee W-C. Killing of cancer cell line by photoexcitation of folic acid-modified titanium dioxide nanoparticles. *J Photochem Photobiol, A* 2009; **204**: 148-53.
198. Lomer MCE, Hutchinson C, Volkert S, Greenfield SM, Catterall A, Thompson RPH et al. Dietary sources of inorganic microparticles and their intake in healthy subjects and patients with Crohn's disease. *Brit J Nutr* 2004; **92**: 947-55.

Assessing renal function in children with hydronephrosis - additional feature of MR urography

George Hadjidekov^{1,2}, Savina Hadjidekova³, Zahari Tonchev^{1,2}, Rumiana Bakalova^{2,4}, Ichio Aoki⁴

¹ Department of Radiology, University Hospital "Lozenets", Sofia, Bulgaria

² Department of Physics, Biophysics & Radiology, Medical Faculty, University Sofia University "St. Kl. Ohridski", Sofia, Bulgaria

³ Department of Medical Genetics, Medical University, Sofia, Bulgaria

⁴ Molecular Imaging Center, National Institute of Radiological Sciences (NIRS), Chiba, Japan.

Received 21 April 2011

Accepted 5 October 2011

Correspondence to: Assist. Prof George V. Hadjidekov, MD, Department of Radiology, University Hospital "Lozenetz" -1, Koziak str. Sofia 1407, Bulgaria. Tel.: +359 898 797612; Fax: +359 2 962 4771; E-mail: jordiman76@yahoo.com

Disclosure: No potential conflicts of interest were disclosed.

Background. Magnetic resonance urography (MRU) is one of the most attractive imaging modalities in paediatric urology, providing largest diagnostic information in a single protocol. Therefore, the aim of our study was to assess the diagnostic value of MRU in children with urogenital anomalies (especially anomalies of the renal pelvis and ureter) and the renal function using different post-processing functional software.

Patients and methods. Ninety six children (7 days – 18 years old) were examined. In 54 patients of them, a static T₂ MRU was completed by excretory T₁ MRU after gadolinium administration and functional analysis has been performed using two functional analysis softwares "CHOP-fMRU" and "ImageJ" software.

Results. MRU showed suspicious renal and the whole urinary tract anomalies with excellent image quality in all children. In ureteropelvic obstruction, MRU was confirmatory to the other imaging techniques, but it was superior modality concerning the evaluation of end-ureteral anomalies. There was an excellent correlation between the MRU data and diagnosis, determined by surgery. The renal transit times, renal volumes and volumetric differential renal function were assessed separately by "CHOP-fMRU" and "ImageJ" with excellent agreement with ^{99m}Tc-DTPA and among them.

Conclusions. MRU overcomes a lot of limitations of conventional imaging modalities and has a potential to become a leading modality in paediatric urology. Synthesis of both anatomical and functional criteria in MR urography enables to select the best candidates for surgical treatment. Even small kidney dysfunction can be detected by functional analysis software.

Key words: MR urography; children; functional analysis; urinary tract

Introduction

The imaging of urinary tract is important clue in paediatrics. Different methods for evaluation of the genitourinary system are routinely used in the clinic. However, there is no single method providing the whole information, necessary for the diagnostic. The conventional methods have many limitations. For example: ultrasound examination is operator-dependant, with sometimes difficult visualization of the end-ureter; in intravenous urography, there is a risk of contrast media and ionizing

radiation; retrograde methods are invasive with limited application; scintigraphy has a poor anatomical resolution.¹

Novel methods have developed to overcome the limitations of the conventional methods and MR urography (MRU) is one of the most attractive. MRU is a promising method for early diagnosis, having an impact on the management of congenital malformations and other urogenital anomalies in children.¹ This diagnostic modality provides a detailed visualization of various morphologic abnormalities of the genitourinary system and avoids

radiation, which is mutagenic.^{1,2} To avoid ionizing radiation is one of the most important diagnostic approaches in children.³

Currently, MRI is used in paediatrics for assessment of the congenital abnormalities of the genitourinary system, different cases of obstruction of the excretory system and evaluation of renal tumours, which are prevalent solid tumours in infants.^{1,4} In addition to the morphological imaging, MRI can be used to quantify the renal function. Following contrast administration and using appropriate software, time-intensity curves can be generated and other parameters (*e.g.*, renal transit times, renal volumes and differential renal function) can be quantified.¹ This is the reason some authors to define MRI as a potential “one-stop-shop” imaging technique for a variety of renal diseases.⁶⁻⁸

In the present study, we assess the diagnostic value of MRU in a cohort of paediatric patients with various urogenital anomalies (especially with anomalies of the renal pelvis and ureter) using two post-processing functional software “CHOP-fMRU” and ImageJ and in comparison to ^{99m}Tc-DTPA scintigraphy.

Materials and methods

Patient population

We retrospectively reviewed all 96 children (age: between 7 days and 18 years) referred from the Department of Urology and Paediatrics, between 2006 and 2010 with suspected congenital urinary tract anomalies, controversial findings from the conventional imaging studies and difficulties to establish the final diagnosis. In 54 of them an excretory, T₁ MRU after contrast administration of gadolinium has been performed for renal function assessment in addition to T2 MR urography. In the remaining 42 patients, static T2 MR urography has been employed in order to confirm conditions affecting the urinary tract without impact on the renal function, co-existing renal pathology or due to contraindications for gadolinium (Gd) injection in cases of renal failure. The frequency of age distribution in the patient population was as follows: 0 day – 1 month: 7 patients (7.3% from the whole study group of 96 patients); 1 month – 1 year: 29 patients (30.2%); 1 year – 6 years: 18 patients (18.8%); 6 years – 14 years: 15 patients (15.6%); 14 years – 18 years: 27 patients (28.1%).

Cross-sectional sequences, MR angiography in the arterial and venous phase, serial evaluation of the renal parenchymal perfusion and contrast-en-

hanced MRU were combined in one imaging session instead of lining up several different imaging modalities. Time-intensity curves were generated, based on the dynamic 3D post-contrast sequences. “CHOP-fMRU” and ImageJ analysis software was used for calculation the functional curves, plots and maps, renal transit times, renal volumes and differential renal function.^{5,10} In all cases, an informed consent was obtained after the procedure was fully explained to the parents and older children and the study was approved by the Ethics Committee of the University Hospital “Lozenets”, Sofia, Bulgaria.

Ultrasonography was conducted in all patients prior to MRU examination. Voiding cystourethrography (VCUG) was performed in 10 children with suspicion for dilatation of urinary tract in accordance to vesicoureteral reflux (VUR). In 8 children intravenous urography (IVU) has been previously done and in 19 cases ^{99m}Tc-DTPA scintigraphy as a part of the urological work-up has been done with a delay prior or after the MRI exam no longer than 1 month, in another institution. The ^{99m}Tc-DTPA protocol was similar to our MRU protocol in terms of hydration with intravenous administration of 10 ml/kg sodium chloride solution 30 min prior to the scan. The amount furosemide (1 mg/kg, *i.v.*) was the same as in our examination, although diuretics have been given when maximum pelvicalyceal distension was observed (usually 10-15 min after administration of ^{99m}Tc-DTPA).

Patient preparation

The adequate preparation is a prerequisite for a good image quality.⁵⁻¹¹ We didn't place routinely a bladder catheter, although catheterisation of small children is recommended in case of megaureter (with or without reflux). We used catheter in few patients with suspected VUR, but due to technical problems we abandoned this procedure. Then we started to scan without catheterization and we were happy with cooperative, toilet-trained children, without cases of severe discomfort or inability to conduct the examination. The intravenous hydration and administration of furosemide are crucial for reducing the concentrations of Gd.¹⁰ Diuretics are recommended in both static urography and dynamic urography before contrast administration. In this context, we administered standardised hydration (10-15 ml/kg sodium chloride or Ringer's solution) and diuretics (furosemide – 1 mg/kg, max. dose 20 mg) 15 min prior to Gd injection, in order to reduce artefacts, to distend

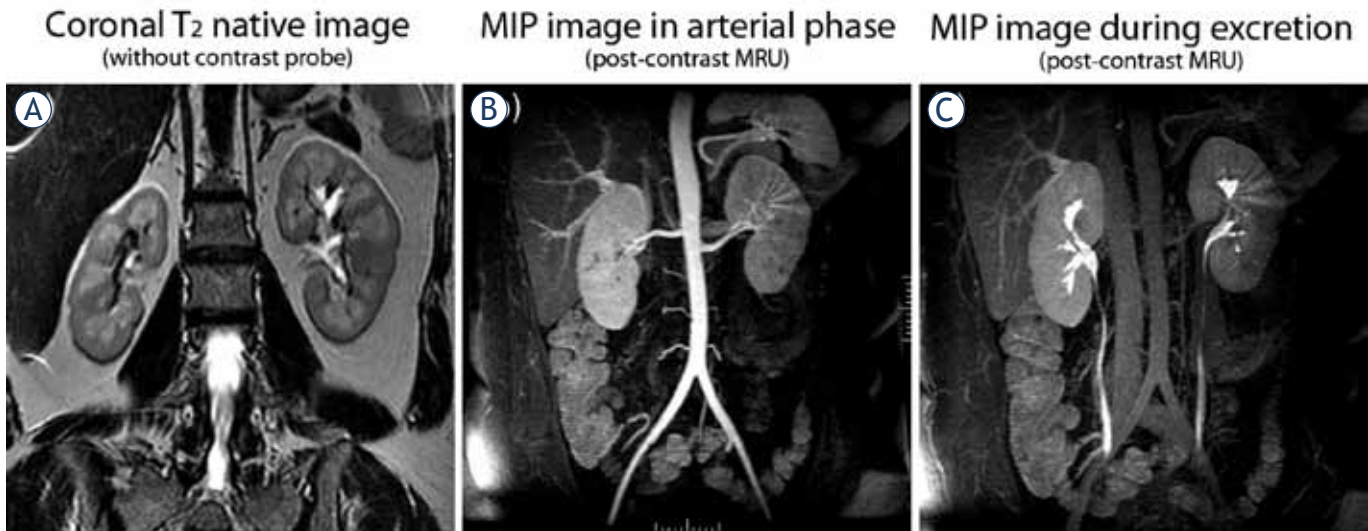


FIGURE 1A-C. Normal MR urogram in 5-year-old boy. **A.** Coronal T₂ native image of both kidneys. **B,C.** MIP images from two separated time-points of the excretory post-contrast MRU in arterial phase (B) and during excretion (C).

the urinary tract, to maintain the linearity between signal intensity and concentration of Gd and to shorten the examination time, adopting the F-15 protocol, proposed by Grattan-Smith.¹² In children younger than 6-year-old and non-cooperative for breath-hold techniques, successful sedation was performed with ketamine (Ketalar) and midazolam (Dormicum) according to the department's standard sedation protocol with no serious adverse effects. In 15 patients intravenous sedation (Ketalar – 1 mg/kg or Thiopental 4-5 mg/kg) was successfully performed with minor motion artefacts in 2 infants without any impact on the diagnostic value of the image quality. Oral sedation using midazolam (Dormicum - 0.5 mg/kg) was sufficient to perform MRU with excellent diagnostic image quality in 32 patients and there was no major complaint of nausea and vomiting that could be related to antiemetic effects of midazolam.¹³⁻¹⁴ The blood pressure, respiration, heart rate, and oxygen saturation were continuously monitored throughout MR imaging in all patients.

MRU protocol

High-field strength tomographs (1.5 Tesla) (Signa, General Electric Medical Systems and Magnetom Essenza, Siemens Medical Solutions) were used with large field of view (FOV) above diaphragm to avoid artefacts from aliasing or post-contrast signal intensity decline in the upper renal poles and obtain an oblique coronal plan angled parallel to the long axis of the kidneys, including ureters and bladder. Our MRU protocol consisted of

native MR examination with T₂ coronal, T₁ and T₂ axial sequences, followed by dynamic study with Gd injection, administration of furosemide prior to the dynamic acquisitions and 3D reconstructions. Following the coronal T₂ plan, we performed axial T₂ and T₁ sequences. Fat-suppression techniques were used in T₁ and T₂ hyperintense findings and in cases of suspicion of tumour formation – In/Out phase dual-echo sequences for contour delineation. The most important pre-contrast sequence was 3D T₂ urogram with fat-suppression and respiratory-triggering. T₁-weighted gradient-echo sequence with fat-saturation (3D Dyn SPGR for GE 1.5 T Signa and 3D VIBE Dynamic for Siemens Essenza 1,5T) was used for the post-contrast scan. The dynamic scan was repeated within 15 min, following Gd injection with increasing intervals between acquisitions, for the need of post-processing. Our sequences were compatible on both MR units and the software used for post-processing has been properly validated for correctness and applicability in our MR protocols. We employed a standard dose of 0.1 mmol/kg of Gd in the majority of our studies, however in some occasions low-dose Gd opacification – 0.01 mmol/kg has been employed, especially in small infants and in cases of glomerular filtration between 30 and 60 ml/min/1.73 m². In all our patients, serum creatinine levels were strictly observed and we estimated individually the glomerular filtration rate according to the Schwartz's formula.¹⁵ New-borns and small infants were scanned with a head-coil and the older children were scanned with a phased-array torso coil. Normal MR urogram is shown in Figure 1.

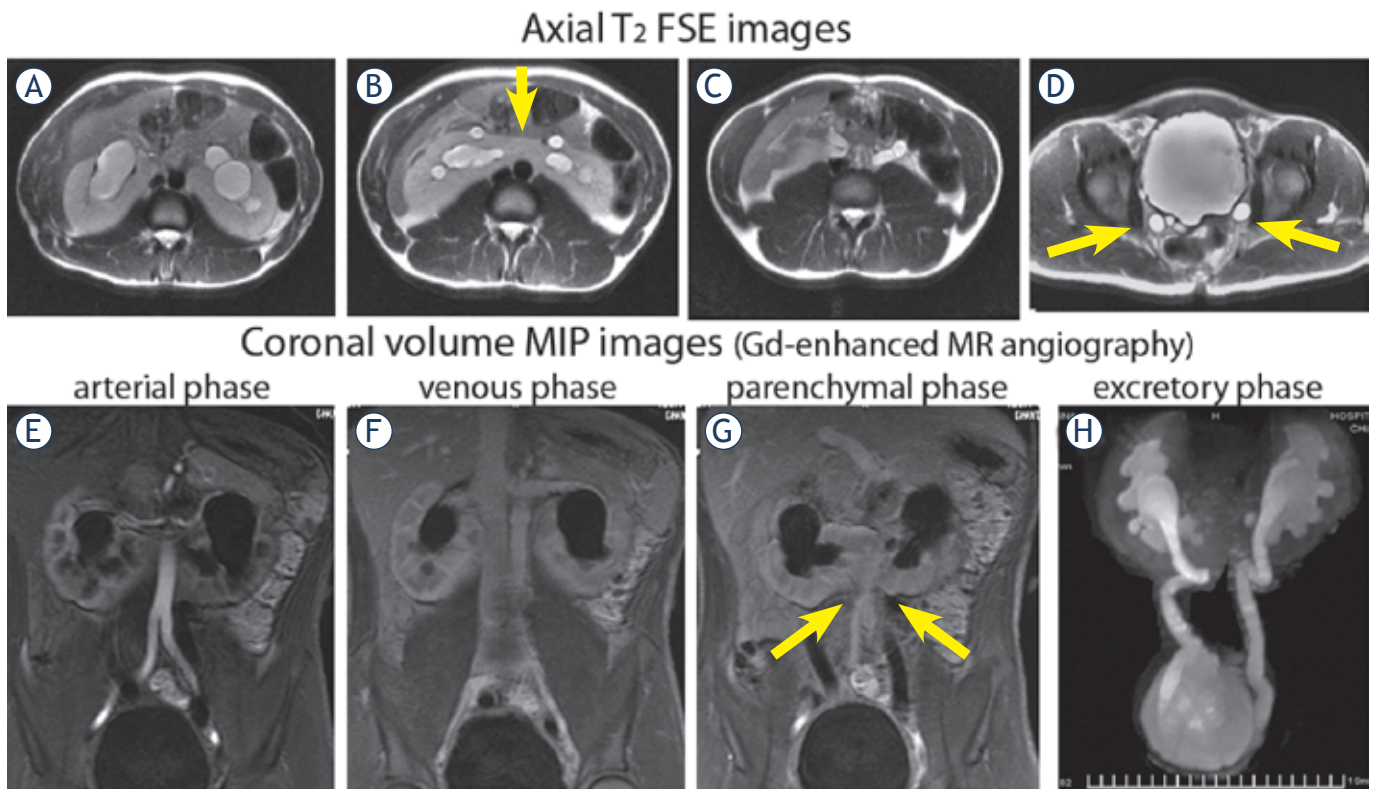
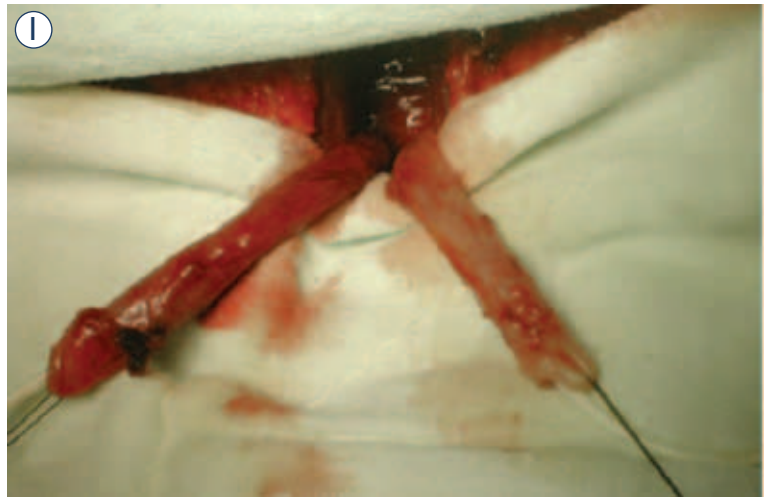


FIGURE 2A-I. MR imaging of horseshoe kidney in 12-year-old boy. **A-D.** Axial T₂ FSE images – clearly dilated pyelocalyceal system and ureters in horseshoe kidney. **E.** Coronal volume MIP image from arterial phase of 3D Gd-enhanced MR angiography – the main left and right renal arteries extending from the anterior aspect of the aorta. **F.** Coronal volume MIP image from venous phase – both renal veins in their expected locations. **G.** Coronal volume MIP image from parenchymal phase – lower poles of the kidneys without any parenchymal abnormalities. **H.** Coronal volume MIP image from excretory phase – marked dilatation of both pyelocalyceal systems and ureters. **I.** Intraoperative findings prove the diagnosis of bilateral megaureters in horseshoe kidney with dysplastic changes in their distal thirds.



Statistical analysis and ethical consideration

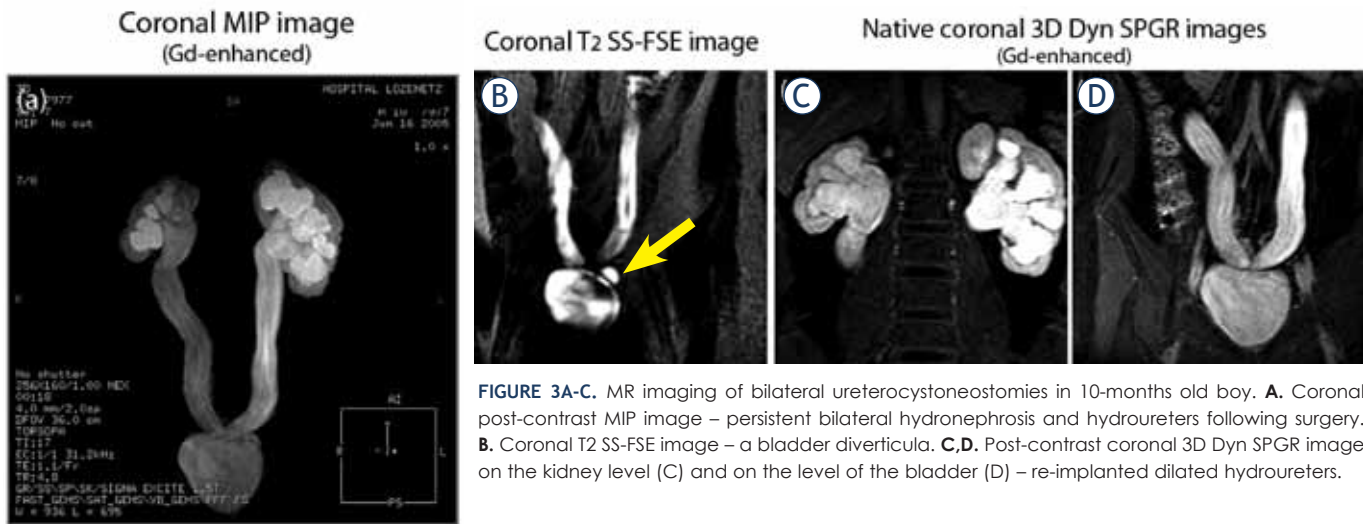
Groups were compared with Mann-Whitney *U*-test, *P*-values >0.05 were taken as indicators of no statistically significant differences. SPSS 13.0 (SPSS Inc., Chicago, Illinois, USA) was used.

The investigators strictly followed recommendations of the Helsinki Declaration (1964, with later amendments) and of the European Council Convention on Protection of Human Rights in Bio-Medicine (Oviedo 1997).

Results

MR urography for visualization of morphological renal anomalies in children

Static, T₂ MR urography was successfully performed in 96 children with 99 exams, totally 197 kidneys (in three children follow-up MRI exams after surgery have been done and in one patient left nephrectomy was performed). T₂ images for anatomic evaluation were helpful in the assess-



ment of children with severe hydronephrosis and poorly functioning systems. The majority of the population (91 cases) presented with congenital anomalies of the renal pelvis and ureter, including megacalycosis, ureteropelvic (UPJ) obstruction and primary megaureters. We also detected 36 cases of congenital anomalies of the kidney, including: renal agenesis – 6; renal hypoplasia – 5; cystic anomalies of the kidneys – 8; anomalies of renal rotation, horseshoe kidney – 6 (Figure 2); renal dystopia – 3; abnormal renal vessels – 6; Fraley's syndrome -2. Static, T2 MRU allows us also to find the following anomalies: (i) bladder anomalies – in 3 children; (ii) encountered lower urinary tract anomalies of urogenital sinus – in 7 children, including disorders of sex development with ambiguous genitalia (hermaphroditism) (n=3), anorectal and vaginal malformations (n=4); (iii) renal infections – in 18 children. 11 cases of renal neoplasms were confirmed or detected on MRU. In 13 cases, no abnormalities were detected on the static, T2 MR urography.

MR urography for assessment of renal function in children

In 54 children (from the whole population), T1 excretory MR urography with injection of Gd has been performed in addition to static, T2 MR urography for the main purpose of our study – to assess the renal function. The majority of them had anomalies of the renal pelvis and ureter: ureteropelvic (UPJ) obstruction (hydronephrosis) – 43 (bilateral – 10, right side – 14, left side – 19); primary megaureter and anomalies of vesicoureteral segment (UVJ) – 30 (bilateral – 8, right side – 8, left side – 14) including 7 patients with vesicoureteric reflux

(VUR), diagnosed by VCUG, ureter duplication – 2; ureterocele – 2. We observed obstructed systems on MR urography morphologically by the presence of narrowed ureter with proximal dilatation and we were able to distinguish obstructed from non-obstructed systems functionally by the presence of delayed contrast excretion into the collecting system and ureter on the basis of the functional analysis in particular by the calculation of renal transit times (RTT). In 40 children MR functional analysis proved the presence of obstructive systems and the remaining 14 children were classified as non-obstructive and they have been followed-up. Both static and excretory MR urography was helpful in differentiating the causes of hydronephrosis in these patients. Typical images of a child with several bilateral ureterocystoneostomies and persistent bilateral hydronephrosis and hydroureters following surgery are shown in Figure 3.

We consider images quality of the kidney and the collecting system to be superior with MR urography in comparison to ultrasound and DTPA renogram in all 96 cases. The agreement of grading of hydronephrosis was equal in MR urography and ultrasound (US), however MR provides a detailed visualization of the entire ureters and presents ureteric pathology clearly US.

A correlation between MRU data and final diagnosis determined by surgery or observation was excellent in all 96 patients. 40 children benefits from surgical interventions for obstructive systems. Pyeloplasty has been performed in 11 with MR findings of ureteropelvic junction (UPJ) obstruction (Figure 4). In 29 children with UVJ obstruction and primary megaureter, reimplantation of the ureters - ureterocystoneostomy (UCNS) has been

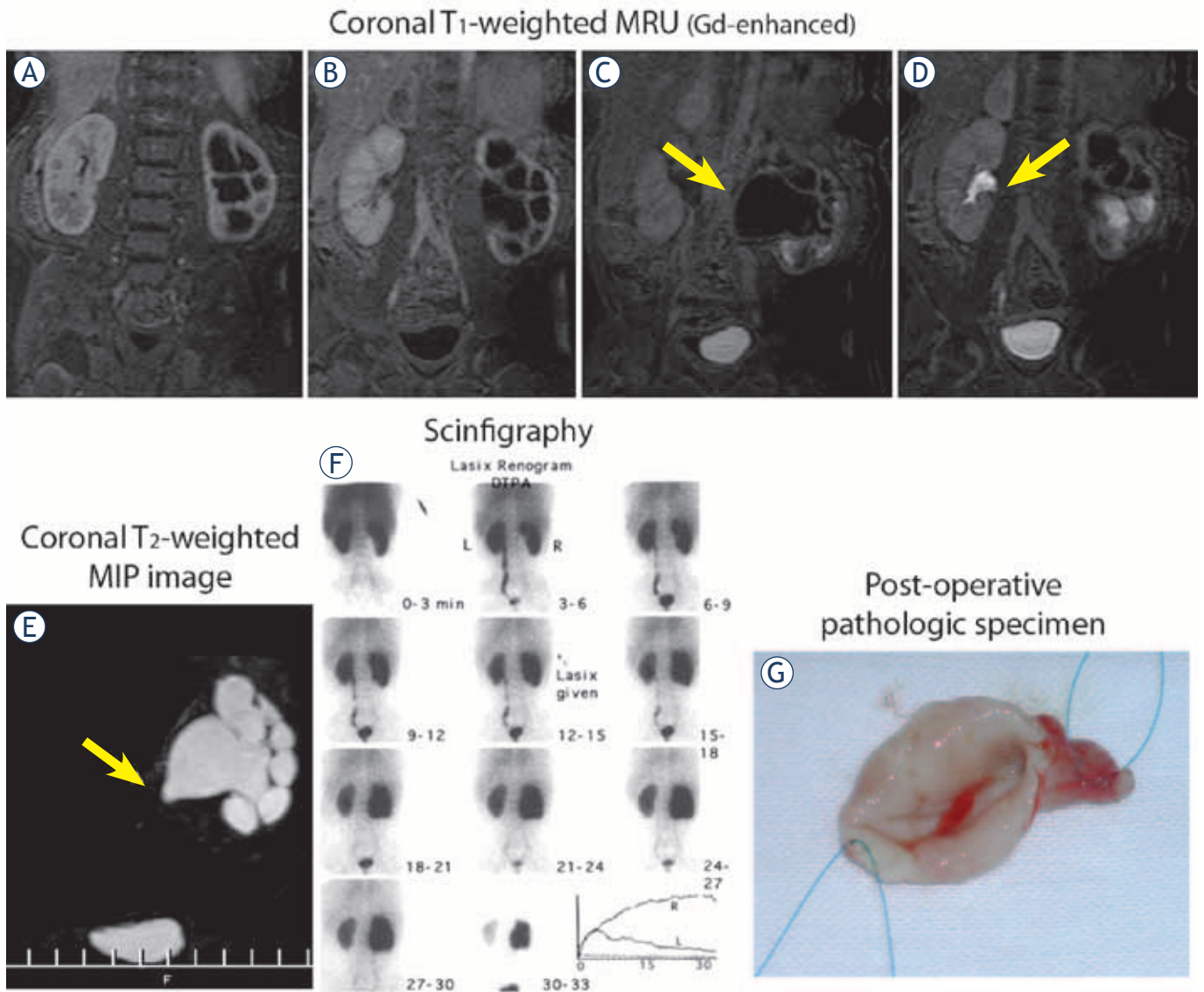


FIGURE 4A-G. Imaging of UPJ obstruction in 9-month-old boy. **A-D.** Consecutive coronal T1-weighted MR images (Gd-enhanced) – successively filling of the right renal pelvis with preservation of the right kidney function. **E.** Coronal T2-weighted MIP image – on the left side an outflow tract obstruction with marked dilatation of the left pyelocalyceal system; **F.** Dynamic ^{99m}Tc -DTPA presenting urinary obstruction of the left kidney; **G.** Postoperative pathologic specimen in the same child following pyeloplasty a modo Anderson-Hynes.

performed (Figure 3). Other surgical interventions (74 in total for the whole study population), such as nephrectomies, partial or atypical kidney resection, nephrostomies, external genitalia corrections, masculinizing surgical procedures, retroperitoneal tumours resections etc. were also confirmed at MR urography.

VCUG was performed in 10 patients. Vesico-ureteric reflux (VUR) in 7 patients and in one case an ureterocele was identified. The vesico-ureteric reflux was classified as grade III in 4 children, grade IV in 2 and grade V in 1; in both cases pre-

sented dilatation of the ureter and the pyelocalyceal system were clearly visible on MR urograms. In two cases VCUG present normal findings.

A comparison of the results from the functional analysis has been done by two different softwares – “CHOP-fMRU” and “ImageJ”, as well as by the data from the ^{99m}Tc -DTPA. The results from the functional analysis of transit times, volumes and volumetric differential renal function are presented on Table 1. No statistically significant differences ($P > 0.05$) were found between the calyceal and renal transit times and the parenchymal kidney

TABLE 1. Calculated transit times, parenchymal volumes and volumetric differential renal function

Transit times		Parenchymal volumes		Volumetric differential renal function			
CHOP-fMRU/ ImageJ	Time (range)	CHOP-fMRU/ ImageJ	Volume (range)	CHOP-fMRU/ ImageJ/NucMed	Percent (range)	SE	SD
CHOP-CTT-R	313 sec. (150-476)	CHOP-Volume-R	134,9 ml (14,3-255,6)	CHOP-vDRF-R	54,15% (44,18-64,11)	3,88	9,50
ImageJ-CTT-R	279 sec. (151-407)	ImageJ-Volume-R	129,2 ml (19,5-238,9)	CHOP-vDRF-L	48,85% (35,88-55,82)	3,88	9,50
CHOP-CTT-L	267 sec. (141-393)	CHOP-Volume-L	147,2 ml (12,4-282,0)	ImageJ-DRF-R	52,40% (44,60-60,20)	3,04	7,44
ImageJ-CTT-L	243 sec. (126-361)	ImageJ-Volume-L	150,3 ml (15,7-284,9)	ImageJ-DRF-L	47,60% (39,80-55,40)	3,04	7,44
CHOP-RTT-R	534 sec. (287-780)			NucMed-DRF-R	51,92% (47,27-56,56)	1,81	4,43
ImageJ-RTT-R	550 sec. (306-793)			NucMed-DRF-L	48,08% (43,44-52,73)	1,81	4,43
CHOP-RTT-L	476 sec. (290-663)						
ImageJ-RTT-L	475 sec. (277-673)5						

Legend: R = right kidney, L = left kidney; CHOP-CTT = mean calyceal transit time measured with CHOP-fMRU; CHOP-RTT = mean renal transit time measured with CHOP-fMRU; ImageJ-CTT = mean calyceal transit time measured with ImageJ; ImageJ-RTT = mean renal transit time measured with ImageJ; CHOP-Volume and ImageJ-Volume = parenchymal volumes, measured with CHOP-fMRU and ImageJ; CHOP-vDRF, ImageJ-vDRF and NucMed-DRF = volumetric differential renal function, measured resp. with CHOP-fMRU, ImageJ and Nuclear Medicine; SE = standard error; SD = standard deviation.

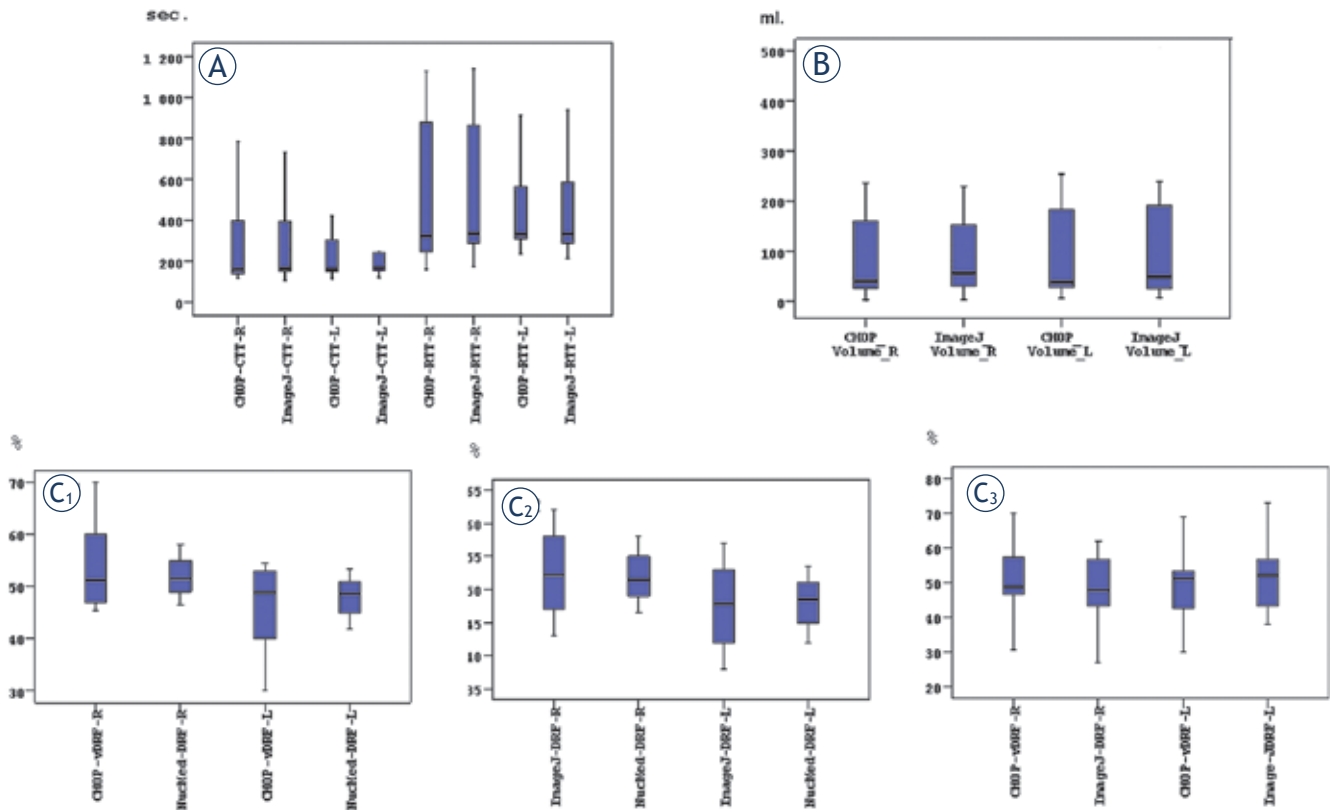


FIGURE 5A-C. Box-plots of different parameters for right and left kidney evaluated by CHOP-fMRU and ImageJ. A. cTT and rTT. B. Parenchymal volumes. C1,2,3. Volumetric differential renal function, as well as 99mTc-DTPA renal function.

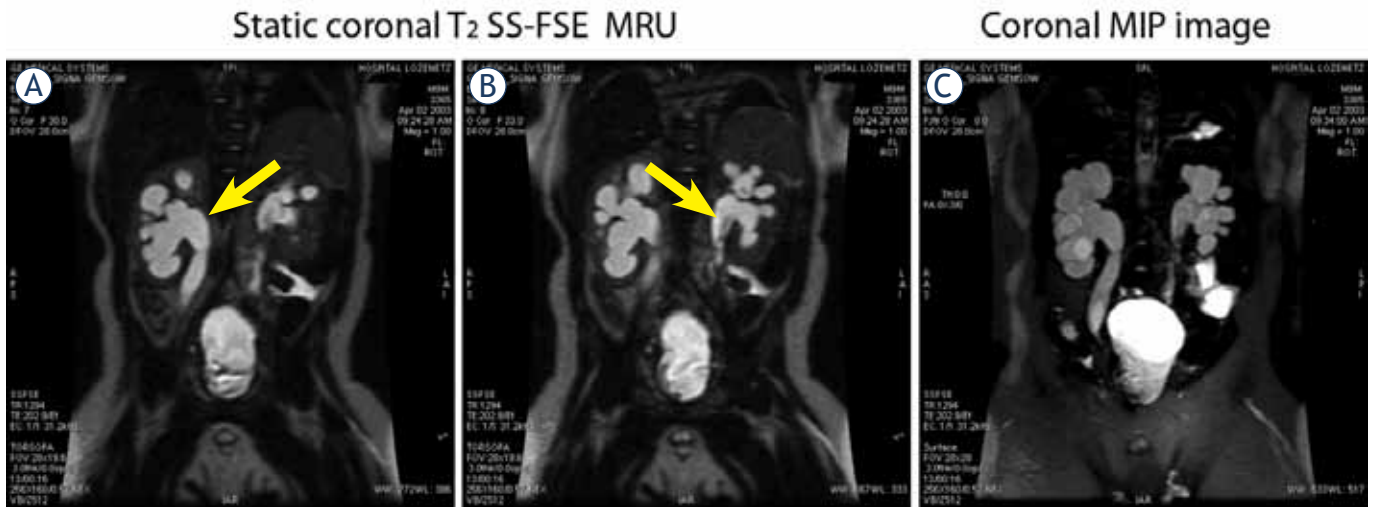


FIGURE 6A-C. MR imaging of persistent bilateral hydronephrosis and hydroureters in 9-month old boy, following ureterocystoneostomy. **A,B.** Static coronal T2-weighted MR images using single-shot fast spin echo (SS-FSE). **C.** Coronal MIP image.

volumes, measured by CHOP-fMRU and ImageJ (Figure 5A,B). The values for the volumetric differential kidney function assessed by CHOP-fMRU and ImageJ measured separately for each kidney were not statistically different to those derived from the Tc-DTPA study ($P>0.05$) (Figure 5C_{1,2,3}). MR urography and renal scintigraphy showed confirmatory results in the diagnosis of obstruction both UPJ and UVJ in terms of volumetric differential renal function values.

Discussion

MRU is a feasible method for evaluation of urinary tract pathology in neonates and infants.^{1,16} It overcomes the limitations of the conventional imaging techniques and is superior tool in many aspects, especially in the evaluation of parenchymal kidney diseases and poorly functioning systems, assessment of ureteral anatomy and renal vasculature as shown in our study. The method is particularly helpful for further therapeutic decisions, planning of surgical intervention and future diagnostic work-up.

The most common MRU techniques, used to visualize the urinary tract, are the static (T_2) MRU and excretory (T_1) MRU.¹⁷⁻¹⁹ Three-dimensional (3D) sequences are used to obtain thin-section data sets that can be further post-processed to create volume-rendered (VR) or maximum-intensity-projection (MIP) images of the entire urinary tract (Figure 6). Similar observations have been as reported by Roy *et al.* and O'Malley *et al.*, using MRU.²⁰⁻²¹ Excretory

(T_1) MRU is similar to CT urography and intravenous urography. The use of dose of Gd (0.1 mmol/kg) and in some occasions low-dose Gd opacification (0.01 mmol/kg) allowed us to maintain the linearity between signal and Gd concentration, which is essential for quantitative measurements and analysis. Administration of diuretics improved the quality of MRU by increasing the quantity of the urine and therefore, leads to better dilution and appropriate distribution of Gd in the urinary tract.²²⁻²³ The most important sequence of excretory MRU in our study was 3D gradient-echo. Fat-suppression is recommended for better demonstration of the ureters. Modern MR-units scan simultaneously in one volume the kidneys, the ureters and the bladder, using 3D gradient-echo sequences in one breath-hold.^{19,24} Sometimes segmental scanning of the kidneys or bladder separately for visualization of image details is recommended.

Currently, there are two major MRU processing software available free of charge, which we have verified, compared each other and used in our practice routinely.^{5,9} Post-processing algorithms permits us to evaluate and compare to scintigraphy several parameters – (i) calycial (cTT) and renal transit times (rTT); (ii) parenchymal volumes; (iii) differentiated renal function (vDRF) and (iv) the time-intensity curves representative for the renal function.

Our results demonstrate that MRU should be a method of choice for visualization of the upper urinary tract in children as it is difficult to assess by US or scintigraphy. In some cases, such as UPJ obstruction, MRU was confirmatory to ultrasound,

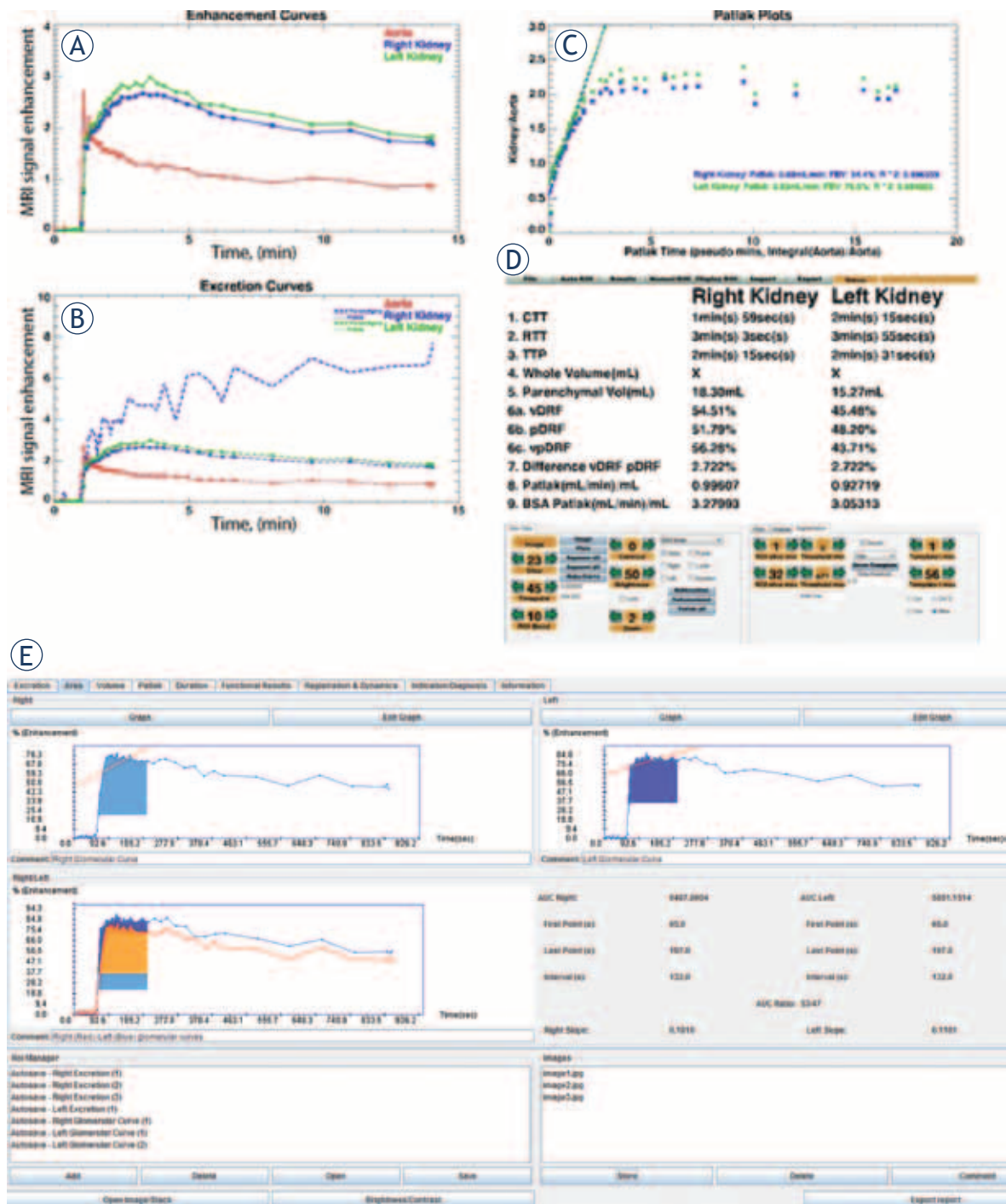


FIGURE 7A-E. Automated functional analysis of MRU data in bilateral normal kidney with vesicoureteral reflux(VUR) – grade 1 on the right side using "CHOP-fMRU". A. Enhancement curves. B. Excretion curves. C. Patlak plots. D. Calculation of renal transit times and differential renal function. E. Enhancement curves, generated on "ImageJ".

but superior concerning the evaluation of end-ureteral anomalies. US provides initial information concerning renal parenchyma, bladder morphology, presence and degree of dilated systems, but failed in visualization of non-accessible ureters, hidden in the retroperitoneum and is pretty weak in information about renal excretion.

The graphic presentation of time-intensity curves, obtained by the dynamic MRU studies, was in accordance with the renal curves, obtained by scintigraphy. Moreover, the calculated values of the volumetric differential renal function, using "CHOP-fMRU" software were similar to those calculated on the basis of ImageJ software; both corresponded to the values from the dynamic ^{99m}Tc -DTPA scintigraphy. Comparable results regarding parenchymal volumes and transit times were observed using the two different software programs. Scintigraphy also supplies information about the renal function and morphology; however it is time-consuming ionizing imaging method with low spatial resolution.^{6,25} In our study, the basic parameters of the curves (amplitude, washout) were assessed, as well as the presence of certain characteristic features of the curve. The data from the "signal-intensity versus time-curve" analysis were combined with the other parameters, derived from the MRU analysis, including estimation of the renal transit times, parenchymal volumes and differential renal function. The resulted data-set provided a powerful tool, of high importance for the diagnosis of obstruction.

In the data processing, several parameters were also calculated, using "CHOP-fMRU" and "ImageJ": CTT – calyceal transit time; RTsT – renal transit time; TTP – time to peak; parenchymal volume; vDRF – volumetric differential renal function; pDRF – Patlak differential renal function etc. Typical example of data processing is shown in Figure 7 – a child with recurrent renal infections and a low-grade vesicoureteral reflux (VUR) on the left side. On non-contrast MRU images dilatation of the distal part of the left ureter was observed, the resulting enhancement curves were non-obstructive and the patient was referred to ultrasonography follow-up. No significant difference concerning the listed parameters was found whatever functional analysis software has been used.

Our results as well as the presented case (Figure 7) showed that both renal and calycial transit times, parenchymal volumes and differential renal function are indicators for kidney dysfunction.

Even small functional disorders can be detected using MRU and analysing these parameters. The complex software functional analysis of the whole patient population confirmed this assumption.

In addition to the advantages of MRU, mentioned above, it is necessary to note that this technique has also some limitations. Sometimes it requires a placement of bladder catheter, administration of furosemide and Gd, sedation and even anaesthesia (for newborns and younger children), as a complementary risk. Breath-hold techniques could not be applied in neonates and small infants and motion artefacts should be at a minimum. Patient preparation and examination itself are time-consuming; post-processing and calculation of functional curves and differential renal function requires additional time.

In 2006, it was demonstrated that some Gd-based contrast agents may provoke the development of nephrogenic systemic fibrosis (NSF) and/or a generalized fibrotic disorder in renal failure patients.²⁶ Gd-ions, released from Gd-based MR contrast agents, are the likely etiologic agent of NSF.²⁷ The ESUR guidelines suggest a very careful administration of Gd in children with renal failure. Absolute contraindications are high levels of creatinine and a glomerular filtration under 30 ml/min/1.73 m². Individual assessment for the indications and the need of contrast-enhanced MR examination was performed after discussions with paediatric nephrologists in cases of glomerular filtration between 30 and 60 ml/min/1.73 m². Written consent should be obtained in spite of the fact that most cases of NSF occurs in adults and the reported cases of NSF without Gd administration. In all patients with high risk for development of NSF and in the paediatric group, we used cyclic Gd-helators due to their higher stability.²⁸ We didn't observe any adverse effects or cases of NSF, following contrast administration in our study-group.

In conclusion, MR urography is useful, non-ionizing method for assessment of obstructive uropathies and facilitates surgical decisions. There is growing number of publications concerning the criteria for assessment of the renal function in children by dynamic MRU, but the achievement of consensus requires more and deeper investigations. The advances of molecular imaging techniques provide new insights about the nature of hereditary diseases in paediatric nephrology and urology.

References

- Vegar-Zubovic S, Kristic S, Lincender L. Magnetic resonance urography in children - when and why? *Radiol Oncol* 2011; **45**: 174-9.
- Miklos M, Gajski G, Garaj-Vrhovac V. Usage of the standard and modified comet assay in assessment of DNA damage in human lymphocytes after exposure to ionizing radiation. *Radiol Oncol* 2009; **43**: 97-107.
- Apaydin M, Varer M, Oztekin O. Radiological considerations in von Hippel-Lindeau disease: imaging findings and the review of the literature. *Radiol Oncol* 2010; **44**: 164-7.
- Kachanov DY, Dobrenkov KV, Shamanskaya TV, Abdullaev RT, Inushkina EV, Savkova RF, et al. Solid tumors in young children in Moscow Region of Russian Federation. *Radiol Oncol* 2008; **42**: 39-44.
- Khrichenko D, Darge K. Functional analysis in MR urography – made simple. *Pediatr Radiol* 2010; **40**: 182-99.
- Avni EF, Bali MA, Regnault M, Damry N, Degroot F, Metens T, et al. MR urography in children. *Eur J Radiol* 2002; **43**: 154-66.
- Grattan-Smith JD, Jones RA. MR urography in children. *Pediatr Radiol* 2006; **36**: 1119-32; quiz 228-9.
- Vivier PH, Blondiaux E, Dolores M, Marouteau-Pasquier N, Brasseur M, Petitjean C, et al. [Functional MR urography in children]. [French]. *Journal de Radiologie* 2009; **90**: 11-9.
- Vivier PH, Dolores M, Taylor M, Dacher JN. MR urography in children. Part 2: how to use ImageJ MR urography processing software. *Pediatr Radiol* 2010; **40**: 739-46.
- Grattan-Smith JD, Little SB, Jones RA. MR urography in children: how we do it. *Pediatr Radiol* 2008; **38** Suppl 1: S3-17.
- Leyendecker JR, Barnes CE, Zagoria RJ. MR urography: techniques and clinical applications. *Radiographics* 2008; **28**: 23-46; 46-7.
- Grattan-Smith JD, Perez-Bayfield MR, Jones RA, Little S, Broecker B, Smith EA, et al. MR imaging of kidneys: functional evaluation using F-15 perfusion imaging. *Pediatr Radiol* 2003; **33**: 293-304.
- Cengiz M, Baysal Z, Ganidagli S. Oral sedation with midazolam and diphenhydramine compared with midazolam alone in children undergoing magnetic resonance imaging. *Paediatr Anaesth* 2006; **16**: 621-6.
- Lin TF, Yeh YC, Yen YH, Wang YP, Lin CJ, Sun WZ. Antiemetic and analgesic-sparing effects of diphenhydramine added to morphine intravenous patient-controlled analgesia. *Br J Anaesth* 2005; **94**: 835-9.
- Ring E, Riccabona M, Fotter R. Normal values: pediatric urology. Berlin: Springer; 2008. p. 507-14.
- Riccabona M, Simbrunner J, Ring E, Ruppert-Kohlmayr A, Ebner F, Fotter R. Feasibility of MR urography in neonates and infants with anomalies of the upper urinary tract. *Eur Radiol* 2002; **12**: 1442-50.
- Nolte-Ernsting CC, Staatz G, Tacke J, Gunther RW. MR urography today. *Abdom Imaging* 2003; **28**: 191-209.
- Garcia-Valtuille R, Garcia-Valtuille AI, Abascal F, Cerezal L, Arguello MC. Magnetic resonance urography: a pictorial overview. *Br J Radiol* 2006; **79**: 614-26.
- Nolte-Ernsting CC, Adam GB, Gunther RW. MR urography: examination techniques and clinical applications. *Eur Radiol* 2001; **11**: 355-72.
- Roy C, Saussine C, Guth S, Horviller S, Tuchmann C, Vasilescu C, et al. MR urography in the evaluation of urinary tract obstruction. *Abdom Imaging* 1998; **23**: 27-34.
- O'Malley ME, Soto JA, Yucel EK, Hussain S. MR urography: evaluation of a three-dimensional fast spin-echo technique in patients with hydronephrosis. *AJR Am J Roentgenol* 1997; **168**: 387-92.
- Szopinski K, Szopinska M, Borowka A, Jakubowski W. Magnetic resonance urography: initial experience of a low-dose Gd-DTPA-enhanced technique. *Eur Radiol* 2000; **10**: 1158-64.
- Hughes J, Jan W, Goodie J, Lund R, Rankin S. MR urography: evaluation of different techniques in non-dilated tracts. *Clin Radiol* 2002; **57**: 989-94.
- Sudah M, Vanninen R, Partanen K, Heino A, Vainio P, Ala-Opas M. MR urography in evaluation of acute flank pain: T2-weighted sequences and gadolinium-enhanced three-dimensional FLASH compared with urography. Fast low-angle shot. *AJR Am J Roentgenol* 2001; **176**: 105-12.
- Borthne A, Pierre-Jerome C, Nordshus T, Reiseter T. MR urography in children: current status and future development. *Eur Radiol* 2000; **10**: 503-11.
- Thomsen HS, Marckmann P. Extracellular Gd-CA: differences in prevalence of NSF. *Eur J Radiol* 2008; **66**: 180-3.
- Abraham JL, Thakral C, Skov L, Rossen K, Marckmann P. Dermal inorganic gadolinium concentrations: evidence for in vivo transmetallation and long-term persistence in nephrogenic systemic fibrosis. *Br J Dermatol* 2008; **158**: 273-80.
- Martin DR, Sharma P, Salman K, Jones RA, Grattan-Smith JD, Mao H, et al. Individual kidney blood flow measured with contrast-enhanced first-pass perfusion MR imaging. *Radiology* 2008; **246**: 241-8.

Cathepsin H indirectly regulates morphogenetic protein-4 (BMP-4) in various human cell lines

Matija Rojnik¹, Zala Jevnikar¹, Bojana Mirkovic¹, Damjan Janes¹, Nace Zidar², Danijel Kikelj², Janko Kos¹

¹ Department of Pharmaceutical Biology, Faculty of Pharmacy, University of Ljubljana, Ljubljana, Slovenia

² Department of Pharmaceutical Chemistry, Faculty of Pharmacy, University of Ljubljana, Ljubljana, Slovenia

Received 15 July 2011

Accepted 13 September 2011

Correspondence to: Prof. Dr. Janko Kos, University of Ljubljana, Faculty of Pharmacy, Aškerčeva 7, SI-1000 Ljubljana, Slovenia. Phone: +386 1 4769 604; Fax: +386 1 4258 031; E-mail: janko.kos@ffa.uni-lj.si

Disclosure: No potential conflicts of interest were disclosed.

Background. Cathepsin H is a cysteine protease considered to play a major role in tumor progression, however, its precise function in tumorigenesis is unclear. Cathepsin H was recently proposed to be involved in processing of bone morphogenetic protein 4 (BMP-4) in mice. In order to clarify whether cathepsin H also regulates BMP-4 in humans, its impact on BMP-4 expression, processing and degradation was investigated in prostate cancer (PC-3), osteosarcoma (HOS) and pro-monocytic (U937) human cell lines.

Materials and methods. BMP-4 expression was found to be regulated by cathepsin H using PCR array technology and confirmed by real time PCR. Immunoassays including Western blot and confocal microscopy were used to evaluate the influence of cathepsin H on BMP-4 processing.

Results. In contrast to HOS, the expression of BMP-4 mRNA in U937 and PC3 cells was significantly decreased by cathepsin H. The different regulation of BMP-4 synthesis could be associated with the absence of the mature 28 kDa cathepsin H form in HOS cells, where only the intermediate 30 kDa form was observed. No co-localization of BMP-4 and cathepsin H was observed in human cell lines and the multistep processing of BMP-4 was not altered in the presence of specific cathepsin H inhibitor. Isolated cathepsin H does not cleave mature recombinant BMP-4, neither with its amino- nor its endopeptidase activity.

Conclusions. Our results exclude direct proteolytic processing of BMP-4 by cathepsin H, however, they provide support for its involvement in the regulation of BMP-4 expression.

Key words: bone morphogenetic protein 4; cancer; cathepsin H; human cell lines; proteolytic enzymes

Introduction

Cathepsin H (CTSH) (EC.4.22.16), a cysteine protease, is ubiquitous in cells and tissues, but its physiological role is poorly understood.^{1,2} CTSH acts mainly as an aminopeptidase but also exhibits limited endopeptidase activity.³ In addition to heavy and light chains, which are typical of a number of mammalian papain-like cysteine proteases, mature CTSH also contains an octapeptide EPQNCSAT, termed the mini-chain, that originates from the propeptide and is bound to the

mature form by a disulphide bond.⁴ The mini-chain is essential for the aminopeptidase activity of CTSH.⁵

CTSH is synthesized as a preproenzyme of 41 kDa which is proteolytically activated through a multistep process to a 30 kDa intermediate form and finally to the single chain mature form of 28 kDa.⁶ This form can be further processed to a 22 kDa heavy chain and a 5-6 kDa light chain.^{2,3,7}

CTSH was identified to play an important role in the establishment and development of a functional tumor vasculature and increases the meta-

static potential of human hepatoma cell lines.⁸⁻¹⁰ Expression of CTSH differs in breast carcinoma¹¹, colorectal cancer¹², melanoma¹³, head and neck carcinoma^{14,15}, glioma¹⁶ and prostate cancer¹⁷ and from that in normal tissue. CTSH is associated with physiological and pathological processes of the lung.¹⁸⁻²⁰ Furthermore, it is involved in the N-terminal processing step of surfactant protein C in type II pneumocytes and pro-granzyme B in cytotoxic lymphocytes.^{21,22} Bone morphogenetic protein 4 (BMP-4) is a potential target for CTSH endopeptidase activity during the differentiation of mouse lungs, and lower activity was proposed to lead to marked accumulation of BMP-4 protein and disruption of branching morphogenesis.²³

BMP-4, as a member of the transforming growth factor β family is involved in the development of many organs and tissues and was shown to play a role in cancer progression.²⁴⁻²⁶ BMP-4 is synthesized as a large inactive precursor which is proteolytically cleaved to the mature protein in a multi-step process.²⁷ Non-processed BMP-4 is targeted to the lysosomes for degradation which can lead to severe loss of BMP-4 activity in specific tissues.^{28,29}

Lü *et al.*²³ presented evidence that CTSH and BMP-4 expression coincides during branching morphogenesis in mouse models. They showed that inhibition of CTSH leads to accumulation of the mature BMP-4 in embryonic mouse lungs. However, they failed to demonstrate the cleavage of BMP-4 by mature 28 kDa CTSH *in vitro*.

In this study we have evaluated the role of human CTSH in BMP-4 processing and regulation at the mRNA and protein level, using various human cell lines.

Materials and methods

Cell culture

Human U937 pro-monocytic (CRL-1593.2; ATCC, Manassas, VA, USA) and WEHI231 mouse lymphoma cells (CRL-1702 cell line; ATCC, Manassas, VA, USA) were maintained in advanced RPMI 1640 (Gibco, Invitrogen, Scotland) supplemented with 2mM glutamine (Sigma, St. Louis; MO, USA), antibiotics (Penicillin-Streptomycin, Sigma, St. Louis, USA) and 10% fetal bovine serum (FBS) (HyClone, Logan, USA). U937 cells were differentiated with PMA (50 nM) (Sigma, St. Louis; MO, USA) for 24 h to achieve attachment. Human osteosarcoma HOS cells (CRL-1543 cell line, ATCC, Manassas, VA, USA) were grown in minimal essential medium (MEM) (Sigma, St. Louis, MO, USA) supple-

mented with 2.2 g/L sodium bicarbonate (Riedel de Haën, St. Louis, MO, USA), 2 mM glutamine, antibiotics and 10% FBS. Human prostate cancer PC-3 cells (cell line CRL-1435, ATCC, Manassas, VA) were cultured in DMEM/F12 (1:1) medium (Gibco, Invitrogen, Scotland) supplemented with antibiotics, 2 mM glutamine and 10% FBS.

Western blot analysis

Lysates of HOS, PC-3 and PMA differentiated U937 cells were prepared in 50 μ l of 0.05 M sodium acetate buffer (pH 6) with added 1mM EDTA, 0.1 M NaCl, 0.25% Triton X-100 (lysis buffer). Complete lysis of the cells was achieved by three 5 to 7 s sonication cycles. Clear supernatants were obtained after centrifugation at 4°C and 16200 g for 15 min. Total protein concentration was determined by the Bradford method using Coomassie Plus Protein Assay reagent (Pierce, Thermo Fischer Scientific) with BSA (Sigma, St. Louis; MO, USA) as standard. Samples containing 100 μ g of proteins were heated at 100°C in reducing sample buffer for 10 min, separated by 12% SDS-PAGE and transferred to nitrocellulose membranes. The molecular weight of the proteins was determined using SeeBlue® Plus2 Pre-Stained Standard (Invitrogen, USA). The membrane was blocked in 5% skimmed milk in Tween-PBS for 30 min and incubated with sheep polyclonal anti-cathepsin H (5 μ g/ml)³⁰ or goat polyclonal anti-BMP4 (dilution 1:400, sc-6896, Santa Cruz Biotechnology, CA, USA) antibodies overnight at 4°C. After washing with Tween-PBS the membrane was incubated with secondary HRP conjugated rabbit anti-sheep (1:10000, sc-2770, Santa Cruz Biotechnology, CA, USA) or donkey anti-goat (1:10000, Santa Cruz Biotechnology, CA, USA) antibodies for 2 h at room temperature.

Real Time PCR analysis

PCR-arrays (Common Cytokine PCR Array; PAHS-021, SABiosciences, MD, USA) were used according to the manufacturer's protocol. RNA was isolated from U937 cells treated with 0.5 μ M native human liver CTSH (nCTSH) and compared to RNA from control cells. Data was analyzed using RT² Profiler PCR Array Data Analysis (SABiosciences, MD, USA). Quantitative Real Time PCR (qPCR) was performed as reported.³¹ Total RNA was isolated from U937, HOS and PC-3 cells using RNeasy Mini kit (Qiagen, Hilden, Germany) according to manufacturer's protocol.

For cDNA synthesis 1 µg of total mRNA was reverse transcribed using OmniscriptRT Kit (Qiagen, Hilden, Germany). qPCR was carried out on an ABI PRISM 7000 apparatus (Applied Biosystems, Life Technologies Corporation, CA, USA) in a total reaction volume of 25 µl containing 5 µl cDNA of different concentrations, BMP4 QuantiTect Primer Assay (Qiagen, Hilden, Germany) and Maxima™ SYBR Green/ROX qPCR Master Mix (2x) (Fermentas International Inc, Ontario, Canada). The cycling program was 2 min at 50°C, 10 min at 95°C, followed by 40 cycles (15 s at 95°C and 60 s at 60°C). Multiple housekeeping genes were checked (the primer sequences were found in the Real Time PCR Primer and Probe Data Base) for their stability using geNorm normalization. The data was normalized to the endogenous controls HPRT and GAPD for U937, HPRT and YWHAZ for HOS and PC-3. A melting curve of PCR products (60-95°C) was also performed to ensure the absence of artefacts. All assays were performed in parallel and in three biological repetitions.

Confocal immunofluorescence microscopy

HOS and PC-3 cells were grown on glass coverslips in 24-well plates for 24 h prior to the experiment; U937 cells were differentiated with PMA (50 nM) for 24 h. WEHI231 were seeded on slides and cytopinned for 6 min at 2500 g. Before labeling, cells were fixed with 4% paraformaldehyde in PBS (pH 7.4) for 30 min and permeabilized with 0.1% Triton X-100 in PBS (pH 7.4) for 10 min. Non-specific staining was blocked with 3% BSA in PBS (pH 7.4). CTSH was labeled with primary mouse monoclonal anti-CTSH 1D10 antibody (10 µg/ml of 3% BSA in PBS).³⁰ Goat polyclonal anti-human BMP4-N16 antibody was used for BMP-4 labeling (Santa Cruz Biotechnology, CA, USA). After 2 h of incubation, cells were washed three times with PBS and treated with Alexa 488-labeled rabbit anti-mouse and Alexa 555-labeled donkey anti-goat (2:1000, Molecular Probes, Invitrogen, USA) antibodies for 2 h. After washing with PBS, ProLong Antifade kit (Molecular Probes, Invitrogen, USA) was mounted on dried coverslips and allowed to dry overnight at 4°C. Cells were studied by fluorescence microscopy at room temperature using a Carl Zeiss LSM 510 confocal microscope (Carl Zeiss Inc., Jena, Germany); immersion oil was used as imaging medium. Images were analyzed using Carl Zeiss LSM image software 3.0.

Synthesis of specific synthetic irreversible inhibitor of CTSH - H₂N-Ser(OBzl)-CHN₂ (CTSHi)

(S)-(9H-Fluoren-9-yl)methyl (1-(benzyloxy)-4-diazo-3-oxobutan-2-yl)carbamate (A). Triethylamine (0.175 mL, 1.258 mmol) in THF (3 mL) was added to a stirred solution of Fmoc-L-Ser(Bzl)-OH (1, 500 mg, 1.198 mmol) in THF (6 mL) at -20°C under argon, followed by the addition of ethyl chloroformate (0.120 mL, 1.258 mmol) in THF (3 mL). The mixture was stirred for 30 minutes at -5°C, after which the precipitated Et₃NH⁺Cl⁻ was filtered off. Acetonitrile (5 mL) and trimethylsilyldiazomethane (2.0 M sol. in hexane, 1.198 mL, 2.395 mmol) were added to the filtrate and the mixture was stirred overnight at +4°C. Ethyl acetate (50 mL) was added and organic phase washed successively with 10% aq. citric acid (2 × 20 mL), sat. aq. NaHCO₃ (2 × 20 mL) and brine (2 × 20 mL). The organic phase was dried over Na₂SO₄, filtered and the solvent evaporated under reduced pressure. The crude product was purified with flash column chromatography using ethyl acetate/petroleum ether (1:4) as eluent to afford 2 as a pale yellow solid (378 mg, 0.856 mmol). Yield: 71%; R_f = 0.43 (EtOAc/petroleum ether = 1:1); IR (KBr): ν = 3552, 3414, 3311, 3076, 2859, 2106 (C=N=N), 1800, 1696, 1630, 1534, 1450, 1385, 1293, 1266, 1103, 1029, 736 cm⁻¹. ¹H NMR (DMSO-d₆): δ 3.60-3.69 (m, 2H, CH₂), 4.21-4.37 (m, 4H, CH, CH, CH₂), 4.49 (s, 2H, CH₂Ph), 6.07 (s, 1H, CHN₂), 7.26-7.44 (m, 9H, Ar-H), 7.74 (d, 2H, J = 7.2 Hz, Ar-H), 7.84 (d, 1H, J = 8.1 Hz, NH), 7.90 (d, 2H, J = 7.5 Hz, Ar-H). MS (ESI): m/z (%) = 464 ([M+Na]⁺, 33), 414 ([MH-N₂]⁺, 35). (S)-3-Amino-4-(benzyloxy)-1-diazobutan-2-one (B). To a solution of A (150 mg, 0.340 mmol) in acetonitrile (10 mL), diethylamine (10 mL) was added and the mixture stirred at room temperature. After 20 min the mixture was concentrated under reduced pressure and purified with flash column chromatography using dichloromethane/methanol (20:1) as eluent, to afford 3 as a yellow oil (20 mg, 0.091 mmol). Yield: 27%; R_f = 0.23 (CH₂Cl₂/MeOH = 10:1); ¹H NMR (CDCl₃): δ 1.73 (br s, 2H, NH₂), 3.59-3.70 (m, 3H, CH, CH₂), 4.55 (s, 2H, CH₂Ph), 5.79 (s, 1H, CHN₂), 7.31-7.40 (m, 5H, Ph).

Analytical TLC was performed on silica gel Merck 60 F254 plates (0.25 mm), using visualization with UV light and ninhydrin. Column chromatography was carried out on silica gel 60 (particle size 240-400 mesh). ¹H NMR spectra were recorded at 300 MHz on a Bruker AVANCE DPX300 spectrometer in CDCl₃ or DMSO-d₆ solution, with TMS as the internal standard. IR spectra were re-

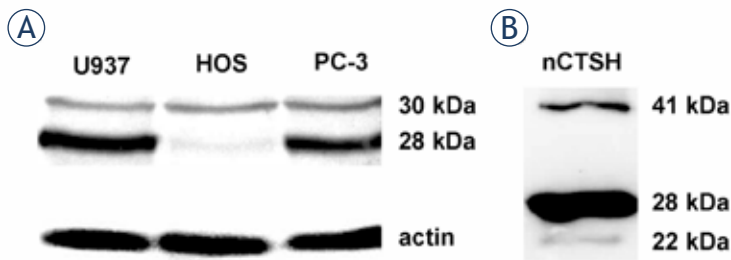


FIGURE 1. CTSH processing forms. (A) Different forms of CTSH were detected in human cell lines and (B) in the sample of nCTSH using Western blot. CTSH was visualized with sheep anti-CTSH primary pAb and rabbit anti-sheep horse radish peroxidase (HRP) labeled secondary antibody. The intermediate 30 kDa CTSH form is present in all of the selected cell lines, while the mature 28 kDa CTSH form is missing in HOS cells. A procathepsin H (41 kDa) and single chain form (22 kDa) could be detected in smaller amounts compared to the mature forms. nCTSH contains the procathepsin H, the mature and heavy chain forms.

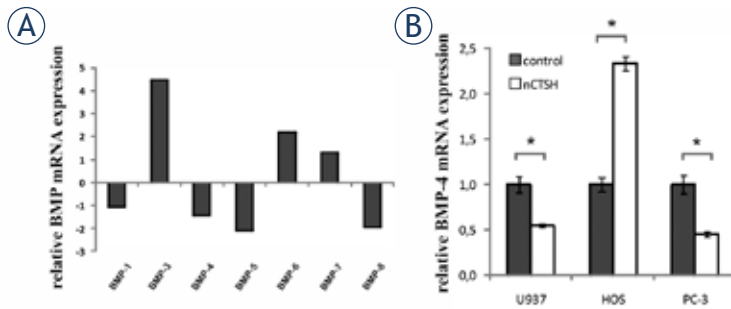


FIGURE 2. CTSH dependent cytokine mRNA expression. (A) The effect of CTSH on the mRNA expression of cytokines from BMP family. Differentiated U937 cells were incubated with 0.5 μ M nCTSH and the mRNA levels were screened by PCR-arrays enabling simultaneous screen of the of 84 cytokine genes. The expression of BMP-2 is not presented, while it was probably an artifact, as shown by the analysis of the melting curve. (B) The influence of CTSH on BMP-4 mRNA expression was further evaluated with quantitative real time PCR analysis in U937, HOS and PC-3 cell lines. Cells were treated with 0.5 μ M nCTSH for 24 h. The mRNA levels obtained from control samples were normalized to 1. Each bar represents the mean \pm SD. Ns, non-significant, * P <0.05.

recorded on a Perkin-Elmer 1600 FT-IR spectrometer. Mass spectra were obtained using a VGAnalytical Autospec Q mass spectrometer.

Inhibition constants for CTSH (k_2 2938.3 $s^{-1}M^{-1}$) and CTSB (k_2 5.1 $s^{-1}M^{-1}$) were similar as referred in the literature.³²

Cleavage of mature human recombinant BMP-4 protein

nCTSH was tested for its ability to degrade human recombinant BMP-4 protein (GenwayBio, San Diego, CA, USA). BMP-4 (7.5 μ M) was incubated with nCTSH (0.75 μ M) for 1.5 h at 37°C in

CTSH activity buffer (pH 6.8) using the same protocol as Obermajer *et al.*³³ nCTSH was pretreated with 10 μ M CTSHi or DMSO for controls. Samples were analyzed using 12% SDS-PAGE followed by Western blot or reverse-phase HPLC (Shimadzu Cooperation, Japan) using a Discovery BIO Wide Pore C5 column (Sigma, St.Louis, MO, USA) with UV-VIS detector.

Statistical analysis

SPSS PC software (Release 13.0) was used for statistical analysis. Statistical significance was evaluated by Student's t test. P values of less than 0.05 were considered to be statistically significant.

Results

Different processing forms of CTSH

The presence of different processing forms of CTSH was determined by Western blot in U937, HOS and PC-3 cell lines (Figure 1A). A 30 kDa intermediate form was detected in all selected cell lines, while the mature single chain 28 kDa form was absent in HOS cells. Only small quantities of the 22 kDa heavy chain (from the two-chain form) were detected in human cell lines (data not shown). The sample of CTSH isolated from human liver (nCTSH)³⁰ contains predominantly mature 28 kDa form (Figure 1B), with a small amount of 22 kDa heavy chain. It is likely that the 30 kDa form was further processed to mature and heavy chain forms.

CTSH regulates the expression of BMP family genes

The effect of CTSH on human cytokine mRNA levels was screened by PCR-array, enabling simultaneous expression of 84 cytokine genes. Incubation of differentiated U937 cells with nCTSH (0.5 μ M) induced significant changes in the expression of several BMP family genes. BMP-3, 6 and 7 were significantly up-regulated, while BMP-4, 5 and 8 were down-regulated (Figure 2A). The expression of BMP-1 was not altered. CTSH dependent regulation of BMP-4 mRNA expression in human cell lines was further confirmed by specific quantitative real time PCR analysis (Figure 2B). After the addition of nCTSH, BMP4 mRNA levels in HOS increased 2.33 ± 0.08 fold, while BMP-4 mRNA levels in U937 and PC-3 were decreased 0.55 ± 0.01 and 0.45 ± 0.03 fold.

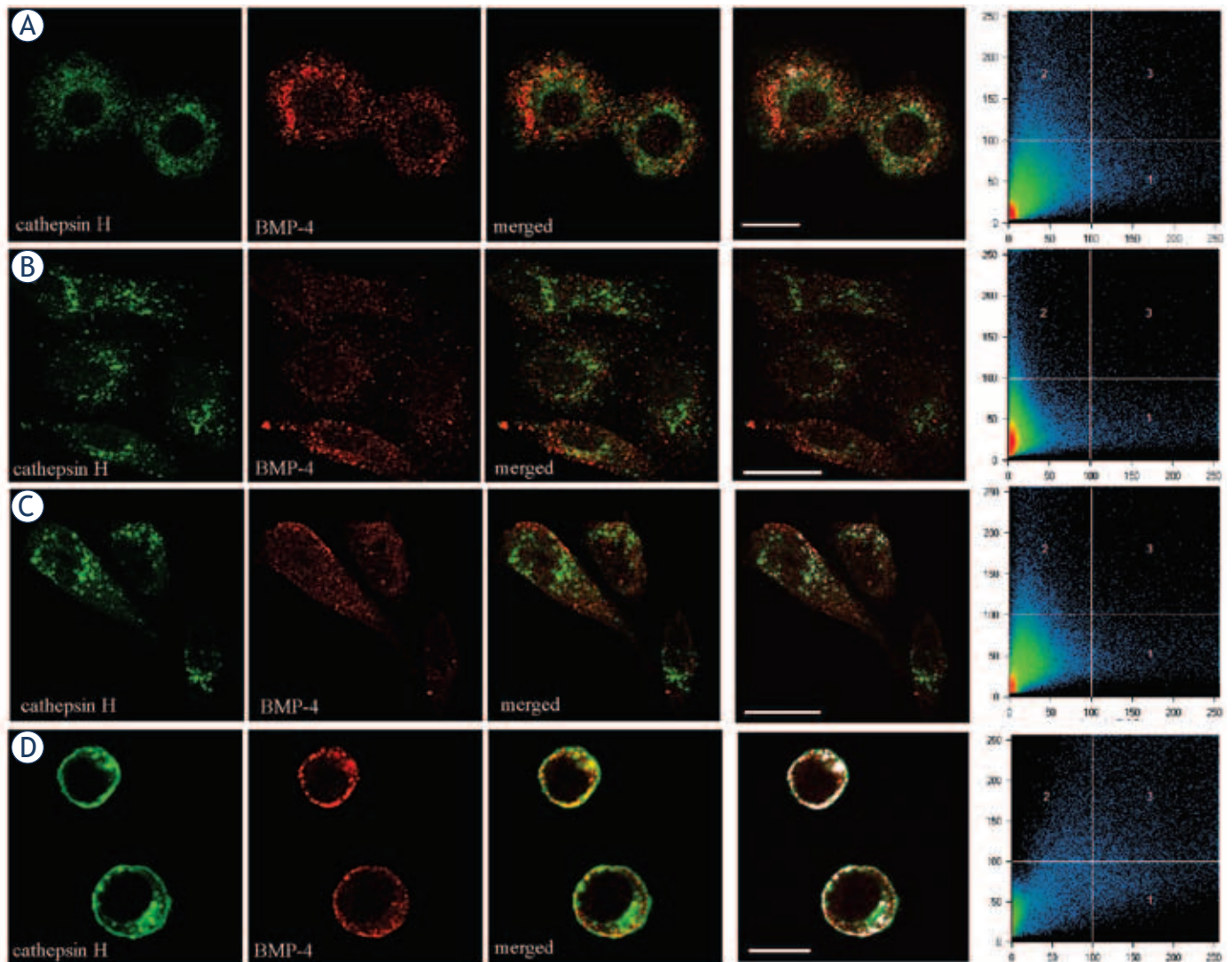


FIGURE 3. Co-localization of CTSH (green fluorescence) and BMP-4 (red fluorescence) in U937 (A), HOS (B), PC-3 (C) and WEHI231 (D) cells. Weak or no co-localization was found in selected human cells (A, B, C), while clear co-localization can be seen in mouse WEHI231 cell line (D). CTSH was labeled with 1D10 monoclonal primary antibody and anti-mouse AlexaFluor™488 secondary antibody. BMP-4 was labeled with primary goat polyclonal anti-BMP-4 antibody (Santa Cruz) and anti-goat AlexaFluor™ 555 secondary antibody. The sites of co-localization are shown in white (frame 4) and correspond to the pixels that are over the threshold in both channels (frame 5). Scale bars represent 5 μm (A and D) and 20 μm (B and C).

CTSH is not involved in the proteolytic processing of BMP-4

No significant co-localization of CTSH and BMP-4 was observed in human U937, HOS, PC-3 cells under confocal microscopy. To present the difference between the co-localization of CTSH and BMP-4 in human and in mouse cells mouse WEHI231 cells were used revealing strong co-localization of both proteins (Figure 3). Furthermore, the role of CTSH in the intracellular degradation of mature BMP-4 was determined using a specific synthetic irreversible inhibitor of CTSH – $\text{H}_2\text{N-Ser(OBzl)-CHN}_2$ (CTSHi; 5 μM).³² The inhibition of CTSH was fol-

lowed by SDS-PAGE and Western blot analysis (Figure 4A). No increase of mature BMP-4 was observed in U937, HOS and PC-3 cells treated with CTSHi, indicating that CTSH inhibition does not have a direct impact on BMP-4 processing or degradation in human cells. Intramolecular cleavage of BMP-4 by CTSH endopeptidase activity was excluded *in vitro* by incubation of recombinant BMP-4 and nCTSH. No additional protein bands appeared on Western blots (Figure 4B). The products of the proteolytic cleavage were also analyzed by reverse phase HPLC to detect possible N-terminal cleavage of BMP-4 by CTSH aminopeptidase activity. No changes in the height or area of the BMP-4

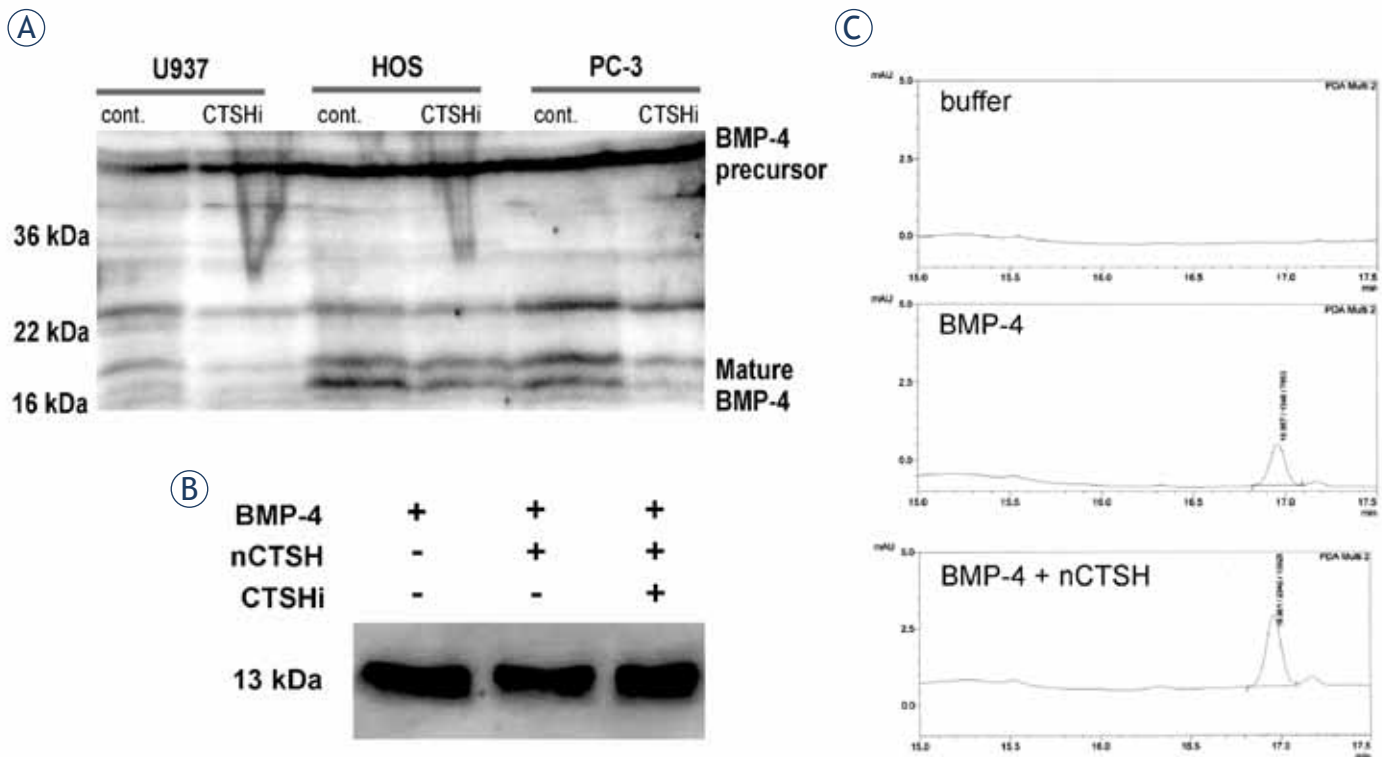


FIGURE 4. CTSH processing of mature BMP-4 protein. (A) Human cell lines were treated with 5 μ M CTSHi for 24 h and then cell lysates were analyzed using Western blot. Proteins (50 μ g) from cell lysates were separated on SDS-PAGE and transferred on to PVDF membrane. BMP-4 was detected with anti-BMP-4 N16 antibody (Santa Cruz) and then with secondary antibody labelled with HRP. The molecular mass in kDa is indicated on the left hand side of the blots. Molecular mass of the mature BMP-4 is detected to be approximately 18 kDa. (B) Using Western blot we analyzed the products of the reaction between mature human recombinant BMP-4 and nCTSH. Mature human recombinant BMP-4 was incubated for 1.5 h at 37°C in CTSH activity buffer (lane 1), with 60 ng of nCTSH in CTSH activity buffer (lane 2) and 60 ng of nCTSH in CTSH activity buffer that was pre-treated for 10 min with 10 μ M CTSHi (lane 3). Mature human recombinant BMP-4 has a molecular mass of 13 kDa. (C) Using reverse phase HPLC we analyzed CTSH activity buffer (buffer), mature human recombinant BMP-4 in CTSH activity buffer (BMP-4) and the products of the reaction between mature human recombinant BMP-4 and nCTSH in CTSH activity buffer (BMP-4 + nCTSH). BMP-4 was eluted in the fraction around 17.0 min.

peak were observed after incubation with nCTSH, excluding significant amounts of aminopeptidase processing (Figure 4C).

Discussion

BMP-4 regulates cell proliferation, differentiation, apoptosis and cell fate throughout mammalian development.³⁴ CTSH has been suggested to regulate its recycling or degradation in the developing lung of mice.²³ In the current study, we identified CTSH as a regulator of BMP-4 mRNA expression in human cell lines, however, we excluded direct proteolytic processing of BMP-4 by CTSH amino- or endopeptidase activity.

CTSH expression is ubiquitous, with very high levels in the kidney.³⁵ There is growing evidence that its expression changes under various pathological conditions, the most extensively studied

being its role in cancer.^{17,36,37} However, its natural substrates and mechanism of action are not known. Using Western blot we have detected different processing forms of CTSH in human prostate cancer (PC-3), osteosarcoma (HOS) and pro-monocytic (U937) cell lines. Whereas the 41 kDa proenzyme and 30 kDa intermediate were present in all cell lines, the mature 28 kDa form was missing in human osteoblasts HOS. The 28 kDa single chain is believed to be the most important form of active CTSH in exerting specific aminopeptidase activity.⁵ However, del Re *et al.*³⁶ demonstrated that in colorectal carcinoma the expression of the 30 kDa form is decreased, while the expression of the mature 28 kDa form is increased in tumor comparing to normal tissue, thus showing the importance of different CTSH processing forms.

We attempted to identify potential targets of CTSH proteolytic activity in human cells, using PCR array technology. In U937 cells a strong as-

sociation between CTSH and mRNA expression of BMP family members was observed. The results of quantitative real time PCR demonstrate that CTSH affects BMP-4 mRNA expression differently in selected cell lines. In U937 and PC-3 cells the addition of nCTSH decreased the expression of BMP-4, whereas in HOS cells the level of BMP-4 mRNA was increased. Interestingly, in HOS cells, where the 28 kDa single chain form of CTSH is missing, the trend of BMP-4 mRNA regulation by nCTSH is opposite to that in U937 and PC-3 cells, where this form is present. This implies that CTSH dependent regulation of BMP-4 mRNA expression is probably controlled by the mature chain form of CTSH, possibly interfering with the promoter of BMP-4 biosynthesis.

Proteolytic processing by BMP-4 is dependent on the proteolytic activity at the two different sites, S1 and S2, in BMP-4 pro-domain.³⁸ Cleavage of the S2 site is enhanced in slightly acidic conditions, as occurs in subcellular organelles like endosomes and lysosomes. Other studies also stressed the need of lysosomal (and proteasomal) function for processing of BMP-4.²⁸ Therefore, CTSH as a lysosomal protease could be involved in BMP-4 proteolytic cleavage and, indeed, the endopeptidase activity of the 22 kDa form of CTSH was proposed to cleave BMP-4.²³ Confocal microscopy was used to determine whether CTSH protein is co-localized with BMP-4, thus being capable of its proteolytic degradation. No co-localization between the two proteins was found in human cell lines, indicating that CTSH and BMP-4 are not present in the same subcellular organelles, so it is unlikely that CTSH is involved directly in the processing or degradation of BMP-4. Furthermore, inhibition of CTSH did not alter the processing of BMP-4 or increase the levels of mature BMP-4 in human cells. These results strongly suggest that CTSH has no direct role in intracellular BMP-4 proteolytic cleavage in the selected human cells. On the other hand, in mouse WEHI231 cells, the significant co-localization of CTSH and BMP-4 indicates the possible involvement of CTSH in BMP-4 protein processing and showing presumably different processing of BMP-4 in mice compared to humans

To confirm a possible indirect action of nCTSH on human recombinant BMP-4 by either endopeptidase or aminopeptidase activity *in vitro*, Western blot analysis was performed, clearly showing that nCTSH, which contains both the mature 28 kDa and heavy chain 22 kDa, does not cleave mature BMP-4 as an endopeptidase. Moreover, using reverse phase HPLC analysis of BMP-4 following

incubation with nCTSH, we demonstrated that the N-terminal of human recombinant BMP-4 is also not cleaved by its aminopeptidase activity. The latter is consistent with the fact that CTSH is not able to hydrolyze substrates by its aminopeptidase activity if proline is at the S₁' position³⁹, as is the case at the N-terminal of mature human BMP-4, which starts with the Ser-Pro-Lys-His-His- sequence.⁴⁰

BMP-4 plays an important role in the differentiation and proliferation of neural⁴¹, and colorectal cancer stem cells⁴² and is a critical component in regulating hematopoietic stem cell function.⁴³ The involvement of cysteine cathepsins in the migratory potential and differentiation of stem cells was studied before.⁴⁴ Our results imply that CTSH might be important in the processes of stem cell differentiation by regulating the expression of BMP-4.

In conclusion, we have demonstrated that CTSH activity is not directly involved in proteolytic processing of BMP-4 in human cells but can regulate mRNA expression of BMP family members, depending on the presence of different processing forms of CTSH. However, the mechanisms of regulation of its mRNA expression, as well as the impact of CTSH on members of BMP family other than BMP-4, remain to be elucidated.

Acknowledgements

The work was supported by Research Agency of the Republic of Slovenia (grant P4-127 J.K.) and partially by 7th EU project Nanophoto.

References

1. Turk V, Turk B, Turk D. Lysosomal cysteine proteases: facts and opportunities. *EMBO J* 2001; **20**: 4629-33.
2. Kirschke H. Cathepsin H. In: Barret AJ, Rawlings ND, Woessner JF. *Handbook of proteolytic enzymes*. 2nd edition. London: Elsevier Academic Press; 2004. p. 1089-92.
3. Kirschke H, Barrett AJ, Rawlings ND. *Lysosomal cysteine proteases*. 2nd edition. Oxford: Oxford University Press; 1998.
4. Ritonja A, Popovic T, Kotnik M, Machleidt W, Turk V. Amino acid sequences of the human kidney cathepsins H and L. *FEBS Lett* 1988; **228**: 341-5.
5. Vasiljeva O, Dolinar M, Turk V, Turk B. Recombinant human cathepsin H lacking the mini chain is an endopeptidase. *Biochemistry* 2003; **42**: 13522-8.
6. Nishimura Y, Kato K. Identification of latent procathepsin H in microsomal lumen: characterization of proteolytic processing and enzyme activation. *Arch Biochem Biophys* 1988; **260**: 712-8.
7. Kominami E, Tsukahara T, Hara K, Katunuma N. Biosyntheses and processing of lysosomal cysteine proteinases in rat macrophages. *FEBS Lett* 1988; **231**: 225-8.
8. Gocheva V, Chen X, Peters C, Reinheckel T, Joyce JA. Deletion of cathepsin H perturbs angiogenic switching, vascularization and growth of tumors in a mouse model of pancreatic islet cell cancer. *Biol Chem* 2010; **391**: 937-45.

9. Wu SM, Huang YH, Yeh CT, Tsai MM, Liao CH, Cheng WL, et al. Cathepsin H regulated by the thyroid hormone receptors associate with tumor invasion in human hepatoma cells. *Oncogene* 2011; **30**: 2057-69.
10. Ciric E, Sersa G. Radiotherapy in combination with vascular-targeted therapies. *Radiol Oncol* 2010; **44**: 67-78.
11. Gabrijelcic D, Svetic B, Spaic D, Skrk J, Budihna M, Dolenc I, et al. Cathepsins B, H and L in human breast carcinoma. *Eur J Clin Chem Clin Biochem* 1992; **30**: 69-74.
12. Schweiger A, Christensen IJ, Nielsen HJ, Sørensen S, Brüner N, Kos J. Serum cathepsin H as a potential prognostic marker in patients with colorectal cancer. *Int J Biol Markers* 2004; **19**: 289-94.
13. Kos J, Stabuc B, Schweiger A, Krasovec M, Cimerman N, Kopitar-Jerala N, et al. Cathepsins B, H, and L and their inhibitors stefin A and cystatin C in sera of melanoma patients. *Clin Cancer Res* 1997; **3**: 1815-22.
14. Budihna M, Strojan P, Smid L, Skrk J, Vrhovec I, Zuperc A, et al. Prognostic value of cathepsins B, H, L, D and their endogenous inhibitors stefins A and B in head and neck carcinoma. *Biol Chem Hoppe Seyler* 1996; **377**: 385-90.
15. Strojan P. Cysteine cathepsins and stefins in head and neck cancer: an update of clinical studies. *Radiol Oncol* 2008; **42**: 69-81.
16. Sivaparvathi M, Sawaya R, Gokaslan ZL, Chintala SK, Rao JS. Expression and the role of cathepsin H in human glioma progression and invasion. *Cancer Lett* 1996; **104**: 121-6.
17. Friedrich B, Jung K, Lein M, Türk I, Rudolph B, Hampel G, et al. Cathepsins B, H, L and cysteine protease inhibitors in malignant prostate cell lines, primary cultured prostatic cells and prostatic tissue. *Eur J Cancer* 1999; **35**: 138-44.
18. Schweiger A, Staib A, Werle B, Krasovec M, Lah TT, Ebert W, et al. Cysteine proteinase cathepsin H in tumours and sera of lung cancer patients: relation to prognosis and cigarette smoking. *Br J Cancer* 2000; **82**: 782-8.
19. Ueno T, Linder S, Na CL, Rice WR, Johansson J, Weaver TE. Processing of pulmonary surfactant protein B by napsin and cathepsin H. *J Biol Chem* 2004; **279**: 16178-84.
20. Serveau-Avesque C, Martino MF, Hervé-Grépinet V, Hazouard E, Gauthier F, Diot E, et al. Active cathepsins B, H, K, L and S in human inflammatory bronchoalveolar lavage fluids. *Biol Cell* 2006; **98**: 15-22.
21. Brasch F, Ten Brinke A, Johnen G, Ochs M, Kapp N, Müller KM, et al. Involvement of cathepsin H in the processing of the hydrophobic surfactant-associated protein C in type II pneumocytes. *Am J Respir Cell Mol Biol* 2002; **26**: 659-70.
22. D'Angelo ME, Bird PI, Peters C, Reinheckel T, Trapani JA, Sutton VR. Cathepsin H is an additional convertase of pro-granzyme B. *J Biol Chem* 2010; **285**: 20514-9.
23. Lü J, Qian J, Keppler D, Cardoso WV. Cathepsin H is an Fgf10 target involved in Bmp4 degradation during lung branching morphogenesis. *J Biol Chem* 2007; **282**: 22176-84.
24. Hogan BL. Bone morphogenetic proteins: multifunctional regulators of vertebrate development. *Genes Dev* 1996; **10**: 1580-94.
25. Deng H, Ravikumar TS, Yang WL. Overexpression of bone morphogenetic protein 4 enhances the invasiveness of Smad4-deficient human colorectal cancer cells. *Cancer Lett* 2009; **281**: 220-31.
26. Maegdefrau U, Amann T, Winklmeier A, Braig S, Schubert T, Weiss TS, et al. Bone morphogenetic protein 4 is induced in hepatocellular carcinoma by hypoxia and promotes tumour progression. *J Pathol* 2009; **218**: 520-9.
27. Cui Y, Jean F, Thomas G, Christian JL. BMP-4 is proteolytically activated by furin and/or PC6 during vertebrate embryonic development. *EMBO J* 1998; **17**: 4735-43.
28. Degnin C, Jean F, Thomas G, Christian JL. Cleavages within the prodomain direct intracellular trafficking and degradation of mature bone morphogenetic protein-4. *Mol Biol Cell* 2004; **15**: 5012-20.
29. Goldman DC, Hackenmiller R, Nakayama T, Sopory S, Wong C, Kulesha H, et al. Mutation of an upstream cleavage site in the BMP4 prodomain leads to tissue-specific loss of activity. *Development* 2006; **133**: 1933-42.
30. Schweiger A, Stabuc B, Popović T, Turk V, Kos J. Enzyme-linked immunosorbent assay for the detection of total cathepsin H in human tissue cytosols and sera. *J Immunol Methods* 1997; **201**: 165-72.
31. Jevnikar Z, Obermajer N, Bogyo M, Kos J. The role of cathepsin X in the migration and invasiveness of T lymphocytes. *J Cell Sci* 2008; **121**: 2652-61.
32. Anglikler H, Wikstrom P, Kirschke H, Shaw E. The inactivation of the cysteinyl exopeptidases cathepsin H and C by affinity-labelling reagents. *Biochem J* 1989; **262**: 63-8.
33. Obermajer N, Svajger U, Bogyo M, Jeras M, Kos J. Maturation of dendritic cells depends on proteolytic cleavage by cathepsin X. *J Leukoc Biol* 2008; **84**: 1306-15.
34. Chen D, Zhao M, Mundy GR. Bone morphogenetic proteins. *Growth Factors* 2004; **22**: 233-41.
35. Kominami E, Tsukahara T, Bando Y, Katunuma N. Distribution of cathepsins B and H in rat tissues and peripheral blood cells. *J Biochem* 1985; **98**: 87-93.
36. del Re EC, Shuja S, Cai J, Murnane MJ. Alterations in cathepsin H activity and protein patterns in human colorectal carcinomas. *Br J Cancer* 2000; **82**: 1317-26.
37. Waghray A, Keppler D, Sloane BF, Schuger L, Chen YQ. Analysis of a truncated form of cathepsin H in human prostate tumor cells. *J Biol Chem* 2002; **277**: 11533-8.
38. Cui Y, Hackenmiller R, Berg L, Jean F, Nakayama T, Thomas G, et al. The activity and signaling range of mature BMP-4 is regulated by sequential cleavage at two sites within the prodomain of the precursor. *Genes Dev* 2001; **15**: 2797-802.
39. Takahashi T, Dehdarani AH, Tang J. Porcine spleen cathepsin H hydrolyzes oligopeptides solely by aminopeptidase activity. *J Biol Chem* 1988; **263**: 10952-7.
40. Ohkawara B, Iemura S, ten Dijke P, Ueno N. Action range of BMP is defined by its N-terminal basic amino acid core. *Curr Biol* 2002; **12**: 205-9.
41. Zhou Z, Sun L, Wang Y, Wu Z, Geng J, Miu W, et al. Bone morphogenetic protein 4 inhibits cell proliferation and induces apoptosis in glioma stem cells. *Cancer Biother Radiopharm* 2011; **26**: 77-83.
42. Lombardo Y, Scopelliti A, Cammareri P, Todaro M, Iovino F, Ricci-Vitiani L, et al. Bone morphogenetic protein 4 induces differentiation of colorectal cancer stem cells and increases their response to chemotherapy in mice. *Gastroenterology* 2011; **140**: 297-309.
43. Goldman DC, Bailey AS, Pfaffle DL, Al Masri A, Christian JL, Fleming WH. BMP4 regulates the hematopoietic stem cell niche. *Blood* 2009; **114**: 4393-401.
44. Ardebili SY, Zajc I, Gole B, Campos B, Herold-Mende C, Drmota S, Lah TT. CD133/prominin1 is prognostic for GBM patient's survival, but inversely correlated with cysteine cathepsins' expression in glioblastoma derived spheroids. *Radiol Oncol* 2011; **45**: 102-15.

Sinonasal inverted papilloma associated with squamous cell carcinoma

Jasna But-Hadzic¹, Klemen Jenko², Mario Poljak³, Bostjan J Kocjan³, Nina Gale⁴, Primož Strojjan¹

¹ Department of Radiation Oncology, Institute of Oncology Ljubljana, Ljubljana, Slovenia

² University Department of Otorhinolaryngology and Cervicofacial Surgery, University Clinical Centre Ljubljana, Ljubljana, Slovenia

³ Institute of Microbiology and Immunology, Medical Faculty, University of Ljubljana, Ljubljana, Slovenia

⁴ Institute of Pathology, Medical Faculty University of Ljubljana, Ljubljana, Slovenia

Received 21 August 2011

Accepted 1 September 2011

Correspondence to: Prof. Primož Strojjan, M.D., Ph.D., Department of Radiation Oncology, Institute of Oncology, Zaloška 2, SI-1000 Ljubljana, Slovenia. Phone: +386 1 5879 110, Fax: +386 1 5879 400; E-mail: pstrojjan@onko-i.si

Disclosure: No potential conflicts of interest were disclosed.

Background. The aims of the study were to review single-institution experiences with sinonasal inverted papilloma associated with squamous cell carcinoma (IP/SCC), to analyze the presence of human papillomavirus (HPV) and to evaluate the role of radiotherapy.

Patients and methods. Five patients with IP/SCC were identified in the prospective institutional databases (1995-2005) and HPV status was determined in all five tumors.

Results. Four out of five patients had T3-4 tumors; no nodal involvement was seen in any of them. Four patients had curative surgery, supplemented in three of them with radiotherapy. Debulking surgery was performed in the patient with a non-resectable tumor followed by radical radiotherapy. Tumor was controlled locally in three patients at 8, 46 and 58 months post-surgery. Local failure occurred in two patients: after endoscopic resection of a T1 tumor (the recurrent tumor was successfully salvaged with additional surgery) and in a patient with an inoperable tumor. No regional or distant metastases occurred. HPV status was determined in all five tumors and three of them were found positive for HPV type 11.

Conclusions. In operable sinonasal IP/SCC, upfront surgery and postoperative radiotherapy to the tumor bed with dose levels comparable to those used for invasive SCC are recommended. For non-resectable disease, radical radiotherapy to a dose of 66-70 Gy could be of benefit.

Key words: inverted papilloma; squamous cell carcinoma; radiotherapy; human papillomavirus infection; outcome

Introduction

Inverted papilloma (IP, one of three types of Schneiderian papilloma) of the nasal cavity and paranasal sinuses is a benign epithelial tumor of unknown etiology, first described by Ward in 1854.¹ IP represents 0.5-4% of all sinonasal tumor and arises from the mucosa of the lateral wall of the nasal cavity, almost always unilaterally. IP is best characterized by the male-to-female ratio of 3:1 with the peak incidence between 5th and 6th decade of life, destructive pattern of local growth, tendency to recur and, occasionally, associated malignancy.^{2,3}

The most common presenting symptom is unilateral nasal obstruction; the duration of symptoms is variable, with an average of >5 years but even up to >45 years.²⁻⁴

The frequency of carcinoma in patients with sinonasal IP is around 11%. In two thirds of cases, carcinoma occurs synchronously with IP, but in some patients carcinoma develops at a later time, after previous resection of IP (metachronous carcinoma). The associated malignancy is predominantly squamous cell carcinoma (SSC), which may arise within the papilloma or is merely associated with a histologically bland IP.² This group of patients is

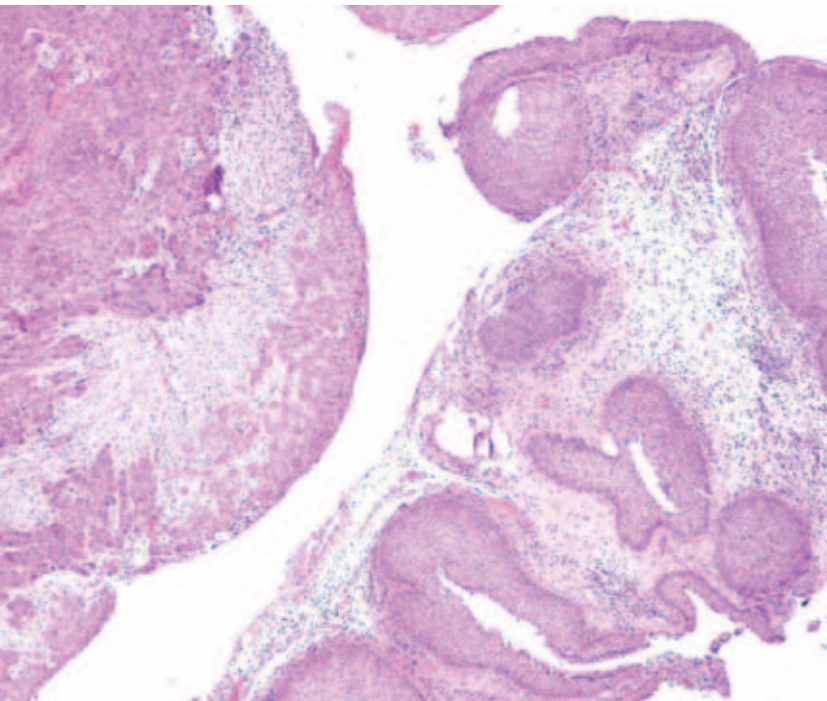


FIGURE 1. Inverted squamous papillomas are seen on the right side, synchronous moderately differentiated non-keratinizing invasive squamous cell carcinoma on the left side.

characterized by older age and male preponderance compared with those without associated malignancy.^{2,3} An etiological role for human papillomavirus (HPV) and the mutation of the p53 tumor suppressor gene in malignant transformation of IP has been suggested.⁵⁻⁷

Literature reports on IP associated with SCC (IP/SCC) are scarce, describing only small cohorts of patients treated with varying degree of success. In the present report, we describe a group of five patients treated for IP/SCC. The presence of HPV was analyzed and the role of adjuvant radiotherapy was discussed.

Patients and methods

The databases of the University Department of Otorhinolaryngology and Cervicofacial Surgery, Clinical Center Ljubljana and the Institute of Pathology, Medical Faculty University of Ljubljana for the years 1995–2005 were used for identification of patients with a diagnosis of IP of the nasal cavity and paranasal sinuses. Out of 89 patients with this diagnosis, 5 patients (5.62%) were found to have IP/SCC. Pathology specimens of all 5 patients were re-examined by an experienced head and neck pa-

thologist (N.G.) (Figure 1) and the medical records of identified patients were reviewed for clinical characteristics, treatment and outcome.

Detection of HPV DNA

Tissue processing, DNA extraction and quantification as well as HPV detection and genotyping were described elsewhere.⁷ Briefly, total DNA was extracted from two 10- μ m sections of paraffin blocks using QIAamp DNA FFPE Tissue Kit (Qiagen, Hilden, Germany), following the manufacturer's instructions. For detection of HPV, PCR amplification was performed on all samples using HotStarTaq® Plus DNA Polymerase kit (Qiagen) and consensus GP5+ and GP6+ primers targeting approximately 150-bp fragments of alpha-HPV L1 gene. The PCR products that appeared as visible bands of the expected size were purified by QIAquick PCR Purification Kit (Qiagen) and sequenced directly using BigDye Terminator v1.1 Cycle Sequencing Kit (PE Applied Biosystems, Foster City, USA) with GP5+/GP6+ primers. A comparison of the HPV-DNA sequences obtained with those of officially designated alpha-HPV genotypes was carried out using the Blast server.⁸ Results from the Blast comparison software were confirmed additionally by pairwise alignment using the sequence of interest and full L1 gene of a reference HPV genotype.⁹

Results

Patients and tumors

Detailed information on the clinical characteristic of patients and their tumors, treatment and outcome is given in Table 1. There were four males and one female, from 45 to 77 years old (median 73 years). Unilateral nasal obstruction was the most frequent presenting symptom reported by four patients. The duration of symptoms before a diagnosis of IP with or without associated SCC was confirmed ranged from 2–6 months (median: 5 months).

In all but one patient, the disease extended from the nasal cavity to neighboring structures and no nodal or distant metastases were presented at the time of diagnosis in any of them. According to the UICC TNM staging system (7th edition, 2009) for malignant tumors of the nasal cavity and ethmoid sinus, four patients had locally advanced T3-4 disease, whereas using the Krouse staging system,¹⁰ all tumors were categorized as stage T4 (*i.e.* due to associated malignancy).

TABLE 1. Sinonasal inverted papilloma associated with squamous cell carcinoma: clinical and tumor characteristics, treatment and outcome

Parameter	Patients				
	1	2	3	4	5
Sex/Age (yrs.)	M/45	M/77	M/75	F/73	M/62
Presenting symptoms	Unilateral nasal obstruction	Unilateral nasal obstruction, nasal discharge, anosmia, pain	Nasal discharge	Unilateral nasal obstruction, headache, diplopia	Unilateral nasal obstruction blurred vision, headache, anosmia
Duration of symptoms	6 mos.	5 mos.	2 mos.	2 mos.	6 mos.
Extent of disease	Lt nasal cavity	Rt nasal cavity, nasopharynx	Rt nasal cavity, ethmoid, orbit	Rt nasal cavity, ethmoid, maxillary sinus, orbit	Rt nasal cavity, ethmoid, fossa pterygopalatina, maxillary sinus, sphenoid, orbit
TNM stage*	T1N0M0	T4bN0M0	T3N0M0	T4aN0M0	T4bN0M0
Histology at 1 st biopsy	P	IP	P	IP	IP
No. of recurrences	1	0	1	6	0
SCC type	M	S	M	M	S
Histopathological grade of SCC	n.s.	G II-III	G II-III	G II	n.s.
Surgery	Endoscopic resection; R0	Endoscopic resection; R0	Lateral rhinotomy; R0	Sublabial and external supraclavicular approach; R0	Sublabial approach, explorative and debulking procedure; R2
HPV status	Positive (type 11)	Positive (type 11)	Positive (type 11)	Negative	Negative
Radiotherapy	Not irradiated	60 Gy, 30#, 5MV, 3 fields, continuous course; Tu site & Rt region II	60 Gy, 30#, 6MV, 3 fields, continuous course; Tu site	60Gy, 24#, 5MV, 3 fields, continuous course; Tu site & Rt neck	70 Gy, 35#, Co-60, 3 fields, continuous course; Tu site
Follow-Up	Local recurrence at 8 mos., NED 62 mos. after salvage surgery	DOC at 46 mos., no evidence of IP/SCC	NED at 58 mos.	DOC at 8 mos., no evidence of IP/SCC	DOD at 14 months, locally progressive disease

M – Male; F – Female; Rt – Right; Lt – Left; P – Papilloma; IP – Inverted papilloma; M – Metachronous; S – Synchronous; n.s. – Not specified; SCC – Squamous cell carcinoma; # – No. of fractions; Tu – Tumor. NED – No evidence of disease; DOD – Died of disease; DOC – Died of other cause.

*TNM clinical classification of malignant tumors of the nasal cavity and ethmoid sinuses.

The presence of SCC was confirmed by histopathological examination of resected specimen (*i.e.* after a biopsy proved negative for the presence of SCC) in two patients (pts. 2 and 5). The other three patients had metachronous SCC found in recurrent IP at 3, 10 and 24 years after first surgery (in pt. 4 at the time of resection of the sixth recurrence of IP). An invasive SCC component was found in all cases.

Treatment

Four patients were operated on with curative intent. The surgical technique was dictated by the extent of the disease: a transnasal endoscopic technique and an external approach were used in two patients each. Surgery was declared as radical, without microscopic residual disease left behind,

in all four patients, and all but one were irradiated postoperatively. The patient with extensive local disease, extending to the right ethmoid complex, sphenoid, pterygopalatal fossa and orbita, had only debulking surgery followed by radiotherapy as a definitive treatment. None of the patients received systemic chemotherapy.

Postoperatively, continuous-course radiotherapy of 5 fractions per week was delivered in three patients, using megavoltage 5-MV or 6-MV linear accelerator photon beams, to a total tumor dose of 60 Gy. In two patients, the daily dose was 2 Gy and in one patient 2.5 Gy per fraction. The patient with gross residual disease after surgical debulking received definitive radiotherapy using megavoltage Co-60 photons in daily fractions of 2 Gy to a total dose of 70 Gy. Two-dimensional computer-based planning was used to cover the postopera-

tive tumor bed or gross tumor volume including sinuses at risk for containing microscopic disease with a $\geq 95\%$ isodose curve. A conventional three-field technique employing a heavily weighted anterior field and two opposed lateral wedged fields to achieve dose homogeneity in the range of $\pm 5\%$ inside the treated volume, head holders with thermoplastic casts and individual shielding blocks were used. When appropriate, optic structures were shielded after a dose of 54 Gy. The ipsilateral regional lymphatics (regions II–V) were irradiated postoperatively in one patient (pt. 5), through an anterior field and with 2.5 daily fractions to a total dose of 40 Gy, whereas in another patient (pt. 2), region II was covered ipsilaterally to a dose of 50 Gy in 2-Gy daily fractions. In both patients, indication for neck irradiation was extensive local disease.

Outcome

After diagnosis of IP/SCC, two patients were alive at 58 and 70 months. In the patient treated solely with endoscopic resection (patient 1), isolated local recurrence, histologically confirmed as IP/SCC, developed on the nasal septum 8 months later; an endoscopic salvage procedure resulted in a permanent local control of 62 months. Two patients died of disease-unrelated causes without disease reappearance at 8 and 46 months after diagnosis of IP/SCC; at the time of death, they were 74 and 81 years old, respectively. The patient who underwent definitive radiotherapy died due to progression of residual disease at 14 months from biopsy.

No severe or unexpected complications of treatment were documented during therapy and none of the patients had severe late therapy-related sequelae that would demand surgical intervention or hospitalization.

Human papillomavirus

Three out of five tumors analyzed for the presence of HPV were found positive, with type 11 being present in all positive cases.

Discussion

In IP, whether or not associated with SCC, complete surgical removal of the tumor is advocated as the treatment of choice. Endoscopic treatment is preferred, whereas for lesions less accessible endoscopically, or in those with peripheral extension, open surgery is indicated.^{11,12} When complete

resection is not possible, or for tumors with associated malignancy, radiotherapy is recommended as an adjunct to surgery.^{13,14}

While the experiences with IP are extensive^{4,10-12}, series describing IP/SCC are limited and feature a limited number of cases. Tanvetyanon *et al.*¹⁵ collected survival data of 76 patients from his series and ten additional series published during the last 30 years, covering a recruitment period of almost six decades.^{4,13-22} The corresponding pooled median overall survival was 126 months with 3-year survival estimate of 63%, which is in the range reported for invasive SCC of the nasal cavity and paranasal sinuses²³ but much lower compared to figures appearing in IP series.^{4,11,12}

Recommendations for the use of radiotherapy are based on clinical observations rather than scientific analyses. More than three quarters of 76 patients from pooled group reported by Tanvetyanon *et al.* had one or another form (*i.e.* pre- or postoperative, definitive, palliative) of irradiation but no analysis on the value of radiotherapy versus surgery alone was carried out in their study.¹⁵ After detailed review of the studies analyzed in the paper mentioned above, we conclude that the low quality of information on the tumor extent and treatment, including completeness of surgical resection, in some publications must be the reason.

According to Hug *et al.*¹³ and Gomez *et al.*¹⁴, the probability of regional or systemic dissemination of IP/SCC is low. Consequently, they proposed elective irradiation of regional lymphatics only in patients with extensive involvement of the nasopharynx or clinically or radiologically apparent neck metastases. Our limited experience corroborates their recommendations.

Because of generally accepted opinion that radiotherapy should not be used as an adjunct to surgery in bland IP, in IP/SCC cases the choice of irradiation dose level is usually dictated by the recommendations for invasive SCC. This is obviously the case when series with sufficiently described radiotherapy details are reviewed.^{14,15,17,20} In 19 pre- or postoperatively irradiated patients, radiotherapy doses ranged from 45 Gy to 70.4 Gy (median 60 Gy); all but four patients received 58.4-66.8 Gy. Furthermore, in a group of 13 patients with IP/SCC reported by Hugh *et al.*¹³ only one local failure occurred after gross total resection and adjuvant hyperfractionated or conventionally fractionated radiotherapy to a mean dose of 59 Gy or 60 Gy, respectively. Following subtotal resection, one out of three tumors failed locally after hyperfractionated irradiation to a mean dose of 66 Gy.¹³ In the present

series, all three tumors postoperatively irradiated were locally controlled at 8, 46 and 58 months post-diagnosis; an irradiation dose of 60 Gy was adjusted to the tumor stage (T3-T4) and the presence of the SCC component.

Experience with chemotherapy in IP/SCC is very scarce. In the majority of cases, chemotherapy was aimed at palliating symptoms of unresectable disease, locally or at distant sites,^{15,20} or has exceptionally been used for reducing tumor size before surgery^{15,21}, or in a postoperative setting, usually with irradiation.^{15,19-21} The chemotherapeutics used were platinum compounds, 5-fluorouracil, paclitaxel, etoposide, and methotrexate.^{15,21} No conclusions could be made on the effectiveness of chemotherapy in SCC/IP; however, none of the three patients with distant metastases reported by Tanvetyanon *et al.*¹⁵ responded to any of the chemotherapy regimens used.

Presence of HPV type 11 was confirmed in three out of five tumors from the present series. Similarly, Cheung *et al.*⁵ demonstrated the presence of HPV in four out of seven IP/SCC cases, one of them being type 11 (typing was not done in other cases because of inadequate HPV DNA content). Simultaneously decreased expression of p16 found in above cited and other studies indicates that the role of HPV in the oncogenesis of IP/SCC differs from that in cervical SCC. It seems that HPV infection occurs as an early event in the multistep process of malignant transformation from IP to SCC.^{5,6,24} However, others suggested that HPV infection may represent incidental colonization rather than being an important etiological factor.⁷

Rather high prevalence of HPV infection in IP but also IP/SCC specimens poses clinically relevant question on the potential prognostic significance of HPV status. Patients with HPV-positive SCCs of the head and neck, oropharynx in particular, have superior outcome, attributed to enhanced radiation and chemo-sensitivity due to an intact apoptotic mechanism in response to radiation and chemotherapy.^{25,26} Because in oropharyngeal SCCs HPV types 16 and 18 rather than 11 are usually found, the question of radio/chemo-sensitivity of HPV-positive IPs and IP/SCCs at this point remains to be elucidated. However, unexpectedly favorable responses after radiotherapy have also been reported in extensive IPs and SCC/IPs. Myers *et al.*¹⁷ described a case of IP/SCC destroying the bony walls of the antrum with orbital invasion; no residual IP or SCC was found in the surgical specimen after 60 Gy of preoperative radiotherapy. A similar experience with preoperative irradiation was reported by

Gomez *et al.*¹⁴, whereas in the patient with non-resectable IP with bilateral involvement of the nasal cavity and paranasal sinuses, radiotherapy alone with 65 Gy was deemed curative (no recurrence at 7 years). The authors draw attention to the rather long interval after irradiation, from 3 to 6 months, for gross disease to disappear.¹⁴ Also, after surgical debulking of locally recurrent IP associated with carcinoma *in situ*, affecting the zygomatic area and with extension into the infratemporal fossa, Levendag *et al.*²⁷ found irradiation to 64 Gy highly effective, resulting in complete regression of the lesion for almost one year.

Conclusions

According to clinical experiences, combination of surgery and postoperative irradiation with radiotherapy dose levels in a range used for invasive SCC are recommended for operable IP/SCC. Elective neck irradiation should be considered only for patients with extensive nasopharyngeal involvement or apparent regional metastases. For non-resectable disease, radical radiotherapy to a dose of 66-70 Gy could be of benefit with potential for long-lasting remission or even cure.

Acknowledgement

A study was supported by Slovenian Research Agency Grant P3-0307.

References

1. Ward N. A mirror of the practice of medicine and surgery in the hospitals of London: London hospital. *Lancet* 1854; **2**: 480-2.
2. Barnes L. Schneiderian papillomas and nonsalivary glandular neoplasms of the head and neck. *Mod Pathol* 2002; **15**: 279-97.
3. Eggers G, Muhling J, Hassfeld S. Inverted papilloma of paranasal sinuses. *J Craniomaxillofac Surg* 2007; **35**: 21-9.
4. Vrabec DP. The inverted Schneiderian papilloma: a 25-year study. *Laryngoscope* 1994; **104**: 582-605.
5. Cheung FMF, Lau TWS, Cheung LKN, Li ASM, Chow SK, Lo AWI. Schneiderian papillomas and carcinomas: a retrospective study with special reference to p53 and p16 suppressor gene expression and association with HPV. *Ear Nose Throat J* 2010; **89**: E5-12.
6. Kim SG, Lee OY, Choi JW, Park YH, Kim YM, Yeo MK, et al. Pattern of expression of cell cycle-related proteins in malignant transformation of sinonasal inverted papilloma. *Am J Rhinol Allergy* 2011; **25**: 75-81.
7. Jenko K, Kocjan B, Zidar N, Poljak M, Strojanc P, Žargi M, et al. Inverted papilloma HPV more likely represents incidental colonization than an etiological factor. *Virchows Arch* (in press).
8. The National Center for Biotechnology Information Database [http://www.ncbi.nlm.nih.gov/blast/]

9. The European Molecular Biology Open Software Suite [<http://www.ebi.ac.uk/emboss/>]
10. Krouse JH. Development of a staging system for inverted papilloma. *Laryngoscope* 2000; **111**: 965-8.
11. Lawson W, Patel ZM. The evolution of management for inverted papilloma: an analysis of 200 cases. *Otolaryngol Head Neck Surg* 2009; **140**: 330-5.
12. Lombardi D, Tomenzoli D, Buttà L, Bizzoni A, Farina D, Sberze F, et al. Limitations and complications of endoscopic surgery for treatment for sinonasal inverted papilloma: a reassessment after 212 cases. *Head Neck* 2011; **33**: 1154-61.
13. Hug EB, Wang CC, Montgomery WW, Goodman ML. Management of inverted papilloma of the nasal cavity and paranasal sinuses: importance of radiation therapy. *Int J Radiat Oncol Biol Phys* 1993; **26**: 67-72.
14. Gomez JA, Mendenhall WM, Tannehill SP, Stringer SP, Cassisi NJ. Radiation therapy in inverted papillomas of the nasal cavity and paranasal sinuses. *Am J Otolaryngol* 2000; **21**: 174-8.
15. Tanvetyanon T, Qin D, Padhya T, Kapoor R, McCaffrey J, Trotti A. Survival outcomes of squamous cell carcinoma arising from sinonasal inverted papilloma: report of 6 cases with systematic review and pooled analysis. *Am J Otolaryngol* 2009; **30**: 38-43.
16. Yamaguchi KT, Shapshay SM, Incze JS, Vaughan CW, Strong S. Inverted papilloma and squamous cell carcinoma. *J Otolaryngol* 1977; **8**: 171-8.
17. Myers EN, Schramm VL, Barnes EL. Management of inverted papilloma of the nose and paranasal sinuses. *Laryngoscope* 1981; **91**: 2071-84.
18. Myers EN, Fernau JL, Johnson JT, Tabet JC, Barnes EL. Management of inverted papilloma. *Laryngoscope* 1990; **100**: 481-90.
19. Segal K, Atar E, Mor C, Har-El G, Sidi J. Inverting papilloma of the nose and paranasal sinuses. *Laryngoscope* 1986; **96**: 394-8.
20. Lesperance MM, Esclamado RM. Squamous cell carcinoma arising in inverted papilloma. *Laryngoscope* 1995; **105**: 178-83.
21. Shipchandler TZ, Batra PS, Citardi MJ, Bolger WE, Lanza DC. Outcomes for endoscopic resection of sinonasal squamous cell carcinoma. *Laryngoscope* 2005; **115**: 1983-7.
22. Oikawa K, Furuta Y, Itoh T, Oridate N, Fukuda S. Clinical and pathological analysis of recurrent inverted papilloma. *Ann Otol Rhinol Laryngol* 2007; **116**: 297-303.
23. Dulguerov P, Jacobsen MS, Allal AS, Lehmann W, Calcaterra T. Nasal and paranasal sinus carcinoma: are we making progress? A series of 220 patients and a systematic review. *Cancer* 2001; **92**: 3012-29.
24. Kim JY, Yoon JK, Citardi MJ, Batra PS, Roh HJ. The prevalence of human papilloma virus infection in sinonasal inverted papilloma specimens classified by histological grade. *Am J Rhinol* 2007; **21**: 664-9.
25. Marur S, D'Souza G, Westra WH, Forastiere AA. HPV-associated head and neck cancer: a virus-related cancer epidemic. *Lancet Oncol* 2010; **11**: 781-9.
26. Ragin CC, Taioli E. Survival of squamous cell carcinoma of the head and neck in relation to human papillomavirus infection: review and meta-analysis. *Int J Cancer* 2007; **121**: 1813-20.
27. Levendag PC, Annys AA, Escajadillo R, Elema JD. Radiotherapy for inverted papilloma: a case report. *Radiother Oncol* 1994; **2**: 13-7.

Comparison of survival of patients receiving laparoscopic and open radical resection for stage II colon cancer

Cui-Zhen Fan¹, Yu-Ping Chu¹, Ping Wei², Hong Dai², Wenming Chen³

¹ Department of Oncology, Beijing Chaoyang Hospital, Capital University of Medical Science, Beijing, China

² Department of Pathology, Beijing Chao yang Hospital, Capital University of Medical Science, Beijing, China

³ Department of Hematologic Neoplasms and Oncology, Beijing Chaoyang Hospital, Capital University of Medical Science, Beijing, China

Received 28 March 2011

Accepted 10 July 2011

Correspondence to: Wenming Chen, Department of Hematologic Neoplasms & Oncology, Beijing Chaoyang Hospital, No.8 Baijiazhuang Road Beijing 100020, China. Phone: +86 10 85231240; Fax: +86 10 85231244; Email: chenq52000@163.com

Disclosure: No potential conflicts of interest were disclosed.

Background. The aim of the study was to compare the survival of patients receiving laparoscopic vs. open radical resection for stage II colon cancer.

Patients and methods. Two hundred and twenty patients with stage II colon cancer were enrolled from Beijing Chaoyang Hospital of Capital Medical University from January 2000 to December 2009, including 61 patients in the laparoscopic radical resection group and 159 patients in the open radical resection group. The survival data in both groups were compared using the log rank test based on Kaplan-Meier survival curves.

Results. There was no statistically significant difference in the 3-year survival (88.5% vs. 80.5%; $X^2=1.98$, $P=0.159$) and the 5-year survival (81.9% vs. 69.2%; $X^2=1.98$, $P=0.159$) between both groups. However, statistically significant difference was found in median overall survival (mOS), which was 102.6 (95% CI: 76.8-122.7) months in the laparoscopic group and 90.0 (95% CI: 70.4-109.6) months in the open radical resection group ($X^2=4.183$, $P=0.041$). mOS was 96 (95% CI: 68.6-111.4) months and 92.6 (95% CI: 56.8-107.2) months in those with and without postoperative chemotherapy, respectively ($X^2=6.389$, $P=0.011$). For patients older than 75 years the mOS was 90.0 (95% CI: 25.3-105.0) months and 83.4 (95% CI: 13.1-96.9) months in the laparoscopic and open group, respectively. The difference between the both groups was statistically significant ($X^2=6.191$, $P=0.013$).

Conclusions. The mOS of patients receiving laparoscopic radical resection was better than open radical resection for stage II colon cancer, especially for patients over 75 years old.

Key words: stage II colon cancer; laparoscopy; chemotherapy; prognosis

Introduction

The incidence of colorectal cancer is 3.6-59.1 per 100,000 people worldwide.¹ It is one of the most common malignancies in the world. Its incidence is still increasing as people's lifestyle changes; especially in developing countries.^{2,3} Surgical resection is still the only approach for curing colorectal cancer. The gold criterion of successful removal is that the cancer margins and lymph nodes in relative regions are completely resected. Currently there are

many reports available on laparoscopic radical resection for colorectal cancer. Laparoscopic radical resection achieves rapid recovery and few postoperative complications with recognized short-term outcomes better than open radical resection.^{4,7} Latest follow-up data of laparoscopic radical resection also confirm the long-term outcomes of laparoscopic radical resection for colorectal cancer; the 1-year, 3-year, and 5-year survival following laparoscopic radical resection is similar to that following open radical resection.⁵⁻⁷ However, the survival might depend on post-treatment surveillance of

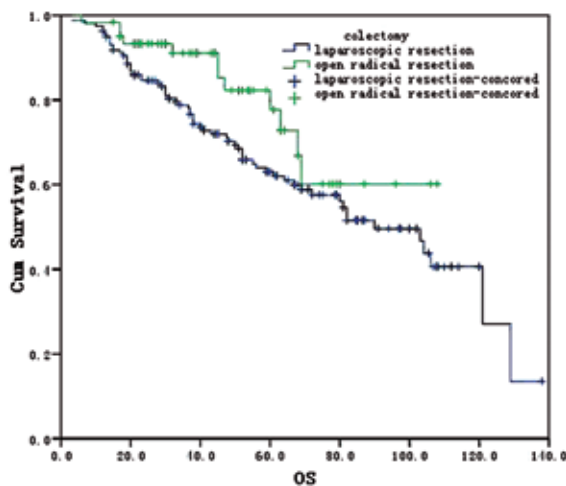


FIGURE 1. Overall survival curves for 220 patients undergoing laparoscopic and open radical resection.

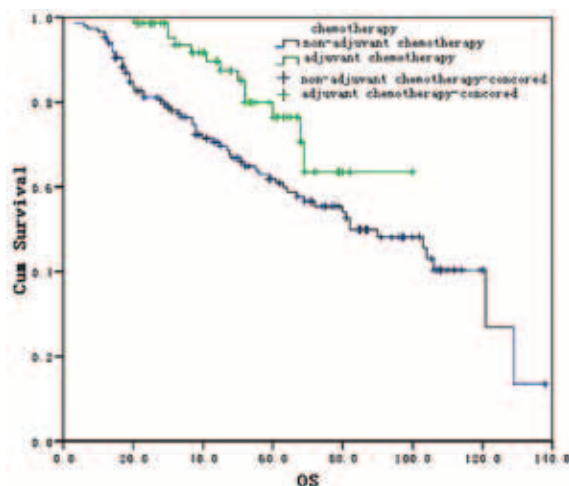


FIGURE 2. Overall survival curves for 220 patients with or without adjuvant chemotherapy.

patients.⁸ There is also report on better efficacy of laparoscopic radical resection than open radical resection as laparoscopic radical resection reduces cancer recurrence, cancer-related mortality and other risks.⁹ In the present study, the survival of patients receiving laparoscopic and open radical resection for stage II colon cancer in 220 patients with stage II colon cancer enrolled from Beijing Chaoyang Hospital of Capital Medical University between January 2000 and September 2009 were retrospectively compared.

Patients and methods

Two hundred and forty-nine patients with stage II colon cancer were treated in Beijing Chaoyang Hospital of Capital Medical University from January 2000 to December 2009. Twenty-nine patients were lost during the follow up. Two hundred and twenty of them were included into the present study according to the inclusion criteria. There were 61 in the laparoscopic radical resection group and 159 in the open radical resection group. The inclusion criteria were: (a) complete medical records with definitive pathology diagnosis of colon cancer treated with radical resection; (b) stage II in the TNM staging system and neoadjuvant chemotherapy not practiced. Exclusion criteria were: (a) synchronous or metachronous colorectal carcinoma, or familial adenomatous polyposis; (b) multiple primary malignant tumours; (c) surgery complication related death; and (d) laparoscopic radical resection replaced by open radical resection. Informed consent was obtained from all these

patients. Sixty-four patients underwent postoperative 5-fluorouracil based chemotherapy, while 156 patients were only underwent radical resection.

Preparations prior to laparoscopic and open radical resection were similar. Tracheal catheterization and general anaesthesia were administered. Surgical procedure was performed according to instructions for tumour-free surgery.

Among 64 patients treated with chemotherapy, fifty-three patients underwent 5-fluorouracil based chemotherapy, complemented by calcium folinate, cis-platinum and oxaliplatin for 4-6 courses, and 11 patients were treated by xeloda alone or combination of xeloda and oxaliplatin for 6-8 courses.

Evaluation of recurrence of colon cancer comprised physical examination, chest X-ray, abdominal CT, and colonoscopy (once a year). The patients were followed up through telephone, outpatient visits and inpatient records. The follow up started from the day of surgery and ended on December 31, 2010. The end-point-data would be 3, 5-year survival and median overall survival (mOS).

Statistical analyses were done using SPSS 15.0. χ^2 test was performed for general data including age and gender. The Kaplan-Meier survival curves and the log rank test were used to analyse the survival data with the selection of operation and treatment. For all analyses, the level of significance was set at $P < 0.05$.

Results

There was no statistically significant differences in the gender, age, cancer site, histological classifica-

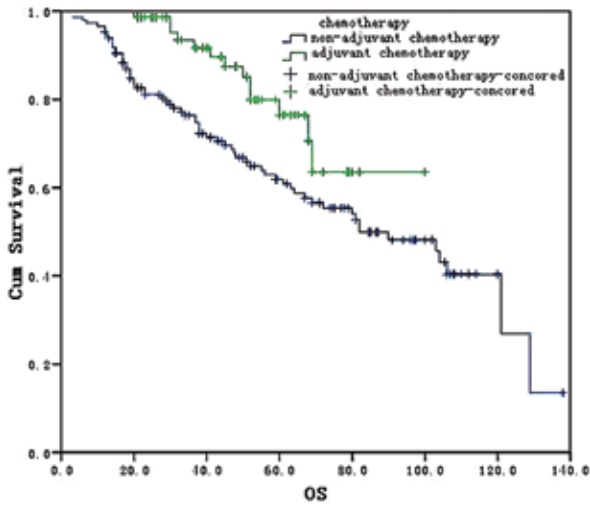
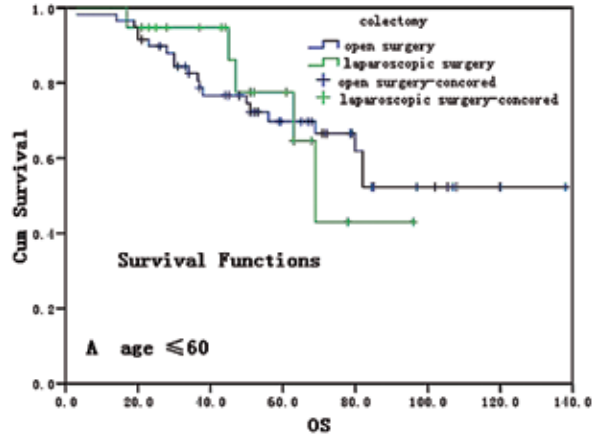


FIGURE 3. Survival curves for 220 patients undergoing laparoscopic or open radical resection in different age periods: A: less than 60 years old; B, 60-75 years old; C=A+B; D, 75 years old.

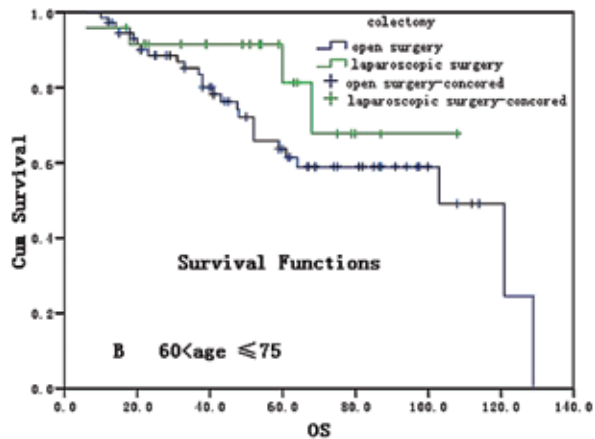
tion, differentiation, vascular thrombus, nerve invasion, lymph nodes revealed by postoperative pathology, or postoperative chemotherapy between the laparoscopic and open radical resection groups ($P>0.05$) (Table 1).

Twenty-nine patients were lost to the follow up with a loss rate of 11.6%. The follow up period ranged from 3 to 128 months with an average of 52.5 months. There was no statistically significant difference in the 3-year survival (88.5% vs. 80.5%; $X^2=1.98$, $P=0.159$) and the 5-year survival (81.9% vs. 69.2%; $X^2=1.98$, $P=0.159$) between both groups. However, statistically significant difference was found in mOS, which was 102.6 (95% CI: 76.8-122.7) months in the laparoscopic group and 90.0 (95% CI: 70.4-109.6) months in the open radical resection group ($X^2=4.183$, $P=0.041$) (Figure 1). mOS was 96 (95% CI: 68.6-111.4) months and 92.6 (95% CI: 56.8-107.2) months in those with or without postoperative chemotherapy, respectively ($X^2=6.389$, $P=0.011$) (Figure 2).

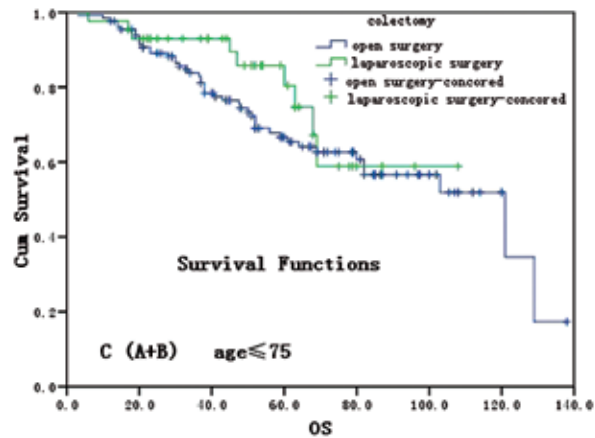
For patients below 75 years old, the mOS was 108 (95% CI: 68.9-173.0) months and 120.8 (95% CI: 69.5-172.5) months in the laparoscopic and open radical resection groups, without statistically significant difference ($X^2=1.0136.191$, $P=0.314$). For patients older than 75 years the mOS was 90.0 (95% CI 25.3 - 105.0) months and 83.4 (95% CI: 13.1 - 96.9) months in the laparoscopic and open group, respectively. The difference between these two groups was statistically significant ($X^2=6.191$, $P=0.013$) (Figure 3).



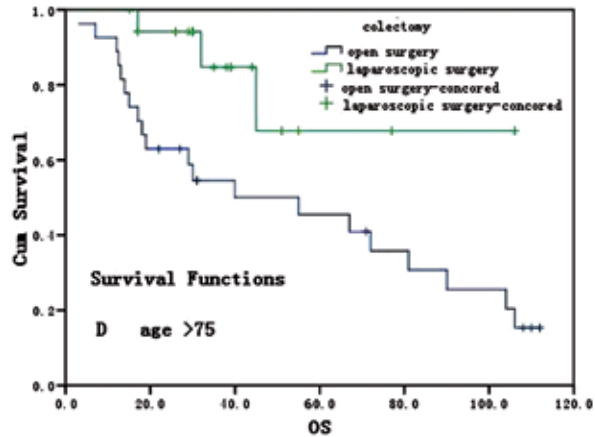
(A)



(B)



(C)



(D)

TABLE 1. General information of 220 patients with stage II colon cancer

	Laparoscopic radical resection	Open radical resection	X ²	P
Total	61	159		
Sex				
Male	28	86	1.183	0.276
Female	33	73		
Age				
~60 years	19	59	4.255	0.119
~75 years	24	73		
>75 years	18	27		
Tumor site				
Ascending colon	20	75	3.910	0.418
Transverse colon	6	14		
Descending colon	10	22		
Sigmoid colon	25	48		
Pathological classification				
Highly differentiated adenocarcinoma	1	4	0.608	0.962
Moderately differentiated adenocarcinoma	50	123		
Mucous adenocarcinoma	6	20		
Lowly differentiated adenocarcinoma with signet ring cells	4	12		
Chemotherapy				
Yes	23	41	2.485	0.115
No	38	118		
Vascular thrombus				
Yes	54	145	0.364	0.546
No	7	14		
Nerve invasion				
Yes	54	146	0.1829	0.669
No	6	13		
Lymph node metastasis				
≥12	24	90	1.418	0.492
<12	37	69		

Discussion

Since Jacobs *et al.* reported the initial use of laparoscopic radical resection of sigmoid colon, laparoscopic radical resection has been increasingly used for colorectal cancer.¹⁰ However, questions are raised regarding whether the long-term outcomes of laparoscopic radical resection are comparative to that of open radical resection and whether it leads to tumour metastasis.

This study showed that the 3-year survival was 88.5% and 80.5% in the laparoscopic and open radical resection groups in 220 patients with stage II colon cancer. Bonjer *et al.*⁶ reported that the 3-year survival was 82.2% and 83.5% respectively for both groups in stage II colon cancer. Kitano *et al.*¹¹ found that the 5-year survival was 94.8% for laparoscopic radical resection, comparable to open radical resection. Fleshman *et al.*⁷ reported that the 5-year survival was 74.6% and 76.4% respectively for laparoscopic and open radical resection group in a multi-centre study in 872 patients with colon cancer and concluded that there was no statistically significant difference in the overall survival and the disease-free survival between two groups, suggesting

that the long-term efficacy is similar for two procedures. This current study found similar results in stage II colon cancer patients, again confirming that laparoscopic radical resection can achieve favourable outcomes for early-stage colon cancer.

In our study the mOS was 102.6 months and 90.0 months in the laparoscopic and open radical resection groups with a statistically significant difference, further demonstrating laparoscopic radical resection has better survival outcomes than open radical resection. Bilimoria *et al.*¹² reported that the 5-year survival was apparently better for laparoscopic radical resection in patients with stages I and II colon cancer. Lacy *et al.*⁹ revealed that laparoscopic radical resection reduced cancer recurrence, risks of mortality from cancer, and other risks, and that the tumour-bearing survival was better for laparoscopic radical resection than open radical resection in a long-term follow up of 218 cases of colon cancer. These results may be attributable to minimal invasion of the surgery and rapid rehabilitation of immune function following laparoscopic radical resection.¹³⁻¹⁵

The 5-year survival is 75% -80% for stage II colon cancer following radical resection and 20%-25% pa-

tients die of recurrence or distant metastasis.¹⁶ As there are no large-scale clinical trials that conclude that stage II colon cancer patients can benefit from postoperative adjuvant chemotherapy, postoperative chemotherapy is thus controversial for stage II colon cancer.^{17,18} The National Surgical Adjuvant Breast and Bowel Project (NSABP) thought that stage II colon cancer patients could benefit from adjuvant chemotherapy as stage III patients.¹⁹ In this study, the mOS was 96 months for patients with postoperative chemotherapy and 92.6 months for those without chemotherapy with a statistically significant difference, showing that chemotherapy is advantageous whatever surgical technique is adopted.

Although meta-analyses could not substitute large randomised clinical studies²⁰, we cannot neglect that a pooled analysis of five randomized trials did not show the radical resection with adjuvant chemotherapy was better than radical resection alone.²¹ Therefore, the National Comprehensive Cancer Network (NCCN) guidelines recommend adjuvant chemotherapy for stage II colorectal cancer patients with risks for poor prognosis (high risks), such as poor histological differentiation, stage T4, invasion to blood vessels or lymph vessels, intestinal obstruction or perforation, tumours too near resection margins, and less than 12 lymph nodes for pathology examination.²² Moreover, some proteins are accepted as predictors for adjuvant chemotherapy for high-risk stage II colorectal cancer.²³ Though this study indicates that chemotherapy was beneficial for patients like in the metastatic disease²⁴, multi-centre trials with a large sample size and different chemotherapy regimens are required to demonstrate the effect of adjuvant chemotherapy for stage II colon cancer. Additionally, there was no statistically significant difference in the cancer site, histological classification, nerve invasion, lymph nodes, or postoperative chemotherapy between the laparoscopic and open radical resection groups.

About 50% colorectal cancer patients are over 70 years old and colorectal cancer thus becomes a common disease for patients over 70 years old.²⁵ According to the Colorectal Cancer Collaborative Group in UK, the risk of surgery for the old increases with age; the mortality was 1.3%-5.2% for patients of 65 years old or above, and 7.1%-8.9% for patients of 85 years or above.²⁶ But another study demonstrates that radical resection is safe in old patients with colorectal cancer and high risks of radical resection are mainly correlated with complications and emergency treatment instead of age.²⁷ In

this study, there were 18 patients over 75 years old in the laparoscopic radical resection group and 27 patients over 75 years old in the open radical resection group. For patients of over 75 years old, it is suggested that the survival of laparoscopic radical resection is superior over open radical resection for stage II colon cancer. The advantage in survival is probably related to less invasive nature of laparoscopic procedure, which can be of greatest benefit in the patients older than 75 years

Conclusions

The survival of patients receiving laparoscopic radical resection was better than that of open radical resection for stage II colon cancer, especially for patients over 75 years old. Thus laparoscopic radical resection should be selected for these stage II colon cancer patients as well as postoperative adjuvant chemotherapy for better survival.

References

- Center MM, Jemal A, Smith RA, Ward E. Worldwide variations in colorectal cancer. *CA Cancer J Clin* 2009; **59**: 366-8.
- Hendon SE, DiPalma JA. U.S. practices for colon cancer screening. *Keio J Med* 2005; **54**: 179-83.
- Horvat M, Stabuc B. Microsatellite instability in colorectal cancer. *Radiol Oncol* 2011; **45**: 75-81.
- Hewett PJ, Allardyce RA, Bagshaw PF, Frampton CM, Frizelle FA, Rieger NA, et al. Short-term outcomes of the Australasian randomized clinical study comparing laparoscopic and conventional open surgical treatments for colon cancer: the ALCCaS trial. *Ann Surg* 2008; **248**: 728-38.
- Bonjer HJ, Hop WC, Nelson H, Sargent DJ, Lacy AM, Castells A, et al. Laparoscopically assisted vs open colectomy for colon cancer: a meta-analysis. *Arch Surg* 2007; **142**: 298-303.
- Buunen M, Veldkamp R, Hop WC, Kuhry E, Jeekel J, Haglind E, et al. Survival after laparoscopic surgery versus open surgery for colon cancer: long-term outcome of a randomised clinical trial. *Lancet Oncol* 2009; **10**: 44-52.
- Fleshman J, Sargent DJ, Green E, Anvari M, Stryker SJ, Beart RW Jr, et al. Laparoscopic colectomy for cancer is not inferior to open surgery based on 5-year data from the COST Study Group trial. *Ann Surg* 2007; **246**: 655-62.
- Velenik V. Post-treatment surveillance in colorectal cancer. *Radiol Oncol* 2010; **44**: 135-141.
- Lacy AM, Delgado S, Castells A, Prins HA, Arroyo V, Ibarzabal A, et al. The long-term results of a randomized clinical trial of laparoscopy-assisted versus open surgery for colon cancer. *Ann Surg* 2008; **248**: 1-7.
- Jacobs M, Verdeja JC, Goldstein HS. Minimally invasive colon resection (laparoscopic colectomy). *Surg Laparosc Endosc* 1991; **1**: 144-50.
- Kitano S, Kitajima M, Konishi F, Kondo H, Satomi S, Shimizu N; Japanese Laparoscopic Surgery Study Group. A multicenter study on laparoscopic surgery for colorectal cancer in Japan. *Surg Endosc* 2006; **20**: 1348-52.
- Bilimoria KY, Bentrem DJ, Nelson H, Stryker SJ, Stewart AK, Soper NJ, et al. Use and outcomes of laparoscopic-assisted colectomy for cancer in the United States. *Arch Surg* 2008; **143**: 832-9.

13. Milsom JW, Jerby BL, Kessler H, Hale JC, Herts BR, O'Malley CM. Prospective, blinded comparison of laparoscopic ultrasonography vs. Contrast-enhanced computerized tomography for liver assessments undergoing colorectal carcinoma asurgery. *Dis Colon Rectum* 2000; **43**: 44-9.
14. Tang CL, Eu KW, Tai BC, Soh JG, MacHin D, Seow-Choen F. Randomized clinical trial of the effect of open versus laparoscopically assisted colectomy on systemic immunity in patients with colorectal cancer. *Br J Surg* 2001; **88**: 801-7.
15. O'Connell J, Maggard M, Ko C. Colon cancer survival rates with the new American Joint Committee On Cancer sixth edition staging. *J Natl Cancer Inst* 2004; **96**: 1420-5.
16. Braga M, Vignali A, Zuliani W, Radaelli G, Gianotti L, Martani C, et al. Metabolic and functional results after laparoscopic colorectal surgery: a randomized, controlled trial. *Dis Colon Rectum* 2002; **45**: 1070-7.
17. Ota D, Nelson H. The surgeon and adjuvant therapy for stage colon cancer. *Anna Surg Oncol* 2007; **14**: 272-3.
18. Brain MW, Jeffreg AM, Harvey JM, Robert JM. Adjuvant treatment of colorectal cancer. *CA Cancer J Clin* 2007; **57**: 168-85.
19. Mamounas E, Wieand S, Wolmark N, Bear HD, Atkins JN, Song K, et al. Comparative efficacy of adjuvant chemotherapy in patients with Dukes'B versus Dukes'C colon cancer: results form founational surgical adjuvant breast and bowel project adjuvant studies(C-01, C-02, C-03, and C-04). *J Clin Oncol* 1999; **17**: 1349-55.
20. Kovač V, Smrdel U. Meta-analyses of clinical trials in patients with non-small cell lung cancer. *Neoplasma* 2004; **51**: 334-40.
21. Efficacy of adjuvant fluorouracil and folinic acid in B2 colon cancer. International Multicentre Pooled Analysis of B2 Colon Cancer Trials (IMPACT B2) Investigators. *J Clin Oncol* 1999; **17**: 1356-63.
22. Benson AB 3rd, Schrag D, Somerfield MR, Cohen AM, Figueredo AT, Flynn PJ, et al. American Society of Clinical Oncology recommendations on adjuvant chemotherapy for stage II colon cancer. *J Clin Oncol* 2004; **22**: 3408-19.
23. Strzelczyk B, Szulc A, Rzepko R, Kitowska A, Skokowski J, Szutowicz A, et al. Identification of high-risk stage colorectal tumors by combined analysis of the NDRG1 gene expression and the depth of tumor invasion. *Ann Surg Oncol* 2009; **16**: 1287-94.
24. Ocvirk J. Advances in the treatment of metastatic colorectal carcinoma. *Radial Oncol* 2009; **43**: 1-8.
25. Parkin DM, Bray F, Ferlay J, Pisani P. Global cancer statistics, 2002. *CA Cancer J Clin* 2005; **55**: 74-108.
26. Colorectal Cancer Collaborative Group. Surgery for colorectal cancer in the elderly: a systematic review. *Lancet* 2000; **16**: 968-74.
27. Kruschewski M, Germer CT, Rieger H, Buhr HJ. Radical resection of colorectal carcinoma in the oldest old. *Chirurg* 2002; **73**: 241-4.

Expression of NF- κ B p65 phosphorylated at serine-536 in rectal cancer with or without preoperative radiotherapy

Andreas Lewander¹, Jinfang Gao¹, Gunnar Adell², Hong Zhang³, Xiao-Feng Sun¹

¹ Department of Oncology, Institute of Clinical and Experimental Medicine, University of Linköping, Linköping, Sweden

² Department of Oncology, Karolinska University Hospital, Stockholm, Sweden

³ Department of Biomedicine, University of Skövde, Sweden

Received 16 July 2011

Accepted 8 August 2011

Correspondence to: Prof. Xiao-Feng Sun, M.D., Ph.D., Department of Oncology, Institute of Clinical and Experimental Medicine, University of Linköping, SE-581 85 Linköping, Sweden. Phone: +46-10-10-32066; Fax: +46-10-10-33090; Email: xiao-feng.sun@liu.se

Disclosure: No potential conflicts of interest were disclosed.

Background. In the present study, we investigated NF- κ B p65 phosphorylated at Serine-536 (phosphor-Ser536-p65) in rectal cancer and its relationship to preoperative radiotherapy (RT), clinicopathological variables and biological factors.

Patients and methods. Expression of phosphor-Ser536-p65 was examined by using immunohistochemistry in 141 primary rectal cancers, 149 normal mucosa specimens and 48 metastases in the lymph nodes, from rectal cancer patients who participated in a Swedish clinical trial of preoperative RT.

Results. The expression of phosphor-Ser536-p65 in the cytoplasm increased from normal mucosa to primary tumour ($p < 0.0001$, for both the group that did and the group that did not received RT). The expression did not further increase from primary tumour to metastasis in either group ($p > 0.05$). Expression of phosphor-Ser536-p65 was positively related to, or tended to be related to, the expression of tumour endothelium marker 1 (TEM1, $p = 0.02$), FXD-3 ($p = 0.001$), phosphatase of regenerating liver (PRL, $p = 0.02$), p73 ($p = 0.048$) and meningioma associated protein (MAC30, $p = 0.05$) in the group that received RT but there were no such relationships in the group that did not received RT ($p > 0.05$). The expression of phosphor-Ser536-p65 was not related to clinicopathological factors including survival ($p > 0.05$).

Conclusions. The increased expression of phosphor-Ser536-p65 may be involved in rectal cancer development. After RT, phosphor-Ser536-p65 seems to be positively related to the biological factors, which associated with more malignant features of tumours. However, phosphor-Ser536-p65 was not directly related to the response of RT based on recurrence and survival.

Key words: NF- κ B, serine-536; radiotherapy; rectal cancer; immunohistochemistry; recurrence; prognosis

Introduction

Nuclear factor-kappaB (NF- κ B) is responsible for expression by regulating many genes for immune response, cell adhesion, differentiation, proliferation, angiogenesis and apoptosis. The function of NF- κ B is inhibited by binding to NF- κ B inhibitory proteins, and imbalance of NF- κ B and its inhibitors has been associated with development of tumours and other diseases.¹⁻³ Five members of the NF- κ B family have been found in human cells, RelA (p65), p105/p50, p100/p52, RelB and c-Rel. The most common form in human cells is p65/p50 heterodimer.

The regulation of the NF- κ B protein family is very important. Upon activating signals the inhibitory proteins are degraded and the protein translocates into the nucleus where it exerts its effect. The regulation also occurs at the posttranslational level, where protein phosphorylation of the different subunit is one very important mechanism of regulation. Several different phosphorylation sites on the subunits have been discovered. An important site of phosphorylation of p65 subunit is at Serine-536 (phospho-Ser536-p65), and this phosphorylation is involved in regulation of transcriptional activity, nuclear localisation and protein stability.^{1,2,4,5}

TABLE 1. Characteristics of patients and rectal cancers

Characteristics	Non-Radiotherapy		Radiotherapy	
	No.	(%)	No.	(%)
Gender				
Male	45	(57)	39	(63)
Female	34	(43)	23	(37)
Age (years)				
≤66	29	(37)	23	(37)
>66	50	(63)	39	(63)
Stage				
I	22	(28)	16	(25)
IIA	18	(23)	22	(36)
IIIA	9	(11)	0	
IIIB	12	(15)	16	(25)
IIIC	14	(18)	3	(5)
IV	4	(5)	5	(8)
Differentiation				
Well	5	(6)	4	(6)
Moderately	56	(71)	40	(65)
Poorly	18	(23)	18	(29)
Numbers of tumours				
Single	68	(86)	51	(82)
Multiple*	9	(11)	11	(18)
Unknown	2	(3)	0	
Surgical type				
Rectal amputation	42	(53)	22	(35)
Anterior resection	37	(47)	40	(65)
Resection margin				
Tumour free	75	(95)	59	(95)
Tumour involved margin	4	(5)	3	(5)
Distance to anal verge (cm)				
Mean	7.3		8.8	

*Other colorectal cancer or other type of tumour besides the present rectal cancer.

It has also been shown that in some tumours NF- κ B activation can enhance radiosensitivity.^{6,7} Preoperative radiotherapy (RT) is today a standard treatment for rectal cancer patients in Sweden and other countries.⁸ It has been shown to increase survival of the patients.^{9,10} In the present study, we investigated whether the phospho-Ser536-p65 was related to response of RT in rectal cancer patients who received or did not receive RT, and whether there were any relationships of the phospho-Ser536-p65 with clinicopathological variables and biological factors.

Patients and methods

Patients

This study included the patients with rectal adenocarcinoma from the Southeast Swedish Health Care region that participated in a Swedish clinical trial of preoperative RT between 1987 and 1990.⁹ Surgical specimens were obtained by either rectal amputation or anterior resection from 141 patients.

The mean age at diagnosis was 66 years (range 36-85). The mean follow-up time was 83 months (range 0-193). Seventy-nine patients had surgery alone. Sixty-two patients were randomised to preoperative radiotherapy, receiving 25 Gy in 5 fractions over a median of 6 days (range 5-12). Surgery was performed after a median of 3 days (range 1-13) after radiotherapy. The characteristics of the patients and tumours are given in Table 1.

The data regarding expression of tumour endothelium marker 1 (TEM1, unpublished data), FXD-3 (also known as MAT-8), phosphatase of regenerating liver (PRL, also known as PTP4A3, protein-tyrosine phosphatase), p73 and meningioma associated protein (MAC30) on the same material used as in the present study, determined by immunohistochemistry, were taken from previous studies performed at our laboratory.¹¹⁻¹⁴ The number of the patients listed in Table 2 was less than the number of the patients mentioned in the materials of the present study due to available numbers of the previous cases¹¹⁻¹⁴, which matched, with the present study. The immunohistochemical staining

TABLE 2. Expression of NF- κ B phosphorylated at Serine-536 in relation to biological factors expressed in rectal cancer

	Non-radiotherapy		p-value	Radiotherapy		p-value
	Weak (%)	Strong (%)		Weak (%)	Strong (%)	
TEM1						
Weak	9 (39)	14 (61)	0.43	10 (59)	7 (41)	0.02
Strong	13 (30)	31 (70)		8 (25)	24 (75)	
FXD3						
Weak	13 (45)	16 (55)	0.08	13 (68)	6 (32)	0.001
Strong	10 (25)	30 (75)		7 (21)	27 (79)	
PRL						
Weak	12 (34)	23 (66)	1.00	11 (50)	11 (50)	0.024
Strong	9 (33)	18 (67)		5 (19)	21 (81)	
p73						
Weak	7 (29)	17 (71)	0.55	9 (56)	7 (44)	0.048
Strong	16 (36)	28 (64)		8 (27)	22 (73)	
MAC30						
Weak	9 (31)	20 (69)	0.73	9 (53)	8 (47)	0.05
Strong	13 (35)	24 (65)		8 (25)	24 (75)	

for those factors was performed on the normal mucosa, primary tumour and metastasis in the lymph nodes from both the non-RT and RT groups.

Immunohistochemistry

Five-micrometer sections were deparaffinised in xylene and rehydrated in graded ethanol. As the method for antigen retrieval we used was high-pressure cooking in 0.01 M Tris-EDTA buffer (pH 9.0). The sections were heated to 125°C for 30 sec and then cooled to 90°C for 10 sec, the sections were then kept in the buffer till room temperature. The sections were incubated with 3% H₂O₂-methanol for 20 min and washed with phosphate-buffered saline (PBS, pH 7.4). After that the sections were incubated with rabbit anti-phospho-Ser536-p65 antibody (phospho S536, ab28856, Abcam, Cambridge, MA) at 20 mg/ml in antibody diluent (Dako, Carpinteria, CA) overnight, followed by rinsing with PBS. The antibody binds specifically to the Ser536-phosphorylated form of p65 and does not cross-react with non-phosphorylated p65 or any other members of the NF- κ B family. Subsequently, the sections were incubated with a goat anti-rabbit/mouse, coupled with peroxidase provided by the Dako ChemMate EnVision Detection Kit (Dako) for 25 min, and washed with PBS. The peroxidase reaction, using 3,3'-diaminobenzidine tetrahydrochloride, was performed (Dako) for 8 min. Sections known to stain positively were included as positive controls. The negative controls used PBS instead of the primary antibody. In all staining procedures, the positive controls showed clear staining, and there was no staining in the negative controls.

The sections were microscopically examined and scored independently by Lewander A and Gao J without any information on the clinicopathological data. The slides were initially classified as weak including negative (<5% of positive cells) and strong staining in the cytoplasm of normal epithelial cells, and tumour cells and metastasis irrespectively of the percentage of positive cells. To avoid artificial effects, cells in areas with necrosis, with poor morphology, or in the margins of sections were excluded from the analysis.

Statistical analysis

The significance of the difference in phospho-Ser536-p65 expression between normal mucosa, primary tumour and metastasis was tested by Chi-square and McNemar methods. The relationships between phospho-Ser536-p65 expression and clinicopathological/biological variables were examined by Chi-square method, and the relationships to survival were tested by using Cox's proportional hazard model. Survival curves were calculated by using the Kaplan-Meier method. Two-sided p values of <0.05 were considered statistically significant.

Results

Phospho-Ser536-p65 expression in the cytoplasm of normal mucosa, primary tumour and metastasis in the lymph node

When we compared staining intensity of phospho-Ser536-p65 expression in the cytoplasm of normal

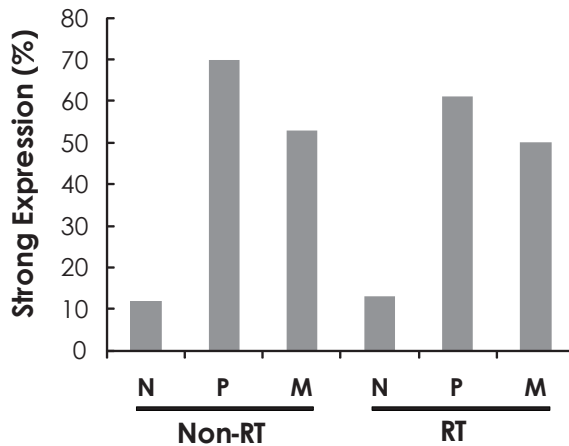


FIGURE 1. Frequency of strong phospho-Ser536-p65 expression in normal mucosa (N), primary tumour (P) and metastasis in the lymph nodes (M) in non-radiotherapy (non-RT) and radiotherapy (RT).

mucosa, primary tumour and metastasis in the lymph node we found significantly more samples with the strong staining of phospho-Ser536-p65 expression in primary tumour than in normal mucosa in the both non-RT and RT groups ($p < 0.0001$ for both Chi-square and McNemar tests for both non-RT and RT groups, Figure 1). There was no significant difference between primary tumour and metastases in either non-RT or RT groups ($p > 0.05$, Figure 1).

We compared phospho-Ser536-p65 expression before and after RT and found there were no differences in normal mucosa ($p = 0.06$), primary tumour ($p = 0.30$) as well as metastases ($p = 0.81$) with chi-square test.

Figure 2 shows phospho-Ser536-p65 expression in normal mucosa, primary tumour and surgical specimens) and metastases in the lymph node. There was weak phospho-Ser536-p65 expression in normal mucosa, while strong expression in the cytoplasm of primary surgical and metastatic tumours.

Phospho-Ser536-p65 expression in the cytoplasm in relation to clinicopathological and biological factors

We compared the expression of phospho-Ser536-p65 expression with the expression of TEM1, FXD3, PRL, p73 and MAC30 (Table 2). Phospho-Ser536-p65 expression was positively related to or tended to be positively related to TEM1 ($p = 0.02$), FXD-3 ($p = 0.001$), PRL ($p = 0.02$) and p73 ($p = 0.048$) and MAC30 ($p = 0.05$) in the RT group. However

in the non-RT group, there were no such relationships ($p > 0.05$, Table 2).

We analysed the relationship of phospho-Ser536-p65 expression in the cytoplasm of primary tumour with clinicopathological variables and did not find any statistically significant relationship of phospho-Ser536-p65 expression with gender, age, differentiation, stage, local/distant recurrence and survival in the two sub-groups of non-RT and RT, or in the whole group of the patients ($p > 0.05$, data not shown).

Discussion

In this study we examined materials from rectal cancer patients included in the Swedish rectal cancer trial of preoperative RT⁹, *i.e.*, the patients divided into two groups, one that received and one that did not received preoperative RT.

When we compared staining intensity of phospho-Ser536-p65 expression in the cytoplasm of normal mucosa, primary tumour and metastasis in the lymph node we found significantly more samples with strong staining in primary tumour than in normal mucosa in either the non-RT or RT group. There was no significant difference between primary tumour and metastases in either the non-RT or RT group. Others have found similar results, that NF- κ B is upregulated in tumour cells compared with the corresponding normal cells in previous studies. Lind *et al.* used electrophoretic mobility shift assay (EMSA) technique and demonstrated that NF- κ B in primary tumour was greatly increased compared with adjacent normal tissue from the same patients.¹⁵ Yu *et al.* examined the expression of NF- κ B p65 by using a monoclonal antibody against NF- κ B p65 in normal colorectal mucosa, colorectal adenomas and colorectal adenocarcinomas, and showed that NF- κ B p65 expression was significantly increased from normal mucosa to adenoma and to adenocarcinoma, furthermore the expression was increased with the transition from low to moderate and to high dysplasia of adenoma.¹⁶ Our previous study in colorectal cancer by immunohistochemistry using the same antibody, showed primary tumour had stronger phospho-Ser536-p65 expression than normal mucosa but had no difference between primary tumours and metastases in the lymph node (unpublished data). Taken together, these results indicate that the NF- κ B p65 may play a role in earlier development of colorectal cancer.

In the same materials used here we have previously studied expression of TEM1 (unpublished

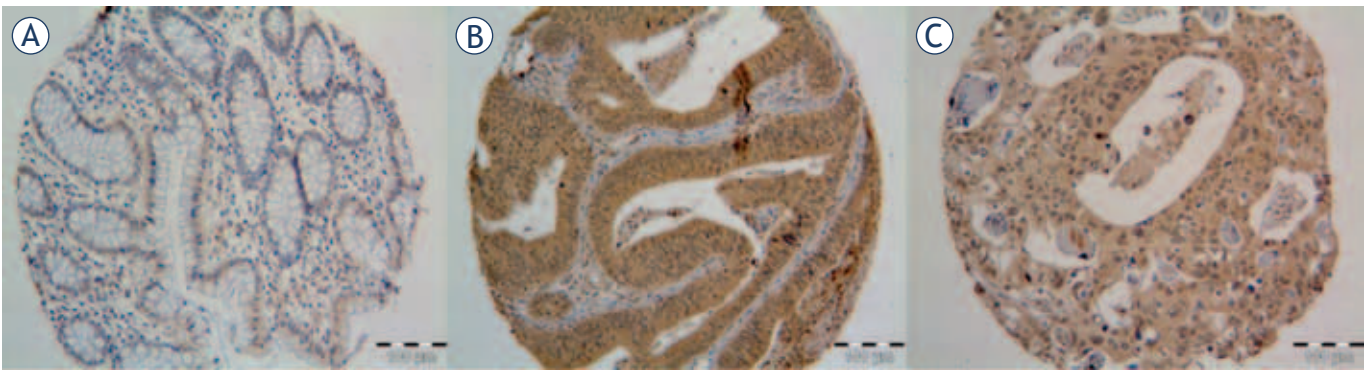


FIGURE 2. The expression of phospho-Ser536-p65 was weak in normal mucosa (A) and strong expression in primary tumour (B) and metastases in the lymph node (C).

data), FXYD3 (9), PRL (11), p73 (10) and MAC30 (12). We found that phospho-Ser536-p65 expression was positively related to TEM1, FXYD-3, PRL, p73 and MAC30 in tumours that received RT, however there were no such relationships in the non-RT group. TEM1 was expressed on periendothelial mural cells (*i.e.*, pericytes) and activated tumour fibroblasts, probably played a role in the tumour vasculature.¹⁷⁻¹⁹ In our previous study we found TEM1 expression in the stroma increased from normal mucosa to primary tumour both in the non-RT and RT group. In the RT group, TEM1 expression in the stroma significantly increased from Dukes' A to B-D. FXYD-3 is an 8-kDa trans-membrane protein and acts as a chloride channel or chloride channel regulator.²⁰ FXYD-3 is overexpressed in several types of cancers including colorectal cancer.^{11,20,21} In our previous study, we found that FXYD-3 expression in the primary tumours was, or tended to be increased compared with normal mucosa regardless of RT. Furthermore in the RT group, strong FXYD-3 expression alone or combined with PRL was related to an unfavourable prognosis independent of both, the TNM stage and tumour differentiation, which are important prognostic factors.²² In tumours with strong FXYD-3 expression, there were less tumour necrosis and a trend of increased incidence of distant metastasis after RT. None of these effects was seen in the non-RT group.¹¹ PRL was identified as an important protein in the metastatic process of colorectal cancer. The PRL family consists of three members, PRL-1, -2, and -3. PRL-3, as a tyrosine phosphatase, may play critical roles in the regulation of cellular growth and cell cycle.^{23,24} We earlier found that PRL expression was increased from normal mucosa to primary tumour. In the RT group, strong PRL expression was related to distant recurrence and poor survival,

independent of both stage and differentiation, but not in the non-RT group. Overexpression of p73 protein has also been correlated with a poor prognosis in colorectal, hepatocellular and breast cancers.^{25,26} In the same material, we earlier found that p73 was overexpressed in rectal cancer compared with normal mucosa. The patients with p73-overexpressing tumours tended to have a higher local recurrence after RT compared to non-RT cases.¹² MAC30 mRNA is expressed in the foetal liver, but not in the adult liver, suggesting a possible role in growth and differentiation of liver.^{27,28} The expression of MAC30 is stronger in breast, stomach and colorectal cancers than the corresponding normal tissues^{14,29,30}, indicating that MAC30 may act as an oncogene in the cancers and might play a role in tumour development and aggressiveness. Why the relationship of phospho-Ser536-p65 expression with TEM1, FXYD-3, PRL, p73 and MAC30 in the RT cases but not in the non-RT cases in this study? One possible speculation is due to the effect of RT, namely, RT resulted in these proteins being more active, temporarily or permanently, and the cells tried to survive. The results may raise a notion that one should consider the targets of RT and the checkpoints controlling the pathways which those factors were involved in. The impact of RT on phospho-Ser536-p65 protein needs to be further investigated in a larger number of patients.

In conclusion, the positive expression of phospho-Ser536-p65 may be involved in rectal cancer development. After RT, the expression of phospho-Ser536-p65 was positively related to the biological factors which associated with more malignant features of tumours. However, we did not find that the NF- κ B protein was directly related to the response of RT based on local/distant recurrence and survival.

Acknowledgement

The study was supported by grants from the Swedish Cancer Foundation, Swedish Research Council and the Health Research Council in the South-East of Sweden. The authors thank Helen Richard, Cecilia Bergenwald, Gertrud Stridh, Gunnel Lindell and Kerstin Ingels, Department of Pathology, Linköping Hospital, Sweden, for kindly preparing tissue sections. We are grateful for the linguist revision by Dr. David Hinselwood.

References

- Hanahan D, Weinberg RA. The hallmarks of cancer. *Cell* 2000; **100**: 57-70.
- Moynagh PN. The NF- κ B pathway. *J Cell Sci* 2005; **118**: 4589-92.
- Sun XF, Zhang H. NF κ B and NF κ BI polymorphisms in relation to susceptibility of tumour and other diseases. *Histol Histopathol* 2007; **22**: 1387-98.
- Sakurai H, Chiba H, Miyoshi H, Sugita T, Toriumi W. IkappaB kinases phosphorylate NF- κ B p65 subunit on serine 536 in the transactivation domain. *J Biol Chem* 1999; **274**: 30353-6.
- Viatour P, Merville MP, Bours V, Chariot AL. Phosphorylation of NF- κ B and IkappaB proteins: implications in cancer and inflammation. *Trends Biochem Sci* 2005; **30**: 43-52.
- Miyakoshi J, Yagi K. Inhibition of I κ B- α phosphorylation at serine and tyrosine acts independently on sensitization to DNA damaging agents in human glioma cells. *Br J Cancer* 2000; **82**: 28-33.
- Yamagashi N, Miyakoshi J, Takebe H. Enhanced radiosensitivity by inhibition of nuclear factor kappa B activation in human malignant glioma cells. *Int J Radiat Biol* 1997; **72**: 157-62.
- Velenik V, Oblak I, Anderluh F. Quality of life in patients after combined modality treatment of rectal cancer: Report of a prospective phase II study. *Radiol Oncol* 2008; **42**: 207-14.
- Improved survival with preoperative radiotherapy in resectable rectal cancer. Swedish Rectal Cancer Trial. *New Eng J Med* 1997; **336**: 980-7.
- Velenik V. Locally recurrent rectal cancer: treatment options. *Radiol Oncol* 2009; **43**: 144-51.
- Loftås P, Önesjö S, Widegren E, Adell G, Kayed H, Kleeff J, et al. Expression of FXD-3 is an independent prognostic factor in rectal cancer patients with preoperative radiotherapy. *Int J Radiat Oncol Biol Phys* 2009; **75**: 137-42.
- Pfeifer D, Gao J, Adell G, Sun X-F. Expression of the p73 protein in rectal cancers with or without preoperative radiotherapy. *Int J Radiat Oncol Biol Phys* 2006; **65**: 1143-8.
- Wallin Å, Svanvik J, Adell G, Sun X-F. Expression of PRL proteins at invasive margin of rectal cancers in relation to preoperative radiotherapy. *Int J Radiat Oncol Biol Phys* 2006; **65**: 452-8.
- Zhang ZY, Zhao ZR, Adell G, Jarlstedt I, Cul YX, Kayed H, et al. MAC30 in rectal cancers with or without preoperative radiotherapy. *Oncology* 2006; **71**: 259-65.
- Lind DS, Hochwald SN, Malaty J, Rekkas S, Hebig P, Mishra G, et al. Nuclear factor- κ B is upregulated in colorectal cancer. *Surgery* 2001; **130**: 363-9.
- Yu HG, Yu LL, Yang Y, Luo H-S, Yu J-P, Meier JJ, et al. Increased expression of RelA/nuclear factor- κ B protein correlates with colorectal tumorigenesis. *Oncology* 2003; **65**: 37-45.
- Christian S, Winkler R, Helfrich I, Boos AM, Besemfelder E, Schadendorf D, et al. Endosialin (Tem1) is a marker of tumor-associated myofibroblasts and tumor vessel-associated mural cells. *Am J Pathol* 2008; **172**: 486-94.
- MacFadyen J, Savage K, Wienke D, Isacke CM. Endosialin is expressed on stromal fibroblasts and CNS pericytes in mouse embryos and is downregulated during development. *Gene Expr Patterns* 2007; **7**: 363-69.
- Tomkowicz B, Rybinski K, Foley B, Ebel W, Kline B, Routhier E, et al. Interaction of endosialin/TEM1 with extracellular matrix proteins mediates cell adhesion and migration. *Proc Natl Acad Sci (USA)* 2007; **104**: 17965-70.
- Morrison BW, Moorman JR, Kowdley GC, Kobayashi YM, Jones LR, Leder P. Mat-8, a novel phospholemmann-like protein expressed in human breast tumors, induces a chloride conductance in *Xenopus* oocytes. *J Biol Chem* 1995; **270**: 2176-82.
- Kayed H, Kleeff J, Kolb A, Ketterer K, Keleg S, Felix K, et al. FXD3 is overexpressed in pancreatic ductal adenocarcinoma and influences pancreatic cancer cell growth. *Int J Cancer* 2006; **118**: 43-54.
- Ocvirk J. Advances in the treatment of metastatic colorectal carcinoma. *Radiol Oncol* 2009; **43**: 1-8.
- Bardelli A, Saha S, Sager JA, Romans KE, Xin B, Markowitz SD, et al. PRL-3 expression in metastatic cancers. *Clin Cancer Res* 2003; **15**: 5607-15.
- Sager JA, Benvenuti S, Bardelli A. PRL-3: a phosphatase for metastasis? *Cancer Biol Ther* 2004; **3**: 952-3.
- Bénard J, Douc-Rasy S, Ahomadegbe JC. TP53 family members and human cancers. *Hum Mutat* 2003; **21**: 182-91.
- Sun XF. p73 overexpression is a prognostic factor in patients with colorectal adenocarcinoma. *Clin Cancer Res* 2002; **8**: 165-70.
- Malhotra K, Luehrsens KR, Costello LL, Raich TJ, Sim K, Foltz L, et al. Identification of differentially expressed mRNAs in human fetal liver across gestation. *Nucleic Acids Res* 1999; **27**: 839-47.
- Murphy M, Pykett MJ, Harnish P, Zang KD, George DL. Identification and characterization of genes differentially expressed in meningiomas. *Cell Growth Differ* 1993; **4**: 715-22.
- Moparthi S, Arbman G, Wallin Å, Kayed H, Kleeff J, Zentgraf H, et al. Expression of MAC30 protein is related to survival and biological variables in primary and metastatic colorectal cancers. *Int J Oncol* 2007; **30**: 91-5.
- Kayed H, Kleeff J, Ding J, Hammer J, Giese T, Zentgraf H, et al. Expression analysis of MAC30 in human pancreatic cancer and tumors of the gastrointestinal tract. *Histol Histopathol* 2004; **19**: 1021-31.

Efficacy of first-line systemic treatment in correlation with BRAF V600E and different KRAS mutations in metastatic colorectal cancer - a single institution retrospective analysis

Martina Reberšek¹, Marko Boc¹, Petra Cerkovnik², Jernej Benedik¹, Zvezdana Hlebanja¹, Neva Volk¹, Srdjan Novakovic², Janja Ocvirk¹

¹ Department of Medical Oncology, ² Department of Molecular Diagnostics, Institute of Oncology Ljubljana, Ljubljana, Slovenia

Received 4 August 2011
Accepted 20 September 2011

Correspondence to: Martina Reberšek, Department of Medical Oncology, Institute of Oncology Ljubljana, Zaloška 2, 1000 Ljubljana Slovenia. Phone: +386 1 5879 220; Fax: +3861 5879 400; E-mail: mrebersek@onko-i.si

Disclosure: No potential conflicts of interest were disclosed.

Background. KRAS mutation status in codons 12 and 13 is recognized as a predictive factor for resistance to anti-EGFR monoclonal antibodies. Despite having a wild type KRAS (wt-KRAS), not all patients with wt-KRAS respond to anti-EGFR antibody treatment. Additional mechanisms of resistance may activate mutations of the other main EGFR effectors pathway. Consequently, other molecular markers in colorectal cancer are needed to be evaluated to predict the response to therapy.

Patients and methods. In this retrospective study, objective responses (OR), time to progression (TTP), overall survival (OS) were analyzed in 176 metastatic colorectal cancer (mCRC) patients treated with first-line chemotherapy in combination with monoclonal antibodies in respect of KRAS status in codons 12 and 13 and BRAF mutational status.

Results. The KRAS mutations were found in 63 patients (35.8%), the KRAS mutation in codon 12 in 53 patients (30.1%) and the KRAS mutation in codon 13 in 10 patients (5.7%). The BRAF V600E mutation was detected in 13 of 176 patients (7.4%). In the subgroup of mCRC patients having wt-KRAS and wild type BRAF (wt-BRAF), the objective response rates were higher (OR 54.0%, CR 14.7%, PR 39.3%) than in the patients with wt-KRAS and mt-BRAF (OR 38.5%, CR 15.4%, PR 23.1%), the difference was not statistically significant ($p=0.378$). Median OS in patients with wt-KRAS wt-BRAF, and in patients with wt-KRAS mt-BRAF, was 107.4 months and 45 months, respectively. The difference was statistically significant ($p=0.042$). TTP in patients with wt-KRAS wt-BRAF, and in patients with wt-KRAS mt-BRAF, was 16 months and 12 months, respectively. The difference was not statistically significant ($p=0.558$).

Conclusions. Patients with BRAF V600E mutation have statistically significantly worse prognosis than the patients with wt-BRAF and progress earlier during treatment. The definitive role of the BRAF V600E mutation as a prognostic and predictive factor for the response to anti-EGFR monoclonal antibodies needs to be analyzed in large prospective clinical studies.

Key words: metastatic colorectal cancer; KRAS; BRAF; prognostic factors

Introduction

Colorectal cancer (CRC) is the fourth most common cancer and one of the leading causes of cancer death in the world. It is the most common cancer in Slovenia and, according to the Cancer Registry of Slovenia, 1279 new patients were diagnosed with CRC in 2007.¹ The majority of patients need

combined modality treatment and careful post-treatment surveillance is necessary to offer patient an optimal treatment approach.^{2,3} Metastatic disease is still incurable, with 5% five-year survival without treatment. With the introduction of new chemotherapy, using oxaliplatin and irinotecan in the current management of metastatic disease, in combination with biologicals, targeting epidermal

growth factor- mediated growth regulatory pathway and the vascular endothelial growth factor-mediated angiogenesis pathway, we can prolong the progression-free survival (PFS) and overall survival (OS) of these patients.⁴⁻⁸ In selected patients with appropriate combination of therapy and surgery we can achieve approximately a 50% five-year survival.

The development of CRC is a multistep process which accumulates different gene mutations, chromosomal abnormalities and epigenetic changes.^{9,10} The mutations within KRAS proto-oncogen, predominately within codons 12 and 13, activate RAS/RAF signalling and are thought to occur early in carcinogenesis of CRC. The KRAS status is the first molecular marker to predict the response to anti-EGFR monoclonal antibodies cetuximab and panitumumab in metastatic CRC (mCRC) patients, and it needs to be determined before deciding in favor of treatment with anti-EGFR antibodies. As the KRAS mutations occur early in CRC formation, there is a high concordance between the KRAS mutations of primary tumour and metastases, which was confirmed in previous studies.¹¹⁻¹³ In a recent retrospective study, de Roock with his colleagues raised the possibility that the patients with the KRAS mutation in codon 13 might have benefited from anti-EGFR antibodies treatment.¹⁴ The mutations in KRAS gene are found in approximately 30 to 40% of mCRC patients, reported in previous literature, but only 40 to 60% of these patients with wt-KRAS will respond to anti-EGFR antibodies treatment.^{15,16} Therefore, other molecular markers downstream of EGFR in the RAS/RAF/MAPK pathway and other effector pathways are found to be involved to predict the response to specific systemic therapy.

The BRAF gene encodes a serine/threonine protein kinase of the RAS/RAF/MEK/ERK kinase pathway and it is also involved in CRC carcinogenesis.^{9,10} The most common mutation of the BRAF gene is V600E which is found in approximately 5 to 9% of mCRC.^{17,18} The same was reported in our previous study carried on Slovenian patients with CRC where the BRAF V600E mutation was found in 5.1% of patients.¹⁹ Previous retrospective studies suggested that mt-BRAF was a marker of resistance to anti-EGFR therapy and that the patients with mt-BRAF had significantly shorter PFS and OS than the patients with wt-BRAF tumours.²⁰ The mutations in the KRAS and BRAF genes have been reported to be mutually exclusive.^{21,22} In the retrospective analysis by Fariña-Sarasqueta *et al.*, it was also shown that the BRAF V600E mutation was

an independent prognostic factor for the survival of patients with colon cancer in stages II and III, while the KRAS mutations did not have any effect on the overall survival of these patients. They concluded that the prognostic role of the KRAS mutations in an adjuvant setting has to be determined.²³ In recent clinical studies, it was published that the BRAF V600E mutation in metastatic colorectal cancer is conferred to a poor prognosis regardless of treatment, but these patients may have some benefit from the treatment with cetuximab in combination with chemotherapy as the first-line therapy, but not when used in the patients in whom the disease has progressed after the first-line therapy.¹⁷

The aim of this retrospective study was to analyze objective responses, time to progression and overall survival of the patients with metastatic colorectal cancer treated with first-line systemic therapy in respect of KRAS and BRAF status.

Patients and methods

Patients

In the study, 176 patients with histologically confirmed metastatic colorectal cancer (mCRC), primarily metastatic or progressed during or after adjuvant therapy were retrospectively analyzed. They were treated according to the national and NCCN guidelines, including performance status of patients and comorbidity. They were treated with chemotherapy, including fluoropyrimidins, capecitabine or 5-fluorouracil (5-FU), oxaliplatin or irinotecan in combination with biologicals, bevacizumab or cetuximab in respect of previously determined KRAS status. The treatment was continued according to the RECIST criteria, until the planned operation or until the progression of disease or toxicity occurred.

Methods and assessment of response

All relevant data from medical files were collected and entered into the data base. Baseline data was analyzed with regard to age, sex, primary site (colon and rectum), number and location of metastases. Efficacy was evaluated according to the Response Evaluation Criteria in Solid Tumours (RECIST, version 1.1) by using computed tomography (CT) scans, magnetic resonance scans, abdominal ultrasound, chest X-ray, bone scans, clinical examination and laboratory tests.²⁴ The study was conducted in the conformance with the principles of the Declaration of Helsinki.

Molecular analysis of KRAS and BRAF mutations

DNA for molecular analysis was extracted from formalin-fixed, paraffin-embedded tumour tissue of primary tumours or metastases with at least 70% of tumour cells. TheraScreen KRAS Mutation Kit® (Roche Applied Science, Mannheim, D) was used to determine seven most common mutations in codons 12 and 13 of the KRAS gene. The V600E mutation in BRAF was detected by end-point genotyping using the TaqMan MGB probes (Applied Biosystems, Warrington, UK) as described previously.¹⁹ The mutation V600E in BRAF in positive tumour samples was confirmed by direct sequencing after amplification of the exon 15 of the BRAF gene.¹⁹

Statistical analysis

The primary end-points of the analysis were overall response rate (ORR), based on RECIST criteria, overall survival (OS) and time to progression (TTP) according to the KRAS and BRAF status.

The χ^2 -test was used to compare ORR, OS and TTP between groups, with 95% confidence intervals (CI) calculated for the medians. OS and TTP were estimated by using Kaplan-Meier Estimates and compared using the log-rank test. TTP was measured in all patients from the beginning of the first-line systemic chemotherapy to the first evidence of progression. The duration of survival was calculated from the beginning of systemic treatment until the date of death. p value < 0.05 was considered statistically significant. Statistical data were obtained using the SPSS software package PASW statistics 18.0.

Results

Patients' characteristics

In total, 176 patients with mCRC who received first-line therapy between May 2005 and October 2010 were included in the retrospective analysis. The cut-off date for the present analysis was April 2011. All patients were treated at the Institute of Oncology Ljubljana, all were Caucasian. The median age was 62 years (range 27-86 years) and the majority of the patients were males (61.4%). Most of the patients had metastatic colon cancer (71.4%). One hundred and four patients had primary metastatic disease (59.1%). The most common sites of metastases were liver and lung. The most com-

TABLE 1. Baseline and disease characteristic of patients

Characteristics	Patients , n= 176 (%)
Gender	
Male	108 (61.4)
Female	68 (38.6)
Age(years)	
Median	62
Range	(27- 86)
WHO PS*	
0	126 (71.6)
1	50 (28.4)
Primary tumour localization,	
Colon	125 (71)
Rectum	51 (28)
Metastatic site	
Liver	68 (38.6)
Lung	11 (6.3)
Liver and lung	12 (6.8)
Other	85 (49.3)
KRAS status	
KRASw	113 (64.2)
KRASm 12	53 (84.0)
KRASm 13	10 (16.0)
BRAF status	
BRAFW	163 (92.6)
BRAFM	13 (7.4)

*WHO PS- World Health Organization performance status

mon therapies the patients received were irinotecan, capecitabine with bevacizumab (29.5%) and oxaliplatin, capecitabine with cetuximab (22.1%). Twenty-four patients (13.6%) were treated only with chemotherapy, capecitabine in monotherapy, or with fluoropyrimidines in combination with oxaliplatin or irinotecan. Patients' baseline and disease characteristics are shown in Table 1.

KRAS mutations were found in 63 patients (35.8%), to be more precise, the KRAS mutation in codon 12 in 53 patients (84.0%) and the KRAS mutation in codon 13 in 10 patients (16.0%). The BRAF V600E mutation was detected in 13 of 176 patients (7.4%).

The mutations of the KRAS or BRAF gene were detected in total in 76 patients (43.4%) (Table1).

Efficacy

The response rates according to RECIST criteria with regard to the KRAS and BRAF status are shown in Table 2. The overall response rates in pa-

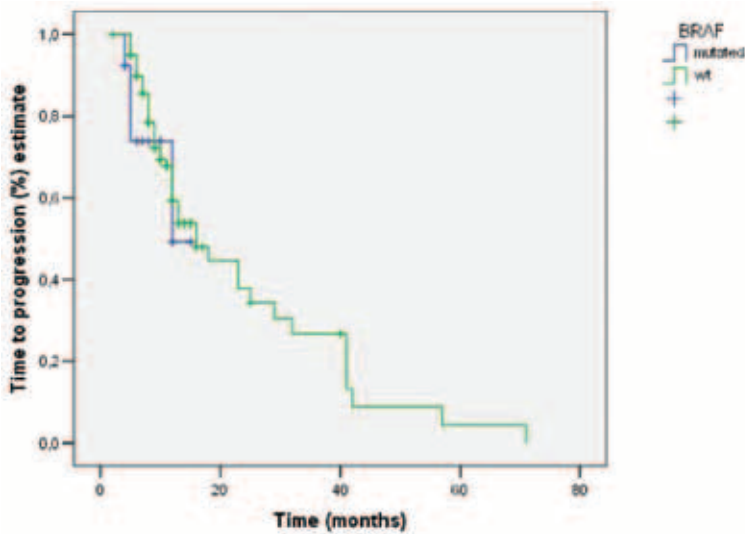


FIGURE 1. Time to progression in patients with wt-KRAS/wt-BRAF and wt-KRAS/mt-BRAF.

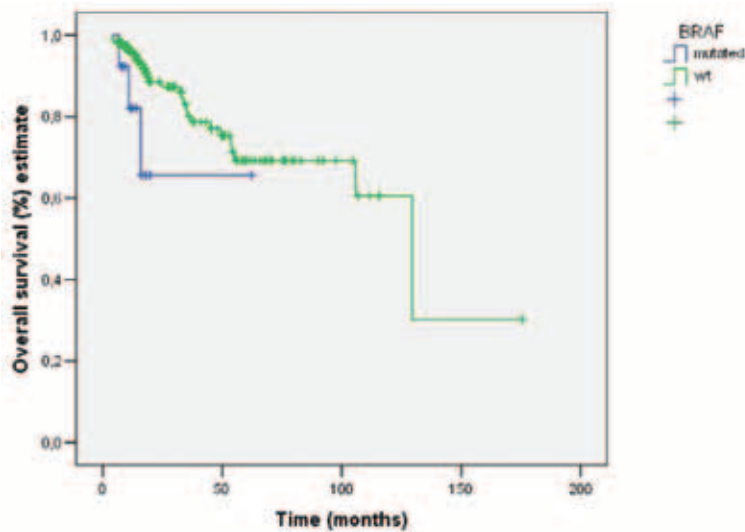


FIGURE 2. Overall survival in patients wt-KRAS/wt-BRAF and wt-KRAS/mt-BRAF.

tients with wt-KRAS and wt-BRAF and in patients with wt-KRAS and mt-BRAF were CR 14.7% + PR 39.3% + SD 35.5% and CR 15.4% + PR 23.1% + SD 46.1% respectively. The objective response rates in the group of patients with wt-KRAS and wt-BRAF tumours were 54.0% (CR 14.7%, PR 39.3%), while in the group of patients with wt-KRAS and mt-BRAF were 38.5% (CR 15.4%, PR 23.1%). The difference was not statistically significant ($p=0.378$). The median OS in the group of patients with wt-KRAS and wt-BRAF tumours was 107.4 months (95% CI: 82- 132.9 months) and in the group of patients with wt-KRAS and mt-BRAF tumours 44.9

months (95% CI: 28.4- 61.5 months) (Figure 1). The difference in median OS between those two groups was statistically significant ($p=0.042$). TTP in the group of patients with wt-KRAS and wt-BRAF tumours and in the group of patients with wt-KRAS and mt-BRAF tumours was 16 months (95% CI: 10.7- 21.2 months) and 12 months (95% CI: 4.0- 15.0 months), respectively (Figure 2). It was not statistically significant ($p=0.558$).

In the KRAS mutation subgroups, the objective response rate of 53 patients with the mutation in codon 12 was 47% (CR 20.7%, PR 26.4%) and, in 10 patients with the mutation in codon 13, the objective response was 33% (CR 11.1%, PR 22.2%). The difference was not statistically significant ($p=0.08$). TTP in the patients with the mutation in codon 12 and the patients with the mutation in codon 13 was 13.5 months (95% CI: 9- 18 months) and 9.3 months (95% CI: 5.1- 13.5 months), respectively. The difference was not statistically significant ($p=0.106$).

Surgical resection of liver metastases was performed in 47/176 patients (26.7%); more specifically, in 31 patients with wt-KRAS tumours and in 16 patients with mt-KRAS tumours. R0 resection was achieved in 38/176 patients (21.6%), of whom 37 patients had wt-BRAF and only one had mt-BRAF tumour.

Discussion

In our study population, the KRAS mutations in codons 12 and 13 were found in 35.8% of patients, in most of them in codon 12; while the mutation V600E in BRAF gene was detected in 13 patients (7.4%). The results of testing are comparable with those previously reported, where the KRAS mutations were found in 30 to 40% and the BRAF V600E mutation in 5 to 9% of the patients.^{11-13,17-19}

The presented data demonstrate that the patients with the BRAF V600E mutation have worse prognosis than the patients with wt-BRAF tumour and progress early during treatment. The patients with wt-BRAF tumours have higher response rates than the patients harbouring the BRAF V600E mutation, but the difference was not statistically significant. One third of the patients with wt-KRAS or mt-BRAF tumour still respond to the treatment, alluding that the BRAF status is not predictive for the response to anti-EGFR antibody therapy. This was also reported in previously published analyses and, in recently published retrospective meta-analysis of the CRYSTAL and OPUS studies, it was also concluded, that the patients with BRAF muta-

TABLE 2. Response rates in KRAS wild type patients according to BRAF status in first-line therapy

	wKRAS	wKRAS/wBRAF	wKRAS/mBRAF
Overall response rate (CR+ PR), n (%)	93 (52.8)	88 (54.0)	5 (38.5)
Disease control rate (CR+PR+SD), n (%)	157 (89.2)	146 (89.5)	11 (84.6)
CR	26 (14.8)	24 (14.7)	2 (15.4)
PR	67 (38.0)	64 (39.3)	3 (23.1)
SD	64 (36.4)	58 (35.5)	6 (46.1)
PD	19 (10.8)	17 (10.5)	2 (15.4)
Median OS, months estimate	129.4 (95% CI: 52.4- 206.4)	107.4 (95% CI: 82- 132.9)*	44.9 (95% CI: 28.4- 61.5) *
Median TTP, months estimate	15.9 (95% CI: 10.8- 21.0)	16.0 (95% CI: 10.7-21.2)**	12.0 (95% CI: 4.0-15.0) **

* p= 0.042

** p= 0.558

tion might have also benefited from the treatment with anti-EGFR antibodies.^{17,18,21-23,25} At this point it should be highlighted that not all patients in our retrospective analysis with wt-KRAS received cetuximab-based first-line systemic therapy; the therapy was selected in accordance to the patients' baseline characteristics, the purpose of treatment or planned operation for metastases.

The difference in TTP between the patients with wt-KRAS and wt-BRAF tumours and the patients with wt-KRAS and mt-BRAF tumours was 4 months. The difference was not statistically significant, probably due to our small group of patients and, consequently, small proportion of the patients with BRAF mutation. The comparison of median OS of those two groups showed a statistically significant difference which was also accompanied with a better prognosis of patients with wt-KRAS and wt-BRAF tumour. These results are comparable with those reported earlier.^{17,20,21} The results of retrospective pooled analysis from randomized CRYSTAL and OPUS trials showed that cetuximab as the first-line chemotherapy based on irinotecan or oxaliplatin significantly improved OS, ORR and PFS the in patients with wt-KRAS tumours. According to the results of the same meta-analysis, the patients with BRAF mutations also appeared to have benefited from cetuximab as the first-line systemic treatment.^{25,26}

In our retrospective study, the KRAS mutations were most frequently detected in codon 12. This is in accordance with the results of our previous study.¹⁹ Comparing the patients having KRAS mutations in codon 12 with the ones having the muta-

tion in codon 13 after the treatment with chemotherapy and bevacizumab, the response rates were higher in the patients with the mutations in codon 12. Nevertheless, the differences in response rates, OS and TTP between these two groups were not statistically significant; we assume that the groups of patients were too small. In the contrast, in their retrospective study, De Roock *et al.* showed that the patients with the mutation in codon 13 KRAS who were treated with cetuximab had better overall and progression-free survival than the patients with other KRAS mutations and might have benefited from the treatment with cetuximab.¹⁴ In an abstract recently published in the 2011 ASCO Annual Meeting Proceedings, Tejpar *et al.* retrospectively analyzed the influence of KRAS G13D mutations on the efficacy of treatment with cetuximab as the first-line systemic therapy and compared it with the pooled results of randomized studies CRYSTAL and OPUS. The patients with the KRAS mutation in codon 13 had a much lower treatment effect compared to the patients with wt-KRAS tumours and might have nevertheless benefited from treatment with cetuximab.²⁷

Although not studied in our retrospective analysis, other KRAS mutations were also reported to predict the response to anti-EGFR monoclonal antibodies. The results of a small study of 74 patients, conducted by Loupakis with his colleagues, suggested that rare KRAS mutations in codon 61 and in codon 146 might also be responsible for in the treatment resistance to anti-EGFR monoclonal antibodies.^{28,29} In contrast, in their large retrospective analysis, De Roock *et al.* concluded that the codon

146 mutations did not affect the response to cetuximab and that the patients with codon 61 mutant tumours had lower response rate.²⁰ According to the analysis of other mutations, they proposed testing of KRAS status, if not mutated, then of BRAF and NRAS status, and PIK3CA exon 20 mutation in order to improve the objective response up to 40% in selected patients.

In our retrospective study, 26.7% of patients, all with KRAS wild-type tumours, who had previously unresectable liver-only metastases, underwent surgical resection after systemic therapy, with R0 resection achieved in 38 patients (21.6%); one of those was patient with the BRAF V600E mutation. Although it is difficult to make any comparison, because our patients were not selected according to specific systemic therapy, these results are comparable with those reported in previous studies claiming that 19 to 23% patients treated with bevacizumab- and irinotecan-based chemotherapy and with previously unresectable liver-only metastases underwent resection.³⁰⁻³² In a recently published clinical study BOXER, where the patients with unresectable liver-only metastases were treated with oxaliplatin, capecitabine and bevacizumab, R0 resection was achieved in 40% of patients.³³ The proportion of patients with resected liver metastases in our retrospective study was higher than that reported in earlier studies including the patients with previously unresectable liver-only metastases and treated with cetuximab in combination with irinotecan- or oxaliplatin-based chemotherapy; resection was achieved in 4 to 10%.^{34,35} In the randomized phase II CELIM study, in which the patients with liver-only metastases were treated with irinotecan- or oxaliplatin-based chemotherapy with cetuximab as the first-line systemic therapy, the proportion of R0 resection was higher; it was achieved in 34% of patients.³⁶ In another phase II POCHER trial, the proportion of R0 resection was even higher; it was achieved in 60% of patients who were treated with chronomodulated chemotherapy with irinotecan, oxaliplatin, 5-fluorouracil and leucovorin.³⁷

In conclusion, the results of our retrospective study showed that the patients with BRAF V600E mutation had worse prognosis than those with wt-BRAF, with lower response rates and progressed early during systemic treatment, consequently, with less possibilities to achieve resectability of metastatic disease. The definitive role of the BRAF V600E mutation as a prognostic and predictive factor to response to the anti-EGFR monoclonal antibodies needs to be analyzed in large prospec-

tive clinical studies. Different KRAS mutations in codon 12 and 13 and other molecular markers, predictive or prognostic, downstream of EGFR in the RAS/RAF/MAPK pathway, and other effector pathways, are needed to be defined to select the patients, who will benefit from specific systemic therapy in a way of individualized treatment.

References

1. Cancer in Slovenia 2007. Ljubljana: Institute of Oncology Ljubljana, Epidemiology and Cancer Registry, Cancer Registry of Republic of Slovenia, 2010.
2. Meyerhardt JA, Mayer RJ. Systemic therapy for colorectal cancer. *N Engl J Med* 2005; **352**: 476-87.
3. Velenik V, Oblak I, Anderluh F. Quality of life in patients after combined modality treatment of rectal cancer: Report of a prospective phase II study. *Radiol Oncol* 2008; **42**: 207-14.
4. Velenik V. Post-treatment surveillance in colorectal cancer. *Radiol Oncol* 2010; **44**: 135-41.
5. National Comprehensive Cancer Network: NCCN clinical practice guidelines in oncology: colon cancer. V.3.2011 (on line). Available: http://www.nccn.org/professionals/physician_gls/PDF/colon.pdf. Accessed April 20, 2011.
6. Advanced colorectal cancer: ESMO clinical practice guidelines for diagnosis, treatment. *Ann Oncol* 2010; **21**: v93-7.
7. Kohne CH. How to integrate molecular targeted agents in the continuum of care. *Ann Oncol* 2010; **21**: vii134-9.
8. Ocvirk J. Advances in the treatment of metastatic colorectal carcinoma. *Radiol Oncol* 2009; **43**: 1-8.
9. Cohen SJ, Cohen RB, Meropol NJ. Targeting signal transducing pathways in colorectal cancer- More than skin deep. *J Clin Oncol* 2005; **23**: 5374-85.
10. Markowitz SD, Bertagnolli MM. Molecular basis of colorectal cancer. *N Engl J Med* 2009; **361**: 2449-60.
11. Artale S, Sartore-Bianchi A, Veronese SM, Gambi V, Sarnataro CS, Gambacorta M, et al. Mutations of KRAS and BRAF in primary and matched metastatic sites of colorectal cancer. *J Clin Oncol* 2008; **26**: 4217-9.
12. Etienne-Grimaldi M-C, Formento J-L, Francoeur M, François E, Formento P, Renée N, et al. K-Ras mutations and treatment outcome in colorectal cancer patients receiving exclusive fluoropyrimidine therapy. *Clin Cancer Res* 2008; **14**: 4830-5.
13. Ličar A, Cerkovnik P, Ocvirk J, Novaković S. KRAS mutations in Slovene patients with colorectal cancer: frequency, distribution and correlation with the response to treatment. *Int J Oncol* 2010; **36**: 1137-44.
14. De Roock W, Jonker DJ, Di Nicolantonio F, Sartore-Bianchi A, Tu D, Siena S, et al. Association of KRAS p.G13D mutation with outcome in patients with outcome with chemotherapy- refractory metastatic colorectal cancer treated with cetuximab. *JAMA* 2010; **304**: 1812-20.
15. Amado RG, Wolf M, Peeters M, Van Cutsem E, Siena S, Freeman DJ, et al. Wild-type KRAS is required for panitumumab efficacy in patients with metastatic colorectal cancer. *J Clin Oncol* 2008; **26**: 1626-34.
16. Roth AD, Tejpar S, Dolorenzi M, Yan P, Fiocca R, Klingbiel D, et al. Prognostic role of KRAS and BRAF in stage II and III resected colon cancer: Results of the translational study on the PETACC-3, EORTC 40993, SAKK 60-00 trial. *J Clin Oncol* 2010; **28**: 466-74.
17. Van Cutsem E, Lang I, D'haens G, Moiseyenko V, Zaluski J, Kohne C, et al. The crystal study: Assessment of the predictive value of KRAS status on clinical outcome in patients with mCRC receiving first-line treatment with cetuximab or cetuximab plus folfox. [Abstract]. *Ann Oncol* 2008; **19**(Suppl 6): vi17-8.
18. Tol J, Nagtegaal ID, Punt CJA. BRAF mutation in metastatic colorectal cancer. *N Engl J Med* 2009; **361**: 98-99.

19. Ličar A, Cerkovnik P, Novaković S. Distribution of some activating KRAS and BRAF mutations in Slovene patients with colorectal cancer. *Med Oncol* 2010 Jul 20. [Epub ahead of print]
20. De Roock W, Claes B, Bernasconi D, De Schutter J, Biesmans B, Fountzilas G, et al. Effect of KRAS, BRAF, NRAS, and PIK3CA mutations on the efficacy of cetuximab plus chemotherapy in chemotherapy-refractory metastatic colorectal cancer: a retrospective consortium analysis. *Lancet Oncol* 2010; **11**: 753-62.
21. Tejpar S, De Roock W. PIK3CA, BRAF and KRAS mutations and outcome prediction in chemorefractory metastatic colorectal cancer (mCRC) patients treated With EGFR targeting monoclonal antibodies (MoAbs): results of a European Consortium. *Eur J Cancer* 2009; **7**: 322.
22. Lambrechts D, De Roock W, Prenen H, De Schutter J, Jacobs B, Biesmans B, et al. The role of KRAS, BRAF, NRAS and PIK3CA mutations as a marker of resistance of cetuximab in chemorefractory metastatic colorectal cancer. [abstract] *J Clin Oncol* 2009; **27 (Suppl)**: 172.
23. Fariña-Sarasqueta A, van Lijnschoten G, Moerland E, Creemers GJ, Lemmens VE, Rutten HJ, et al. The BRAF V600E mutation is an independent prognostic factor for survival in stage II and stage III colon cancer patients. *Ann Oncol* 2010; **21**: 2396-2402.
24. Eisenhauer EA, Therasse P, Bogaerts J, Schwartz LH, Sargent D, Ford R, Dancey J, et al. New response evaluation criteria in solid tumours: Revised RECIST guideline (version 1.1). *Eur J Cancer* 2009; **45**: 228-247.
25. Kohne CH, Rougier P, Stroh C, Schlichting M, Bokemeyer C, Van Cutsem E, et al. Cetuximab with chemotherapy as 1st- line treatment for metastatic colorectal cancer: A meta- analysis of the CRYSTAL and OPUS studies according to KRAS and BRAF mutation status. *ASCO GI* 2010 [abstract 406].
26. Bokemeyer C, Kohne CH, Rougier P, Stroh C, Schlichting M, Van Cutsem E, et al. Cetuximab with chemotherapy as 1st- line treatment for metastatic colorectal cancer: Analysis of the CRYSTAL and OPUS studies according to KRAS and BRAF mutation status [abstract]. *J Clin Oncol* 2010; **28 (Suppl)**: 3506.
27. Tejpar S, Bokemeyer C, Celik I, Schlichting M, Sartorius U, Van Cutsem E, et al. Influence of KRAS G13D mutations on outcome in patients with metastatic colorectal cancer (mCRC) treated with first- line chemotherapy with or without cetuximab. *ASCO* 2011 [abstract 3511].
28. Loupakis F, Ruzzo A, Cremolini C, Vincenzi B, Salvatore L, Santini D, et al. KRAS codon 61, 146 and BRAF mutations predict resistance to cetuximab + irinotecan in KRAS codon 12 and 13 wild-type metastatic colorectal cancer. *Br J Cancer* 2009; **101**: 715-21.
29. Smith G, Bounds R, Wolf H, Steele RJ, Carey FA, Wolf CR, et al. Activating K-ras mutations outwith 'hotspot' codons in sporadic colorectal tumours-implications for personalised cancer medicine. *Br J Cancer* 2010; **102**: 1-11.
30. Okines A, Del Puerto O, Cunningham D, Chau I, Van Cutsem E, Saltz L, et al. Surgery with curative-intent in patients treated with first-line chemotherapy plus bevacizumab for metastatic colorectal cancer First BEAT and the randomised phase-III NO16966 trial. *Br J Cancer* 2009; **101**: 1033-8.
31. Terrebbonne E, Smith D, Becouarn Y, Michel P, Guimbaud M, Fourrier- Reglat A, et al. Resection of colorectal cancer (CRC) metastases after bevacizumab (BV) treatment for first-line therapy: results of the ETNA cohort study (abstract 3594). *J Clin Oncol* 2010; **28 (Suppl)**:15s.
32. Ocvirk J, Rebersek M, Boc M. Bevacizumab in first- line therapy of metastatic colorectal cancer: A retrospective comparison of FOLFIRI and XELIRI. *Anticancer Res* 2011; **31**: 1777-82.
33. Wong R, Cunningham D, Barbachano Y, et al. A multicentric study of capecitabine, oxaliplatin plus bevacizumab as perioperative treatment of patients with poor- risk colorectal liver- only metastases not selected for upfront resection. *Ann Oncol* 2011; **22**: 2042-8.
34. Van Cutsem E, Kohne CH, Hitre E, Zaluski J, Chang Chien CR, Makhson A, et al. Cetuximab and chemotherapy as initial treatment for metastatic colorectal cancer. *N Engl J Med* 2009; **360**: 1408-17.
35. Bokemeyer C, Bondarenko I, Makhson A, Hartmann JT, Aparicio J, de Braud F, et al. Fluorouracil, leucovorin, and oxaliplatin with or without cetuximab in the first- line treatment of metastatic colorectal cancer. *J Clin Oncol* 2009; **27**: 663-71.
36. Folprecht G, Gruenberger T, Bechstein WO, Raab HR, Lordick F, Hartmann JT, et al. Tumour response and secondary resectability of colorectal liver metastases following neoadjuvant chemotherapy with cetuximab: the CELIM randomised phase 2 trial. *Lancet Oncol* 2010; **1**: 38-47.
37. Garufi C, Torsello A, Tumolo S, Ettorre GM, Zeuli M, Campanella C, et al. Cetuximab plus chronomodulated irinotecan, 5- fluorouracil, leucovorin and oxaliplatin as neoadjuvant chemotherapy in colorectal liver metastases: POCHER trial. *Br J Cancer* 2010; **103**: 1-6.

Hepatocellular carcinoma with subcutaneous metastasis of the scalp

Yilmaz Tezcan and Mehmet Koc

Selcuk University, Meram Faculty of Medicine, Department of Radiation Oncology, Konya, Turkey

Received 6 April 2011
Accepted 23 May 2011

Correspondence to: Yilmaz Tezcan, M.D. Department of Radiation Oncology, Meram Faculty of Medicine, Selcuk University, 42090-Konya, Turkey. Phone: +332 223 6942; Fax: +0332 223 6182; E-mail: yilmaztezcan@yahoo.com

Disclosure: No potential conflicts of interest were disclosed.

Background. The majority of subcutaneous metastases from hepatocellular carcinoma (HCC) originate from needle tracks or surgical wound contamination. Non-iatrogenic subcutaneous metastasis from hepatocellular carcinoma was rarely reported.

Case report. A 70-year-old man presented with a mass in his left occipital region of the scalp. The surgical complete resection was performed. The histopathology report of the scalp mass showed a characteristic metastatic HCC. Computed tomography (CT) of the abdomen showed no primary or metastatic lesion in the abdomen; that's why the adjuvant treatment was not given after the surgery. Five months later, magnetic resonance imaging (MRI) of the brain revealed a 6 x 5.5 cm mass at the left posterior parietal region of the scalp. Second surgery was performed and histopathology of the specimen excised was again metastatic HCC. The external beam radiation therapy (XRT) was administered after the surgery. A follow-up MRI of the brain showed no recurrent disease after 9 months from XRT.

Conclusions. HCCs should be considered in the differential diagnosis of carcinomas metastatic to the skin, even in the absence of liver symptoms.

Key words: hepatocellular carcinoma; radiation therapy; cutaneous metastases

Introduction

Hepatocellular carcinoma (HCC) is the most common primary tumour of the liver. Lungs, abdominal lymph nodes, and bones are the most common extrahepatic metastatic sites of HCC.

Cutaneous metastases from HCC are very rare.^{1,2} We report a case who has a subcutaneous mass on his scalp which was the first clue for the diagnosis of the HCC. Aggressive recurrence was occurred three months after surgery that was well controlled with radiation therapy.

Case report

In November 2009, a 70-year-old man presented with a mass in his left occipital region of the scalp. His ECOG status was 0. He has a history of hepatitis-C virus (HCV) positivity for 30 years. The magnetic resonance imaging (MRI) revealed a 6.5 x 6.0

cm mass invading bone in the left occipital region of the scalp which has extra and intracranial components (Figure 1). Fine needle aspiration biopsy showed a malign tumour.

The mass was completely resected. The macroscopic size of mass was measured 6.0 x 5.5 x 2.0 cm. Pathology of the mass showed a characteristic metastatic hepatocellular carcinoma (HCC) invading the occipital bone. All surgical margins were free of tumour. Immunohistochemical staining showed Pan-CK, CK8, CEA(p) and CD10 positivity.

Complete blood count, liver function tests, and α -fetoprotein (AFP) level were normal. Abdominopelvic computed tomography (CT) showed no abnormalities; that's why no adjuvant treatment was given after the surgery. Five months later (on April 2010) he noticed a mass at the same region. MRI revealed a 5.2 x 2.3 cm (Figure 2) mass invading bone in his left posterior parietal portion of the scalp. For the second time the surgery was performed and once again the metastasis of HCC was

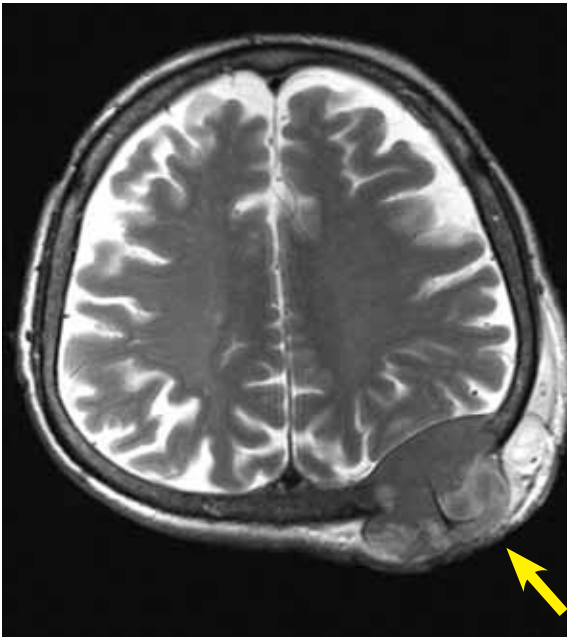


FIGURE 1. Brain MRI with a subcutaneous metastasis from hepatocellular carcinoma.

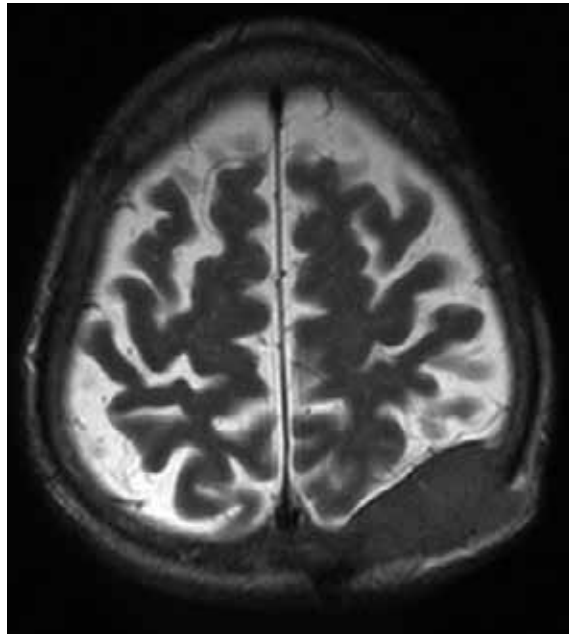


FIGURE 2. Brain MRI with a recurrent subcutaneous metastasis from hepatocellular carcinoma.

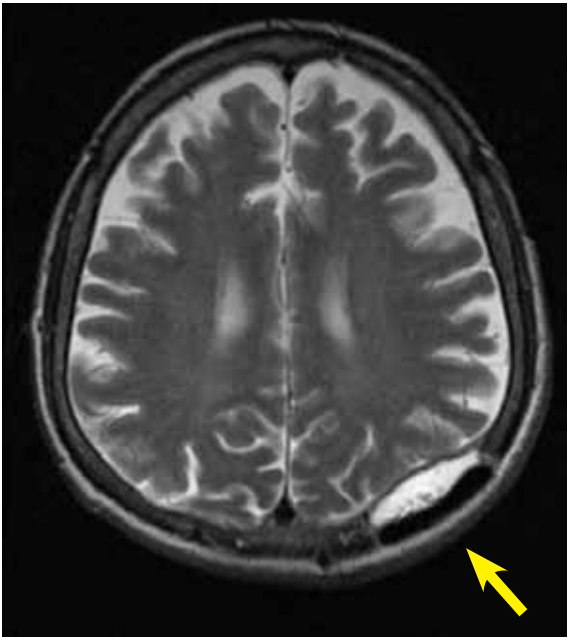


FIGURE 3. Brain MRI after second surgery which is contrast enhanced residual lesion.

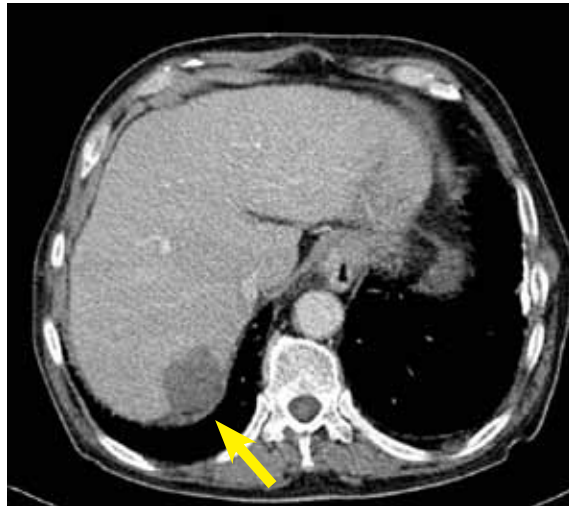


FIGURE 4. CT scan of hepatocellular carcinoma in right lobe of the liver.

confirmed on the histopathological examination of the resected tissue specimen. Postoperative MRI of the brain revealed a contrast enhancing mass on the left parietal region (Figure 3). CT of the abdomen showed a hypodense lesion in the right lobe of the liver (Figure 4). Due to the bone invasion and

residual disease, the palliative external beam radiation therapy (XRT) was applied after the surgery. Three-dimensional treatment planning was used and the radiation dose to the scalp was 300 cGy per day for 5 days a week; the total dose was 3000 cGy (Figure 5). Radiofrequency ablation (RFA) was administered to the metastatic mass of the right liver and the systemic therapy with a targeting agent (sorafenib) treatment was started. A follow-up MRI of the brain showed no recurrent disease 9 months

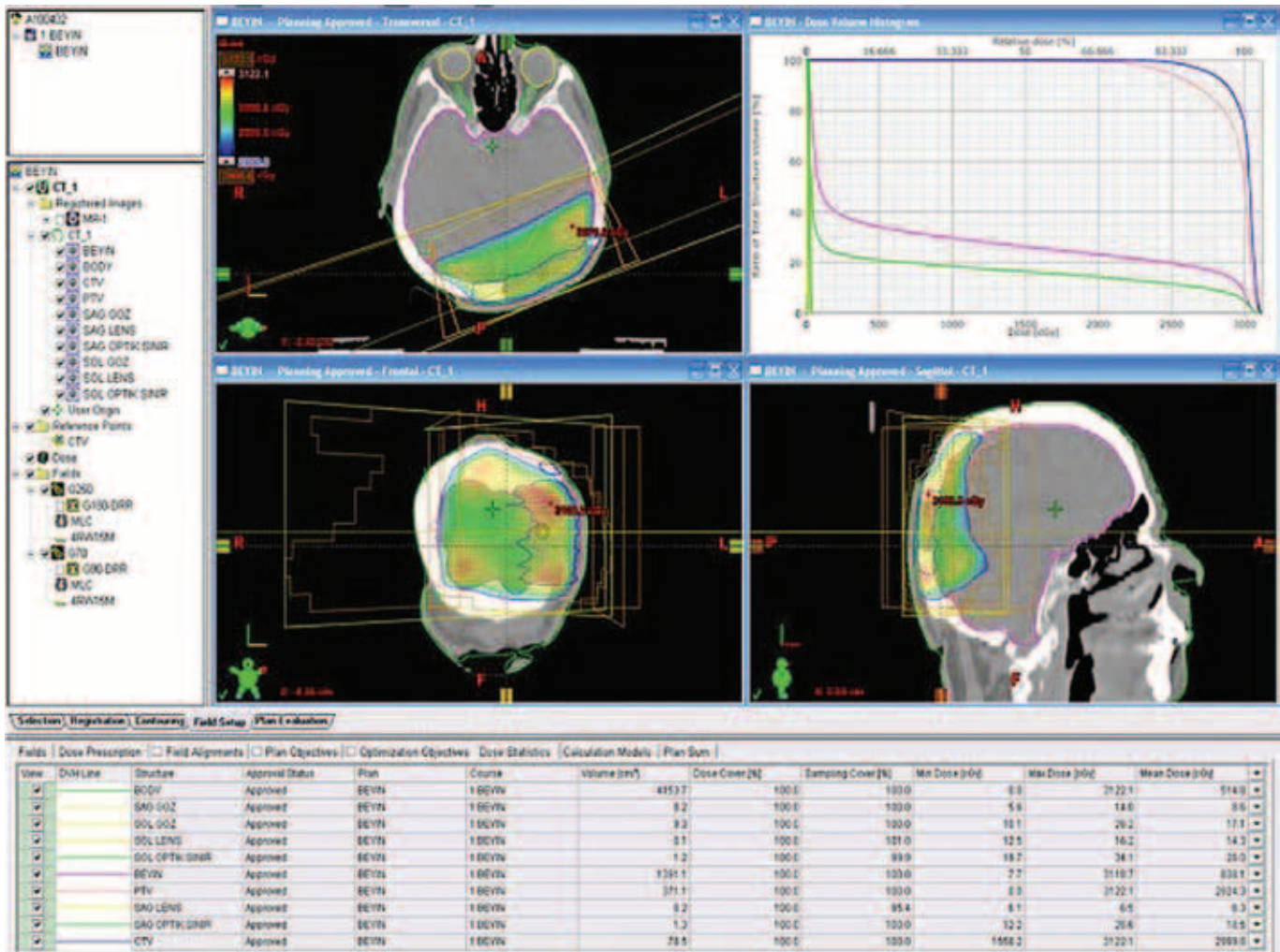


FIGURE 5. The typical dose distribution from 2 posterior oblique field using 6 MV photon beams from conformal radiotherapy plan.

from XRT (Figure 6). After 17-month follow-up from the diagnosis, the patient could perform his daily activities although he developed hypo albuminemia and fatigue.

Discussion

The majority of subcutaneous metastasis from HCC originates from needle tracks or the surgical wound contamination.³⁻⁵ The non-iatrogenic subcutaneous metastasis from hepatocellular carcinoma was rarely reported. Since these patients are usually considered at their terminal period, they are usually observed without any treatment. However, the surgical resection of the metastatic lesion has been performed in a few cases.^{5,6} In one study, skin metastases were detected in only 2.7 % of cirrhotic HCCs, and none in noncirrhotic HCC.⁷

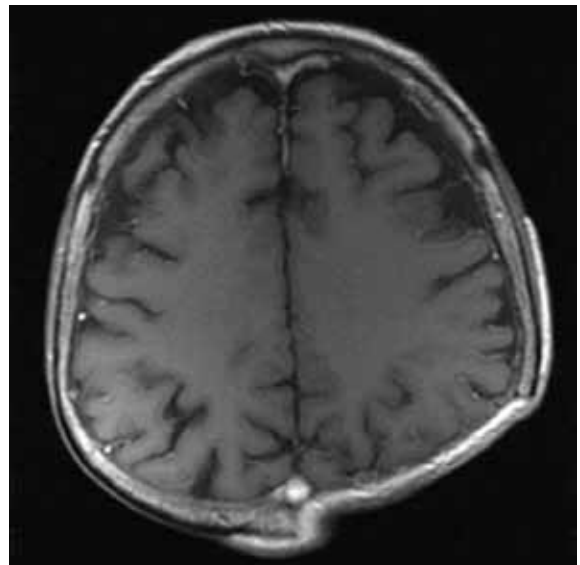


FIGURE 6. MRI of the brain 9-month later of the XRT.

Although the subcutaneous metastasis of HCC is unusual, it could be presented as the sole and initial sign of the HCC.⁸

Huang *et al.*⁹ reported that the radiation therapy was found XRT an efficient treatment modality when subcutaneous metastases of HCC are in question. They observed at least a partial response in 20 of 24 lesions (83.3%), with radiation doses ranging from 8 to 64 Gy. No severe sequelae were recorded. The overall 6-month survival was 43.4%, and the overall 1-year survival was 22.8%. At these patients, the treatment response was good, and the side-effect profile was acceptable. Due to our palliative aim, we applied 30 Gy in 10 fraction XRT over 2 weeks and achieved a good local control during last 9-month.

HCCs should be considered in the differential diagnosis of carcinomas metastatic to the skin, even in the absence of liver symptoms or absence of imaging finding with ultrasonography or CT that usually reveal the primary lesion.¹⁰ Surgery is the primary treatment choice, like in some other cases of metastases¹¹, in particular, when superficial (skin) metastases are to be resected. Radiotherapy seems to be a reasonable alternative in patients with advanced disease and poor performance status and in other clinical scenarios when surgery could not be implemented.

10. Botros M, Quevedo JF, Miller RC. Angiosarcoma of the liver after multimodality therapy for gallbladder carcinoma. *Radiol Oncol* 2009; **43**: 126-31.
11. Strojan P. Role of radiotherapy in melanoma management. *Radiol Oncol* 2010; **44**: 1-12.

References

1. Okuda K, Konda Y. Primary carcinoma of the liver. In: Haubrich WS, Schaffner F, Berk JE, editors. *Bockus gastroenterology*. 5th edition. Philadelphia, PA: WB Saunders; 1995. p. 2444-89.
2. MacDonald RA. Primary carcinoma of the liver: a clinicopathological study of 108 cases. *Arch Intern Med* 1967; **99**: 266-79.
3. Casella G, Cacopardo E, Rovere G, Buda CA, Cascinu S, Baldini V. Cutaneous seeding after ultrasound-guided percutaneous ethanol injection for treatment of hepatocellular carcinoma. *J Clin Ultrasound* 2001; **29**: 354-8.
4. Navarro F, Taourel P, Michel J, Perney P, Fabre JM, Blanc F, et al. Diaphragmatic and subcutaneous seeding of hepatocellular carcinoma following fine-needle aspiration biopsy. *Liver* 1998; **8**: 251-4.
5. Koffi E, Moutardier V, Sauvanet A, Noun R, Flejou JF, Belghiti J. Wound recurrence after resection of hepatocellular carcinoma. *Liver Transpl Surg* 1996; **2**: 301-3.
6. Koffi E, Moutardier V, Sauvanet A, Noun R, Flejou JF, Belghiti J. Wound recurrence after resection of hepatocellular carcinoma. *Liver Transpl Surg* 1996; **2**: 301-3.
7. Peters RL. Metastatic patterns of HCC. In: Okuda K, Peters RL, editors. *Hepatocellular Carcinoma*. New York: John Wiley & Sons, Inc; 1976. p. 156-64.
8. Amador A, Monforte NG, Bejarano N, Martí J, Artigau E, Navarro S, et al. Cutaneous metastases from hepatocellular carcinoma as the first clinical sign. *J Hepatobiliary Pancreat Surg* 2007; **14**: 328-30.
9. Huang YJ, Tung WC, Hsu HC, Wang CY, Huang EY, Fang FM. Radiation therapy to non-iatrogenic subcutaneous metastasis in hepatocellular carcinoma: results of a case series. *Br J Radiol* 2008; **81**: 143-50.

Genotyping of *BRCA1*, *BRCA2*, *p53*, *CDKN2A*, *MLH1* and *MSH2* genes in a male patient with secondary breast cancer

Ana Lina Vodusek¹, Srdjan Novakovic², Vida Stegel², Berta Jereb¹

¹ Department of Radiation Oncology, Institute of Oncology, Ljubljana, Slovenia

² Department of Molecular Diagnostics, Institute of Oncology, Ljubljana, Slovenia

Received 12 May 2011

Accepted 23 June 2011

Correspondence to: Ana Lina Vodusek, MD, Institute of Oncology, Zaloška 2, 1000 Ljubljana, Slovenia. Phone: +386 1 5879 629; Fax: +386 1 5879 304; E-mail: avodusek@onko-i.si

Disclosure: No potential conflicts of interest were disclosed.

Background. Some tumour suppressor genes (*BRCA2*) and mismatch repair genes (*MSH2*, *MLH1*) are correlated with an increased risk for male breast cancer.

Case report. Our patient developed secondary breast cancer after the treatment for Hodgkin's disease in childhood. DNA was isolated from the patients' blood and screened for mutations, polymorphisms and variants in *BRCA1*, *BRCA2*, *p53*, *CDKN2A*, *MLH1* and *MSH2* genes. We found no mutations but common polymorphisms, and three variants in mismatch repair genes.

Conclusions. Nucleotide variants c.2006-6T>C and p.G322D in *MSH2* might be correlated with male breast cancer.

Key words: gene screening; breast cancer; male; secondary neoplasm

Introduction

Secondary neoplasms (SN) are the most serious late effects of the treatment of childhood cancers. Their incidence is increasing with time of observation to 25% at 25 years from diagnosis of the primary tumor.^{1,2} Patients treated with radiotherapy for Hodgkin's disease (HD) are at highest risk for SN.³

Male breast cancer (MBC) is rare, accounting for less than 1% of all breast cancers.^{4,5} Risk factors for primary MBC include testicular disease, benign breast conditions, age, family history, the Klinefelter syndrome, gynecomasty and non-therapeutic radiation exposure.^{5,6} The highest risk for primary MBC is among the carriers of mutations in the *BRCA2* gene. Besides mutations in the *BRCA2* gene, additional germ line mutations in MBC have been reported also in the androgen receptor gene and *PTEN*.⁷ There is likely to be a number of genes more commonly mutated correlated with a modest increase in primary MBC, such as mismatch repair (MMR) genes - *MSH2*, *MLH1*, *PMS1*, *PMS2*.^{7,8}

In literature we found two case reports on secondary MBC, one after the treatment for HD and

one after the treatment for acute lymphoblastic leukaemia including total body irradiation and bone marrow transplantation.^{3,9} There are no data on genetic factors predisposing the development of secondary MBC after the treatment for HD.

The aim of this case report was to elucidate the genetic conditions in a patient with secondary MBC, screening the genes already known to be correlated with primary MBC - *BRCA1*, *BRCA2*, *p53*, *CDKN2A*, *MLH1* and *MSH2*.

Case report

Patient

A 37 year old man developed breast cancer 24 years after the treatment for HD. In 1983, when 13 years old, he was treated with chemotherapy (6 cycles of MOPP/ABVD) and irradiation of the neck and upper thorax, retroperitoneal and inguinal nodes (25 Gy) for stage IIIIBS HD. Afterwards he was followed, at the Department of Paediatrics and after 1995 at the Late Effect Clinic at the Institute of Oncology in Ljubljana.

TABLE 1. Nucleotide variations detected in male breast cancer patient

Gene	BIC*	HGVS nomenclature**	Genotype	Clinical significance
MLH1		c.453+79A>G	heterozygote AG	polymorphism
		c.1668-19A>G	homozygote AA	polymorphism
		c.655A>G (p.I219V)	heterozygote AG	unclassified variant
MSH2		c.211+9G>C	homozygote GG	polymorphism
		c.1511-9A>T	heterozygote AT	polymorphism
		c.1661+11G>A	heterozygote GA	polymorphism
		c.2006-6T>C	heterozygote TC	unclassified variant
		c.965G>A (p.G322D)	heterozygote AG	unclassified variant
BRCA1	2201C>T	c.2082C>T (p.S694S)	heterozygote CT	polymorphism
	2430T>C	c.2311T>C (p.L771L)	heterozygote TC	polymorphism
	2731C>T	c.2612C>T (p.P871L)	heterozygote CT	polymorphism
	3232A>G	c.3113A>G (p.E1038G)	heterozygote AG	polymorphism
	3667A>G	c.3548A>G (p.K1183R)	heterozygote AG	polymorphism
	4427T>C	c.4308T>C (p.F1436S)	heterozygote TC	polymorphism
	4956A>G	c.4837A>G (p.S1613G)	heterozygote AG	polymorphism
BRCA2				
	203G>A	c.1-25G>A	homozygote GG	polymorphism
	1342C>A	c.1114C>A (p.H372N)	homozygote CA	polymorphism
	3624A>G	c.3396A>G (p.L1132L)	heterozygote AG	polymorphism
	4035T>C	c.3807T>C (p.V1269V)	heterozygote TC	polymorphism
	7470A>G	c.7242A>G (p.S2414S)	heterozygote AG	polymorphism
IVS16-14C>T	c.7806-14C>T	heterozygote TC	polymorphism	
P53		c.96 + 41_56 del CCCCAGCCCTCCAGGT	homozygote	polymorphism
		c.215 C>T (p. Pro72Arg)	heterozygote CT	polymorphism
		c.782 + 72 A>C	heterozygote AG	polymorphism
		c.782 + 92 A>G	heterozygote AC	polymorphism
CDKN2A				
		c.1-191A>G	homozygote GG	polymorphism
		c.471+69C>T	heterozygote CT	polymorphism

*Nucleotide variations described as in BIC (Breast Cancer Information Core) database. DNA variants are numerated according to NCBI reference sequence HSU14680 for mRNA of BRCA1, or U43746 for mRNA of BRCA2. First nucleotide of mRNA is numerated as 1.

**Description of nucleotide variations is in accordance with HGVS (Human Genome Variation Society) nomenclature. DNA variants are numerated according to NCBI reference sequence NM_000249 for MLH1, NM_000251 for MSH2, NM_007294.2 for BRCA1, NM_000059.3 for BRCA2, NM_000546 for p53 and NM_000077.3 for CDKN2A. First nucleotide of start codon ATG is numerated as 1.

Eleven years after the treatment we observed primary hypogonadism with low levels of testosterone, bilateral gynecomasty and azoospermia and at the age of 37 a palpable tumour 6 cm in diameter in the central part of the left breast, infiltrating the skin, with an inverted nipple. Ultrasounds of both axillae, of the abdomen, chest X-ray films and Technetium bone scan were normal.

Histology showed an invasive ductal carcinoma, grade III, with negative progesterone and estrogen receptors and positive Her2 status. His family history was negative. He was treated with neoadjuvant chemotherapy, left mastectomy with axillary node dissection, adjuvant treatment with trastuzumab and postoperative irradiation of the left mammary region.

Methods of genetic investigations

Patient's DNA was isolated from peripheral blood using the DNA blood isolation kit Quiagen (Hilden, Germany). It was screened for variants in tumour suppressor genes (*BRCA1*, *BRCA2*, *p53*, *CDKN2A*) and MMR genes (*MLH1* and *MSH2*).

Four methods were used: DGGE (denaturing gradient gel electrophoresis) or HRM (high resolution melting), direct sequencing and MLPA (multiplex ligation-dependent probe amplification). The screening of *BRCA1/2* genes was performed for all exons by the DGGE while *MLH1* and *MSH2* genes were screened using the HRM. Positive fragments were subsequently sequenced to determine the nucleotide change. Genes *BRCA1*, *BRCA2*, *MLH1* and *MSH2* were also screened for large deletions or insertions using the MLPA method. All coding regions of *p53* and *CDKN2A* were sequenced.

HRM was used for discrimination between two DNA molecules with different sequences for the detection of SNPs (single nucleotide polymorphism) and small deletions and insertions. PCR (polymerase chain reaction) was performed on LC480 instrument using the LC 480 High-resolution Melting Master Kit (Roche, Mannheim, Germany) according to manufacturer's instructions.

DGGE was used for detection of SNPs and small deletions or insertions. The PCR amplification of DNA samples was performed using a set of GC-clamped primers (Ingeny International BV, Goes, Netherlands) according to the cycling conditions provided by the primer-manufacturer. Different denaturing and running conditions were used for specific primer sets. When electrophoresis was complete, gels were stained with EtBr and documented using the GelDoc system.

Direct sequencing was performed using the ABI PRISM Big Dye Terminator Cycle Sequencing Kit (Applied Biosystems, Warrington, UK) and products analyzed on the ABI Prism® 310 Genetic Analyzer (Applied Biosystems). Data were collected with ABI Prism 310 software (Applied Biosystems), and the results analyzed with the ABI Prism DNA sequencing analysis software (Applied Biosystems). Sequence data were analyzed utilizing the Gene Runner software tool.

The MLPA was applied for the detection of large deletions and insertions. The probe-mixes labelled as P003 for *MLH1* and *MSH2*, P045-B1 for *BRCA2*, and P002 for *BRCA1* from MRC Holland (MRC Holland, Amsterdam, Netherlands) were used, according to manufacturer's instructions.

Results of genetic investigations

BRCA1 in BRCA2

With MLPA, DGGE and direct sequencing we did not find any changes in the sample. We detected some polymorphisms at the frequently polymorphic loci but no mutations.

However, we found a rare polymorphism in *BRCA2* gene p.V1269V which did not code a different amino acid; therefore, it did not affect protein function (Table 1). The sample was also tested for the presence of mutation 1100delC in *CHEK2* gene with MLPA kit P045-B1. In the samples mutation 1100delC was not detected.

P53

Tumour suppressor gene *p53* was sequenced in total. No mutations were found, but some common polymorphisms were (Table 1).

CDKN2A

By direct sequencing of exons of *CDKN2A* gene (p16 and p14^{ARF}) we detected two polymorphisms: c.1-191A>G in 5'-UTR (untranslated region) and c.471+69C>T in 3'-UTR (Table 1).

MLH1 in MSH2

We detected no changes by means of the MLPA. The screening of the patients' DNA was therefore continued through HRM and sequencing. With these two methods no mutations were discovered, but we found some polymorphisms which were frequently detected in a general population. We also detected three variants of DNA which were described as variants with unknown influence on the protein function (Table 1).

Discussion

Secondary breast cancer is the most common SN among women who have received high dose radiotherapy.¹⁰ However, secondary breast cancer is a rare disease in men and very little is known about its aetiology. It has been suggested that the carcinogenic effect of ionizing radiation may be similar in the male and prepubertal female breast.¹¹

Beside the radiation exposure, some of the risk factors for primary MBC⁶ were also found in our

patient with secondary MBC – *i.e.* hormonal imbalances and gynecomasty.

Genetic factors associated with an increased risk of primary MBC include *BRCA2* mutations that account for 4% to 14% of all primary MBC.^{6,12} We found no such mutations; only a rare V1269V polymorphism that does not affect protein function.

Since p53 is often mutated in female breast cancers, it could be mutated also in MBC. Even though the mutations in tumour suppressor gene *p53* are correlated with numerous malignancies^{13,14}, no mutations were found in our patient while screening this gene. Also in MMR genes (*MLH1* and *MSH2*) and in *CDKN2A* no deleterious mutations have been detected (Table1).

We found polymorphisms in MMR genes – *MLH1* and *MSH2*, frequently detected in a general population, but also three variants (two in *MSH2* and one in *MLH1*) which are described as variants with unknown influence on the protein function. This finding could be of interest since recent reports allude that two of these variants in *MSH2* (c.2006-6T>C and p.G322D) might influence the process of cancer development. Nucleotide variant c.2006-6T>C may be associated with an increased risk for of Non-Hodgkin's Lymphomas.¹⁵ Additionally, the risk of some haematological malignancies in individuals carrying c.2006-6T>C variant is increased after the treatment with alkylating agents such as procarbazine, dacarbazine, cyclophosphamide.¹⁶

According to some recent reports the variant p.G322D is associated with changes in *MSH2* protein function. Individuals with this variant have slightly reduced release efficiency of mismatched targeted DNA compared to the wild type.¹⁷

Conclusions

To our knowledge there are no reports of genetic screening in secondary MBC. We found three unclassified variants that could be correlated with an increased risk of secondary MBC but further studies should be performed.

References

- Jazbec J, Todorovski L, Jereb B. Classification tree analysis of second neoplasms in survivors of childhood cancer. *BMC Cancer* 2007; **7**: 1-6.
- Metayer C, Lynch CF, Clarke EA, Glimelius B, Storm H, Pukkala E, et al. Second cancers among long-term survivors of Hodgkin's disease diagnosed in childhood and adolescence. *J Clin Oncol* 2000; **18**: 2435-43.
- Boussen H, Kochbati L, Besbes M, Dhiab T, Makhlof R, Jerbi G, et al. [Male secondary breast cancer after treatment for Hodgkin's disease. Case report and review of the literature]. [French]. *Cancer Radiother* 2000; **4**: 465-8.
- Ozet A, Yavuz AA, Kömürçü S, Öztürk B, Safalı M, Arpacı F, et al. Bilateral male breast cancer and prostate cancer: a case report. *Jpn J Clin Oncol* 2000; **30**: 188-90.
- Weiss JR, Moysich KB, Swede H. Epidemiology of male breast cancer. *Cancer Epidemiol Biomarkers Prev* 2005; **14**: 20-26.
- Giordano SH, Buzdar AU, Hortobagyi GN. Breast cancer in men. *Ann Intern Med* 2002; **137**: 678-87.
- Leinung S, Horn LC, Backe J. [Male breast cancer: history, epidemiology, genetic and histopathology]. [German]. *Zentralbl Chir* 2007; **132**: 379-85.
- Murata H, Khattar NH, Gu L, Li GM. Roles of mismatch repair proteins hMSH2 and hMLH1 in the development of sporadic breast cancer. *Cancer Lett* 2005; **223**: 143-50.
- Latz D, Alfrink M, Nassar N, Beyerle C. Breast cancer in a male patient after treatment of acute lymphoblastic leukemia including total body irradiation and bone marrow transplantation. *Onkologie* 2004; **27**: 477-9.
- Zebic-Sinkovec M, Kadivec M, Podobnik G, Skof E, Snoj M. Mammographically occult high grade ductal carcinoma in situ (DCIS) as second primary breast cancer, detected with MRI: a case report. *Radiol Oncol* 2010; **44**: 228-31.
- Thomas DB, Rosenblatt K, Jimenez LM, McTiernan A, Stalsberg H, Stemhagen A, et al. Ionizing radiation and breast cancer in men (United States). *Cancer Causes and Control* 1994; **5**: 9-14.
- Eeles RA. Future possibilities in the prevention of breast cancer: intervention strategies in BRCA1 and BRCA2 mutation carriers. *Breast Cancer Res* 2000; **2**: 283-90.
- Malkin D. The role of p53 in human cancer. *J Neurooncol* 2001; **51**: 231-43.
- Zager V, Cemazar M, Hreljac I, Lah TT, Sersa G, Filipic M. Development of human cell biosensor system for genotoxicity detection based on DNA damage-induced gene expression. *Radiol Oncol* 2010; **44**: 42-51.
- Cesar Paz-y-Mino, Perez CJ, Fiallo BF, Leone PE. A polymorphism in the *hMSH2* gene (g1VS12-6T>C) associated with non-Hodgkin lymphomas. *Cancer Genet Cytogenet* 2002; **133**: 29-33.
- Worrillow LJ, Travis LB, Smith AG, Rollinson S, Smith AJ, Wild CP, et al. An intron splice acceptor polymorphism in *hMSH2* and risk of leukemia after treatment with chemotherapeutic alkylating agents. *Clin Cancer Res* 2003; **9**: 3012-20.
- Ollila S, Delmadi Bebek D, Jiricny J, Nystrom M. Mechanisms of pathogenicity in human *MSH2* missense mutants. *Human Mutation* 2008; **29**: 1355-63.

Periampullary localized pancreatic intraepithelial neoplasia-3 (PanIN-3): evaluation with contrast-enhanced MR cholangiography (MRCP)

Oktay Algin¹, Evrim Ozmen¹, Pamir Eren Ersoy², Mustafa Karaoglanoglu¹

¹ Department of Radiology, Atatürk Training and Research Hospital, Bilkent, Ankara, Turkey

² Department of General Surgery, Atatürk Training and Research Hospital, Bilkent, Ankara, Turkey

Received 19 January 2011

Accepted 19 July 2011

Correspondence to: Oktay Algin, Department of Radiology, Atatürk Training and Research Hospital, Bilkent-Ankara, Turkey. Phone: 0090 312 2912525; Fax: 0090 312 2912707; E-mail: droktayalgin@gmail.com

Disclosure: No potential conflicts of interest were disclosed.

Background. The early determination of premalignant lesions of pancreas can prevent unnecessary excessive surgical procedures and can reduce morbidity and mortality. Pancreatic intraepithelial neoplasia-3 (PanIN-3) is a preinvasive form of adenocarcinoma (carcinoma *in situ*). PanINs have not taken place in the literature of radiology yet, it should be considered in differential diagnosis of pancreatic cystic lesions.

Case report. A patient with preliminary diagnosis of chronic cholecystitis who had choledocolithiasis and periampullary pancreatic cyst detected by noncontrast-enhanced (NCE) and contrast-enhanced (CE) magnetic resonance cholangiography (MRCP) is presented. Pathological examination results of gallbladder and pancreatic cyst were reported as gallbladder adenocarcinoma and PanIN-3, respectively.

Conclusions. Pancreatic cystic lesions with thin septa which enhances slightly with the administration of contrast material may represent PanIN-3. In patients with cystic pancreatic lesion localized at periampullary region, using CE-MRCP together with NCE-MRCP could be useful in the evaluation of pancreatic cystic masses as well as other abdominal pathologies.

Key words: multidetector computed tomography; pancreatic cysts; magnetic resonance cholangiography; carcinoma; pancreatic intraepithelial neoplasia; magnetic resonance imaging

Introduction

Pancreatic cystic lesions are often detected with imaging techniques incidentally and can be differentiated from other lesions with some characteristic imaging findings. These findings could be useful for optimal classification, accurate clinical approach, and early diagnosis and correct therapy planning. An early determination of premalignant lesions can prevent unnecessary excessive surgical procedures and can reduce morbidity and mortality. It may increase the survival of patients by providing simple surgical procedures as well.¹

Most of pancreatic cystic lesions are pseudocysts.² Serous micro-cystic adenomas, mucinous cystic neoplasms, intraductal papillary mucinous

neoplasms and solid pseudopapillary tumours consist about 90% of all pancreatic tumors.¹ The remaining 10% is made by metastases, cystic endocrine tumours, teratomas, lymphangiomas, primary pancreatic adenocarcinomas and acinar cell cystadenomas-carcinomas, etc.¹⁻³ Although there are some reports related to the diagnostic features of the diseases mentioned above, as far we are aware, there is no paper about pancreatic intraepithelial neoplasia-3 (PanIN-3) which is a premalignant lesion (carcinoma *in situ*) in radiology literature. In this paper, we present a patient with preliminary diagnosis of chronic cholecystitis who had choledocolithiasis and periampullary pancreatic cystic lesion detected by noncontrast-enhanced (NCE) and contrast-enhanced (CE) magnetic reso-

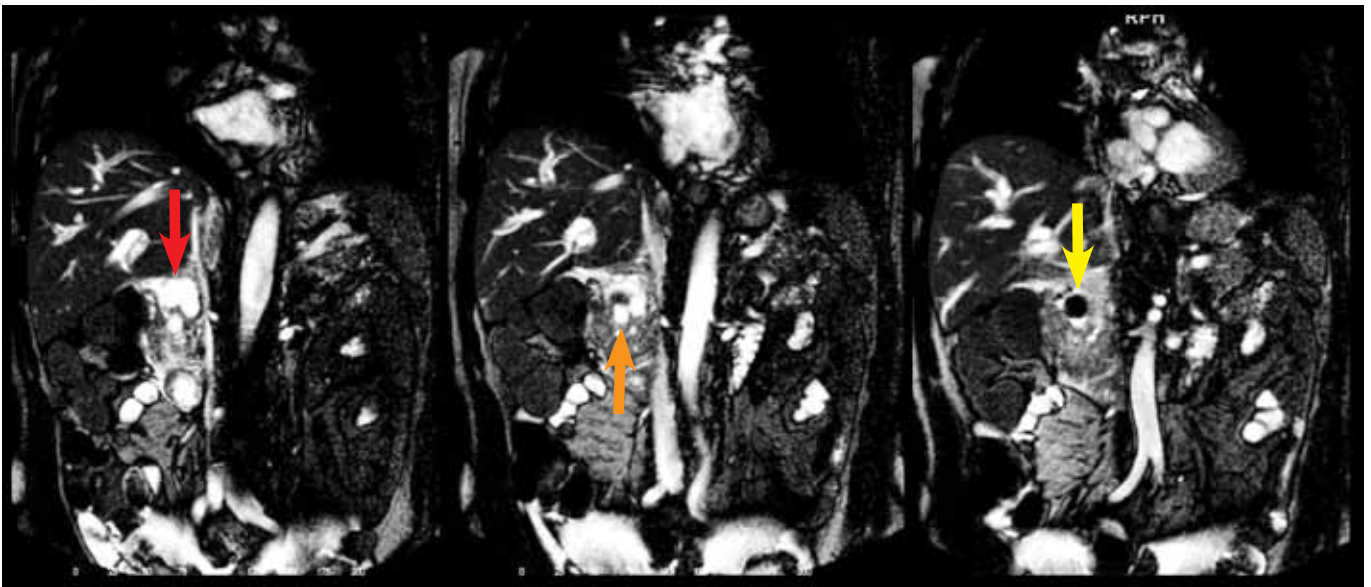


FIGURE 1. Sequential T2 weighted (noncontrast-enhanced) MR cholangiography images of the patient. The images show stone (yellow arrow) in ductus choledochus (orange arrow) and cystic lesion (red arrow) in the pancreas.

nance cholangiography (MRCP) examinations. Pathological examination results of gallbladder and pancreatic cyst were reported as gallbladder adenocarcinoma and PanIN-3, respectively. In this case report we aimed to discuss the role of NCE-MRCP and CE-MRCP in cystic tumours of periapillary region, to evaluate radiologic features of PanINs and review the literature.

Case report

A 58-year-old man was admitted to the emergency department with right upper quadrant pain and jaundice. Though gallbladder could not be demonstrated optimally, the ultrasonographic examination revealed an increase in gallbladder wall thickness but it was contracted. Dilatation of intra and extrahepatic bile duct was detected. As a result, 64-detector multidetector computed tomography (MDCT) was performed since we could not evaluate gallbladder and choledochus optimally with ultrasound. In MDCT, gallbladder was contracted and could not be demonstrated clearly. The enlargement of choledochus and multiple choledochus stones were determined. For a better evaluation of the biliary stones, T2 weighted (T2W) MRCP (NCE-MRCP) was performed. T2W images showed multiple stones in ductus choledochus and intrahepatic bile ducts. A 15x20 mm cystic lesion including thin septa was demonstrated at the head of pancreas at periapillary region (Figure 1).

There was no relationship between cystic lesion and pancreatic duct. Gadoteric-acid enhanced MRCP (CE-MRCP) was performed at the same session to examine the bile duct obstruction and to evaluate the pancreatic cystic lesion (Figure 2). A slight enhancement was detected at the wall and septi of the cystic lesion in CE-MRCP. There was no relationship between cyst and choledochus or pancreatic duct. There was no obstruction in the biliary tract as well. The transition of contrast material to the lumen of gallbladder was not seen at either early or late phase images. The patient was planned to undergo the surgical treatment according to these findings.

At surgical exploration, the size of gallbladder was significantly reduced. There were fibrotic adhesions between gallbladder, liver and transverse colon. Cholecystectomy was done; the pancreatic cystic lesion was aspirated and excised, as well. The histopathologic examination revealed a moderately differentiated adenocarcinoma of gallbladder with positive surgical margins and the pancreatic lesion was reported as PanIN-3. The patient was referred to the medical oncology department. The patient was in good condition the 6th month after the operation.

Discussion

The most important features of pancreatic adenocarcinomas are their progressive course and their

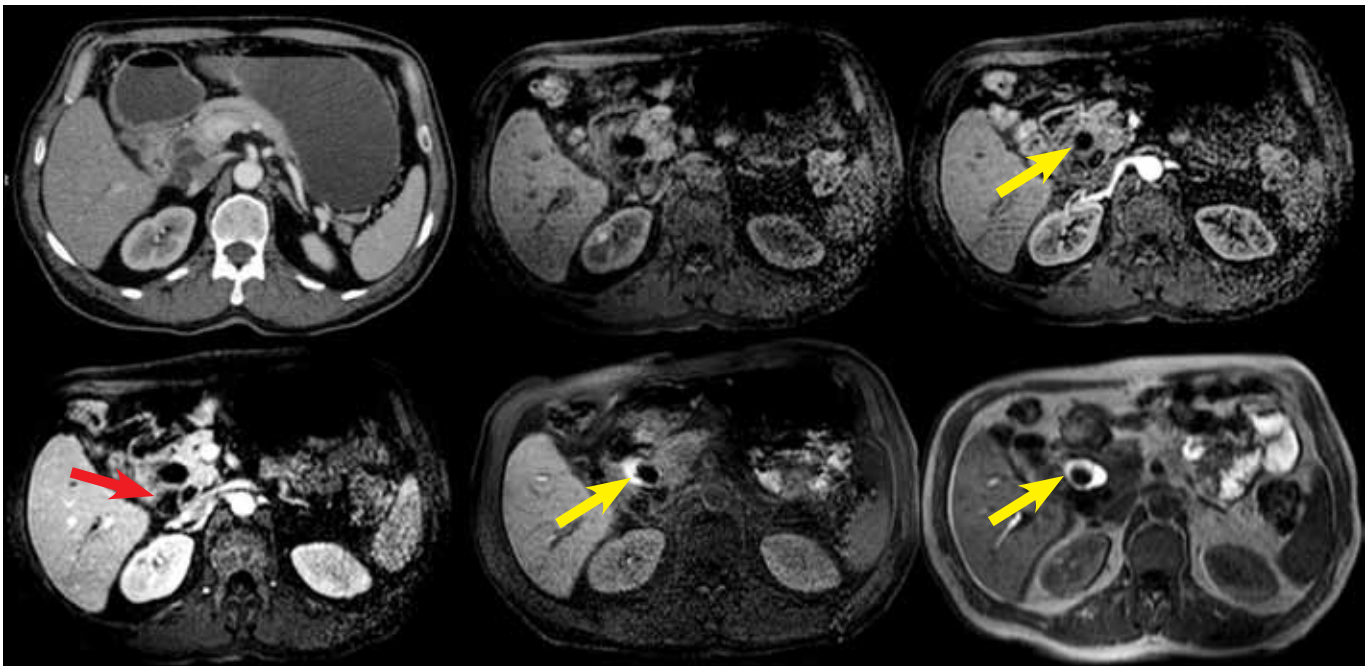


FIGURE 2. Axial contrast enhanced multidetector computed tomography (upper left), noncontrast-enhanced T1 weighted (upper medium), arterial phase contrast-enhanced T1 weighted (upper right), portal phase contrast-enhanced T1 weighted (left below), delayed phase contrast-enhanced T1 weighted with and without fat saturation (middle below and right below, respectively) images of the patient. Pancreatic cystic lesion with contrast-enhanced thin septi-wall (red arrows) can be differentiated from ductus choledochus (yellow arrows) by gadoteric-acid enhanced T1 weighted images. Also, delayed phase T1 weighted images show stone in the ductus choledochus.

high mortality rate. The majority of patients have locally advanced or distant metastatic disease (inoperable stage) during the diagnosis. Therefore, a detection of premalignant and malignant pancreatic lesions at early stage is necessary for curative surgery and improving the survival rates like in other oncological diseases.⁴⁻⁶

PanIN is the most common and histologically well-defined precursor that leads to pancreatic ductal carcinoma.⁷ Histologically PanINs could be divided into 3 subtypes. PanIN-1 and PanIN-2 are low-grade lesions, whereas PanIN-3 (carcinoma *in situ*) is a preinvasive form of adenocarcinoma.⁷ In conclusion PanIN-3 is a premalignant lesion similar to intraductal papillary mucinous neoplasm and mucinous cystic neoplasm and these lesions should be diagnosed early before they improve to invasive carcinoma. Although PanINs have not taken place in the literature of radiology yet, it should be considered in differential diagnosis of pancreatic cystic lesions.³ The existence of genetic, biochemical, and histological relation between PanINs and hepatobiliary/pancreatic carcinomas was reported in recent pathology literature.^{4,7,8} Gallbladder adenocarcinoma of our patient is a good example for this situation.

To evaluate the relation between the lesion and pancreatic duct at the heavily T2W sequences (NCE-MRCP) may differentiate PanIN-3 from intraductal papillary mucinous neoplasm.² Although NCE-MRCP cannot always show the relationship, it often contributes to the diagnosis.³ Endoscopic ultrasound and endoscopic ultrasound-guided fine needle aspiration might be useful when NCE-MRCP is inadequate.³ Mucinous cystic neoplasms are often seen among women during the 4-6th decades (also called mother lesions).¹ They consist of one or multiple cystic lesions and 10-25 % of the lesions may include peripheral curvilinear calcification. They are well demarcated and generally larger than 2 cm.¹ Wall or septa of cysts could be enhanced after the contrast material administration similar to PanIN-3.²

Serous cystadenomas are generally seen among women after the 6th decade (also called grandmother lesions).¹ They include fibrous central scars with or without a characteristic stellate pattern of calcification and these fibrous central scars are enhanced with contrast material.¹ Demonstration of fibrous central scars with or without other characteristic features could provide differentiation serous cystadenomas from other cystic lesions ra-

diologically. Pseudocysts should be included to the differential diagnosis of pancreatic cystic lesions. Also, percutaneous or endoscopic ultrasound-guided fine needle aspiration of cystic fluid may be helpful in many cases with pancreatic cystic mass; since levels of amylase increase in the cystic fluid of pseudocysts, CEA levels are elevated in many mucinous cystic neoplasms, keratinous and amorphous debris can be seen in lymphoepithelial cysts, and mucin-rich fluid and columnar mucinous cells within this fluid can be observed in intraductal papillary mucinous neoplasm.¹⁻³ Solid pseudopapillary tumour and acinar cell cystadenoma/carcinoma are the other rare cystic neoplasms that should be considered in differential diagnosis as well.^{1,2,9}

MDCT, abdominal magnetic resonance imaging (MRI) and MRCP were reported as most useful techniques to evaluate pancreatic cystic lesions.^{3,10} Nevertheless, periapillary cystic lesions cannot be evaluated optimally by the tomographic examination in patients with dilated distal choledochus and choledocholithiasis as in our case.¹¹ In such cases MRI and NCE-MRCP are supposed to be better in determination of cyst morphology and classification.¹¹ However, there is not a published report related to the role of CE-MRCP in the evaluation of pancreatic cysts. CE-MRCP could be useful in determination of the relationship between the cystic lesions adjacent to choledochus and pancreatic duct or choledochus itself. It may also detect possible causes of the pancreatic duct obstruction at the periapillary region and it can provide functional data. CE-MRCP could evaluate the entire abdomen (especially in hepatobiliary system, duodenum, and pancreatic evaluation) at a single session with the addition of T2W images (NCE-MRCP).¹² Moreover, CE-MRCP could supply an optimal assessment in case with suspicious malignant cyst by the detection of the contrast enhancement of cystic lesion with dynamic sequences, without a risk for radiation exposure or nephrotoxic contrast-material application.

Conclusions

Pancreatic cystic lesions with thin septa which enhances slightly with the administration of contrast material may represent PanIN-3. Early diagnosis and treatment of these lesions increase the duration and quality of lifetime by preventing excessive surgical procedures. Therefore, radiologists should be aware of the premalignant pancreatic cystic lesions. In patients with cystic pancreatic tumour localized at the periapillary region, using CE-

MRCP together with NCE-MRCP could be useful in the evaluation of pancreatic cystic masses as well as other abdominal pathologies.

References

1. Acar M, Tatlı S. Cystic tumors of the pancreas: a radiological perspective. *Diagn Interv Radiol* 2011; **17**: 143-9.
2. Gumus M, Ugras S, Algin O, Gundogdu H. Acinar cell cystadenoma (acinar cystic transformation) of the pancreas: the radiologic-pathologic features. *Korean J Radiol* 2011; **12**: 129-34.
3. Dumitrescu D, Săftoiu A, Stoica M, Ciurea T, Popescu C. Natural evolution of an intraductal papillary mucinous neoplasm of the pancreas: A case report. *J Gastrointest Liver Dis* 2007; **16**: 105-8.
4. Feldmann G, Beaty R, Hruban RH, Maitra A. Molecular genetics of pancreatic intraepithelial neoplasia. *J Hepatobiliary Pancreat Surg* 2007; **14**: 224-32.
5. Botros M, Quevedo JF, Miller RC. Angiosarcoma of the liver after multimodality therapy for gallbladder carcinoma. *Radiol Oncol* 2009; **43**: 126-31.
6. Debevec L, Jeric T, Kovac V, Bitenc M, Sok M. Is there any progress in routine management of lung cancer patients? A comparative analysis of an institution in 1996 and 2006. *Radiol Oncol* 2009; **43**: 47-53.
7. Recavarren C, Labow DM, Liang J, Zhang L, Wong M, Zhu H, et al. Histologic characteristics of pancreatic intraepithelial neoplasia associated with different pancreatic lesions. *Human Pathol* 2011; **42**: 18-24.
8. Sanada Y, Yoshida K, Ohara M, Tsutani Y. Expression of orotate phosphoribosyltransferase (OPRT) in hepatobiliary and pancreatic carcinoma. *Pathol Oncol Res* 2007; **13**: 105-13.
9. Chung WJ, Byun JH, Lee SS, Lee MG. Imaging findings in a case of mixed acinar-endocrine carcinoma of the pancreas. *Korean J Radiol* 2010; **11**: 378-81.
10. Sahani DV, Saokar A, Hahn PF, Brugge WR, Fernandez-Del Castillo C. Pancreatic cysts 3 cm or smaller: how aggressive should treatment be? *Radiology* 2006; **238**: 912-9.
11. Sainani NI, Saokar A, Deshpande V, Fernández-del Castillo C, Hahn P, Sahani DV. Comparative performance of MDCT and MRI with MR cholangiopancreatography in characterizing small pancreatic cysts. *AJR Am J Roentgenol* 2009; **193**: 722-31.
12. Algin O, Ozlem N, Kilic E, Karaoglanoglu M, Arslan H. Gd-BOPTA enhanced MR cholangiography findings in gall bladder perforation. *Emerg Radiol* 2010; **17**: 487.

Brain meningioma invading and destructing the skull bone: replacement of the missing bone *in vivo*

Tomaz Velnar¹, Rado Pregelj¹, Clara Limbaeck-Stokin²

¹ University Medical Centre Ljubljana, Department of Neurosurgery, Ljubljana, Slovenia

² Institute of Pathology, Medical Faculty, Ljubljana, Slovenia

Received 12 May 2011

Accepted 18 June 2011

Correspondence to: Tomaž Velnar, MD, MSc, Department of Neurosurgery, University Medical Centre Ljubljana, Ljubljana, Slovenia. Phone: +368 1 522 32 62; Fax: +386 1 522 22 18; E-mail: tvelnar@hotmail.com or t.velnar.s06@cranfield.ac.uk

Disclosure: No potential conflicts of interest were disclosed.

Background. Meningiomas are frequently encountered tumours. In those invading locally into the adjacent tissue, reconstructions may pose a problem.

Case report. We report a case of a benign convexity brain meningioma with invasion into the skull bone and subcutaneous tissue. The tumour was removed completely, together with the infiltrated tissue and the defects were successfully closed with *in vivo* bone reconstruction.

Conclusions. The reconstruction of the skull bone is sometimes needed after the benign meningioma excision. Artificial bone may be a suitable material, allowing fast intraoperative reconstruction with excellent brain protection and cosmetic effect during the one-stage procedure.

Key words: meningioma; brain; invasion; bone reconstruction

Introduction

In neurosurgical practice, meningiomas are frequently encountered tumours and they represent about 20% to 25% of central nervous system neoplasms.¹⁻³ Arising from arachnoidal cells lining the brain and spinal cord, they may be found intracranially and intraspinally. In addition, meningiomas may originate as extracranial or extraspinal masses. These types of tumours are referred to as ectopic and have been described in various locations, the most frequent being the head, neck and soft tissue alongside the vertebral column.^{1,2,4}

Meningiomas usually affect middle aged and older adults and contrary to oligodendroglial tumours are twice as frequent in women as in men.^{4,5} Progesterone receptors have been found in meningeal tumour cells and possibly this hormone positively influences tumour development and progression. Genetic mutations in the neurofibromatosis 2 gene (NF2), immunological factors and

exposure to both high and low dose of ionizing radiation have been recognised among risk factors.²

Ninety percent of meningiomas are slow growing and benign tumours, the remaining ones are invasive or truly malignant.¹ Most meningiomas have good long-term prognosis after the treatment, some display an aggressive clinical behaviour. The vicinity and compression of the eloquent brain zones, venous sinuses, skull base location and adjacent bone destruction may often lead to serious and potentially lethal consequences.^{1,4} Clinically, meningiomas are revealed by various symptoms including neurologic deficits and epileptic seizures.¹ Surgery still remains the principal form of the treatment and must be preceded by appropriate preoperative diagnostics.⁶⁻⁸

Although the majority of meningiomas behave as expansive lesions, compressing the brain tissue, they may cause erosion on the neighbouring structures, especially bone. It is the location and particularly invasion of tumour into adjacent tissue that

may hamper radical resections and reconstructions by simple surgical means.^{1,9,10} In such cases, the reconstruction of the skull bone is problematic due to tissue deficit. Many alternatives exist, from autografts, allografts or artificial replacement material.^{11,12} We report an unusual case of a meningioma of the brain, located in the premotor and motor cortex in the frontoparietal region, invading and destroying the skull bone and subcutaneous tissue. The tumour was removed completely, together with the infiltrated tissue and the defects after the operation were successfully reconstructed with *in vivo* bone reconstruction.

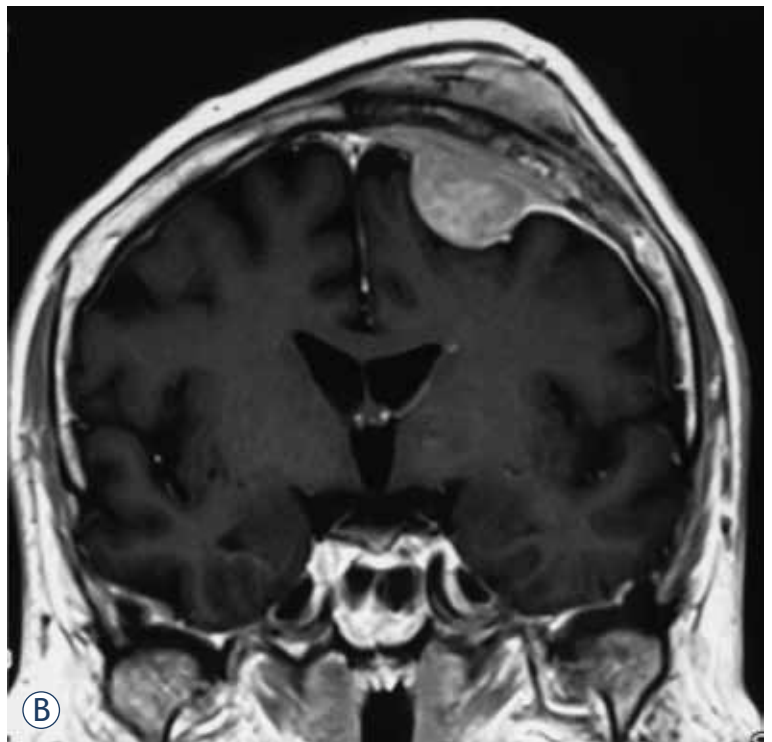
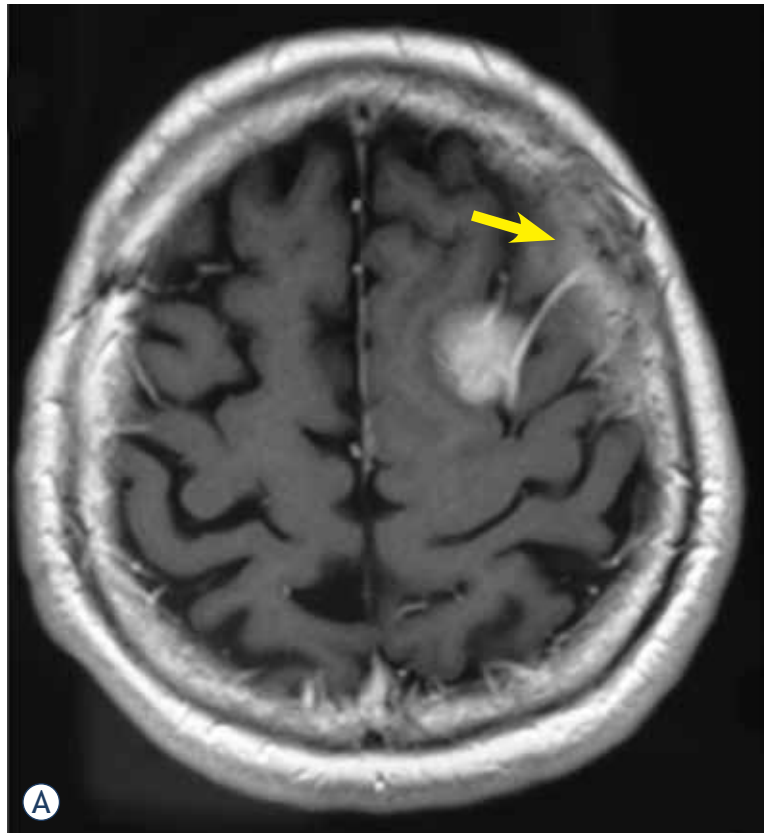
Case report

A 66-year old gentleman in otherwise good general health was admitted to the neurosurgical department due to a skull deformation in the left frontoparietal region, which was growing progressively. He first noticed it approximately seven months ago and complained of dull headaches, located in the left half of the head that were noticed a few times weekly. No other complaints in connection with his health status were reported at the admission.

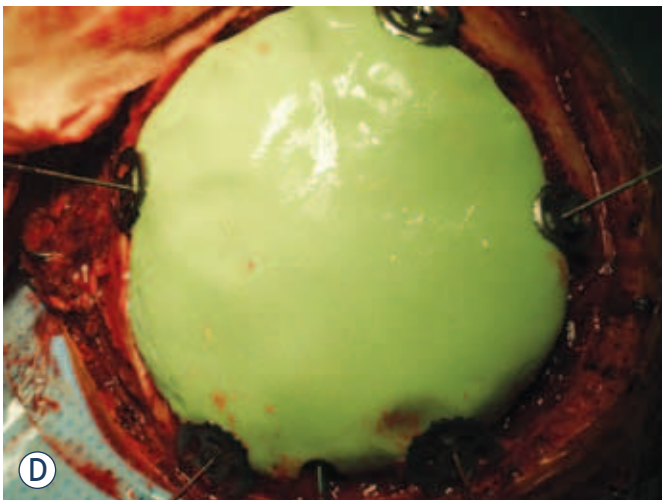
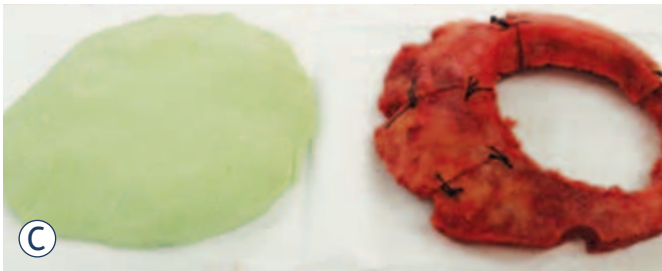
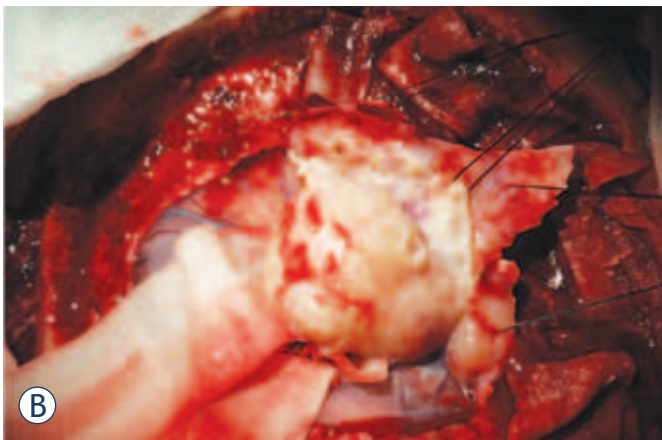
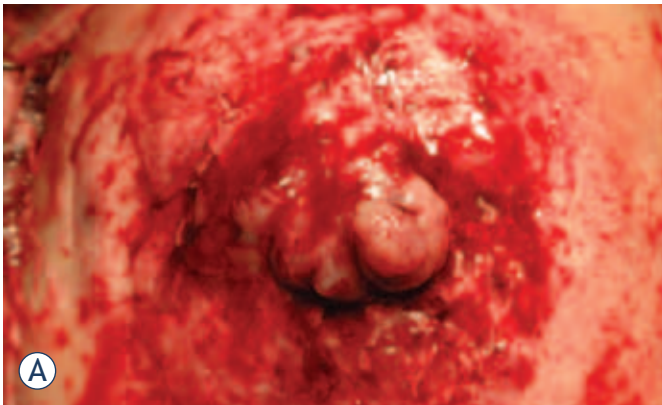
The neurological status during the clinical examination was normal. Locally, a skull tumour of 5 cm in diameter was felt. It was immobile and insensitive on palpation and the skin covering it was normal.

The computer tomography (CT) and magnetic resonance (MR) imaging revealed an intracranial expansive lesion of 8 cm in diameter, compressing the cortex and invading the skull bone and subcutaneous tissue (Figures 1A and 1B). The CT angiography did not show any signs about sinus invasion. Surgery was indicated.

The operation was performed via midline incision. In the subcutis, the tumour mass growing through the bone was seen, infiltrating the periosteum and galea (Figure 2A). A round section of the skull bone was performed, encircling the tumour first. Then, the bone in the very vicinity of the tumour was drilled in such a way that two circular bone flaps were formed around the tumour as it was not possible to elevate the first bone flap due to the tumour adhesion to the bone without damaging the bridging veins and the dura. The tumour was then microsurgically removed, carefully dissected and elevated off the brain substance (Figure 2B). The tumour origin was in the dural convexity over the left motor and premotor cortex. The cortex was



FIGURES 1A, 1B. The axial view of the CT scan showing homogenous lesion in the motor/premotor area, radiologically classified as meningioma, with hyperostotic bone (arrow) (A). The coronal view of the tumour, growing intra- and extracranially (B).



relatively spared, though severely compressed and the superior sagittal sinus was also compressed but otherwise intact. However, the bone was porotic and invaded by the tumour, which spread through the periosteum into the galea. The tumour was completely excised together with all infiltrated extracranial tissue.

Extensive defects of the dura mater and bone were well reconstructed with dura replacement material (lyophilised dura) and water tightly sealed with fibrin glue in order to avoid liquorrhea. Artificial bone was modelled *in vivo* from two component polymethylmetacrylate material, which was moulded and modelled according to the shape of the removed bone just before closure (Figures 2C and 2D). The original bone flap was used as a template. The fit was very good, giving an excellent cosmetic result as well as brain protection. The new artificial bone flap was fixed to the skull bone with titanium plates. Finally, the wound was closed in layers. After the operation, the patient was neurologically intact. The control CT scan showed a good position of the implant with no fluid collection underneath (Figure 3). The rest of the postoperative course was uneventful.

Histology showed that the tumour was a conventional fibrous meningioma, WHO grade 1. It indeed originated from the dural convexity and spread through the bone into the subcutis (Figure 4). No additional treatment was recommended.

Discussion

Our patient was operated on for a benign meningioma, which was especially interesting because of the invasion into the skull bone, its destruction and invasion into the subcutaneous tissue as well as the postoperative question about tissue reconstruction. The majority of meningiomas are benign tumours

FIGURES 2A, 2B, 2C, 2D. Intraoperative view of the meningioma growing through the skull bone into the periosteum and the subcutis. The scalp has been retracted laterally (A). Removal of the intracranial part of the meningioma: the tumour was dissected from the brain tissue, gently lifted off the brain via suspension and removed together with the infiltrated dura. Special care was taken not to damage the vessels (B). The artificial bone modelling and its template. Green material is polymethylmetacrylate. During the operation, the outer ring of the bone visible on the right was removed first, only then the tumour dissection and removal of the inner bony ring started (C). The artificial bone in place, fixed with titanium clamps at the edge (D).

that behave as expansive lesions.^{1,3,10} Symptoms usually arise due to compression of the brain and erosion of the neighbouring tissue.

Some of meningiomas are invasive and about 5% of meningiomas are malignant, more likely causing direct invasion.^{1,3,13-15} Besides invasive and malignant meningiomas, benign meningiomas may also invade bone. In all cases, the reconstruction of the removed bone is necessary.

Patients with meningiomas are often elderly people with associate diseases that preclude radical resections and complicate a postoperative course. Because of tissue deficit and extensive operation, the reconstruction of the missing tissue, especially the skull bone and soft tissue, is problematic.¹⁶⁻¹⁸ There are many alternatives to repair the missing tissue, nowadays three main techniques are used: autografts, allografts and artificial replacement material.^{9,10,19} The selection of the material and operative technique depends on surgeons' experience and preferences in addition to size, location, shape and depth of the bone defect.

About 50% of cases show hyperostosis of the bone overlaying the tumour, with meningotheial tumour cells infiltrating the bone itself.^{9,10} A lot of technical difficulties may arise during the operation and because of that, many skull base tumours, principally those of the anterior or middle cranial fossa and those extending into the orbit were not excised completely. Recently, improved techniques of craniofacial surgery have been developed, allowing a wide range reconstruction and leading to more successful clinical result.¹⁹

In order to accomplish a complete resection, a combined intra- and extracranial resection is required, involving the removal of the hypertrophic bone. It was suggested that strict adherence to oncological principles should be applied also in the case of benign neoplasms in order to prevent contamination of wounds with tumour cells and potential recurrence.²⁰ Often, a radical resection may be attained with low morbidity in operated patients, providing a significantly better long-term clinical outcome.¹⁰ In such extensive resections, the aesthetic reconstruction of large bone defects may pose a significant issue during the operation. Viable tissue in the form of autografts and allografts is one attractive option, another one is artificial replacement material.^{9,11,12}

In this particular case, we decided for *in vivo* reconstruction of the missing bone with artificial replacement material for several reasons. The autografts, which are available in the form of free tissue transfer, rotational flaps and combined as

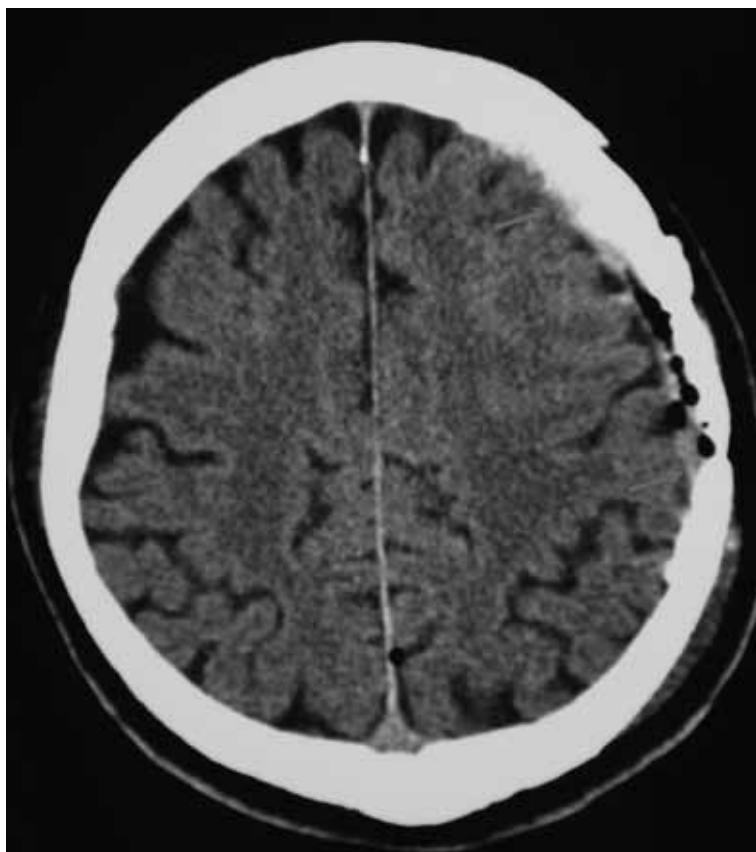


FIGURE 3. The axial view of the postoperative CT scan with the artificial bone (arrows) covering slightly oedematous brain tissue.

well, allow coverings of large volume tissue defects, especially those of soft tissue.^{19,21} Vascularised tissue is less prone to infection and will survive easily than grafts without direct vascular supply. Autografts are safe in terms of disease transmission and exhibit no immune response reactions. Bone grafts show low infection and desorption rate that leads to relatively short term of graft incorporation.²¹ Moreover, vascularised tissue is relatively resistant to postoperative irradiation, which may also become necessary after the resection of grade III and sometimes of grade II meningiomas.^{11,19,21,22} However, to protect healthy tissue, specially brain and vessels, we use limited postoperative irradiated fields in contrast with prophylactic cranial irradiation.²³

On the other hand, the use of viable tissue has many drawbacks, especially morbidity at the donor site after the operation, higher infection rate due to more extensive operative process, longer intraoperative time and a need of plastic surgeon. When allografts are considered, the infection risk is

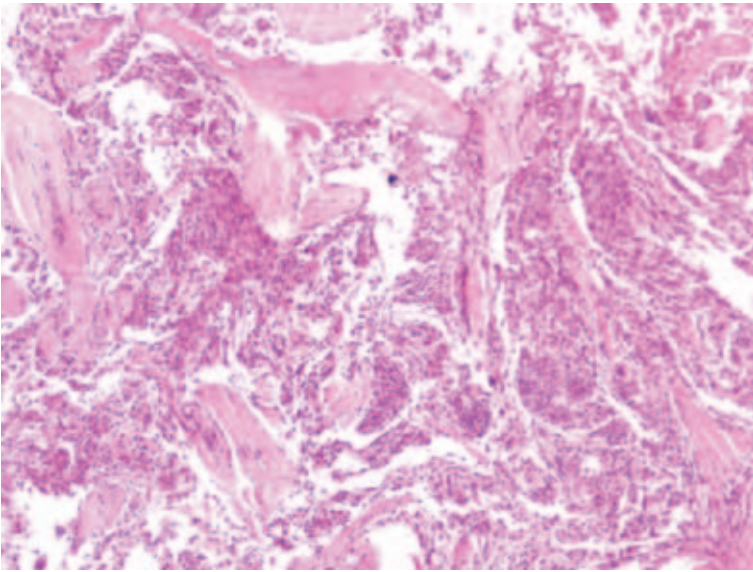


FIGURE 4. The histological image of the extracranial part of the fibrous meningioma, showing tumour cell invasion into the muscle tissue of the galea.

higher and immunological reactions are possible, complicating the recovery and slowing down the healing process.²¹

Further possibilities are cranioplasty implants. Some are manufactured in advance, according to the shape of the bone defect, other may be modelled intraoperatively from titanium meshes or various composite materials. In our case, we decided for the artificial bone reconstruction. Custom made cranio-plasty implants are made in advance according to the shape of the bone defect, therefore, the fit is not always appropriate, increasing the possibilities that the implant may shift. Furthermore, a second operation for the implantation is needed. Our goal was to complete the tumour resection and the reconstruction in one leg, posing less operation-associated risks and enabling faster recovery. We reconstructed the defect from polymethylmethacrylate, which is an efficient and relatively straightforward procedure. It can be performed immediately after the tumour resection, it is fast and yields excellent cosmetic results. After mixing the two components of polymethylmethacrylate, the material is soft and it may be modelled in the shape of the removed bone, exactly filling the bone defect. It hardens in about ten minutes, allowing subtle additional adjustments in shape and fit during modelling. The curvature of the implant may be adjusted according to the curvature of the skull and the implant may be easily fixed with titanium plates and screws, titanium clamps

or absorbable clamps, providing good stability. The implant, when in place and air-dried, yields a solid construct that perfectly matches the patient's natural head shape and has good strength in both compression and tension. Our operative procedure with bone modelling did not pose any particular technical problem and was time saving with good result of the reconstruction.

Among the artificial materials, artificial bone is an efficient alternative to titanium plate or mesh for intraoperative bone reconstruction.⁹ According to our experience, this technique is useful in appropriate conditions, as it is time-saving, straightforward and enables brain protection with good cosmetic result after the extensive cranial vault defect at the time of tumour resection.

Conclusions

This case illustrates how reconstruction of the skull bone is sometimes needed after the benign meningioma excision. Artificial bone may be a suitable material, allowing fast intraoperative reconstruction with excellent brain protection and cosmetic effect during the one-stage procedure.

References

1. Kalamirides M, Goutagny S. Meningiomas. *Rev Prat* 2006; **56**: 1792-8.
2. Perry A, Gutmann DH, Reifenberger G. Molecular pathogenesis of meningiomas. *J Neurooncol* 2004; **70**: 183-202.
3. Vranic A. Antigen expression on recurrent meningioma cells. *Radiol Oncol* 2010; **44**: 107-12.
4. Wiemels J, Wrensch M, Claus EB. Epidemiology and etiology of meningioma. *J Neurooncol* 2010; **99**: 307-14.
5. Velnar T, Smrdel U, Popovic M, Bunc G. Genetic markers in oligodendroglial tumours. *Radiol Oncol* 2010; **44**: 13-8.
6. Wen PY, Quant E, Drappatz J, Beroukhim R, Norden AD. Medical therapies for meningiomas. *J Neurooncol* 2010; **99**: 365-78.
7. Norden AD, Drappatz J, Wen PY. Advances in meningioma therapy. *Curr Neurol Neurosci Rep* 2009; **9**: 231-40.
8. Prabhu SS, Demonte F. Treatment of skull base tumors. *Curr Opin Oncol* 2003; **15**: 209-12.
9. Bloch O, McDermott MW. In situ cranioplasty for hyperostosing meningiomas of the cranial vault. *Can J Neurol Sci* 2011; **38**: 59-64.
10. Shrivastava RK, Sen C, Costantino PD, Della Rocca R. Sphenoorbital meningiomas: surgical limitations and lessons learned in their long-term management. *J Neurosurg* 2005; **103**: 491-7.
11. Moyer JS, Chepeha DB, Teknos TN. Contemporary skull base reconstruction. *Curr Opin Otolaryngol Head Neck Surg* 2004; **12**: 294-9.
12. Salyer KE, Bruce DA, Hardin CE, Hopkins KS, Gendler E. Craniofacial neurosurgical approach for extensive hyperostotic meningioma. *J Craniofac Surg* 1993; **4**: 128-34.
13. Singh RVP, Yeh JS, Campbell DA. Implantation meningioma in temporalis muscle: case report. *Br J Neurosurg* 1994; **8**: 93-5.

14. Akai T, Shiraga S, Iizuka H, Kishibe M, Kawakami S, Ueda Y. Recurrent meningioma with metastasis to the skin incision. *Neurol Med Chir (Tokyo)* 2004; **44**: 600-2.
15. Menal P, Garcia-Tirado FJ, Embun R, Rivas JJ. Is a benign meningioma always an indolent tumor? *Interact Cardiovasc Thorac Surg* 2011; **13**: 94-5.
16. Sughrue ME, Rutkowski MJ, Shangari G, Chang HQ, Parsa AT, Berger MS, et al. Risk factors for the development of serious medical complications after resection of meningiomas. *J Neurosurg* 2011; **114**: 697-704.
17. Black P, Morokoff A, Zauberger J, Claus E, Carroll R. Meningiomas: science and surgery. *Clin Neurosurg* 2007; **54**: 91-9.
18. Li PL, Mao Y, Zhu W, Zhao NQ, Zhao Y, Chen L. Surgical strategies for petroclival meningioma in 57 patients. *Chin Med J* 2010; **123**: 2865-73.
19. Cansiz H, Cambaz B, Papila I, Tahami R, Güneş M. Use of free composite graft for a large defect in the anterior skull base. *J Craniofac Surg* 1998; **9**: 76-8.
20. Velnar T, Bunc G. Iatrogenic metastasis of a benign meningioma to the periosteum at the site of previous craniotomy: a case report. *Wien Klin Wochenschr* 2008; **120**: 766-9.
21. Bauer TW, Muschler GF. Bone graft materials. An overview of the basic science. *Clin Orthop Relat Res* 2000; **371**: 10-27.
22. Angelos PC, Downs BW. Options for the management of forehead and scalp defects. *Facial Plast Surg Clin North Am* 2009; **17**: 379-93.
23. Stanic K, Kovac V. Prophylactic cranial irradiation in patients with small-cell lung cancer: the experience at the Institute of Oncology Ljubljana. *Radiol Oncol* 2010; **44**: 180-6.

Dosimetric verification of compensated beams using radiographic film

Slaven Jurkovic¹, Gordana Zauhar², Dario Faj³, Deni Smilovic Radojic¹, Manda Svabic¹, Mladen Kasabasic³, Ana Diklic¹

¹ University Hospital Rijeka, Radiotherapy Department, Physics Division, Rijeka, Croatia

² School of Medicine, Department of Physics, Rijeka, Croatia

³ University Hospital Osijek, Department of Radiotherapy and Oncology, Osijek, Croatia

Received 19 January 2011

Accepted 25 April 2011

Correspondence to: Slaven Jurković, UH Rijeka, Radiotherapy Department, Physics Division, Krešimirova 42, 51000 Rijeka, Croatia. Phone: + 385 51 658 398; Fax: +385 51 658 391; E-mail: slaven.jurkovic@ri.t-com.hr

Disclosure: No potential conflicts of interest were disclosed.

Introduction. External photon beam modulation using compensators in order to achieve a desired dose distribution when brachytherapy treatment is followed by external beam radiation is a well-established technique. A compensator modulates the central part of the beam, and the dose beneath the thickest part of the compensator is delivered mostly by scattered, low energy photons. A two-dimensional detector with a good spatial resolution is needed for the verification of those beams. In this work, the influence of different types of detectors on the measured modulated dose distributions was examined.

Materials and methods. Dosimetric verification was performed using X-Omat V, Eastman Kodak radiographic films at different depths in a solid water phantom. The film measurements were compared with those made by ionization chambers. Photon beams were also modelled using EGSnrc Monte Carlo algorithm to explain the measured results.

Results. Monte Carlo calculated over-response of the film under the thickest part of the compensator was over 15%, which was confirmed by measurements. The magnitude of over-response could be associated with changes in the spectra of photon energy in the beam.

Conclusions. The radiographic film can be used for the dosimetry of compensated high energy photon beams, with limitations in volumes where photon spectra are hardly degraded.

Key words: radiation therapy; dosimetry; compensators

Introduction

Intracavitary application of brachytherapy sources followed by external beam radiation is a common practice in radiotherapy of carcinoma of the cervix. Since the application of brachytherapy sources results in characteristic dose distributions, modulated external photon beams should be added in a way to achieve the desired cumulative dose distribution over the target volume. Several techniques used in practice have been described.¹⁻⁴

On the other hand, the dosimetry of modulated linear accelerator's photon beams is rather complex, mainly due to dose distribution in homogeneity within the radiation field with large dose gradients. Therefore, dosimetric verification needs

a high spatial resolution and this demand makes the radiographic film a dosimeter of choice.⁵⁻⁸ Nevertheless, it has been shown that the absorbed dose could be related to the energy absorption coefficient.⁹ Furthermore, energy absorption coefficients for film emulsions and water differ significantly in the low energy region below 400 keV, as the data calculated according to Seltzer have shown.¹⁰ Since there is an enhanced contribution of scattered radiation to the total dose in modulated photon beams, a disadvantage of the film which shows over-response to low energy photons may become important.¹¹⁻¹³

In this work, we compared the measured dose distributions of high energy photon beams acquired by different detectors. In order to discuss ex-

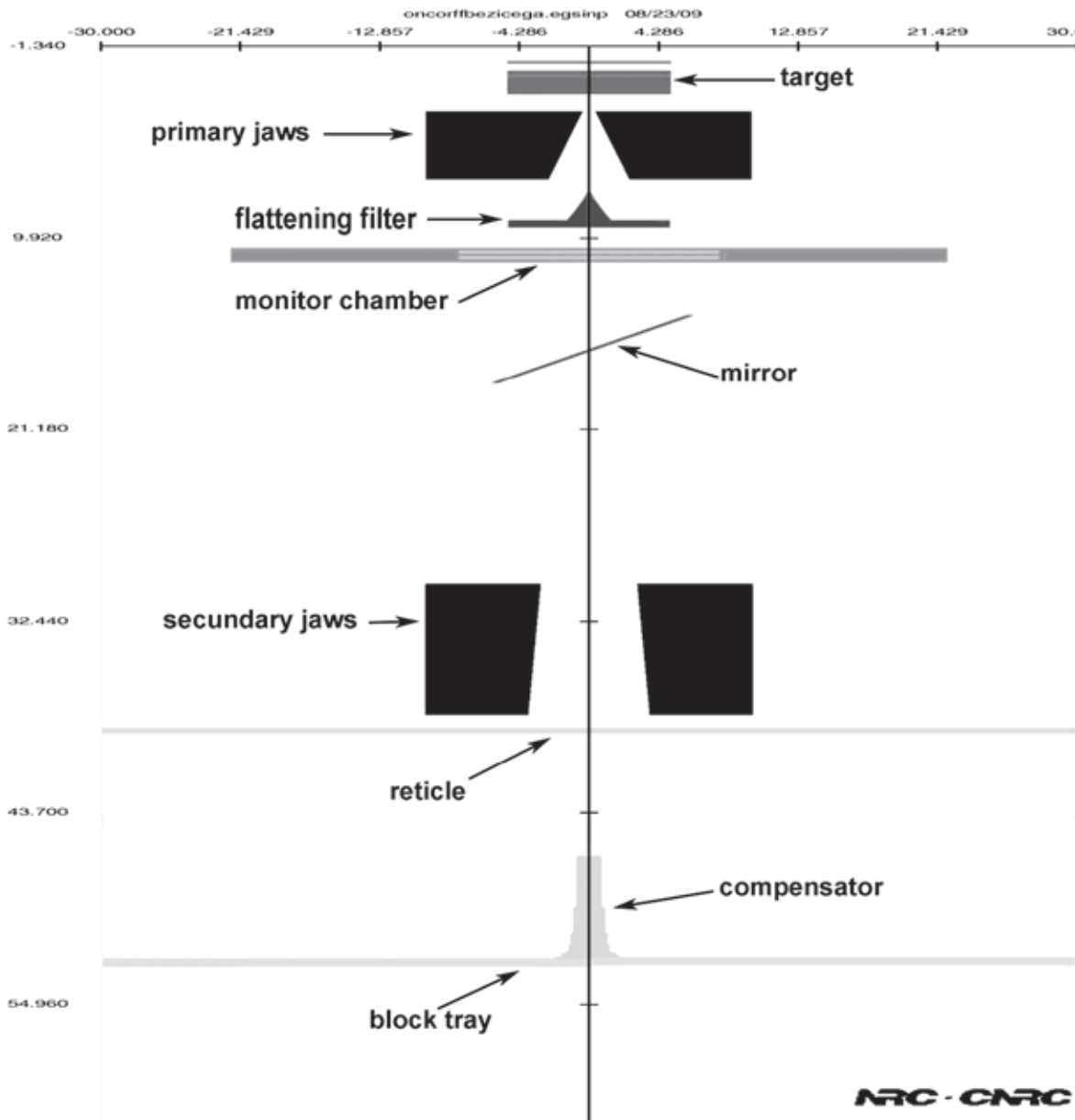


FIGURE 1. Simulated geometry of accelerator's head according to manufacturer's data for modelling compensated beam using BEAMnrc program package.

perimental results, Monte Carlo simulation of particle transport for the measured beams was done.

Materials and methods

Dosimetric verification of open and modulated 6 MV photon beams from Siemens Oncor Impression linear accelerator was performed using X-Omat V (Eastman Kodak) radiographic films at different depths in solid water (PTW Solid Water Phantom). We used fixed source-to-surface (SSD)

geometry with SSD=100 cm on the phantom surface. Film dosimetry was performed using Vidar DosimetryPro Advantage scanner with Coherence Physicist (Siemens Medical Solutions) and PIPSPro (Standard Imaging) software packages for film dosimetry. The dose profiles measured by the film were compared with those made by ionization chambers (IBA Dosimetry, compact chambers CC13 and CC 01) in the water phantom (IBA Dosimetry, Blue Phantom). Regarding a better spatial resolution of a small volume ionisation chamber (CC01), data measured with those chambers in

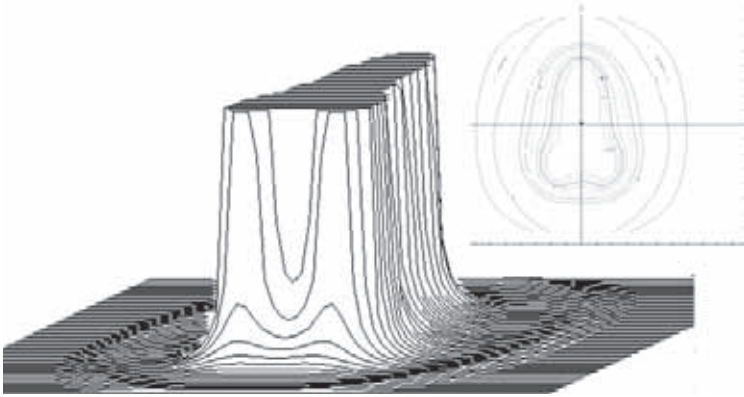


FIGURE 2. Compensator's shape calculated to conform the dose distribution given by an external beam according to the dose distribution around brachytherapy sources. The insert shows thickness of the compensator in a form of level curves in mm.

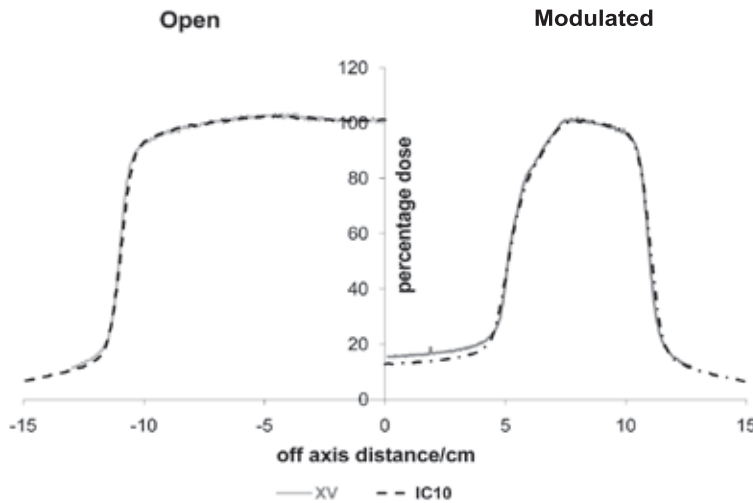


FIGURE 3. Dose profiles measured with ionization chamber (black) and X-Omat V film (grey). Measurements were done with SSD=100 cm, 20×20 cm² field size at 10 cm depth for open and modulated beams. Regarding the symmetry of the dose distributions only half-profiles are shown.

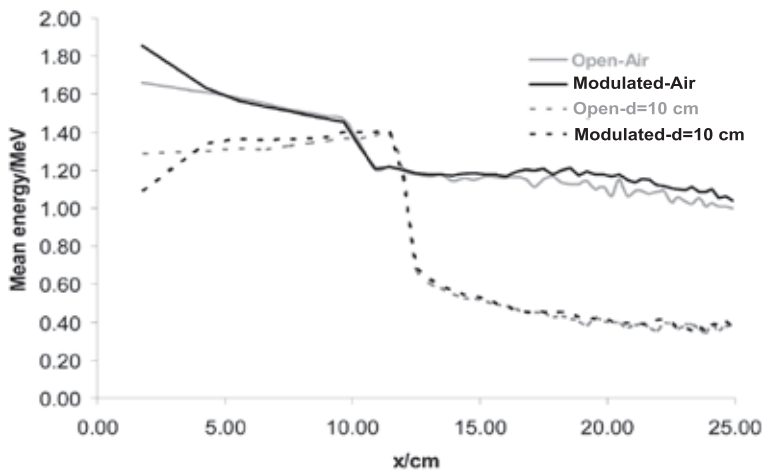


FIGURE 4. Mean energy distributions for open and modulated beams in air and on 10 cm depth in water. Calculations were done with SSD=100 cm and 20×20 cm² field size for open and modulated beams. Regarding the symmetry of the energy distributions only half-profiles are shown.

the high gradient region of the beams were superimposed on measurements with CC13 ionization chamber which had a better signal-to-noise ratio.

Photon spectra for Siemens Oncor Impression linear accelerator photon beams were calculated at the measuring planes using Monte Carlo simulation of particle transport (EGSnrc). The simulation for 6 MV photons with a field size of 20×20 cm² (defined at SSD=100 cm) was performed using OMEGA/BEAM code, developed by the National Research Council of Canada (NRCC). This is an EGSnrc user code capable of complex linear accelerator geometric coding.¹⁴ The detailed geometry and composition of each individual device in the Siemens Oncor Impression linear accelerator were obtained from the manufacturer. Open and modulated beams were modelled using BEAMnrc software. The modelled geometry of compensated beam is shown in Figure 1. Calculated shape of the compensator is shown in Figure 2.

The compensator shape was calculated using the dose distribution around the brachytherapy sources as a pattern according to which the open photon beam was modulated in order to achieve the desired total dose distribution.⁴

Therefore, the shape of the dose distribution is rather characteristic and, from the dose profiles point of view, three different areas can be distinguished: the area under the compensator and the open beam area where the measurements can be performed with high reproducibility and the area near the edge of the compensator which is characterized by high dose gradients and a lower level of measurement reproducibility. In the last area, Monte Carlo calculation is especially used as a guideline for the interpretation of the measured dose distributions. On the other hand, changes in the energy spectrum were expected in the area under the thickest part of the compensator.

The absorbed dose in a material depends on energy absorption coefficients⁹ and there is a large difference in those coefficients for film and water in low energy area.¹⁰ Therefore, an over-response of the film under the thickest part of the compensator was expected at larger depths because the Compton scattered low-energy photons dominate there.⁸ Dose calculations in a material were performed according to:⁹

$$D = -\frac{1}{\rho} \nabla \Psi = \int \Psi_E \frac{\mu_{en}(E)}{\rho} dE = \Psi \overline{\mu_{en}} \quad [1]$$

The BEAM code was implemented using variance reduction techniques: photon forcing, bremsstrahlung splitting and range rejection to speed up

the simulation. The lower charged particle cutoff energy, AE, was 0.7 MeV, and the lower photon cutoff energy, AP, was 0.01 MeV. The energy loss per transport step of the electron, ESTEPE, was controlled by PRESTA.¹⁵ Scored plane was set at Z=100cm to collect the particles after transportation from the accelerator, and to form the phase space file. Information concerning particles in the phase space file included the position (X, Y, Z), direction (U, V, W), energy, charge, weighting, and origin (LATCH). Five to ten million particles were collected in the scored plane. The phase space file served as the source for the following water phantom simulation using DOSXYZ, an EGSnrc user code for 3D absorbed dose calculation in Cartesian coordinates.¹⁶ In DOSXYZ, the water phantom size was 40×40×40cm³ and the phase space source position was on the water surface (Z=0). The origin was at the centre of the radiation field. Voxels with size of 0.5×0.5×0.5 cm³ (X×Y×Z) were set at the depth of the maximum dose for dose profile simulation. 50 voxels from water surface (Z=0) with size 2.0×2.0×0.2 cm³ and 20 voxels with size 2.0×2.0×0.4 cm³ were set along the central axis for central percent depth dose (PDD) simulation. The particles in the phase space file were redistributed and reused to obtain better accuracy in dose calculation.¹⁶ Physical parameters of original electron beam that may influence the dose profile and central-axis PDD curve are the beam energy, the beam spot size and the distance from the point source.^{17,18} These parameters were adjusted to allow dose profiles and percentage depth dose curve to match measured data. Since we calculated changes in beam energies, for the purpose of our work, the accuracy of the beam profiles was not essential. We decided that 3% discrepancy from measurements is acceptable in the high dose region and 20% in the low dose region. Recommended values are 2% and 20% respectively.¹⁹⁻²¹

Results

From the analysis of measured beam profiles, we observed significant discrepancies between measurements with the radiographic film and ionization chambers when measuring beam profiles of modulated beams on larger depths in water. The discrepancies were pronounced under the thickest part of the compensator (Figure 3).

Calculated mean energy distributions in open and modulated beams are shown in Figure 4.

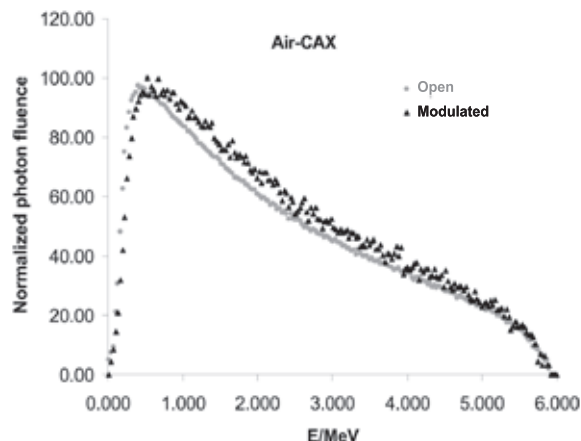


FIGURE 5A. Photon spectral distributions for open and modulated 6MV photon beams on central axis in air. Calculations were done with SSD=100 cm and 20×20 cm² field size.

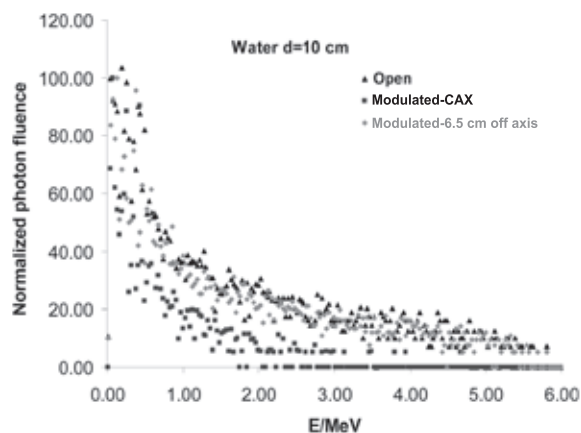


FIGURE 5B. Photon spectral distributions in water for open and modulated 6MV photon beams, on 10 cm depth in water. Calculations were done with SSD=100 cm and 20×20 cm² field size at central axis for open beam and also at central axis and under steep part of the compensator (6.5 cm off axis) for modulated beam.

From the 'in air' simulation analyses, we can see that the compensator removed low energy photons from the beam, so the mean energy of the modulated beam is higher than the one of the open beam (Figure 4). This can also be seen in Figure 5A. On the other hand, at larger depths in water, the Compton scattering low-energy photons dominate, especially under the thickest part of the compensator, so the Figure 4 shows the decrease of the mean energy of the modulated beam there.

Calculated photon spectral distributions for open and modulated beams are shown in Figures 5A and 5B, respectively.

Taking into account the dependence of mass absorption coefficients on photon energy for used

dosimeters and calculated energy distribution of photons in small volumes, we can estimate changes in the film response. Regarding data shown in Figures 4, 5A and 5B, it follows that the largest differences could be expected under the thickest part of the compensator at larger depths in water because of the largest energy degradation. Dose calculations for the film and water were done according to Equation [1]. Calculated over-response of the film in this region was over 15% which was confirmed by measurements (Figure 3).

Discussion

In this paper, we showed that magnitude of over-response of the radiographic film of modulated high energy photon beams could be associated with the changes in the spectra of photon energy in the beam. Since the largest spectral change was under the thickest part of the compensator, there was the largest difference between film and ionisation chamber measurements.

Regarding a high dose gradient beneath the steep part of the compensator, it was not possible to measure doses in this area accurately. Nevertheless, spectra in this area resemble open rather than modulated beam beneath the thickest part of the compensator. In this way, the over-response of the film under the steep part of the compensator would be small.

The radiographic film is often used for verifications of modulated photon beams.^{5,7,8,22} Despite of described limitations, it can be used either on build up depth for the evaluation of compensators shape or for measuring dose distributions of modulated high energy photon beams in phantoms. Special attention should be paid to the interpretation of measured values in volumes where photon spectra are hardly degraded.

References

- Han IH, Malviya V, Chuba P, Orton CG, Devi S, Deppe G, et al. Multifractionated HDR brachytherapy with concomitant daily teletherapy for cervical cancer *Gynecol Oncol* 1996; **63**: 71-7.
- Popple RA, Kim RY, Pareek P, Duan J, Shen S, Brezovich IA. Custom step wedge blocking using dynamic multileaf collimation for parametrial pelvic boost irradiation following brachytherapy carcinoma of the cervix. *Med Phys* 2003; **30**: 2699-702.
- Jurković S, Žauhar G, Bistrović M, Faj D, Kaliman Z, Smilović Radojčić D. An alternative approach to compensators design for photon beams used in radiotherapy. *Nucl Instrum Methods A* 2007; **580**: 530-3.
- Jurković S, Žauhar G, Faj D, Smilović Radojčić D, Švabić M, Radiation therapy photon beams dose conformation according to dose distribution around intracavitary applied brachytherapy sources. *Med Dos* 2010; **35**: 49-52.
- Bucciolini M, Banci F, Casati M. Verification of IMRT fields by film dosimetry. *Med Phys* 2004; **31**: 161-8.
- Bailey DW, Kumaraswamy L, Podgorsak MB. A fully electronic intensity-modulated radiation therapy quality assurance (IMRT QA) process implemented in a network comprised of independent treatment planning, record and verify, and delivery systems. *Radiol Oncol* 2010; **44**: 124-30.
- Salz H, Wiezorek T, Scheithauer M, Schwedas M, Beck J, Wendt TG. IMRT with Compensators for Head-and-Neck Cancers. *Strahlenther Onkol* 2005; **181**: 665-72.
- Srivastava RP, Wagter De C. The value of EDR2 film dosimetry in compensator-based intensity modulated radiation therapy. *Phys Med Biol* 2007; **52**: 449-57.
- Brahme A, Andreo P. Dosimetry and quality specification of high energy photon beams. *Acta Rad Onc* 1986; **25**: 213-23.
- Seltzer SM. Calculation of photon mass energy-transfer and mass energy-absorption coefficients. *Radiat Res* 1993; **136**: 147-70.
- Yeo JJ, Wang CC, Burch SE. A filtration method for improving film dosimetry in photon radiation therapy. *Med Phys* 1997; **24**: 1943-53.
- Wang X, Spirou S, Lo Sasso T, Stein J, Chui C, Mohan R. Dosimetric verification of intensity-modulated fields. *Med Phys* 1996; **23**: 317-27.
- Ju SG, Ahn YC, Huh SJ, Yeo JJ. Film dosimetry for intensity modulated radiation therapy; Dosimetric evaluation. *Med Phys* 2002; **29**: 351-55.
- Rogers DWO, Faddegon BA, Ding GX, Ma CM, We J, Mackie TR. BEAM: a Monte Carlo code to simulate radiotherapy treatment units. *Med Phys* 1995; **22**: 503-24.
- Bielayew AF, Rogers DWO. PRESTA: the parameter reduced electron-step transport algorithm for electron Monte Carlo transport. *Nucl Instrum Methods B* 1987; **18**: 165-81.
- Ma CM, Reckwerdt P, Holmes M, Rogers DWO, Geiser B. *DOSXYZ users manual*. National Research, Council of Canada Report PIRS-0509B; 1995.
- Lin SY, Chu TC, Lin JP. Monte Carlo simulation of a clinical linear accelerator. *App Rad Isotopes* 2001; **55**: 759-65.
- Faj D, Vrtar M, Krajina Z, Jurković S, Margaretić D. Model of total skin electron treatment using the 'six-dual-field' technique. *Coll Antropol* 2003; **27**: 713-21.
- Verhaegen F, Seuntjens J. Monte Carlo modeling of external radiotherapy photon beams. *Phys Med Biol* 2003; **48**: R107-64.
- Rivest DRC, Riauka TA, Murtha AD, Fallone BG. Dosimetric implications of two registration based patient positioning methods in prostate image guided radiation therapy (IGRT). *Radiol Oncol* 2009; **43**: 203-12.
- Mesbahia A, Reilly AJ, Thwaites DI. Development and commissioning of a Monte Carlo photon beam model for Varian Clinac 2100EX linear accelerator. *Applied Radiation* 2006; **64**: 656-62.
- Ting JY, Davis L. Dose verification for patients undergoing IMRT. *Med Dosim* 2001; **26**: 205-13.

Radiol Oncol 2011; 45(4):227-247.
doi:10.2478/v10019-011-0037-0

Titanijev dioksid v vsakdanji uporabi. Je varen?

Skočaj M, Filipič M, Petković J, Novak S

Izhodišča. Na splošno ocenjujejo, da je titanijev dioksid (TiO_2) inerten in varen, zato ga že desetletja uporabljajo v različne namene. Z razvojem nanotehnologij pa se je povečala proizvodnja in uporaba TiO_2 v nanoobliki. Ta ima številne nove koristne lastnosti, vendar lahko pričakujemo povečano izpostavljenost ljudi in okolja. Zato je pomembno boljše poznavanje toksikoloških lastnosti nanodelcev TiO_2 . Mehanistične toksikološke raziskave kažejo, da nanodelci TiO_2 povzročajo toksične učinke predvsem prek oksidativnega stresa. Ta povzroča poškodbe celic, genotoksičnost, vnetja, imunski odziv itd. Obseg in vrste poškodb sta v veliki meri odvisna od fizikalnih in kemijskih lastnosti delcev TiO_2 . Te lastnosti določajo biološko dostopnost in reaktivnost TiO_2 . Na osnovi dokazov poskusov inhalacijske izpostavljenosti živali je Mednarodna agencija za raziskavo raka (IARC) delce TiO_2 opredelila kot »možno karcinogene za ljudi«, Nacionalni inštitut za varnost in zdravje v poklicih (NIOSH) pa je nanodelce TiO_2 opredelil kot karcinogene pri poklicni izpostavljenosti. Raziskave kožne izpostavljenosti, ki je pri ljudeh zelo velika zaradi uporabe v zaščitnih kremah za sončenje, na splošno kažejo, da je prehod prek kože zanemarljiv. Vendar pa ni podatkov o dolgotrajni izpostavljenosti in podatkov o morebitnih škodljivih učinkih fotooksidacijskih produktov. Čeprav je TiO_2 dovoljen kot aditiv v hrani (E171) in v farmacevtskih proizvodih, ni zanesljivih podatkov o njegovi absorpciji, porazdelitvi, izločanju in toksičnosti pri oralni izpostavljenosti. TiO_2 vstopa tudi v okolje, za vodne organizme ni akutno toksičen, pri dolgotrajni izpostavljenosti pa povzroča vrsto subletalnih učinkov.

Zaključki. Dokler ne bodo na voljo relevantni toksikološki podatki in podatki o izpostavljenosti ljudi, ki bodo omogočili zanesljivo oceno tveganj, je pri uporabi nanodelcev TiO_2 potrebna velika previdnost.

Radiol Oncol 2011; 45(4): 248-258.
doi:10.2478/v10019-011-0038-z

Ocena ledvične funkcije pri otrocih s hidronefrozo - dodatna možnost magnetnoresonančne tomografije

Hadjidekov G, Hadjidekova S, Tonchev Z, Bakalova R, Aoki I

Izhodišča. Magnetnoresonančna urografija (MRU) je ena izmed najbolj primernih slikovnih metod v pediatrični urologiji. Z eno samo preiskavo dobimo največ diagnostičnih podatkov. Namen raziskave je bil opredeliti diagnostično vrednost MRU pri otrocih z različnimi prirojenimi razvojnimi nepravilnostmi sečil in rodil, predvsem nepravilnostmi ledvičnega meha in sečevodov, ter naknadno oceniti ledvično funkcijo z različnima računalniškima programoma.

Bolniki in metode. V raziskavo smo zajeli 96 otrok (starost 7 dni do 18 let). Pri 54 smo statično T2 MRU dopolnili z ekskretorno T1 MRU po aplikaciji Gadolinijevega kontrastnega sredstva. Oceno ledvične funkcije smo opravili z dvema računalniškima programoma, s "CHOP-fMRU" in "ImageJ".

Rezultati. Z MRU smo lahko pri vseh otrocih zelo kvalitetno prikazali razvojne nepravilnosti ledvic in celotnega urotrakta. Ob primerih obstrukcije zaradi pielouretalne stenoze smo z MRU potrdili že z ostalimi slikovnimi metodami ugotovljeno diagnozo. Ob primerih razvojnih nepravilnosti končnega dela sečevoda pa je bila MRU bolj natančna metoda. Ugotovili smo veliko skladnost med diagnozo postavljeno z MRU in dokončno kirurško diagnozo. Z računalniškima programoma "CHOP-fMRU" in "ImageJ" smo izračunali čas ledvičnega izločanja, volumen ledvic in volumetrično ledvično funkcijo, ki so bili zelo skladni s scintigrafijo $^{99\text{mTc}}$ -DTPA in tudi med seboj.

Zaključki. Zaradi svojih prednosti postaja MRU najpomembnejša slikovna metoda v pediatrični urologiji. Omogoča sintezo anatomskega prikaza in oceno ledvične funkcije. Na ta način omogoča optimalno izbiro primernih kandidatov za kirurško zdravljenje. Z uporabljenima programoma smo lahko odkrili tudi majhne nepravilnosti v delovanju ledvic.

Radiol Oncol 2011; 45(4): 259-266.
doi: 10.2478/v10019-011-0034-3

Katepsin H posredno regulira kostni morfogenetški protein 4 (BMP-4) v človeških celičnih linijah

Rojnik M, Jevnikar Z, Mirkovic B, Janes D, Zidar N, Kikelj D, Kos J

Izhodišča. Katepsin H je cisteinska proteaza, ki ima pomembno vlogo pri napredovanju raka, vendar pa je njegova natančna funkcija v tem procesu nejasna. Pred kratkim se je uveljavila domneva, da naj bi bil katepsin H udeležen pri izoblikovanju kostnega morfogenetškega proteina 4 (BMP-4) pri miših. Da bi pojasnili, ali je katepsin H udeležen pri regulaciji BMP-4 tudi pri ljudeh, smo raziskovali njegov vpliv na izražanje, izoblikovanje in razgradnjo BMP-4 v človeških celičnih linijah raka prostate (PC-3), osteosarkoma (HOS) in pro-monocitov (U937).

Materiali in metode. Z uporabo tehnologije mikromrež polimerazne verižne reakcije (PCR) smo ugotovili, da katepsin H regulira izražanje BMP-4, kar smo potrdili s PCR v realnem času. S pomočjo prenosa Western ter konfokalne mikroskopije smo raziskovali vlogo katepsina H pri izoblikovanju BMP-4.

Rezultati. Izražanje BMP-4 je v celicah HOS v odvisnosti od katepsina H povečano, vendar pa nasprotno katepsin H značilno zniža izražanje BMP-4 v celicah U937 in PC-3. Drugačno regulacijo BMP-4 bi lahko povezali z odsotnostjo zrele 28 kDa oblike katepsina H v celicah HOS, saj smo tu opazili le vmesno 30 kDa obliko katepsina H. BMP-4 v človeških celičnih linijah ni v neposredni odvisnosti s katepsinom H, poleg tega pa specifični inhibitor katepsina H ne vpliva na večstopenjsko izoblikovanje BMP-4. Ugotovili smo tudi, da izoliran katepsin H ne razgrajuje BMP-4 tako z aminopeptidazo kot tudi ne z endopeptidazo aktivnostjo.

Zaključki. Naši rezultati izključujejo možnost neposredne regulacije kostnega morfogena proteina 4 (BMP-4) s katepsinom H, vendar pa podpirajo hipotezo, da katepsin H posredno regulira izražanje BMP-4.

Radiol Oncol 2011; 45(4): 267-272.
doi:10.2478/v10019-011-0033-4

Sinonazalni invertni papilom združen s ploščatoceličnim karcinomom

But-Hadžić J, Jenko K, Poljak M, Kocjan BJ, Gale N, Strojan P

Izhodišča. Namen raziskave je bil ovrednotiti naše izkušnje s sinonazalnim invertnim papilomom združenim s ploščatoceličnim karcinomom (IP/PCK), analizirati prisotnost humanega virusa papiloma (HPV) in oceniti vlogo radioterapije.

Bolniki in metode. V prospektivnih podatkovnih bazah (1995-2005) smo ugotovili pet bolnikov z IP/PCK. Prisotnost HPV smo določili v vseh petih tumorjih.

Rezultati. Štirje izmed petih bolnikov so imeli tumorje stadijev T3-T4; vsi bolniki so bili brez področnih zasevkov. Štiri bolnike smo zdravili z namenom ozdravitve: z operacijo, ki smo jo pri treh bolnikih dopolnili z radioterapijo. Pri bolniku z neoperabilnim tumorjem smo naredili zmanjševalno operacijo in nato bolnika radikalno obsevali. Lokalno kontrolo tumorja smo dosegli pri treh bolnikih 8, 46 in 58 mesecev po operaciji. Bolezen se je ponovila lokalno pri dveh bolnikih: po endoskopski odstranitvi T1 tumorja (recidivni tumor je bil uspešno zdravljen z dodatno operacijo) in pri bolniku z neoperabilnim tumorjem. Področne ali sistemske ponovitve bolezni nismo videli. HPV status je bil določen pri vseh petih tumorjih in trije izmed njih so bili pozitivni na HPV tip 11.

Zaključki. Pri operabilnih IP/PCK priporočamo zdravljenje z operacijo in pooperativno radioterapijo, omejeno na področje ležišča tumorja ter z uporabo doz, primerljivih s tistimi, ki jih uporabljamo pri invazivnem PCK. V primerih neoperabilnih tumorjev priporočamo radikalno radioterapijo z dozami med 66 in 70 Gy.

Radiol Oncol 2011; 45(4): 273-278.
doi:10.2478/v10019-011-0029-0

Primerjava preživetja bolnikov z laparoskopsko in odprto radikalno resekcijo raka debelega črevesa stadija II

Fan CZ, Chu YP, Wei P, Dai H, Chen W

Izhodišča. Namen raziskave je bil primerjati preživetje bolnikov z laparoskopsko in odprto radikalno resekcijo raka debelega črevesa stadija II.

Bolniki in metode. V raziskavo je bilo vključenih 220 bolnikov z rakom debelega črevesa stadija II, ki so bili obravnavani v *Chaoyang Hospital of Capital Medical University* v Pekingu od januarja 2000 do decembra 2009. Laparoskopska radikalna resekcija je bila narejena pri 61 bolnikih, odprta radikalna resekcija pa pri 159 bolnikih. Primerjava preživetja bolnikov v obeh skupinah je bila narejena s pomočjo Kaplan Meierjevih krivulj preživetja in statističnega testa log rank.

Rezultati. Med skupinama ni bilo statistično značilnih razlik v 3 letnem (88,5% proti 80,5%; $X^2=1,98$, $p=0,159$) in 5 letnem preživetju (81,9% proti 69,2%; $X^2=1,98$, $p=0,159$). Statistično značilno razliko smo ugotovili v srednjem preživetju, ki je bilo v skupini z laparoskopsko resekcijo 102,6 (95% CI: 76,8-122,7) mesecev, v skupini z odprto radikalno resekcijo pa 90,0 (95% CI: 70,4-109,6) mesecev ($X^2=4,183$, $p=0,041$). Pri bolnikih s pooperativno kemoterapijo je bilo preživetje 96,0 (95% CI: 68,6-111,4) mesecev in pri bolnikih brez kemoterapije 92,6 (95% CI: 56,8-107,2) mesecev ($X^2=6,389$, $p=0,011$). Pri bolnikih starejših od 75 let je bilo preživetje v skupini z laparoskopsko resekcijo 90,0 (95% CI: 25,3-105,0) mesecev in v skupini z odprto radikalno resekcijo 83,4 (95% CI: 13,1-96,9) mesecev ($X^2=6,191$, $p=0,013$).

Zaključki. Srednje preživetje bolnikov s karcinomom debelega črevesa stadija II, pri katerih je bila narejena laparoskopska radikalna resekcija, je bilo boljše kot pri tistih, pri katerih je bila narejena odprta resekcija. To zlasti velja za bolnike starejše od 75 let.

Radiol Oncol 2011; 45(4): 279-284
doi:10.2478/v10019-011-0030-7

Izražanje NF- κ B p65, fosforiliranega na serinu-563 pri raku danke brez ali z preoperativnim obsevanjem

Lewander A, Gao J, Adell G, Zhang H, Sun XF

Izhodišča. Namen študije je bil preučiti izražanje NF- κ B p65, fosforiliranega na serinu-536 (fosfor-Ser-p65) pri raku danke. Zanimalo nas je njegovo izražanje pri bolnikih z ali brez preoperativnega obsevanja (RT) ter povezava s kliničnopatološkimi značilnostmi bolnikov in z njihovimi biološkimi dejavniki.

Bolniki in metode. Fosfor-Ser-p65 smo določali pri 141 tumorjih danke, pri 149 normalnih mukozah in pri 48 metastazah v limfnih vozlih bolnikov z rakom danke, ki so bili vključeni v švedsko klinično študijo.

Rezultati. Izražanje fosfor-Ser-p65 je bilo statistično značilno povečano v tumorjih ($p<0,0001$ za obe skupini, ki sta ali nista prejeli RT) v primerjavi z normalno mukozo. Izražanje pa ni bilo še bolj povečano v metastazah, v primerjavi s primarnimi tumorji ($p>0,05$). Izražanje fosfor-Ser-p65 je v precejšnji meri koreliralo z izražanjem označevalca za tumorki endotelij 1 (TEM1, $p=0,02$), FXD-3 ($p=0,001$), fosfatazo za regeneracijo jeter (PRL, $p=0,02$), p73 ($p=0,048$) in s proteinom povezanim z meningeomom (MAC30, $p=0,05$) v skupini, ki je bila obsevana, vendar ne pri skupini, ki ni bila obsevana ($p>0,05$).

Zaključki. Povečano izražanje fosfor-Ser-p65 je lahko udeleženo pri razvoju raka danke. Po radioterapiji tumorjev izražanje fosfor-Ser-p65 korelira z biološkimi dejavniki, ki so povezani z bolj malignimi značilnostmi tumorjev. Vendar izražanje fosfor-Ser-p65 ni bilo direktno povezano z odgovorom na radioterapijo glede na ponovitev bolezni in preživetje.

Radiol Oncol 2011; 45(4): 285-291.

doi:10.2478/v10019-011-0039-y

Učinkovitost sistemskega zdravljenja prvega reda pri bolnikih z razsejanim rakom debelega črevesa in danke v povezavi z BRAF in različnimi KRAS mutacijami

Reberšek M, Boc M, Cerkovnik P, Benedik J, Hlebanja Z, Volk N, Novaković S, Ocvirk J

Izhodišča. Mutacije v kodonu 12 in 13 gena KRAS so napovedni dejavniki za odgovor na zdravljenje z anti-EGFR monoklonalnimi protitelesi pri bolnikih z razsejanim rakom debelega črevesa in danke. Vsi bolniki z nemutiranim tipom gena KRAS žal ne odgovorijo na zdravljenje s temi tarčnimi zdravili. Vzrok so še drugi mehanizmi odpornosti na zdravljenje. Ti nastanejo z aktivacijo mutacij v predelu drugih EGFR signalnih poti in napovedujejo odgovor na specifično sistemske zdravljenje.

Bolniki in metode. V retrospektivni analizi smo ovrednotili objektivni odgovor na zdravljenje, čas do napredovanja bolezni in celokupno preživetje glede na status KRAS v kodonih 12 in 13 ter status BRAF. Analizirali smo podatke pri 176 bolnikih z razsejanim rakom debelega črevesa in danke, ki smo jih zdravili s prvim redom sistemske kemoterapije v kombinaciji z monoklonalnimi protitelesi.

Rezultati. KRAS mutacije smo ugotovili pri 63 bolnikih (35,8%), pri 53 bolnikih v kodonu 12 (30,1%), pri 10 bolnikih pa v kodonu 13 (5,7%). BRAF V600E mutacijo je imelo 13 od 176 bolnikov (7,4%). V podskupini bolnikov z nemutiranim tipom KRAS so tudi bolniki z nemutiranim tipom BRAF odgovorili na zdravljenje v 54,0%, bolniki z mutiranim BRAF pa v 38,5% ($p = 0,378$). Srednje preživetje bolnikov z nemutiranim tipom BRAF je bilo 107,4 mesecev, bolnikov z mutiranim BRAF pa 45 mesecev ($p = 0,042$). Čas do napredovanja bolezni pri bolnikov z nemutiranim tipom BRAF je bil daljši, 16 mesecev, v primerjavi z 12 mesecev pri bolnikih z mutiranim BRAF ($p = 0,558$).

Zaključki. Bolniki z BRAF V600E mutacijo imajo značilno krajše preživetje kot bolniki z nemutiranim tipom BRAF gena, njihova bolezen hitreje napreduje med sistemskim zdravljenjem. Dokončno vlogo BRAF V600E mutacije kot prognoistični in napovedni dejavnik za odgovor na sistemske zdravljenje s kemoterapijo in monoklonalnimi protitelesi bodo opredelili rezultati prospektivnih randomiziranih kliničnih raziskav.

Radiol Oncol 2011; 45(4): 292-295.

doi:10.2478/v10019-011-0022-7

Hepatocelularni rak s podkožnim zasevkom v predelu skalpa

Tezcan Y, Koc M

Izhodišča. Največ podkožnih zasevkov hepatocelularnega raka (HCC) nastane zaradi prenosa rakastih celic ob igelni punkciji ali ob operaciji. O nejatrogenih podkožnih zasevkih hepatocelularnega raka redko poročajo.

Prikaz primera. Opisujemo primer 70-letnega bolnika s tumorsko maso v podkožju levega zatilja. Bolnika smo radikalno operirali, v kirurških robovih ni bilo rakastih celic. Histopatološki pregled pa je pokazal zasevke HCC. Pregled z računalniško tomografijo ni pokazal znakov primarnega tumorja ali zasevkov v trebuhu, zato se nismo odločili za dodatno zdravljenje. Pet mesecev kasneje smo z magnetno resonančno preiskavo (MRI) ugotovili ponovitev bolezni. Tumorska masa je bila velika 6,0 x 5,5 cm in je ležala v podkožju levega posteriornega parietalnega dela. Bolnika smo ponovno operirali in histopatološki pregled je ponovno pokazal zasevke HCC. Operacija ni bila radikalna in bolnika smo pooperativno obsevali. Po 9 mesecih MRI ni pokazal morebitne ponovitve bolezni v predelu glave.

Zaključki. Ob ugotovljenih podkožnih zasevkih moramo v diferencialni diagnozi pomisliti tudi na HCC, čeprav bolniki nima simptomov jetrnega obolenja.

Radiol Oncol 2011; 45(?): 296-299.
doi:10.2478/v10019-011-0031-6

Ugotavljanje genotipov BRCA1, BRCA2, p53, CDKN2A, MLH1 in MSH2 pri moškem s sekundarnim rakom dojke

Vodušek AL, Novaković S, Stegel V, Jereb B

Izhodišča. Nekatere tumor supresorske gene (BRCA2) in gene za popravljanje neujemanja (MSH2, MLH1) povezujejo s povišanim tveganjem za nastanek raka dojke pri moških.

Prikaz primera. Bolnik je zbolel za sekundarnim rakom dojke po zdravljenju Hodgkinove bolezni v otroštvu. Iz bolnikove krvi smo izolirali DNA ter v genih BRCA1, BRCA2, p53, CDN2A, MLH1 in MSH2 iskali mutacije, polimorfizme in variante. Našli smo tri variante v genih za popravljeno neujemanja ter navadne polimorfizme.

Zaključki. Nukleotidne variante c.2006-6T>C in p.G322D v genu MSH2 bi lahko povezovali s povišanim tveganjem za nastanek raka dojke pri moških.

Radiol Oncol 2011; 45(4): 300-303.
doi: 10.2478/v10019-011-0035-2

Ugotavljanje periampularne lokalizirane pankreatične intraepitelijske neoplazije-3 (PanIN-3) z MR holangiografijo, ojačeno s kontrastom

Algin O, Ozmen E, Ersoy P E, Karaoglanoglu M

Izhodišča. Zgodnja določitev premaligne lezije pankreasa prepreči obsežne kirurške posege in tako zmanjša obolelost in smrtnost. Pankreatična intraepitelijska neoplazija-3 (PanIN-3) je preinvazivna oblika adenokarcinoma (karcinom in situ). Pankreatične intraepitelijske neoplazije še nimajo mesta v radiološki literaturi, vendar pa je potrebno v diferencialni diagnostiki pankreatičnih lezij upoštevati tudi te premaligne lezije.

Prikaz primera. Predstavljamo bolnika, ki smo mu postavili začasno diagnozo kroničnega holecistitisa z žolčnimi kamni in periampularno pankreatično cisto. Preiskavi smo naredili z nekontrastno MR holangiografijo in z MR holangiografijo, ojačano s kontrastom. Kasnejši patološki pregled žolčnika in pankreatične ciste je pokazal adenokarcinom žolčnika in PanIN-3.

Zaključki. Cistične lezije pankreasa s tankimi septi, ki so ojačena z dodajanjem kontrastnega sredstva, lahko predstavljajo PanIN-3. Pri bolnikih s cističnimi lezijami pankreasa v periampularni regiji je MR holangiografija, ojačena s kontrastom, skupaj z nekontrastno metodo lahko koristna pri odkrivanju cističnih lezij pankreasa kot tudi druge abdominalne patologije.

Radiol Oncol 2011; 45(4): 304-309.
doi:10.2478/v10019-011-0036-1

In vivo nadomestitev kosti pri meningeomu, ki je vraščal in uničeval lobanjsko kost

Velnar T, Pregelj R, Limbaeck-Stokin C

Izhodišča. Meningeomi so pogosti možganski tumorji. Nekateri z lokalnim vraščanjem uničujejo okoliško kostno tkivo, ki ga je med operacijo skupaj s tumorjem potrebno odstraniti. Rekonstrukcija po operaciji je lahko zato znatno otežkočena.

Prikaz primera. Opisujemo bolnika z benignim meningeomom konveksitete, ki je vraščal skozi lobanjsko kost v podkožje. Tumor smo skupaj z infiltriranim tkivom v celoti odstranili. Vrzeli okoliškega tkiva, ki so nastale po odstranitvi tumorja, smo že med operacijo oskrbeli z rekonstrukcijo kosti iz umetnih materialov.

Zaključki. Po operaciji benignega meningeoma moramo včasih narediti rekonstrukcijo lobanjske kosti. Pri tem lahko uporabimo kost iz umetnih materialov, ki nam omogoča sorazmerno hitro medoperativno rekonstrukcijo z odlično zaščito možganov in dobrim kozmetičnim učinkom.

Radiol Oncol 2011; 45(4): 310-314.
doi:10.2478/v10019-011-0020-9

Dozimetrično preverjanje kompenziranih žarkov z radiografskim filmom

Jurković S, Žauhar G, Faj D, Smilović Radojčić Đ, Švabić M, Kasabašić M, Diklić A

Izhodišča. Modulacija zunanjih fotonskih žarkov, kadar teleterapiji sledi brahiterapija, je uveljavljena tehnika. Pomaga nam, da bolnika obsevamo z želeno dozo. Kompenzator modulira centralni del žarka; pod najdebelejšim delom kompenzatorja pa je doza odvisna predvsem od sipanih nizko energijskih fotonov. Za preverjanje teh žarkov potrebujemo dvo-dimenzionalni detektor z dobro prostorsko ločljivostjo. Proučili smo vpliv različnih tipov detektorjev na merjeno modulirano dozo.

Materiali in metode. Dozimetrično preverjanje smo opravili z X-Omat V, Eastman Kodak radiografskim filmom na različnih globinah v fantomu trde vode. Filmske meritve smo primerjali z meritvami opravljenimi z ionizacijsko celico. Da bi razložili merjene rezultate, smo fotonske žarke modelirali z algoritmom EGSnrc Monte Carlo.

Rezultati. Z algoritmom Monte Carlo izračunan odziv filma pod najdebelejšim delom kompenzatorja je bil več kot 15% prevelik, kar smo potrdili z drugimi meritvami. Velikost prevelikega odziva filma lahko povežemo s spremembami v spektru fotonskih energij žarka.

Zaključki. Čeprav radiografski film ni vedno najprimernejši dozimeter, ga lahko uporabimo za dozimetrijo kompenziranih visoko energijskih fotonskih žarkov, pri tem pa moramo biti pozorni na volumne, kjer je fotonski spekter močno energijsko oslavljen.

Authors Index 2011

- Adell G: 4/279-284
Adim S: 2/116-122
Algin O: **4/300-303**
Anderluh F: 3/209-212
Aoki I: 4/248-258
Ardebili S: **2/102-115**
Ari F: 2/116-122
Aurer I: 1/27-30
- Bakalova R: 4/248-258
Bayol U: 1/53-58
Benedik J: 4/285-291
Bešenski N: 2/147-158
Boc M: 4/285-291
Borštnar S: 1/46-52
Bregant P: 1/64-67
But-Hadžić J: **4/267-272**
- Campos B: 2/102-115
Cebulski W: 1/59-63
Cerkovnik P: 4/285-291
Chen Weicai: 2/123-128;
Chen Wenming: 4/273-278
Chryssou EG: 1/22-26
Chu YP: 4/273-278
Cör A: 1/30-39
Coskun A: **2/129-131**
Cui MH: 3/196-203
- Čemazar M: 1/30-39
Čirić E: 3/209-212
- Dai H: 4/273-278
de Bree E: 1/22-26
de Denaro M: **1/64-67**; 2/143-146
Diklić A: 4/310-314
Ding W: 2/82-90
Dobrenić M: **3/189-195**
- Dogan M: 1/53-58
Drmota S: 2/102-115
- Erkan N: 1/53-58; 2/129-131
Evrensel T: 2/116-122
- Faj D: 4/310-314
Fan CZ: **4/273-278**
Filipič M: 4/227-247
Fornasier MR: 2/143-146
Fu N: 2/82-90
- Gale N: 4/267-272
Gao J: 4/279-284
Gao LF: 3/196-203;
Ghavamnasiri MR: 3/184-188
Giannikaki E: 1/22-26
Glavina K: 2/147-158
Gole B: 2/102-115
Gornicka B: 1/59-63
Grazio Frković S: 1/46-52
Grošev D: 3/189-195
Guan H: 2/123-128
Gundogdu H: 4/300-303
- Hadjidekov G: **4/248-258**
Hadjidekova S: 4/248-258
He J: **2/123-128**
Herold - Mende C: 2/102-115
Hlebanja Z: 4/285-291
Hodolič M: **1/17-21**
Horvat M: **2/75-81**
Hrabak Paar M: 1/27-30
Hrovatić Podvršnik N: 3/209-212
Huić D: 3/189-195
- Janeš D: 4/259-266
Jangjoo A: 3/184-188
- Jenko K: 4/267-272
Jereb B: 4/296-299
Jevnikar Z: 4/259-266
Jurković S: **4/310-314**
- Kakhki VRD: 3/184-188
Kandušer M: 3/204-208
Karaagac E: 2/116-122
Karantanas A: 1/22-26
Karaoglanoglu M: 4/300-303
Kasabašić M: 4/310-314
Kikelj D: 4/259-266
Király R: 1/68-74
Klarić - Čustović R: 2/147-158
Koc M: 3/213-219; 4/292-295
Kocjančič B: 4/267-272
Kos J: 4/259-266
Krasnodebski IW: 1/59-63
Kristić S: 3/174-179
- Lah Turnšek T: 2/102-115
Lavrenčak J: 1/40-45
Letonja M: **3/180-183**
Lewander A: **4/279-284**
Liang H: 2/91-96
Limbaeck-Stokin C: 4/304-309
Lincender L: 3/174-179
Lu G: 2/82-90
- Malhotra H: 2/132-142
Matos E: 1/46-52
Meng Q: **2/82-90**
Miklavčič D: 3/204-208
Mirković B: 4/259-266
Mommenzhad M: **3/184-188**
Mowlavi A: **2/143-146**
Možina B: 1/46-52; 3/209-212

- Novak S: 4/227-247
 Novaković S: 4/285-291;
 4/296-299
- Oblak I: **3/209-212**
 Ocvirk J: 3/209-212; 4/285-291
 Oral A: 2/116-122
 Ovčariček T: **1/46-52**
 Ozmen E: 4/300-303
- Paliwal B: 3/220-226
 Pavlin D: **1/30-39**
 Pavliša Goran: **2/97-101**
 Pavliša Gordana: 2/97-101
 Perdikakis E: **1/22-26**
 Pesznyak C: **1/68-74**
 Petković J: 4/227-247
 Petrović R: 3/189-195
 Podgorsak M: 2/132-142
 Pogačnik A: 1/30-39
 Polgar I: 1/68-74
 Poljak M: 4/267-272
 Prasad D: 2/132-142
 Pregel R: 4/304-309
 Prijič S: **1/1-16**
- Qiu S: 2/123-128
- Radoš M: 2/97-101
 Ramasubramanian V: 3/220-226
 Raposo NRB: 3/166-173
 Reberšek Matej: **3/204-208**
 Reberšek Martina: **4/285-291**
 Rojnik M: **4/259-266**
- Sadeghi R: 3/184-188
 Samardžić T: 3/189-195
 Serša G: 1/1-16; 1/30-39
- Skočaj M: **4/227-247**
 Slodkowski M: 1/59-63
 Smilović Radojčić Đ: 4/310-314
 Stegel V: 4/296-299
 Steinman J: 2/132-142
 Strojan P: 1/40-45; 4/267-272
 Strojan Fležar M: **1/40-45**
 Sun XF: 4/279-284
- Šantl Letonja M: 3/180-183
 Šimunić S: **2/147-158**
 Štabuc B: 2/75-81
 Štern-Padovan R: **1/27-30**
 Švabić M: 4/310-314
- Tezcan Y: **3/213-219; 4/292-295**
 Tokullugil A: 2/116-122
 Tonchev Z: 4/248-258
 Tozon N: 1/30-39
 Tran T: **2/132-142**
- Ulukaya E: **2/116-122**
- Valatsou C: 1/22-26
 Vardar E: **1/53-58**
 Vegar-Zubović S: **3/174-179**
 Velenik V: 3/209-212
 Velnar T: **4/304-309**
 Vitral GSF: **3/166-173**
 Vodušek A: **4/296-299**
 Volk N: 4/285-291
 Vranič A: **3/159-165**
- Wang M: 2/123-128
 Wang Xianming: 2/123-128
 Wang Xuhui: **2/91-96**
 Wang Z: 2/123-128
 Wei P: 4/273-278
- Weisz C: 1/68-74
 Wronski M: **1/59-63**
 Wu H: 2/123-128
 Wu V: 2/132-142
- Xu L: 2/91-96
 Xu M: 2/91-96
 Yadav P: **3/220-226**
 Yang B: 2/82-90
 Yilmaz C: 1/53-58
- Zajc I: 2/102-115
 Zakavi SR: 3/184-188
 Zarand P: 1/68-74
 Zhang H: 4/279-284
 Zhao F: 3/196-203;
 Zhao SH: **3/196-203**
 Zhao XJ: 3/196-203
 Zheng JY: 3/196-203
 Zhou R: 2/123-128
 Ziarkiewicz-Wroblewska B:
 1/59-63
 Zidar N: 4/259-266
 Zuvić M: 3/189-195
 Žauhar G: 4/310-314
 Žganec M: 1/40-45

Subject Index 2011

- ¹³¹I radionuclide: 2/143-146
¹⁸F-choline PET/CT: 1/17-21
 adaptive planning: 3/220-226
 adenoma: 2/129-131
 anaemia: 2/129-131
 apoptosis: 2/116-122; 3/196-203
 apparent diffusion coefficient: 2/97-101
 applications, safety: 4/227-247

 backward wave: 2/82-90
 biopsy: 1/22-26
 body contour: 3/184-188
 body outlining: 3/184-188
 bone morphogenetic protein 4: 4/259-266
 bone reconstruction: 4/304-309
 BRAF: 4/285-291
 brain: 4/304-309
 breast cancer: 2/116-122; 3/166-173; 3/184-188; 4/296-299
 Brunner's gland: 2/129-131

 cancer: 4/259-266
 cancer therapy: 1/1-16
 carcinoma: 4/300-303
 cathepsin H: 4/259-266
 CD133/prominin1: 2/102-115
 central venous catheterization: 1/27-30
 cerebrospinal leak: 2/91-96
 chemotherapy: 2/75-81; 2/116-122; 4/273-278
 children: 4/248-258
 colorectal cancer: 2/75-81
 compensators: 4/310-314
 computed tomography: 3/180-183
 computed tomography dose index: 1/64-67

 cone-beam computerized tomography, kV CBCT: 3/220-226
 conformal radiotherapy: 3/213-219
 Croatian Medical Association, Croatian Society of Radiology: 2/147-158
 CT: 2/91-96
 CT to density table: 3/220-226
 CT, MR imaging, diffusion weighted imaging: 1/22-26
 cutaneous metastases: 4/292-295
 cysteine cathepsins: 2/102-115

 delivery systems: 1/1-16
 desmoid tumour: 1/59-63
 diagnosis: 1/17-21; 2/91-96
 differential diagnosis: 1/59-63
 differentiated thyroid cancer: 3/189-195
 dose profile: 1/64-67
 dosimetry: 2/132-142; 4/310-314

 echocardiography: 3/180-183
 effective circulating blood volume: 2/82-90
 elastic recoil: 2/82-90
 electrodes: 3/204-208
 electrogene therapy: 1/30-39
 electron density phantom: 3/220-226
 electronic portal imaging device: 1/68-74
 electroporation: 1/30-39
 electrotransfection: 1/30-39
 ependymoma: 2/97-101

 fluorescence-guided resection: 3/159-165
 follow-up: 1/17-21
 functional analysis: 4/248-258

 Gafchromic film: 1/64-67
 gamma knife: 2/132-142
 gastrointestinal stromal tumour: 1/59-63
 gene electrotransfer: 3/204-208
 gene screening: 4/296-299
 GIST: 1/59-63
 glioblastoma: 2/102-115
 glioblastoma multiforme: 3/213-219
 glioma stem cells: 2/102-115

 head and neck cancer: 1/40-45
 healthy blood donors: 3/209-212
 helical computed tomography: 1/27-30
 hemangiopericytoma: 1/22-26
 hepatocellular carcinoma: 4/292-295
 history: 2/147-158
 human cell lines: 4/259-266
 human papillomavirus infection: 4/267-272

 IL-12: 1/30-39
 image cytometry: 1/40-45
 image-guided surgery: 3/159-165
 immunohistochemistry: 4/279-284
 INF- γ : 1/30-39
 intradermal injection: 3/184-188
 invasion: 2/102-115; 4/304-309
 inverted papilloma: 4/267-272

 KRAS: 4/285-291

 laparoscopy: 4/273-278
 left ventricular pseudoaneurysm: 3/180-183
 low iodine diet: 3/189-195

- lymphoma, non-Hodgkin:
 1/27-30
 lymphoscintigraphy: 3/184-188

 M30: 2/116-122
 magnetic nanoparticles: 1/1-16
 magnetic resonance
 cholangiography: 4/300-303
 magnetic resonance imaging:
 4/300-303
 magnetic targeting: 1/1-16
 magnetofection: 1/1-16
 male: 4/296-299
 malignant glioma: 3/159-165
 mast cell tumors: 1/30-39
 MCNPX code: 2/143-146
 meningioma: 4/304-309
 mesenteric fibromatosis: 1/59-63
 metastatic colorectal cancer:
 4/285-291
 metastatic tumours: 1/53-58
 microsatellite instability: 2/75-81
 MR urography: 3/174-179;
 4/248-258
 MRI: 2/91-96
 multidetector computed
 tomography: 4/300-303
 multiple basilar skull fracture:
 2/91-96
 multislice CT: 1/64-67

 nanoparticles: 4/227-247
 nanotechnology: 1/1-16
 neural stem cells: 2/102-115
 neuronavigation: 3/159-165
 NF- κ B, serine-536: 4/279-284
 nuclear features: 1/40-45

 oncology: 1/1-16
 outcome: 4/267-272
 ovarian cancer: 3/196-203

 paediatrics: 3/174-179
 pancreatic cysts: 4/300-303
 pancreatic intraepithelial
 neoplasia: 4/300-303
 pelvis: 1/22-26
 pencil chamber: 1/64-67
 perfexion: 2/132-142
 pilocytic astrocytoma: 2/97-101
 pipette tip, CHO cell line:
 3/204-208
 portal film: 1/68-74
 principal wave: 2/82-90
 prognosis: 1/40-45; 2/123-128;
 4/273-278; 4/279-284
 prognostic factors: 1/46-52;
 3/213-219; 4/285-291
 prostate carcinoma: 1/17-21
 proteolytic enzymes: 4/259-266

 quality control: 1/68-74

 radiation therapy: 4/310-314;
 4/292-295
 radioiodine: 3/189-195
 radiological contrast: 3/166-173
 radiology: 2/147-158
 radiotherapy: 1/22-26; 4/267-272;
 4/279-284
 rectal cancer: 3/209-212
 rectal cancer: 4/279-284
 recurrence: 4/279-284
 resistance: 2/82-90
 response to chemotherapy:
 2/116-122
 RNA interference: 3/196-203
 ROLL technique: 3/166-173

 scattered photons: 3/184-188
 secondary malignancies: 1/53-58
 secondary neoplasm: 4/296-299
 shutter effect: 2/132-142

 SKOV3 cells: 3/196-203
 squamous cell carcinoma:
 4/267-272
 stage II colon cancer: 4/273-278
 staging: 1/17-21
 stat3: 3/196-203
 stereotactic radiosurgery:
 2/132-142
 surgery: 3/159-165; 3/166-173

 targeted chemotherapy:
 2/123-128
 temozolomide: 3/213-219
 thyroid gland: 2/143-146
 thyroid malignancy: 1/53-58
 TIMP-1: 3/209-212
 titanium dioxide: 4/227-247
 total energy deposition:
 2/143-146
 toxicity: 4/227-247
 transcranial magnetic
 stimulation: 3/159-165
 treatment outcome: 1/46-52
 triple negative breast cancer:
 1/46-52
 triple-negative breast cancer:
 2/123-128

 urinary tract: 3/174-179;
 4/248-258
 urine iodine concentration:
 3/189-195

 velocity tracing: 2/82-90



FUNDACIJA "DOCENT DR. J. CHOLEWA"
JE NEPROFITNO, NEINSTITUCIONALNO IN NESTRANKARSKO
ZDRUŽENJE POSAMEZNIKOV, USTANOV IN ORGANIZACIJ, KI ŽELIJO
MATERIALNO SPODBUJATI IN POGLABLJATI RAZISKOVALNO
DEJAVNOST V ONKOLOGIJI.

DUNAJSKA 106
1000 LJUBLJANA

ŽR: 02033-0017879431



Activity of "Dr. J. Cholewa" Foundation for Cancer Research and Education - a report for the second half of 2011

The Dr. J. Cholewa Foundation for Cancer Research and Education is a non-profit, non-government and non-political association of individuals, institutions and organisations, its main aim is to support novel initiatives and forward thinking in cancer education, research and prevention. One of its most important aims is to facilitate the flow of relevant information and knowledge from major oncology centres in the world to medical professionals, other experts and general public in Slovenia.

The Foundation thus distributes different types of grants and support to applicants from Slovenia wishing to extend existing or gain new knowledge in oncology. It helps professional and other associations in Slovenia to organise scientific and other meetings of specific interest in different fields of advanced cancer research and education. One of its most important activities is to support the publication of various cancer information and cancer awareness brochures and booklets for the general public.

The Dr. J. Cholewa Foundation for Cancer Research and Education is especially proud to continue its support for the publication of "Radiology and Oncology", an important international medical scientific journal that is edited, published and printed in Ljubljana, Slovenia. As its name suggests, "Radiology and Oncology" is a journal that publishes scientific articles, reviews, case reports, short reports and letters that deal with problems in radiology, radiophysics, experimental and clinical oncology, supportive therapy, prevention and early diagnostics of different types of cancer. It is an open access journal, available free of charge on its website, with an important Science Citation Index impact factor.

The Dr. J. Cholewa Foundation for Cancer Research and Education plans to add a number of new activities to the now well established projects in course in the near future, as the need for changes is becoming ever more necessary. The need for up to date prevention and early detection measures for certain types of cancers has grown substantially in the last few years in Slovenia. An increase in a number of incidence and prevalence rates of various types of cancer has been observed in the last two or three decades in Slovenia and these changes warrant the identification of new priorities and new goals in the national setting. Hopefully, the Foundation may be able to respond and to support at least some of the proposals by the experts active in these new and challenging aspects of oncology in Slovenia.

The Foundation has continued with its activities throughout 2011 with the aim to spread the latest knowledge about cancer and related problems to specialists and other professionals in Slovenia, with important part of its activities being the education and information of the lay public. These activities may already in the near future lead to greater practical application of the latest methods and protocols in the treatment of cancer in Slovenia.

Borut Štabuc, MD, PhD
Andrej Plesničar, MD
Tomaž Benulič, MD

Kakovost • Izbira • Zadovoljstvo

T H E

*Natrelle*TM

C O L L E C T I O N

Prsni vsadki in ekspanderji tkiv



*I*ndividualne ženske
*I*ndividualen izbor

 **ALLERGAN**

DISTRIBUCIJA IN PRODAJA:
SANOLABOR, d.d.,
Leskoškova 4, 1000 Ljubljana, Slovenija
Tel: +386 (0)1 585-42-11
Fax: +386 (0)1 585-42-98
www.sanolabor.si

 **Sanolabor**

PROMOCIJA, MARKETING IN STROKOVNA PODPORA:
EWOPHARMA d.o.o., Cesta 24. junija 23, 1000 Ljubljana, Slovenija
Jurij Pivka, vodja poslovne enote -Medicinska estetika
Tel: +386 (0) 59 084 845, mobilnik: +386 (0) 51 326 058
Fax: +386 (0) 59 084 849

ERBITUX®

CETUKSIMAB

ERBITUX – izbira za izboljšano učinkovitost

- Za zdravljenje metastatskega raka debelega črevesa in danke
- Za zdravljenje raka skvamoznih celic glave in vratu

Merck Serono Onkologija | ključ je v kombinaciji

Erbix 5 mg/ml raztopina za infundiranje (Skrajšan povzetek glavnih značilnosti zdravila)

Sestava: En ml raztopine za infundiranje vsebuje 5 mg cetuximaba in pomožne snovi. Cetuximab je himerno monoklonsko IgG1 protitelo. **Terapevtske indikacije:** Zdravilo Erbitux je indicirano za zdravljenje bolnikov z metastatskim kolorektalnim rakom z ekspresijo receptorjev EGFR in nemutiranim tipom KRAS v kombinaciji s kemoterapijo in kot samostojno zdravilo pri bolnikih, pri katerih zdravljenje z oksaliplatinom in irinotekanom ni bilo uspešno. Zdravilo Erbitux je indicirano za zdravljenje bolnikov z rakom skvamoznih celic glave in vratu v kombinaciji z radioterapijo za lokalno napredovalo bolezen in v kombinaciji s kemoterapijo na osnovi platine za ponavljajočo se in/ali metastatsko bolezen. **Odmerjanje in način uporabe:** Zdravilo Erbitux pri vseh indikacijah infundirajte enkrat na teden. Pred prvo infuzijo mora bolnik prejeti premedikacijo z antihistaminikom in kortikosteroidom. Začetni odmerek je 400 mg cetuximaba na m² telesne površine. Vsi naslednji tedenski odmerki so vsak po 250 mg/m². **Kontraindikacije:** Zdravilo Erbitux je kontraindicirano pri bolnikih z znano hudo preobčutljivostno reakcijo (3. ali 4. stopnje) na cetuximab. **Posebna opozorila in previdnostni ukrepi:** Če pri bolniku nastopi blaga ali zmerne reakcija, povezana z infundiranjem, lahko zmanjšate hitrost infundiranja. Priporočljivo je, da ostane hitrost infundiranja na nižji vrednosti tudi pri vseh naslednjih infuzijah. Če se pri bolniku pojavi huda kožna reakcija (≥ 3. stopnje po kriterijih US NCI-CTC), morate prekiniti terapijo s cetuximabom. Z zdravljenjem smete nadaljevati le, če se je reakcija izboljšala do 2. stopnje. Zaradi možnosti pojava znižanja nivoja magnezija v serumu se pred in periodično med zdravljenjem priporoča določanje koncentracije elektrolitov. Če se pojavi sum na nevtropenijo, je potrebno bolnika skrbno nadzorovati. Potrebno je upoštevati kardiovaskularno stanje bolnika in sočasno dajanje kardiotsičnih učinkovin kot so fluoropirimidini. **Interakcije:** farmakokinetične značilnosti cetuximaba ostanejo nespremenjene po sočasni uporabi enkratnega odmerka irinotekana, tudi farmakokinetika irinotekana je nespremenjena pri sočasni uporabi cetuximaba. Pri kombinaciji s fluoropirimidini se je povečala pogostost srčne ishemije, vključno z miokardnim infarktom in kongestivno srčno odpovedjo ter pogostost sindroma dlani in stopal. V kombinaciji s kemoterapijo na osnovi platine se lahko poveča pogostost hude levkopenije ali hude nevtropenije. **Neželeni učinki:** Zelo pogosti (≥ 1/10): hipomagneziemija, povečanje ravni jetrnih encimov, kožne reakcije, blage ali zmerne reakcije povezane z infundiranjem, blag do zmeren mukozitis. Pogosti (≥ 1/100, < 1/10): dehidracija, hipokalcemija, anoreksija, glavobol, konjunktivitis, driska, navzeja, bruhanje, hude reakcije povezane z infundiranjem, utrujenost. **Posebna navodila za shranjevanje:** Shranjujte v hladilniku (2 °C – 8 °C). **Pakiranje:** 1 viala z 20 ml ali 100 ml raztopine. **Način in režim izdaje:** H. **Imetnik dovoljenja za promet:** Merck KGaA, 64271 Darmstadt, Nemčija. **Datum zadnje revizije besedila:** november 2010.

Pred predpisovanjem zdravila natančno preberite celoten Povzetek glavnih značilnosti zdravila. Podrobne informacije o zdravilu so objavljene na spletni strani Evropske agencije za zdravila (EMA) <http://www.emea.europa.eu>.

Dodatne informacije so na voljo pri: Merck d.o.o., Dunajska cesta 119, 1000 Ljubljana, tel.: 01 560 3810, faks: 01 560 3831, el. pošta: info@merck.si

www.merckserono.net

www.Erbix-international.com

Merck Serono

Merck Serono is a
division of Merck.



POVZETEK GLAVNIH ZNAČILNOSTI ZDRAVILA

Ime zdravila: Temodal 20 mg, 100 mg, 140mg, 180 mg, 250 mg, Temodal 2,5 mg/ml prašek za raztopino za infundiranje **Kakovostna in količinska sestava:** Vsaka kapsula zdravila Temodal vsebuje 20 mg, 100 mg, 140 mg, 180 mg ali 250 mg temozolomida. Ena viala vsebuje 100 mg temozolomida Po rekonstituciji 1 ml raztopine za infundiranje vsebuje 2,5 mg temozolomida. Pomožna snov: Ena viala vsebuje 2,4 mmol natrija. **Terapevtske indikacije:** Zdravilo Temodal 2,5 mg/ml je indicirano za zdravljenje: odraslih bolnikov z novo diagnosticiranim multiformnim glioblastomom, sočasno z radioterapijo (RT) in pozneje kot monoterapija in otrok, starih 3 leta in več, mladostnikov in odraslih bolnikov z malignimi gliomi, npr. multiformnimi glioblastomi ali anaplastičnimi astroцитomi, ki se po standardnem zdravljenju ponovijo ali napredujejo. **Odmerjanje in način uporabe:** Zdravilo Temodal 2,5 mg/ml smejo predpisati le zdravniki, ki imajo izkušnje z zdravljenjem možganskih tumorjev. **Odrasli bolniki z novo diagnosticiranim multiformnim glioblastomom** Zdravilo Temodal 2,5 mg/ml se uporablja v kombinaciji z žariščno radioterapijo (faza sočasne terapije), temu pa sledi do 6 ciklov monoterapije (monoterapijska faza) z temozolomidom (TMZ). **Faza sočasne terapije** TMZ naj bolnik jemlje v odmerku 75 mg/m² na dan 42 dni, sočasno z žariščno radioterapijo (60 Gy, danih v 30 delnih odmerkih). Zmanjševanje odmerka ni priporočeno, vendar se boste vsak teden odločili o morebitni odločitvi jemanja TMZ ali njegovi ukinitvi na podlagi kriterijev hematološke in nehematološke toksičnosti. TMZ lahko bolnik jemlje ves čas 42-dnevnega obdobja sočasne terapije (do 49 dni), če so izpolnjeni vsi od naslednjih pogojev:

- absolutno število nevtrofilcev (ANC – Absolute Neutrophil Count) $\geq 1,5 \times 10^9/l$;
- število trombocitov $\geq 100 \times 10^9/l$;
- skupna merila toksičnosti (SMT) za nehematološko toksičnost ≤ 1 . stopnje (z izjemo alopecije, navzee in bruhanja).

Med zdravljenjem morate pri bolniku enkrat na teden pregledati celotno krvno sliko.

Faza monoterapije Štiri tedne po zaključku faze sočasne terapije s TMZ in RT naj bolnik jemlje TMZ do 6 ciklov monoterapije. V 1. ciklu (monoterapije) je odmerek zdravila 150 mg/m² enkrat na dan 5 dni, temu pa naj sledi 23 dni brez terapije. Na začetku 2. cikla odmerek povečate na 200 mg/m², če je SMT za nehematološko toksičnost za 1. cikel stopnje ≤ 2 (z izjemo alopecije, slabosti in bruhanja), absolutno število nevtrofilcev (ANC) $\geq 1,5 \times 10^9/l$ in število trombocitov $\geq 100 \times 10^9/l$. Če odmerka niste povečali v 2. ciklu, ga v naslednjih ciklih ne smete povečevati. Ko pa odmerek enkrat povečate, naj ostane na ravni 200 mg/m² na dan v prvih 5 dneh vsakega naslednjega cikla, razen če nastopi toksičnost. Zmanjšanje odmerka in ukinitvev zdravila med fazo monoterapije opravite, kot je opisano v preglednicah 2 in 3. Med zdravljenjem morate 22. dan pregledati celotno krvno sliko (21 dni po prvem odmerku TMZ). **Odrasli in pediatrični bolniki, stari 3 leta ali več, s ponavljajočim se ali napredujočim malignim gliomom:** Posamezen cikel zdravljenja traja 28 dni. Bolniki, ki še niso bili zdravljeni s kemoterapijo, naj jemljejo TMZ v odmerku 200 mg/m² enkrat na dan in prvih 5 dni, temu pa naj sledi 23-dnevni premor (skupaj 28 dni). Pri bolnikih, ki so že bili zdravljeni s kemoterapijo, je začetni odmerek 150 mg/m² enkrat na dan, v drugem ciklu pa se poveča na 200 mg/m² enkrat na dan 5 dni, če ni bilo hematoloških toksičnih učinkov. **Kontraindikacije:** Preobčutljivost za zdravilno učinkovino ali katerikoli pomožni snov. Preobčutljivost za dakarbazin (DTIC). **Posebna opozorila in previdnostni ukrepi:** **Piljučnica, ki jo povzroča *Pneumocystis carinii*** Pilotno preskušanje podaljšane 42-dnevne sheme zdravljenja je pokazalo, da pri bolnikih, ki so sočasno prejemali TMZ in RT, obstaja še posebej veliko tveganje za nastanek pljučnice zaradi okužbe s *Pneumocystis carinii* (PCP). **Malignosti** Zelo redko so poročali tudi o primerih mielodisplastičnega sindroma in sekundarnih malignostih, vključno z mieloidno levkemijo. Antimetično zdravljenje Navzea in bruhanje sta pogosto povezana z zdravljenjem s TMZ. **Antimetično zdravljenje** se lahko da pred uporabo TMZ ali po njej. **Odrasli bolniki z novo diagnosticiranim multiformnim glioblastomom** Antimetična profilaksa je priporočljiva pred začetnim odmerkom sočasne faze in je močno priporočljiva med fazo monoterapije. **Ponavljajoči se ali napredujoči maligni gliom** Pri bolnikih, ki so močno bruhal (stopnja 3 ali 4) v prejšnjih ciklih zdravljenja, je potrebno antimetično zdravljenje. **Laboratorijske vrednosti** Pred jemanjem zdravila morata biti izpolnjena naslednja pogoja za laboratorijske izvide: ANC $\geq 1,5 \times 10^9/l$ in število trombocitov $\geq 100 \times 10^9/l$. Na 22. dan (21 dni po prvem odmerku) ali v roku 48 ur od navedenega dne, morate pregledati celotno krvno sliko in jo nato spremljati vsak teden, dokler ni ANC $> 1,5 \times 10^9/l$ in število trombocitov $> 100 \times 10^9/l$. Če med katerikoli ciklom ANC pade na $< 1,0 \times 10^9/l$ ali število trombocitov na $< 50 \times 10^9/l$, morate odmerek zdravila v naslednjem ciklu zmanjšati za eno stopnjo (glejte poglavje 4.2). Stopnje odmerka so 100 mg/m², 150 mg/m² in 200 mg/m². Najmanjši priporočeni odmerek je 100 mg/m². **Pediatrična uporaba** Kliničnih izkušenj z uporabo TMZ pri otrocih, mlajših od 3 let, ni. Izkušnje z uporabo tega zdravila pri starejših otrocih in mladostnikih so zelo omejene. **Starejši bolniki** (stari > 70 let) Videti je, da je pri starejših bolnikih tveganje za neutropenijo ali trombocitopenijo večje, kot pri mlajših. Zato je pri uporabi zdravila TMZ pri starejših bolnikih potrebna posebna previdnost.

Moški bolniki Moškimi, ki se zdravijo s TMZ, je treba svetovati, naj ne zaplodijo otroka še šest mesecev po prejemu zadnjem odmerku in naj se pred zdravljenjem posvetujejo o možnostih za shranitev zmrznele sperme. **Natrij** To zdravilo vsebuje 2,4 mmol natrija na vialo. To je treba upoštevati pri bolnikih na nadzorovani dieti z malo natrija. **Medsebojno delovanje z drugimi zdravili in druge oblike interakcij:** Študije medsebojnega delovanja so izvedli le pri odraslih. V ločeni študiji 1. faze, sočasna uporaba TMZ in ranitidina ni povzročila spremembe obsega absorpcije temozolomida ali izpostavljenosti njegovemu aktivnemu presnovku monometiltrazenomidazol karboksamidu (MTIK). Analiza populacijske farmakokinetike v preskušanih 2. faze je pokazala, da sočasna uporaba deksametazona, proklorperazina, fenitoina, karbamazepina, ondansetrona, antagonistov receptorjev H₂ ali fenobarbitala ne spremeni očistka TMZ. Sočasno jemanje z valprojsko kislino je bilo povezano z majhnim, a statistično pomembnim zmanjšanjem očistka TMZ. Študij za določitev učinka TMZ na presnovo ali izločanje drugih zdravil niso izvedli. Ker pa se TMZ ne presnavlja v jetrih in se na beljakovine veže le v majhni meri, je malo verjetno, da bi vplival na farmakokinetiko drugih zdravil.

Uporaba TMZ v kombinaciji z drugimi mielosupresivnimi učinkovinami lahko poveča verjetnost mielosupresije. **Neželeni učinki:** Pri bolnikih, ki se zdravijo s TMZ v kombinaciji z RT ali monoterapijo po RT zaradi novo diagnosticiranega multiformnega glioblastoma ali z monoterapijo pri bolnikih s ponavljajočim se ali napredujočim gliomom, so bili zelo pogosti neželeni učinki podobni: slabost, bruhanje, zaprtje, neješčnost, glavobol in utrujenost. Pri bolnikih z novo diagnosticiranim glioblastomom multiformne na monoterapiji so zelo pogosto poročali o konvulzijah, medtem ko je bil izpuščaj opisan zelo pogosto pri bolnikih z novo diagnosticiranim multiformnim glioblastomom, ki so prejemali TMZ sočasno z RT, ter pri tistih, ki so zdravilo prejemali v obliki monoterapije, pogosto pa pri tistih s ponavljajočim se gliomom. Pri obeh indikacijah so o večini hematoloških neželenih reakcij poročali pogosto ali zelo pogosto. **Imetnik dovoljenja za promet:** Schering-Plough Europe, Rue de Stalle 73, Bruselj, Belgija **Način in režim izdaje zdravila:** Zdravilo Temodal 20 mg, 100 mg, 140mg, 180 mg, 250 mg se izdaja na recept (Rp/Spec), Temodal 2,5 mg/ml prašek za raztopino za infundiranje pa je namenjeno uporabi samo v bolnišnicah (H). **Datum prijave informacije:** februar 2010

1. Stupp R, et al. Effects of radiotherapy with concomitant and adjuvant temozolomide versus radiotherapy alone on survival in glioblastoma in a randomised III study: 5-year analysis of the EORTC-NCIC trial
2. Povzetek temeljnih značilnosti zdravila Temodal

5 jakosti v 5 barvah za lažje in natančnejše dnevno odmerjanje²



Schering-Plough CE AG
Dunajska cesta 22, 1000 Ljubljana
tel: 01 300 10 70
fax: 01 300 10 80



Resnični napredek

Pomembno izboljšanje preživetja potrjeno
tudi ob daljšem spremljanju bolnikov¹

Temodal[®] [™]
temozolomide
capsules

SKRAJŠAN POVZETEK GLAVNIH ZNAČILNOSTI ZDRAVILA

Samo za strokovno javnost.

Ime zdravila: Tarceva 25 mg/100 mg/150 mg filmsko obložene tablete

Kakovostna in količinska sestava: Ena filmsko obložena tableta vsebuje 25 mg, 100 mg ali 150 mg erlotiniba (v obliki erlotinibijevga klorida).

Terapevtske indikacije: Nedrobnocelični rak pljuč: Zdravilo Tarceva je indicirano za prvo linijo zdravljenja bolnikov z lokalno napredovalim ali metastatskim nedrobnoceličnim rakom pljuč z EGFR-aktivirajočimi mutacijami. Zdravilo Tarceva je indicirano tudi za samostojno vzdrževalno zdravljenje bolnikov z lokalno napredovalim ali metastatskim nedrobnoceličnim rakom pljuč po neuspehu vsaj ene predhodne kemoterapije na osnovi platine v prvi liniji zdravljenja. Zdravilo Tarceva je indicirano tudi za zdravljenje bolnikov z lokalno napredovalim ali metastatskim nedrobnoceličnim rakom pljuč po neuspehu vsaj ene predhodne kemoterapije. Pri predpisovanju zdravila Tarceva je treba upoštevati dejavnike, povezane s podaljšanim preživetjem. Koristnega vpliva na podaljšanje preživetja ali drugih klinično pomembnih učinkov zdravljenja niso dokazali pri bolnikih z EGFR-negativnimi tumorji (glede na rezultat imunohistokemije). **Rak trebušne slinavke:** Zdravilo Tarceva je v kombinaciji z gemcitabinom indicirano za zdravljenje bolnikov z metastatskim rakom trebušne slinavke. Pri predpisovanju zdravila Tarceva je treba upoštevati dejavnike, povezane s podaljšanim preživetjem. Koristnega vpliva na podaljšanje preživetja niso dokazali za bolnike z lokalno napredovalo boleznijo.

Odmerjanje in način uporabe: Zdravljenje z zdravilom Tarceva mora nadzorovati zdravnik z izkušnjami pri zdravljenju raka. Pri bolnikih z lokalno napredovalim ali metastatskim nedrobnoceličnim rakom pljuč, ki še niso prejeli kemoterapije, je treba testiranje za določanje mutacij EGFR opraviti pred začetkom zdravljenja z zdravilom Tarceva. Zdravilo Tarceva vzamemo najmanj eno uro pred zaužitjem hrane ali dve uri po tem. Kadar je potrebno odmerek prilagoditi, ga je treba zmanjševati v korakih po 50 mg. Pri sočasnem jemanju substratov in modulatorjev CYP3A4 bo morda potrebna prilagoditev odmerka. Pri dajanju zdravila Tarceva bolnikom z jetrno okvaro je potrebna previdnost. Če se pojavijo hudi neželeni učinki, pride v poštev zmanjšanje odmerka ali prekinitve zdravljenja z zdravilom Tarceva. Uporaba zdravila Tarceva pri bolnikih s hudo jetrno ali ledvično okvaro ter pri otrocih ni priporočljiva. Bolnikom kadilcem je treba svetovati, naj prenehajo kaditi, saj so plazemske koncentracije erlotiniba pri kadilcih manjše kot pri nekadilcih. **Nedrobnocelični rak pljuč:** Priporočeni dnevni odmerek zdravila Tarceva je 150 mg. **Rak trebušne slinavke:** Priporočeni dnevni odmerek zdravila Tarceva je 100 mg, v kombinaciji z gemcitabinom. Pri bolnikih, pri katerih se kožni izpuščaji v prvih 4 do 8 tednih zdravljenja ne pojavijo, je treba ponovno pretehati nadaljnje zdravljenje z zdravilom Tarceva.

Kontraindikacije: Preobčutljivost za erlotinib ali katero koli pomožno snov.

Posebna opozorila in previdnostni ukrepi: Pri določanju bolnikovega statusa mutacij EGFR je pomembno izbrati dobro validirano in robustno metodologijo, da se izognemo lažno negativnim ali lažno pozitivnim rezultatom. Močni induktorji CYP3A4 lahko zmanjšajo učinkovitost erlotiniba, močni zaviralci CYP3A4 pa lahko povečajo toksičnost. Sočasnemu zdravljenju s temi zdravili se je treba izogibati. Bolnikom, ki kadijo, je treba svetovati, naj prenehajo kaditi, saj so plazemske koncentracije erlotiniba pri kadilcih zmanjšane v primerjavi s plazemskimi koncentracijami pri nekadilcih. Verjetno je, da je velikost zmanjšanja klinično pomembna. Pri bolnikih, pri katerih se akutno pojavijo novi in/ali poslabšajo nepojasneni pljučni simptomi, kot so dispneja, kašelj in vročina, je treba zdravljenje z zdravilom Tarceva prekiniti, dokler ni znana diagnoza. Bolnike, ki se sočasno zdravijo z erlotinibom in gemcitabinom, je treba skrbno spremljati zaradi možnosti pojava toksičnosti, podobni intersticijski boleznijo pljuč. Če je ugotovljena intersticijska bolezen pljuč, zdravilo Tarceva ukinemo in uvedemo ustrezno zdravljenje. Pri približno polovici bolnikov, ki so se zdravili z zdravilom Tarceva, se je pojavila driska (vključno z zelo redkimi primeri, ki so se končali s smrtnim izidom). Zmerno do hudo drisko zdravimo z loperamidom. V nekaterih primerih bo morda potrebno zmanjšanje odmerka. V primeru hude ali dolgotrajne driske, navzee, anoreksije ali bruhanja, povezanih z dehidracijo, je treba zdravljenje z zdravilom Tarceva prekiniti in dehidracijo ustrezno zdraviti. O hipokalemiji in ledvični odpovedi so poročali redko. Posebno pri bolnikih z dejavniki tveganja (sočasno jemanje drugih zdravil, simptomi, boleznijo ali drugi dejavniki, vključno z visoko starostjo) moramo, če je driska huda ali dolgotrajna oziroma vodi v dehidracijo, zdravljenje z zdravilom Tarceva prekiniti in bolnikom zagotoviti intenzivno intravensko rehidracijo. Dodatno je treba pri bolnikih s prisotnim tveganjem za razvoj dehidracije spremljati ledvično delovanje in serumske elektrolite, vključno s kalijem. Pri uporabi zdravila Tarceva so poročali o redkih primerih jetrne odpovedi. K njenemu nastanku je lahko pripomogla predhodno obstoječa jetrna bolezen ali sočasno jemanje hepatotoksičnih zdravil. Pri teh bolnikih je treba zato premisliti o rednem spremljanju jetrnega delovanja. Dajanje zdravila Tarceva je treba prekiniti, če so spremembe jetrnega delovanja hude. Bolniki, ki prejemajo zdravilo Tarceva, imajo večje tveganje za razvoj perforacij v prebavilih, ki so jih opazili občasno (vključno z nekaterimi primeri, ki so se končali s smrtnim izidom). Pri bolnikih, ki sočasno prejemajo zdravila, ki zavirajo angiogenezo, kortikosteroide, nesteroidna protivnetna zdravila (NSAID) in/ali kemoterapijo na osnovi taksanov, ali so v preteklosti imeli peptični ulkus ali divertikularno bolezen, je tveganje večje. Če pride do tega, je treba zdravljenje z zdravilom Tarceva dokončno ukiniti. Poročali so o primerih kožnih bolezni z mehurji in luščenjem kože, vključno z zelo redkimi primeri, ki so nakazovali na Stevens-Johnsonov sindrom/toksično epidermalno nekrolizo in so bili v nekaterih primerih smrtni. Zdravljenje z zdravilom Tarceva je treba prekiniti ali ukiniti, če se pri bolniku pojavijo hude oblike mehurjev ali luščenja kože. Bolniki, pri katerih se pojavijo znaki in simptomi, ki nakazujejo na keratitis

in so lahko akutni ali se poslabšujejo: vnetje očesa, solzenje, občutljivost na svetlobo, zamegljen vid, bolečine v očesu in/ali rdeče oči, se morajo takoj obrniti na specialista oftalmologije. V primeru, da je diagnoza ulcerativnega keratitisa potrjena, je treba zdravljenje z zdravilom Tarceva prekiniti ali ukiniti. V primeru, da se postavi diagnoza keratitisa, je treba skrbno razmisliti o koristih in tveganjih nadaljnjega zdravljenja. Zdravilo Tarceva je pri bolnikih, ki so v preteklosti imeli keratitis, ulcerativni keratitis ali zelo suhe oči, uporabljati previdno. Uporaba kontaktnih leč je prav tako dejavnik tveganja za keratitis in ulceracijo. Med uporabo zdravila Tarceva so zelo redko poročali o primerih perforacije ali ulceracije roženice. Tablete vsebujejo laktozo in jih ne smemo dajati bolnikom z redkimi dednimi stanji: intoleranco za galaktozo, laponsko obliko zmanjšane aktivnosti laktaze ali malabsorpcijo glukoze/galaktoze.

Medsebojno delovanje z drugimi zdravili in druge oblike interakcij: Erlotinib se pri ljudeh presnavlja v jetrih z jetrnimi citokromi, primarno s CYP3A4 in v manjši meri s CYP1A2. Presnova erlotiniba zunaj jeter poteka s CYP3A4 v črevesju, CYP1A1 v pljučih in CYP1B1 v tumorskih tkivih. Zdravilnimi učinkovinami, ki se presnavljajo s temi encimi, jih zavirajo ali pa so njihovi induktorji, lahko pride do interakcij. Erlotinib je srednje močan zaviralec CYP3A4 in CYP2C8, kot tudi močan zaviralec glukuronidacije z UGT1A1 *in vitro*. Pri kombinaciji ciprofloksacina ali močnega zaviralca CYP1A2 (npr. fluvoksamina) z erlotinibom je potrebna previdnost. V primeru pojava neželenih učinkov, povezanih z erlotinibom, lahko odmerek erlotiniba zmanjšamo. Predhodno ali sočasno zdravljenje z zdravilom Tarceva ni spremenilo čistka prototipov substratov CYP3A4, midazolama in eritromicina. Inhibicija glukuronidacije lahko povzroči interakcije z zdravili, ki so substrati UGT1A1 in se izločajo samo po tej poti. Močni zaviralci aktivnosti CYP3A4 zmanjšajo presnovo erlotiniba in zvečajo koncentracije erlotiniba v plazmi. Pri sočasnem jemanju erlotiniba in močnih zaviralcev CYP3A4 je zato potrebna previdnost. Če je treba, odmerek erlotiniba zmanjšamo, še posebno pri pojavu toksičnosti. Močni spodbujevalci aktivnosti CYP3A4 zvečajo presnovo erlotiniba in pomembno zmanjšajo plazemske koncentracije erlotiniba. Sočasnemu dajanju zdravila Tarceva in induktorjev CYP3A4 se je treba izogibati. Pri bolnikih, ki potrebujejo sočasno zdravljenje z zdravilom Tarceva in močnim induktorjem CYP3A4, je treba premisliti o povečanju odmerka do 300 mg ob skrbnem spremljanju njihove varnosti. Zmanjšana izpostavljenost se lahko pojavi tudi z drugimi induktorji, kot so fenitoin, karbamazepin, barbiturati ali šentjanževka. Če te zdravilne učinkovine kombiniramo z erlotinibom, je potrebna previdnost. Kadar je mogoče, je treba razmisliti o drugih načinih zdravljenja, ki ne vključujejo močnega spodbujanja aktivnosti CYP3A4. Bolnikom, ki jemljejo kumarinske antikoagulate, je treba redno kontrolirati protrombinski čas ali INR. Sočasno zdravljenje z zdravilom Tarceva in statinom lahko poveča tveganje za miopatijo, povzročeno s statini, vključno z rhabdomiolizo; to so opazili redko. Sočasna uporaba zaviralcev P-glikoproteina, kot sta ciklosporin in verapamil, lahko vodi v spremenjeno porazdelitev in/ali spremenjeno izločanje erlotiniba. Za erlotinib je značilno zmanjšanje topnosti pri pH nad 5. Zdravila, ki spremenijo pH v zgornjem delu prebavil, lahko spremenijo topnost erlotiniba in posledično njegovo biološko uporabnost. Učinka antacidov na absorpcijo erlotiniba niso proučevali, vendar je ta lahko zmanjšana, kar vodi v nižje plazemske koncentracije. Kombinaciji erlotiniba in zaviralca protonske črpalke se je treba izogibati. Če menimo, da je uporaba antacidov med zdravljenjem z zdravilom Tarceva potrebna, jih je treba jemati najmanj 4 ure pred ali 2 uri po dnevnem odmerku zdravila Tarceva. Če razmišljamo o uporabi ranitidina, moramo zdravili jemati ločeno: zdravilo Tarceva je treba vzeti najmanj 2 uri pred ali 10 ur po odmerku ranitidina. V študiji faze Ib ni bilo pomembnih učinkov gemcitabina na farmakokinetiko erlotiniba, prav tako ni bilo pomembnih učinkov erlotiniba na farmakokinetiko gemcitabina. Erlotinib poveča koncentracijo platine. Pomembnih učinkov karboplatina ali paklitaksela na farmakokinetiko erlotiniba ni bilo. Kapecitabin lahko poveča koncentracijo erlotiniba. Pomembnih učinkov erlotiniba na farmakokinetiko kapecitabina ni bilo.

Neželeni učinki: Zelo pogosti neželeni učinki so kožni izpuščaji in driska, kot tudi utrujenost, anoreksija, dispneja, kašelj, okužba, navzea, bruhanje, stomatitis, bolečina v trebuhu, pruritus, suha koža, suhi keratokonjunktivitis, konjunktivitis, zmanjšanje telesne mase, depresija, glavobol, nevropatija, dispneja, flatulenca, alopecija, okorelost, piroksija, nenormalnosti testov jetrne funkcije. Pogosti neželeni učinki so krvavitve v prebavilih, epistaksa, keratitis, paronihija, fisure na koži. Občasno so poročali o perforacijah v prebavilih, hirzutizmu, spremembah obrvi, krhkih nohtih, odstopanju nohtov od kože, blagih reakcijah na koži (npr. hiperpigmentacija), spremembah trepalnic, hudi intersticijski boleznijo pljuč (vključno s smrtnimi primeri). Redko pa so poročali o jetrni odpovedi. Zelo redko so poročali o Stevens-Johnsonovem sindromu/toksični epidermalni nekrolizi ter o ulceracijah in perforacijah roženice.

Režim izdaje zdravila: H/Rp. **Imetnik dovoljenja za promet:** Roche Registration Limited, 6 Falcon Way, Shire Park, Welwyn Garden City, AL7 1TW, Velika Britanija. **Verzija:** 1.0/1.1. **Informacija pripravljena:** Oktober 2011.

DODATNE INFORMACIJE SO NA VOLJO PRI:

Roche farmacevtska družba d.o.o.

Vodovodna cesta 109, 1000 Ljubljana.

Povzetek glavnih značilnosti zdravila je dosegljiv

na www.roche.si ali www.onkologija.si.



ČAS ZA ŽIVLJENJE.

DOKAZANO PODALJŠA PREŽIVETJE PRI BOLNIKI:

- z lokalno napredovalim ali metastatskim nedrobnoceličnim rakom pljuč¹
- z metastatskim rakom trebušne slinavke¹

¹ Povzetek glavnih značilnosti zdravila TARCEVA, www.ema.europa.eu





odprto

Novartis Oncology prinaša spekter inovativnih zdravil, s katerimi poskuša spremeniti življenje bolnikov z rakavimi in hematološkimi obolenji.

Ta vključuje zdravila kot so Glivec® (imatinib), Tassigna® (nilotinib), Afinitor® (everolimus), Zometa® (zoledronska kislina), Femara® (letrozol), Sandostatin® LAR® (oktreotid/i.m. injekcije) in Exjade® (deferasiroks).

Novartis Oncology ima tudi obširen razvojni program, ki izkorišča najnovejša spoznanja molekularne genomike, razumskega načrtovanja in tehnologij za odkrivanje novih učinkovin.

 **glivec**
imatinib

 **Tassigna**
(nilotinib)

 **AFINITOR**
(everolimus) tablete

ZOMETA
zoledronska kislina

 **Femara**
(letrozol)

 **Sandostatin LAR**
oktreotid / i.m. injekcije

 **EXJADE**
deferasiroks



Že več kot desetletje prinašamo rešitve v Vaš laboratorij!

Za področja:

- bioznanosti **SYNGENE, INVITROGEN, BIOTEK**
diagnostike **MINERVA, MEDAC, BIOTEK**
- gojenja celičnih kultur **INVITROGEN-GIBCO, TPP, SANYO**
- merjenja absorbance, fluorescence in luminiscence
BIOTEK, SHIMADZU
- pipetiranja **BIOHIT** in **BIOTEK**
- laboratorijske opreme in instrumentov **SANYO, SHIMADZU**
- čiste vode za laboratorije **ELGA LABWATER**
- HPLC in GC instrumentov, kolon, vial in filtrov
PHENOMENEX, CHROMACOL/NATIONAL SCIENTIFIC, SHIMADZU



Megace®

megestrolacetat 40mg/ml
peroralna suspenzija

učinkovita in preizkušena
možnost zdravljenja
anoreksije-kaheksije

Megace®

... še vedno EDINO ZDRAVILO, ki je v Sloveniji registrirano za zdravljenje anoreksije-kaheksije pri bolnikih z napredovalim rakom ^{1,2} - predpisovanje na zeleni recept v breme ZZS ⁶

Megace®

- izboljša apetit ^{1,5}
- pomaga ohraniti in pridobiti telesno težo ^{3,4,5}
- izboljša splošno počutje bolnikov ^{3,4}

Megace®

SKRAJŠAN POVZETEK GLAVNIH ZNAČILNOSTI ZDRAVILA: MEGACE 40 mg/ml peroralna suspenzija

Sestava: 1 ml peroralne suspenzije vsebuje 40 mg megestrolacetata. **TERAPEVTSKE INDIKACIJE:** Zdravljenje anoreksije-kaheksije ali nepojasnjene, pomembne izgube telesne mase pri bolnikih z AIDS-om. Zdravljenje anorektično-kahektičnega sindroma pri napredovalem raku. **ODMERJANJE IN NAČIN UPORABE:** Pri aidsu je priporočeni začetni odmerek Megace za odrasle 800 mg (20 ml peroralne suspenzije) enkrat na dan eno uro pred jedjo ali dve uri po jedi in se lahko med zdravljenjem prilagodi glede na bolnikov odziv. V raziskavah bolnikov z aidsom so bili klinično učinkoviti dnevni odmerki od 400 do 800 mg/dan (10 do 20 ml), uporabljeni štiri mesece. Pri anorektično-kahektičnem sindromu zaradi napredovalega raka je priporočljiv začetni odmerek 200 mg (5 ml) na dan; glede na bolnikov odziv ga je mogoče povečati do 800 mg na dan (20 ml). Običajni odmerek je med 400 in 800 mg na dan (10–20 ml). V raziskavah bolnikov z napredovalim rakom so bili klinično učinkoviti dnevni odmerki od 200 do 800 mg/dan (5 do 20 ml), uporabljeni najmanj osem tednov. Pred uporabo je potrebno platenko s suspenzijo dobro pretresti. Uporaba pri otrocih: Varnosti in učinkovitosti pri otrocih niso dokazali. Uporaba pri starostnikih: Zaradi pogostejših okvar jeter, ledvic in srčne funkcije, pogostejših sočasnih obolenj ali sočasnega zdravljenja z drugimi zdravili je odmerek za starejšega bolnika treba določiti previdno in običajno začeti z najnižjim odmerkom znotraj odmernega intervala. **KONTRAINDIKACIJE:** Preobčutljivost za megestrolacetat ali katerokoli pomožno snov. **POSEBNA OPOZORILA IN PREVIDNOSTNI UKREPI:** Uporaba gestagenov med prvimi štirimi meseci nosečnosti ni priporočljiva. Pri bolnikih s tromboflebitisom v anamnezi je treba zdravilo Megace uporabljati previdno. Zdravljenje z zdravilom Megace se lahko začne šele, ko so bili vzroki hujšanja, ki jih je mogoče zdraviti, ugotovljeni in obravnavani. Megestrolacetat ni namenjen za profilaktično uporabo za preprečitev hujšanja. Učinki na razmnoževanje virusa HIV niso ugotovljeni. Med zdravljenjem z megestrolacetatom in po prekinitvi kroničnega zdravljenja je treba upoštevati možnost pojava zavore nadledvične žleze. Morda bo potrebno nadomestno zdravljenje s stresnimi odmerki glukokortikoidov. Megestrolacetat se v veliki meri izloči prek ledvic. Ker je verjetnost zmanjšane delovanja ledvic pri starostnikih večja, je pri določitvi odmerka potrebna previdnost, prav tako je koristno spremljanje ledvične funkcije. Peroralna suspenzija vsebuje saharozo. Bolniki z redko dedno intoleranco za fruktozo, malabsorpcijo glukoze/galaktoze ali pomanjkanjem saharoza-izomaltaze ne smejo jemati tega zdravila. Peroralna suspenzija vsebuje tudi majhne količine etanola (alkohola), in sicer manj kot 100 mg na odmerek. **INTERAKCIJE:** Aminoglutetimid: poročali so o zmanjšanju koncentracije progesterona v plazmi z možno izgubo terapevtskega delovanja zaradi inducirane presnove. Sočasno jemanje megestrolacetata (v obliki peroralne suspenzije) in zidovudina ali rifabutina ne povzroča sprememb farmakokinetičnih parametrov. **NEŽELENI UČINKI:** Pogosti ($\geq 1/100$, $< 1/10$): navzea, bruhanje, driska, flatulenca, izpuščaji, metroragija, impotenca, astenija, bolečina, edem. Neznana pogostnost (pogostnosti ni mogoče oceniti iz razpoložljivih podatkov): poslabšanje osnovne bolezn (širjenje tumorja), adrenalna insuficienca, kušingoidni izgled, Cushingov sindrom, diabetes mellitus, motena toleranca za glukozo, hiperglikemija, spremembe razpoloženja, sindrom karpalnega kanala, letargija, srčno popuščanje, tromboflebitis, pljučna embolija (v nekaterih primerih usodna), hipertenzija, navali vročine, dispneja, zaprtje, alopecija, pogosto uriniranje. **Vrsta ovojnine in vsebina:** Platenka z 240 ml suspenzije. **Režim izdaje:** Rp/Spec. **Imetnik dovoljenja za promet:** Bristol-Myers Squibb spol. s r.o., Olivova 4, Praga 1, Češka. **Odgovoren za trženje v Sloveniji:** PharmaSwiss d.o.o., Ljubljana, tel: 01 236 4 700, faks: 01 236 4 705; MGS-120609. **Pred predpisovanjem preberite celoten povzetek glavnih značilnosti zdravila!**

Reference: 1. Povzetek glavnih značilnosti zdravila Megace – 12. junij 2009; 2. Register zdravil Republike Slovenije XII – leto 2010; 3. Beller, E., 1997. Ann Oncol 8: 277-283; 4. Čufer, T, 2002. Onkologija 9(2): 73-75; 5. Yavuzsen, T., 2005. J Clin Oncol 23(33): 8500-8511; 6. Bilten Recept 8(2), 8.12.2010

MEG0211-01; februar 2011



Bristol-Myers Squibb

PharmaSwiss

Choose More Life

TANTUM® VERDE



Lajšanje bolečine in oteklin pri vnetju v ustni votlini in žrelu, ki nastanejo zaradi okužb in stanj po operaciji in kot posledica radioterapije (t.i. radiomukozitis).

Tantum Verde 1,5 mg/ml oralno pršilo, raztopina

Kakovostna in količinska sestava

1 ml raztopine vsebuje 1,5 mg benzidaminijevega klorida, kar ustreza 1,34 mg benzidamina. V enem razpršku je 0,17 ml raztopine. En razpršek vsebuje 0,255 mg benzidaminijevega klorida, kar ustreza 0,2278 mg benzidamina. En razpršek vsebuje 13,6 mg 96 odstotnega etanola, kar ustreza 12,728 mg 100 odstotnega etanola, in 0,17 mg metilparahidroksibenzoata (E218).

Terapevtske indikacije

Samozdravljenje: lajšanje bolečine in oteklin pri vnetju v ustni votlini in žrelu, ki so lahko posledica okužb in stanj po operaciji. Po nasvetu in navodilu zdravnika: lajšanje bolečine in oteklin v ustni votlini in žrelu, ki so posledica radiomukozitisa.

Odmerjanje in način uporabe

Uporaba 2- do 6-krat na dan (vsake 1,5 do 3 ure). Odrasli: 4 do 8 razprškov 2- do 6-krat na dan. Otroci od 6 do 12 let: 4 razprški 2- do 6-krat na dan. Otroci, mlajši od 6 let: 1 razpršek na 4 kg telesne mase; do največ 4 razprške 2 do 6-krat na dan.

Kontraindikacije

Znana preobčutljivost za zdravilno učinkovino ali katerokoli pomožno snov.

Posebna opozorila in previdnostni ukrepi

Pri manjšini bolnikov lahko resne bolezni povzročijo ustne/žrelne ulceracije. Če se simptomi v treh dneh ne izboljšajo, se mora bolnik posvetovati z zdravnikom ali zobozdravnikom, kot je primerno. Zdravilo vsebuje aspartam (E951) (vir fenilalanina), ki je lahko škodljiv za bolnike s fenilketonurijo. Zdravilo vsebuje izomalt (E953) (sinonim: izomaltitol (E953)). Bolniki z redko dedno intoleranco za fruktozo ne smejo jemati tega zdravila. Uporaba benzidamina ni priporočljiva za bolnike s preobčutljivostjo za salicilno kislino ali druga nesteroidna protivnetna zdravila. Pri bolnikih, ki imajo ali so imeli bronhialno astmo, lahko pride do bronhospazma. Pri takih bolnikih je potrebna previdnost.

Medsebojno delovanje z drugimi zdravili in druge oblike interakcij

Pri ljudeh raziskav o interakcijah niso opravljali.

Nosečnost in dojenje

Tantum Verde z okusom mentola 3 mg pastile se med nosečnostjo in dojenjem ne smejo uporabljati.

Vpliv na sposobnost vožnje in upravljanja s stroji

Uporaba benzidamina lokalno v priporočenem odmerku ne vpliva na sposobnost vožnje in upravljanja s stroji.

Neželeni učinki

Bolezni prebavil Redki: pekoč občutek v ustih, suha usta.

Bolezni imunskega sistema Redki: preobčutljivostna reakcija.

Bolezni dihal, prsnega koša in mediastinalnega prostora Zelo redki: laringospazem.

Bolezni kože in podkožja Občasni: fotosenzitivnost. Zelo redki: angioedem.

Rok uporabnosti

4 leta. Zdravila ne smete uporabljati po datumu izteka roka uporabnosti, ki je naveden na ovojnini. Posebna navodila za shranjevanje Za shranjevanje pastil niso potrebna posebna navodila. Platenko z raztopino shranjujte v zunanji ovojnini za zagotovitev zaščite pred svetlobo. Shranjujte pri temperaturi do 25°C. Shranjujte v originalni ovojnini in nedosegljivo otrokom.



Preprečuje CINV* od samega začetka

z zdravilom EMEND v kombinaciji
z drugimi antiemetiki



* - s kemoterapijo povzročena navzea in bruhanje

EMEND 80 mg trde kapsule EMEND 125 mg trde kapsule **SKRAJŠAN POVZETEK GLAVNIH ZNAČILNOSTI ZDRAVILA** Pred predpisovanjem, prosimo, preberite celoten Povzetek glavnih značilnosti zdravila, ki ga dobite pri naših strokovnih sodelavcih! Sestava: Ena EMEND 125 mg trda kapsula vsebuje 125 mg aprepitanta in 125 mg saharoze. Ena EMEND 80 mg trda kapsula vsebuje 80 mg aprepitanta in 80 mg saharoze. **Terapevtske indikacije:** Preprečevanje akutne in zapoznele navzee in bruhanja povezanih z zelo emetogeno kemoterapijo raka s cisplatinom pri odraslih. Preprečevanje navzee in bruhanja, povezanih z zmerno emetogeno kemoterapijo raka pri odraslih. Zdravilo EMEND 125 mg/80 mg se daje v sklopu kombiniranega zdravljenja. **Odmerjanje in način uporabe:** Zdravilo EMEND se daje 3 dni po shemi zdravljenja, ki vključuje kortikosteroid in antagonist 5-HT₃. Priporočeno odmerjanje zdravila EMEND je 125 mg peroralno (p.o.) enkrat dnevno eno uro pred pričetkom kemoterapije prvi dan ter 80 mg (p.o.) enkrat na dan drugi in tretji dan. Fosaprepitant 115 mg, liofilizirano predzdravilo aprepitanta v obliki 15-minutne infuzije, lahko prvi dan, 30 minut pred kemoterapijo nadomesti uporabo zdravila EMEND (125 mg). Zdravilo EMEND se lahko jemlje s hrano ali brez. Trdo kapsulo je treba pogoltniti celo. Pri starostnikih, bolnikih z okvaro ledvic in pri bolnikih s končno ledvično odpovedjo, ki se zdravijo s hemodializo, bolnikih z blago okvaro jeter ter glede na spol odmerka ni treba prilagajati. Pri bolnikih z zmerno okvaro jeter je število podatkov omejeno, pri bolnikih s hudo okvaro jeter pa podatkov ni. Pri teh bolnikih je treba aprepitant uporabljati previdno. Uporabe pri bolnikih, ki so mlajši od 18 let, zaradi nezadostnih podatkov o varnosti in učinkovitosti ne priporočamo. **Kontraindikacije:** Preobčutljivost za zdravilno učinkovino ali katerokoli pomožno snov. Sočasno jemanje s pimozidom, terfenadinom, z astemizolom ali s cisapridom. **Posebna opozorila in previdnostni ukrepi:** Zdravilo EMEND je treba uporabljati previdno pri bolnikih, ki sočasno jemljejo peroralne zdravilne učinkovine, ki se primarno presnavljajo s CYP3A4 in z ožkim terapevtskim območjem, kot so ciklosporin, takrolimus, sirolimus, everolimus, alfentanil, diergotamin, ergotamin, fentanil in kinidin. Previdnost je še posebej potrebna pri sočasnem dajanju inotekana, saj lahko kombinacija poveča toksični učinek. Pri sočasni uporabi zdravila EMEND z alkaloidi rženega rožička (ergot alkaloidi) svetujemo previdnost zaradi morebitnega tveganja za pojav z ergot alkaloidi povezanih toksičnih učinkov. Sočasna uporaba zdravila EMEND z varfarinom zmanjša protrombinski čas, izražen kot INR. Pri bolnikih, ki se kontinuirano zdravijo z varfarinom, je treba INR skrbno spremljati med zdravljenjem z zdravilom EMEND in 2 meseca po zadnjem odmerku zdravila EMEND je treba uporabljati alternativno ali dodatno kontracepcijsko metodo. Sočasnemu jemanju zdravila EMEND in zdravilnih učinkovin, ki močno inducirajo aktivnost CYP3A4 (npr. rifampicin, fenitoin, karbamazepin, fenobarbital), se je treba izogibati, ker kombinacija povzroči zmanjšanje plazemskih koncentracij aprepitanta. Sočasna uporaba zdravila EMEND in zeliščnih pripravkov, ki vsebujejo šentjanzkevo, ni priporočljiva. Potrebna je previdnost pri sočasni uporabi zdravila EMEND in zdravilnih učinkovin, ki zavirajo aktivnost CYP3A4 (npr. ketokonazol, itraconazol, vorikonazol, posakonazol, klaritromicin, telitromicin, nefazodon in zaviralci proteaz), ker se zaradi kombinacije pričakuje zvišanje plazemskih koncentracij aprepitanta. Zdravilo EMEND vsebuje saharozo. Bolniki z redkimi dednimi motnjami – fruktozno intoleranco, malabsorpcijo glukoze in galaktoze ali insuficienco saharoze-izomaltaze – ne smejo jemati tega zdravila. **Medsebojno delovanje z drugimi zdravili in druge oblike interakcij:** Aprepitant (125 mg/80 mg) je substrat, zmerno zaviralec in induktor CYP3A4. Aprepitant je tudi induktor CYP2C9. Med zdravljenjem se CYP3A4 inhibira. Po koncu zdravljenja pa zdravilo EMEND povzroči blago indukcijo CYP2C9, CYP3A4 in glukuronidacije. Aprepitant nima medsebojnega vpliva z digoksinom, zato verjetno ne interagirata s P-glikoproteinskim prenašalcem. Kot blag induktor CYP2C9, induktor CYP3A4 in glukuronidacije lahko aprepitant zniža plazemske koncentracije substratov, ki se izločajo po teh poteh. Ta učinek se lahko pokaže šele po koncu zdravljenja z zdravilom EMEND. Za substrate CYP2C9 in CYP3A4 je indukcija prehodna, največji učinek pa je dosežen v 3-5 dneh po koncu 3 dnevne zdravljenja z zdravilom EMEND. Učinek traja nekaj dni, potem pa počasa upada in je klinično nepomemben v dveh tednih po koncu zdravljenja. V tem obdobju svetujemo previdnost pri dajanju peroralnih zdravilnih učinkovin, ki se presnavljajo s CYP2C9. **Kortikosteroidi:** Pri sočasnem jemanju je treba običajni peroralni odmerek deksametazona zmanjšati za približno 50 %, običajni intravenski odmerek metilprednizolona zmanjšati za približno 25 % in

običajni peroralni odmerek metilprednizolona zmanjšati za približno 50 %. **Kemoterapevtiki:** Pri bolnikih, ki poleg zdravila EMEND peroralno prejemajo kemoterapevtike, ki se primarno ali delno presnavljajo s CYP3A4 (npr. etopozid, vinorelbin), svetujemo previdnost. Pri takih bolnikih bo morda potreben dodatni nadzor. **Imunosupresivi:** Zmanjšanja odmerka imunosupresivov, ki se presnavljajo s CYP3A4 (npr. ciklosporin, takrolimus, everolimus in sirolimus), ne priporočamo. **Midazolam:** Pri sočasni uporabi z zdravilom EMEND (125mg / 80 mg) je treba upoštevati možne učinke zvišanih plazemskih koncentracij midazolama in drugih benzodiazepinov, ki se presnavljajo predvsem s CYP3A4 (alprazolam, triazolam). **Tolbutamid:** Zdravilo EMEND je pri jemanju po shemi 125 mg prvi dan ter 80 mg/dan drugi in tretji dan zmanjšal AUC tolbutamida (ki je substrat za CYP2C9), ki so ga bolniki prejemali v enkratnem odmerku 500 mg per os pred začetkom 3 dnevne sheme odmerjanja zdravila EMEND ter 4., 8. in 15. dan. **Antagonisti 5-HT₃:** V kliničnih raziskavah medsebojnega delovanja aprepitant ni imel klinično pomembnih učinkov na farmakokinetiko ondansetrona, granisetrona in hidroksisetrona. **Ketokonazol:** Pri enkratnem odmerku 125 mg aprepitanta 5. dan 10 dnevne zdravljenja s ketokonazolom (ki je močan zaviralec CYP3A4) 400 mg na dan, se je AUC aprepitanta povečal za približno 5 krat, srednji končni razpolovni čas aprepitanta pa se je podaljšal za približno za 3 krat. **Rifampicin:** Pri enkratnem odmerku 375 mg aprepitanta 9. dan 14 dnevne zdravljenja z rifampicinom (ki je močan induktor CYP3A4) 600 mg na dan, se je AUC aprepitanta zmanjšal za 91 %, srednji končni razpolovni čas aprepitanta pa se je skrajšal za 68 %. **Neželene učinke:** Pri bolnikih, zdravljenih z aprepitantom, so opazili naslednje neželene učinke, ki so se pojavljali pogosteje kot pri standardni terapiji: Pogosti (>1/100, <1/10): anoreksija, glavobol, omotica, kolcanje, konstipacija, driska, dispneja, spanovanje, astenija/utrujenost, zvišanje ALT, zvišanje AST. Občasni (>1/1000, <1/100): kandidoza, okužbe s stafilokoki, anemija, febrilna nevtropenija, povečanje telesne mase, polidipsija, dezorientacija, evforija, anksioznost, neobičajne sanje, motnje mišljenja, letargija, zaspanost, konjunktivitis, tinitus, bradikardija, palpitacije, bolezen srca in ožilja, zardevanje/navali vročine, faringitis, kihanje, kašelj, zatekanje izcedka iz nosu v zrela, draženje žrela, perforirajoč duodenalni ulkus, navzea, bruhanje, refluks kisline, motnje okusa, neugodje v epigastriju, obstipacija, gastroezofagalna refluksna bolezen, bolečine v trebuhu, suha usta, enterokolitis, vetrovi, stomatitis, napihnjen trebuh, trdo blato, navtropančni kolitis, izpuščaji, akne, fotosenzitivnost, prekomerno znojenje, mastna koža, srbenje, lezije kože, srbeči izpuščaji, mišični krči, bolečine v mišicah, mišična oslabelost, polurija, disurija, polakisurija, edem, nelagodje v prsnem košu, splošno slabo počutje, žejna, mrzlica, motnja hoje, zvišanje alkaline fosfataze, hiperpigmentacija, mikrohematurija, hiponatriemija, zmanjšanje telesne mase, zmanjšano število nevtrofilcev. Poročali so o enem primeru angioedema in urtikarije. Pri enem bolniku, ki je dobival aprepitant ob kemoterapiji zaradi raka, so poročali o pojavu Stevens-Johnsonovega sindroma. V obdobju trženja zdravila so poročali še o (pogostnosti je neznana) truden, izpuščaji, urtikarija, preobčutljivostne reakcije, vključno z anafilaktičnimi reakcijami. EMEND 80mg trde kapsule EMEND 125 mg trde kapsule **Imetih dovoljenja za promet:** Merck Sharp & Dohme Ltd., Harford Road, Hoddesdon, Hertfordshire EN 11 9BU, Velika Britanija **Način in režim izdaje zdravila:** Predpisovanje in izdaja zdravila je le na zdravilni recept. **Datum zadnje revizije besedila:** 01/2010

Samo za strokovno javnost.

EMEND® (aprepitant, MSD)
IVEMEND® (fosaprepitant dimeglumin, MSD)

Preventivno od začetka



Merck Sharp & Dohme, inovativna zdravila d.o.o.

Šmartinska cesta 140, 1000 Ljubljana; telefon: 01/ 5204 201, faks: 01/ 5204 349

Tiskano v Sloveniji, junij 2011.

Prvi na poti individualnega zdravljenja bolnikov z napredovalim nedrobnoceličnim pljučnim rakom.

Iressa je prva in edina tarčna monoterapija, ki dokazano podaljša preživetje brez napredovanja bolezni v primerjavi z dvojno kemoterapijo kot zdravljenje prvega reda pri bolnikih z napredovalim nedrobnoceličnim pljučnim rakom z mutacijo EGFR.



EGFR M⁺

IRESSA® (GEFITINIB)

SKRAJŠAN POVZETEK GLAVNIH ZNAČILNOSTI ZDRAVILA

Sestava: Filmsko obložene tablete vsebujejo 250 mg gefitiniba.

Indikacije: zdravljenje odraslih bolnikov z lokalno napredovalim ali metastatskim nedrobnoceličnim pljučnim rakom z aktivacijskimi mutacijami EGFR-TK

Odmerjanje in način uporabe: Zdravljenje z gefitinibom mora uvesti in nadzorovati zdravnik, ki ima izkušnje z uporabo zdravil proti raku. Priporočeno odmerjanje zdravila IRESSA je ena 250-mg tableta enkrat na dan. Tableto je mogoče vzeti s hrano ali brez nje, vsak dan ob približno istem času.

Kontraindikacije: preobčutljivost za zdravilno učinkovino ali katerokoli pomožno snov, dojenje

Opozorila in previdnostni ukrepi: Pri 1,3 % bolnikov, ki so dobivali gefitinib, so opažali intersticijsko bolezen pljuč (IBP). Ta se lahko pojavi akutno in je bila v nekaterih primerih smrtna. Če se bolniku poslabšajo dihalni simptomi, npr. dispneja, kašelj in zvišana telesna temperatura, morate zdravljenje z zdravilom IRESSA prekiniti in bolnika takoj preiskati. Če je potrjena IBP, morate terapijo z zdravilom IRESSA končati in bolnika ustrezno zdraviti. Opažene so bile nepravilnosti testov jetrnih funkcij, občasno zabeležene kot hepatitis. Opisani so bili posamezni primeri odpovedi jeter. Zato so priporočljive redne kontrole delovanja jeter. V primeru blagih do zmernih sprememb v delovanju jeter je treba zdravilo IRESSA uporabljati previdno. Če so spremembe hude, pride v poštev prekinitev zdravljenja. Zdravilo IRESSA vsebuje laktozo. Bolniki z redko dedno intoleranco za galaktozo, laponsko obliko zmanjšane aktivnosti laktaze ali malabsorpcijo glukoze/galaktoze ne smejo jemati tega zdravila. Bolnikom naročite, da morajo takoj poiskati zdravniško pomoč, če se jim pojavijo kakršnikoli očesni simptomi, huda ali dolgotrajna driska, navzea, bruhanje ali anoreksija, ker lahko vse te posredno povzročijo dehidracijo.

Medsebojno delovanje zdravil: Sočasna uporaba močnih zaviralcev CYP3A4 lahko poveča koncentracijo gefitiniba v plazmi. Močni zaviralci CYP2D6 lahko pri izrazitih metabolizatorjih CYP2D6 povečajo koncentracijo gefitiniba v plazmi za približno 2-krat. Induktorji CYP3A4 lahko povečajo presnovo gefitiniba in zmanjšajo njegovo koncentracijo v plazmi. Zato lahko sočasna uporaba induktorjev CYP3A4 zmanjša učinkovitost zdravljenja in se ji je treba izogniti. Snovi, ki občutno in dolgotrajno zvišajo pH v želodcu, lahko zmanjšajo koncentracijo gefitiniba v plazmi in tako zmanjšajo njegovo učinkovitost. Veliki odmerki kratkodelujočih antacidov, uporabljenih blizu časa jemanja gefitiniba, imajo lahko podoben učinek. Pri nekaterih bolnikih, ki so jemali varfarin skupaj z gefitinibom, so se pojavili zvišanje internacionalnega normaliziranega razmerja (INR) in/ali krvavitve. Bolnike, ki sočasno jemljejo varfarin in gefitinib, morate redno kontrolirati glede sprememb protrombinskega časa (PČ) ali INR.

Neželeni učinki: V kumulativnem naboru podatkov kliničnih preskušanj III. faze so bili najpogosteje opisani neželeni učinki, ki so se pojavili pri več kot 20 % bolnikov, driska in kožne reakcije (vključno z izpuščajem, aknam, suho kožo in srbenjem). Neželeni učinki se ponavadi pojavijo prvi mesec zdravljenja in so praviloma reverzibilni. Ostali pogostejši neželeni učinki so: anoreksija, konjunktivitis, blefaritis in suho oko, krvavitev, npr. epistaksa in hematurija, intersticijska bolezen pljuč (1,3 %), navzea, bruhanje, stomatitis, dehidracija, suha usta, nepravilnosti testov jetrnih funkcij, boleznih nohtov, alopecija, asimptomatično laboratorijsko zvišanje kreatinina v krvi, proteinurija, cistitis, astenija, piroksija.

Vrsta in vsebina ovojnine: škatla s 30 tabletami po 250 mg gefitiniba

Način izdajanja zdravila: samo na recept

Datum priprave besedila: januar 2011

Imetnik dovoljenja za promet: AstraZeneca AB, S-151 85, Sodertalje, Švedska

Pred predpisovanjem, prosimo, preberite celoten povzetek glavnih značilnosti zdravila.

Dodatne informacije so na voljo pri:

AstraZeneca UK Limited, Podružnica v Sloveniji, Verovškova 55, 1000 Ljubljana, telefon: 01/51 35 600.

Samo za strokovno javnost.

Informacija pripravljena: avgust 2011

Instructions for authors

The editorial policy

Radiology and Oncology is a multidisciplinary journal devoted to the publishing original and high quality scientific papers, professional papers, review articles, case reports and varia (editorials, short communications, professional information, book reviews, letters, etc.) pertinent to diagnostic and interventional radiology, computerized tomography, magnetic resonance, ultrasound, nuclear medicine, radiotherapy, clinical and experimental oncology, radiobiology, radiophysics and radiation protection. Therefore, the scope of the journal is to cover beside radiology the diagnostic and therapeutic aspects in oncology, which distinguishes it from other journals in the field.

The Editorial Board requires that the paper has not been published or submitted for publication elsewhere; the authors are responsible for all statements in their papers. Accepted articles become the property of the journal and, therefore cannot be published elsewhere without the written permission of the editors.

Submission of the manuscript

The manuscript written in English should be submitted electronically to: gsera@onko-i.si. In the case the figures are too big to be submitted electronically, authors are asked to send along the printed copy of the manuscript, together with all the files on CD, to the editorial office. The type of computer and word-processing package should be specified (Word for Windows is preferred).

Editorial Office Radiology and Oncology
Zaloska cesta 2
P.O. Box 2217
SI-1000 Ljubljana
Slovenia
Phone: +386 (0)1 5879 434,
Tel./Fax: +386 (0)1 5879 434,
E-mail: gsera@onko-i.si

All articles are subjected to the editorial review and the review by independent referees. Manuscripts which do not comply with the technical requirements stated herein will be returned to the authors for the correction before peer-review. The editorial board reserves the right to ask authors to make appropriate changes of the contents as well as grammatical and stylistic corrections when necessary. Page charges will be charged for manuscripts exceeding the recommended page number, as well as additional editorial work and requests for printed reprints. All articles are published printed and on-line as the open access. To support the open access policy of the journal, the authors are encouraged to pay the open access charge of 500 EUR.

Preparation of manuscripts

Radiology and Oncology will consider manuscripts prepared according to the Uniform Requirements for Manuscripts Submitted to Biomedical Journals by International Committee of Medical Journal Editors (<http://www.icmje.org/>). The manuscript should be typed double-spaced with a 3-cm margin at the top and left-hand side of the sheet. The manuscript should be written in grammatically and stylistically correct language. Abbreviations should be avoided. If their use is necessary, they should be explained at the first time mentioned. The technical data should conform to the SI system. The manuscript, including the references, must not exceed 15 typewritten pages, and the number of figures and tables is limited to 8. If appropriate, organize the text so that it includes: Introduction, Materials and methods, Results and Discussion. Exceptionally, the results and discussion can be combined in a single section. Start each section on a new page, and number each page consecutively with Arabic numerals.

The Title page should include a concise and informative title, followed by the full name(s) of the author(s); the institutional affiliation of each author; the name and address of the corresponding author (including telephone, fax and E-mail), and an abbreviated title. This should be followed by the abstract page, summarizing in less than 250 words the reasons for the study, experimental approach, the major findings (with specific data if possible), and the principal conclusions, and providing 3-6 key words for indexing purposes. Structured abstracts are preferred. Slovene authors are requested to provide title and the abstract in Slovene language in a separate file. The text of the research article should then proceed as follows:

Introduction should summarize the rationale for the study or observation, citing only the essential references and stating the aim of the study.

Materials and methods should provide enough information to enable experiments to be repeated. New methods should be described in detail.

Results should be presented clearly and concisely without repeating the data in the figures and tables. Emphasis should be on clear and precise presentation of results and their significance in relation to the aim of the investigation.

Instructions

Discussion should explain the results rather than simply repeating them and interpret their significance and draw conclusions. It should discuss the results of the study in the light of previously published work.

Illustrations and tables must be numbered and referred to in the text, with the appropriate location indicated. Graphs and photographs, provided electronically, should be of appropriate quality for good reproduction. Color graphs and photographs are encouraged. Picture size must be 2.000 pixels on the longer side. In photographs, mask the identities of the patients. Tables should be typed double-spaced, with a descriptive title and, if appropriate, units of numerical measurements included in the column heading.

References must be numbered in the order in which they appear in the text and their corresponding numbers quoted in the text. Authors are responsible for the accuracy of their references. References to the Abstracts and Letters to the Editor must be identified as such. Citation of papers in preparation or submitted for publication, unpublished observations, and personal communications should not be included in the reference list. If essential, such material may be incorporated in the appropriate place in the text. References follow the style of Index Medicus. All authors should be listed when their number does not exceed six; when there are seven or more authors, the first six listed are followed by "et al.". The following are some examples of references from articles, books and book chapters:

Dent RAG, Cole P. *In vitro* maturation of monocytes in squamous carcinoma of the lung. *Br J Cancer* 1981; **43**: 486-95.

Chapman S, Nakielny R. *A guide to radiological procedures*. London: Bailliere Tindall; 1986.

Evans R, Alexander P. Mechanisms of extracellular killing of nucleated mammalian cells by macrophages. In: Nelson DS, editor. *Immunobiology of macrophage*. New York: Academic Press; 1976. p. 45-74.

Authorization for the use of human subjects or experimental animals

Manuscripts containing information related to human or animal use should clearly state that the research has complied with all relevant national regulations and institutional policies and has been approved by the authors' institutional review board or equivalent committee. These statements should appear in the Materials and methods section (or for contributions without this section, within the main text or in the captions of relevant figures or tables).

When reporting experiments on human subjects, authors should indicate whether the procedures followed were in accordance with the Helsinki Declaration. Patients have the right to privacy; therefore the identifying information (patient's names, hospital unit numbers) should not be published unless it is essential. In such cases the patient's informed consent for publication is needed, and should appear as an appropriate statement in the article.

The research using animal subjects should be conducted according to the EU Directive 2010/63/EU and following the Guidelines for the welfare and use of animals in cancer research (*Br J Cancer* 2010; **102**: 1555 – 77). Authors must identify the committee approving the experiments, and must confirm that all experiments were performed in accordance with relevant regulations.

Transfer of copyright agreement

For the publication of accepted articles, authors are required to send the Transfer of Copyright Agreement to the publisher on the address of the editorial office. A properly completed Transfer of Copyright Agreement, signed by the Corresponding Author on behalf of all the authors, must be provided for each submitted manuscript. A form can be found on the journal's webpage.

Conflict of interest

When the manuscript is submitted for publication, the authors are expected to disclose any relationship that might pose real, apparent or potential conflict of interest with respect to the results reported in that manuscript. Potential conflicts of interest include not only financial relationships but also other, non-financial relationships. In the Acknowledgement section the source of funding support should be mentioned. The Editors will make effort to ensure that conflicts of interest will not compromise the evaluation process of the submitted manuscripts; potential editors and reviewers will exempt themselves from review process when such conflict of interest exists. The statement of disclosure must be in the Cover letter accompanying the manuscript or submitted on the form available on http://www.icmje.org/coi_disclosure.pdf

Page proofs will be sent by E-mail or faxed to the corresponding author. It is their responsibility to check the proofs carefully and return a list of essential corrections to the editorial office within three days of receipt. Only grammatical corrections are acceptable at this time.

Reprints: The electronic version of the published papers will be available on www.versitaopen.com free of charge.

ALIMTA[®] pemetreksed



BUILD A TREATMENT STRATEGY FROM SURVIVAL

SKRAJŠAN POVZETEK GLAVNIH ZNAČILNOSTI ZDRAVILA

Ime zdravila ALIMTA, 100 mg prašek za raztopino za infundiranje in ALIMTA 500 mg prašek za raztopino za infundiranje. **Kakovostna in količinska sestava** ALIMTA 100 mg: vsaka viala vsebuje 100 mg pemetrekseda (v obliki dinatrijevega pemetrekseda). Po pripravi vsebuje vsaka viala 25 mg/ml pemetrekseda. Pomozne snovi: vsaka viala vsebuje približno 11 mg natrija, manitol, klorovodikova kislina, natrijev hidroksid. ALIMTA 500 mg: vsaka viala vsebuje 500 mg pemetrekseda (v obliki dinatrijevega pemetrekseda). Po pripravi vsebuje vsaka viala 25 mg/ml pemetrekseda. Pomozne snovi: vsaka viala vsebuje približno 54 mg natrija, manitol, klorovodikova kislina, natrijev hidroksid. **Terapevtske indikacije** ALIMTA je v kombinaciji s cisplatinom indicirana za zdravljenje bolnikov z neresektibilnim malignim plevralnim mezoteliomom, ki jih še nismo zdravili s kemoterapijo. ALIMTA je v kombinaciji s cisplatinom indicirana kot zdravljenje prvega izbora za bolnike z lokalno napredovalim ali metastatskim nedrobnoceličnim pljučnim karcinomom, ki nima pretežno ploščatocelične histologije. ALIMTA je indicirana kot monoterapija za zdravljenje lokalno napredovelega ali metastatskega nedrobnoceličnega pljučnega karcinoma, ki nima pretežno ploščatocelične histologije pri bolnikih, pri katerih bolezen ni napredovala neposredno po kemoterapiji na osnovi platine. ALIMTA je indicirana kot monoterapija za zdravljenje drugega izbora bolnikov z lokalno napredovalim ali metastatskim nedrobnoceličnim pljučnim karcinomom, ki nima pretežno ploščatocelične histologije. **Odmerjanje in način uporabe** Odmerjanje: ALIMTO smemo dajati le pod nadzorom zdravnika, usposobljenega za uporabo kemoterapije za zdravljenje raka. ALIMTA v kombinaciji s cisplatinom. Priporočeni odmerek ALIMTE je 500 mg/m² telesne površine (TP), dan kot intravenska infuzija v 10 minutah prvi dan vsakega 21-dnevnega ciklusa. Priporočeni odmerek cisplatina je 75 mg/m² TP, infundiran v dveh urah približno 30 minut po zaključku infuzije pemetrekseda prvi dan vsakega 21-dnevnega ciklusa. Bolniki morajo prejeti zadostno antiemetično zdravljenje, pred in/ali po prejetju cisplatina jih moramo tudi ustrezno hidrirati. ALIMTA kot samostojno zdravilo. Priporočeni odmerek ALIMTE je 500 mg/m² TP, dan kot intravenska infuzija v 10 minutah prvi dan vsakega 21-dnevnega ciklusa. **Režim premedikacije** Da zmanjšamo incidenco in resnost kožnih reakcij, dajemo kortikosteroid dan pred dajanjem pemetrekseda, na dan dajanja pemetrekseda in naslednji dan. Kortikosteroid naj ustreza 4 mg deksametazona, danega peroralno dvakrat dnevno. Za zmanjšanje toksičnosti morajo bolniki dnevno jemati tudi peroralno folno kislino ali multivitaminski pripravek, ki jo vsebuje (350 do 1000 mikrogramov). V sedmih dneh pred prvim odmerkom pemetrekseda morajo vzeti vsaj pet odmerkov folne kisline, odmerjanje pa morajo nadaljevati ves čas zdravljenja in še 21 dni po zadnjem odmerku pemetrekseda. Bolniki morajo prejeti tudi intramuskularno injekcijo vitamina B12 (1000 mikrogramov) v tednu pred prvim odmerkom pemetrekseda in enkrat vsake tri cikluse zatem. Kasnejše injekcije vitamina B12 lahko dajemo isti dan kot pemetreksed. **Kontraindikacije** Preobčutljivost za zdravilno učinkovino ali katerokoli pomožno snov. Dolojene. Sočasno cepljenje proti rumeni mrzlici. **Posebna opozorila in previdnostni ukrepi**: Pemetreksed lahko zavre delovanje kostnega mozga, kar se kaže kot nevtropenija, trombocitopenija in anemija (ali pancitopenija). Mielosupresija običajno predstavlja toksičnost za omejitve odmerka. Pri bolnikih, ki pred zdravljenjem niso prejeli kortikosteroidov, so poročali o kožnih reakcijah. Uporabe pemetrekseda pri bolnikih z očistkom kreatinina < 45 ml/min ne priporočamo. Bolniki z blagim do zmernim popuščanjem delovanja ledvic naj se izogibajo jemanju nesteroidnih protivnetnih zdravil (NSAID), denimo, ibuprofena in aceticilsalicilne kisline 2 dni pred dajanjem pemetrekseda, na dan dajanja in še 2 dni po dajanju pemetrekseda. Vsi bolniki, ki jih lahko zdravimo s pemetreksedom, naj se izogibajo jemanju NSAID-ov z dolgi razpolovni čas izločanja vsaj 5 dni pred dajanjem pemetrekseda, na dan dajanja in še vsaj 2 dni po dajanju pemetrekseda. Poročali so o resnih ledvičnih primerih, vključno z akutno ledvično odpovedjo, s pemetreksedom samim ali v povezavi z drugimi kemoterapevtskimi zdravili. Pri bolnikih s klinično pomembno tekočino tretjega prostora moramo razmisliti o drenaži izliva pred dajanjem pemetrekseda. Kot posledico toksičnosti pemetrekseda v kombinaciji s cisplatinom za prebavila so opažali hudo dehidracijo, zato moramo bolnike pred prejetjem terapije in/ali po njej ustrezno hidrirati, prejeti morajo zadostno antiemetično zdravljenje. Običajno so v kliničnih študijah pemetrekseda, običajno ob sočasnem dajanju z drugo citotoksično učinkovino, poročali o resnih srčnožilnih dogodkih, vključno z miokardnim infarktom in možganskožilnimi dogodki. Odsvetujemo uporabo živih oslabljenih cepiv. Spolno zreli moški odsvetujemo zaploditev otroka v času zdravljenja in še 6 mesecev zatem. Priporočamo ukrepe proti zanositvi ali vzdržnost. Zaradi možnosti, da zdravljenje s pemetreksedom povzroči trajno neplodnost, naj se moški pred začetkom zdravljenja posvetujejo o shranjevanju semena. Ženske v rodni dobi morajo v času zdravljenja s pemetreksedom uporabljati učinkovito kontracepcijo. Poročali so o primerih radiacijske pljučnice pri bolnikih, ki so jih zdravili z radiacijo pred, med ali po zdravljenju s pemetreksedom. Poročali so o radiacijskem izpuščaju pri bolnikih, ki so se zdravili z radioterapijo pred tedni ali leti. **Medsebojno delovanje z drugimi zdravili in druge oblike interakcij**: Sočasno dajanje nefrotoksičnih zdravil (denimo, aminoglikozidov, diuretikov zanke, spojini platine, ciklosporina) lahko potencialno povzroči zakasneli očistek pemetrekseda. Sočasno dajanje snovi, ki se tudi izločajo s tubulno sekrecijo (denimo, probencid, penicilin), lahko potencialno povzroči zakasneli očistek pemetrekseda. Pri bolnikih z normalnim delovanjem ledvic lahko visoki odmerki nesteroidnih protivnetnih zdravil (NSAID), denimo, ibuprofena in aceticilsalicilna kislina v visokih odmerkih zmanjšajo eliminacijo pemetrekseda in tako lahko povečajo pojavnost neželenih učinkov pemetrekseda. Pri bolnikih z blagim do zmernim popuščanjem delovanja ledvic se moramo izogibati sočasnemu dajanju pemetrekseda z NSAID-i (denimo, ibuprofonom) ali aceticilsalicilne kisline v visokih odmerkih 2 dni pred dajanjem pemetrekseda, na dan dajanja in še 2 dni po dajanju pemetrekseda. Sočasnemu dajanju NSAID-ov z daljšimi razpolovni časi s pemetreksedom se moramo izogibati vsaj 5 dni pred dajanjem pemetrekseda, na dan dajanja in še vsaj 2 dni po dajanju pemetrekseda. Velika različenost med posamezniki v koagulacijskem statusu v času bolezni ter možnost medsebojnega delovanja med peroralnimi antikoagulantnimi učinkovinami ter kemoterapijo proti raku zahtevata povečano pozornost spremljanja INR. **Kontraindicirana sočasna uporaba**: Cepivo proti rumeni mrzlici, tveganje za smrtno generalizirano bolezen po cepljenju. **Odsvetovana sočasna uporaba**: Živa oslabljena cepiva (razen proti rumeni mrzlici); tveganje za sistemsko, potencialno smrtno bolezen. **Neželeni učinki** Klinične študije malignega plevralnega mezotelioma. **Zelo pogosto**: znižani nevtrofilci/granulociti, znižani levkociti, znižani hemoglobin, znižani trombociti, nevropatija-senzorna, diareja, bruhanje, stomatitis/faringitis, slabost, anoreksija, zaprtje, izpuščaj, alopecija, povišan kreatinin, znižan očistek kreatinina, utrujenost. **Pogosti**: dehidracija, motnje okusa, konjunktivitis, dispneja. Klinične študije nedrobnoceličnega pljučnega karcinoma - ALIMTA monoterapija, zdravljenje 2. izbora. **Zelo pogosti**: znižan nevtrofilci/granulociti, znižani levkociti, znižan hemoglobin, diareja, bruhanje, stomatitis/faringitis, slabost, anoreksija, zaprtje, izpuščaj, alopecija, povišana telesna temperatura. Klinične študije nedrobnoceličnega pljučnega karcinoma - ALIMTA v kombinaciji s cisplatinom, zdravljenje 1. izbora. **Zelo pogosti**: znižan hemoglobin, znižani nevtrofilci/granulociti, znižani levkociti, znižani trombociti, slabost, bruhanje, anoreksija, zaprtje, stomatitis/faringitis, diareja brez kolostomije, alopecija, izpuščaj/luščenje, povišan kreatinin, utrujenost. **Pogosti**: nevropatija-senzorična, motnje okusa, dispneja/zgaga. Klinične študije nedrobnoceličnega pljučnega karcinoma - ALIMTA monoterapija, vzdrževalno in nadaljevalno zdravljenje. **Zelo pogosti**: znižan hemoglobin, slabost, anoreksija, utrujenost. **Pogosti**: znižani levkociti, znižani nevtrofilci, nevropatija-senzorična, bruhanje, mukozitis/stomatitis, povišanje ALT (SGPT), povišanje AST (SGOT), izpuščaj/luščenje, bolečina. Običajno so v kliničnih študijah pemetrekseda poročali o primerih resnih srčnožilnih in možganskožilnih dogodkih, vključno z miokardnim infarktom, angino pektoris, cerebrovaskularnim insultom in prehodnimi ishemičnimi atakami; primerih kolitisa ter o primerih intersticijske pljučnice z respiratorno insuficienco, primerih edema, o ezofagitisu/radiacijskem ezofagitisu in o primerih sepse. Redkeje pa o primerih potencialno resnega hepatitisa in pancitopenije. Po uvedbi zdravila na trg so poročali o primerih akutne odpovedi ledvic s pemetreksedom samim ali v povezavi z drugimi kemoterapevtskimi, primerih radiacijske pljučnice pri bolnikih, ki so jih zdravili z radiacijo pred, med ali po njihovem zdravljenju s pemetreksedom, primerih radiacijskega izpuščaja pri bolnikih, ki so se v preteklosti zdravili z radioterapijo, o primerih periferne ishemije, ki je včasih vodila v nekrozo okončin, redkih primerih buloznih stanj, kot sta Stevens-Johnsonov sindrom in toksična epidermalna nekroliza, ki so bila v nekaterih primerih usodna in o redkih primerih hemotične anemije. **Imetnik dovoljenja za promet** Eli Lilly Nederlanden BV, Grootslag 1 5, NL 3991 RA, Houten, Nizozemska. Datum zadnje revizije besedila 24.10.2011. **Način izdaje zdravila**: H. SAMO ZA STROKOVNO JAVNOST.

Podrobnejše informacije o zdravilu Alimta, so dostopne na spletni strani Evropske agencije za zdravila EMA <http://www.ema.europa.eu> in na lokalnem predstavništvu.

SIALM00025

Eli Lilly Farmaceutvska družba, d.o.o.
Brničeva 41G, 1231 Ljubljana - Črnuče, Slovenija
Telefon: +386 (0)1 5800 010
Faks: +386 (0)1 5691 705

